Electrochemical modification of Si surfaces by methyl groups (CH_3, CD_3), ethynyl derivatives, pyrrole and thiophene

DISSERTATION

zur Erlangung des akademischen Grades
doctor rerum naturalium
(Dr. rer. nat.)
im Fach Chemie

eingereicht an der

Mathematisch-Naturwissenschaftlichen Fakultät I
der Humboldt-Universität zu Berlin

von

M.Sc.-Phys. Florent Yang
geboren am 07.05.1981 in Paris

Präsident der Humboldt-Universität zu Berlin
Prof. Dr. Christoph Markschies

Dekan der Mathematisch-Naturwissenschaftlichen Fakultät I
Prof. Dr. Lutz-Helmut Schön

Gutachter: 1. Prof. Dr. Klaus Rademann
2. Prof. Dr. Norbert Esser

eingereicht am: 16.10.2008
Tag der mündlichen Prüfung: 09.12.2008

To my parents.

Zusammenfassung

Silizium (Si) wird für eine breite Palette von Anwendungen wie z.B. in Solarzellen, Mikroelektronik, Biochips und so weiter eingesetzt. In dieser Arbeit wurden neue Hybridsysteme aus Si und organischen Molekülen, bezüglich der Oberflächenpassivierung des Halbleiters und der resultierenden elektronischen Eigenschaften untersucht. Insbesondere wurden Methyl-Gruppen (CH_3 und CD_3), Ethynyl-Derivate (H−C≡C-, CH_3−C≡C-, und C_6H_5−C≡C-), sowie Pyrrol und Thiophen aus Grignardlösungen untersucht. Bezüglich Stabilität und Defektkonzentration konnte gezeigt werden, dass organisch modifizierte Si-Oberflächen eine höhere Stabilität an Luft haben als Standard wasserstoffpassivierte Si-Oberflächen und dabei eine nur geringfügig höhere Defektkonzentration aufweisen. Untersuchungen mit Infrarot Spektroskopischer Ellipsometrie (IRSE) und Synchrotron Röntgen Photoemissions Spektroskopie (SXPS) zeigen, dass die Oxidationsrate für Oberflächen mit CH_3-Terminierung stark reduziert ist. In der vorliegenden Arbeit gelang es erstmalig mittels IRSE die charakteristische „Umbrella“-Schwingungsmode zu beobachten und SXPS Messungen zeigten die Spin-Orbit-Aufspaltung der Si 2p Emission für CH_3-passivierte Si-Oberflächen. Die CH_3-Gruppen besitzen einen hohen Grad von Ordnung auf der Si(111)-Oberfläche. Das Aufbringen von Ethynyl-Derivaten führt zu extrem dünnen polymerisierten Schichten auf Si durch elektrochemische Radikaloxidation der C≡C Dreifachbindung. Diese Schichten sind homogen und haften sehr gut an der Si-Oberfläche. Weiterhin konnte gezeigt werden, dass die Abscheidung von Ethynyl-Derivaten vom Typ des Halogenatoms im Grignard-Precursor abhängig ist, wobei Br im Vergleich zu Cl zu geringeren Rekombinationsgeschwindigkeiten an der Polymer/Si-Grenzfläche führen. Eine Änderung der Austrittsarbeit von bis zu 0.5 eV und der Bandverbiegung von bis zu 0.24 eV wurde nach der Abscheidung dieser Moleküle gemessen. Diese elektronischen Eigenschaften hängen linear vom Oberflächendipol ab.

Schlagwörter: Silizium, Organischen Schichten, Grignard, Elektrochemie, Passivierung, Infrarot Ellipsometrie, Röntgen Photoemissions Spektroskopie, Photolumineszenz

Abstract

Organic functionalization of silicon (Si) surfaces has received a tremendous interest in the development of organic/semiconductor hetero-structures for plenty of potential applications from microelectronics, molecular electronics, photovoltaics to bio-applications. In this thesis, tailoring of the electronic properties and passivation properties of such organic hetero-structures have been investigated. Direct grafting of organic layers like methyl groups (CH_3 and CD_3), ethynyl derivatives (H−C≡C-, CH_3−C≡C-, and C_6H_5−C≡C-), and heterocyclic molecules (pyrrole and thiophene) onto Si(111) surfaces have been performed in a one-step electrochemical process by anodic treatment in Grignard electrolytes. Organically modified Si surfaces show low interface recombination rates as measured by photoluminescence technique and reveal also a much better passivation with respect to stability in ambient air than H-terminated Si surfaces. Grafting of ethynyl derivatives and heterocyclic molecules lead to the formation of ultrathin polymeric layers, where the thickness depends on charge flow applied to the Si electrode, while methyl groups lead to a monolayer on Si(111) surfaces. Only a very small amount of oxidation states of Si has been observed by infrared spectroscopic ellipsometry (IRSE) and synchrotron X-ray photoemission spectroscopy (SXPS). For the first time, IRSE and SXPS measurements reveal the “umbrella” vibrational mode characteristic from methyl groups and a well-defined spin-orbit splitting of the Si 2p core level emission, respectively, in the case of methylated Si(111) surfaces. For all ethynyl derivatives, high-resolution SXPS investigations reveal the incorporation of halogen atoms in the organic layers obtained. Thereby, exchanging Br for Cl in the Grignard compound leads to lower interface recombination rates at the polymer/Si interface. A shift in work function and surface band bending of up to 0.5 and 0.24 eV has been observed, respectively. The electronic properties reveal a linear relation between the work function and the surface dipole.

Keywords: silicon, organic layers, Grignard, electrochemistry, passivation, infrared ellipsometry, X-ray photoemission spectroscopy, photoluminescence

Table of contents

Chapter 1

Introduction and motivations

Since several years, research in the field of organic modification of semiconductor surfaces, especially for silicon (Si), has revealed an important increase in the development of new semiconductor-based devices. A tremendous interest in such organic/semiconductor systems occurred due to a wide range of potential applications in molecular electronics, biosensors, microelectronics, organic hybrid devices, or photovoltaics, for instance.[1-5] Nowadays, the organic/semiconductor interface is becoming more and more important for surface sciences and for potential technological applications.[6,7]

The formation of covalently attached organic monolayers on silicon surfaces is one of the many possibilities to obtain such heterostructures. Until now, a large variety of methods used to achieve such systems is well-documented including wet chemical processes, e.g., by alkyl-Grignard, alkyllithium reagents, and electrochemical grafting or reaction in ultrahigh vacuum to name a few.[8-11] Organic modification of Si surface is known to possess attractive and prospective properties like superior resistance such as electronic passivation (low concentration of electronic states in the band gap) and chemical stability towards oxidation.[12,13]

In this work, a particular interest has been focused to understand such hybrid Si/organic hetero-interface systems. Direct covalent grafting of various small organic molecules like methyl groups, ethynyl derivatives, and ultrathin polymers like polypyrrole and polythiophene on Si(111) surfaces has been attempted using a one-step Grignard electrochemical route.[14-18]

Recently, several studies have been performed on the methylated terminated Si(111) surfaces since a complete coverage of the Si(111) surface can be achieved. Lewis' group has intensively investigated such surfaces in the last few years. However, these modified Si surfaces have been entirely prepared using a two-step alkylation Grignard method,[19-22] which includes a first halogenation step by chlorination and a subsequent reaction with Li- or Mg-compounds. This procedure requires typically several hours. In the one-step Grignard method presented here no such first step is necessary. Therefore, the process to obtain organically modified Si surfaces is different (faster and more reliable). This electrochemical method has

the advantage to control the grafting process by means of current and potential applied to the Si electrode, and it takes typically only a few minutes.

Electrochemical methods are especially attractive and efficient because they provide a straightforward and very fast way to generate radicals near the surface. The process used here is a one-step reaction where radicals R• are created (arising from the Grignard compounds) when an anodic current is applied to the Si surface. The radicals R• formed react with the H-terminated Si surface to create a dangling bond and, subsequently, another R• can react with the dangling bond from H-passivated Si surface, which allows to obtain Si surfaces organically modified with strong covalent Si−C bondings. The processing in anhydrous solutions avoids oxygen presence or other contaminations from the Si surface.

The atomic distance between adjacent Si surface sites on an unreconstructed 1×1 H−Si(111) surface is 3.84 Å.[23] The van der Waals diameter of methyl groups is estimated to ~ 2 Å,[24] which indicates that methyl groups are small enough to fit on every atop Si(111) surface site. A complete coverage of the Si(111) surface can be thus achieved.[24] Due to steric constraints, other molecules like long alkyl chains or phenyl groups could not yield a complete coverage of the Si(111) surface but a partial coverage of ~ 50% has been reached.[25-27] Further potential candidates for the complete coverage of the Si(111) surface are unsaturated organic species such as ethynyl or propynyl moieties (−C≡C−R, where R = H, CH_3) because of the linearity of these molecules. The modification of Si surfaces by −C≡C− group opens new reaction pathways for further functionalizations of these surfaces, e.g., in biological applications.[28-30] Moreover, pyrrole and thiophene heterocyclic molecules well known to polymerize easily can both present conductivity properties and passivate Si surfaces as well. H-terminated Si(111) surfaces present a flat and well-ordered structure, which can be easily achieved using chemical methods. However, even if these H-passivated Si surfaces show low surface recombination velocity, they tend to degrade rapidly (e.g., oxidation) in ambient air.

One aspect in this thesis is to investigate if such organic monolayers are possible candidates to passivate silicon surfaces as well. Additionally, since the presence of surface contaminants can lead to a strong degradation in device performance and because device dimensions become smaller and smaller, the near surface region will become more and more important. That is the reason why atomically clean surfaces have to be prepared and have been investigated in this work.

In this thesis, the principal investigations were performed on p-type Si(111) surfaces because the orientation presented by this surface shows well-ordered flat structures with atomic steps and terraces. However, other orientations (like Si(100) or porous Si structures) have

been studied as well. Moreover, the deposition of organic molecules on Si surfaces induces the creation of dipoles on the surface. These surface dipoles play an important role in such heterostructures and change the electronic properties (work function, band bending, electronic affinity…). The electronic properties determined for such organically modified Si surfaces will be presented and discussed. Electrochemistry has been chosen since this method is an easy and quick way to prepare such organic hetero-systems. Principally, two routes are used, the reduction (like aryl groups for instance)[31-36] or the anodization of radicals (e.g., alkyl-Grignard).[14,16,17,24,37] For a complete overview of the Grignard compounds used in this thesis, see page 34 (Tab. 4.2).

The work presented here addresses several related issues concerning the covalent grafting of organic layers onto Si surfaces and more particularly in case of Si(111) surfaces through the one-step Grignard electrochemical route. This is summarized as followed:

Chapter 2 briefly introduces the basics of electronic and structure properties of the Si semiconductor. The change in electronic properties of Si surfaces by the organic molecules deposited on Si surfaces and the electrochemical grafting method used by the one-step Grignard electrochemical route to modify Si surfaces are presented.

Chapter 3 outlines the experimental methods performed for the investigations and characterizations of the modified Si surfaces.

Chapter 4 describes the different substrates used and the corresponding preparation methods to obtain H-terminated Si surfaces. IRSE characterizations of such H-terminated Si surfaces are presented. The experimental conditions for the Grignard grafting process are described and the Grignard solutions used are listed. The preparation conditions for both pyrrylmagnesium and thiophen-2-yl magnesium bromide are presented.

Chapter 5 summarizes the intensive characterization of the methylated Si surfaces and shows that a complete coverage of a monolayer has been achieved. The electronic properties induced by the surface dipoles will be discussed. Both p- and n-type methylated Si(111) surfaces are compared. Moreover, passivation and stability properties of such methyl-terminated Si surfaces are investigated.

Chapter 6 concerns the deposition of ethynyl derivatives onto Si(111) surfaces. The formation of ultrathin polymeric layers via the variation of the charge flow applied during the electrochemical grafting is presented. The different molecules are compared and the Grignard mechanism which is different from the grafting of methyl groups is proposed. Moreover, the role of the halogen used in the Grignard solutions and the electronic properties ascertained from such modified Si surfaces are discussed.

Chapter 7 introduces one of the first attempt to anchor covalently bonded polypyrrole and polythiophene using the one-step Grignard electrochemical route. First results reveal the presence of ultrathin, homogeneous, adhesive and robust polymeric films of polypyrrole and polythiophene, respectively. The thickness of the polymeric layers can be influenced by the charge flow.

The last chapter is dedicated to give an overview and to summarize the results discovered during this thesis.

Chapter 2

Basics of organic/Si heterostructures

2.1 Silicon surfaces

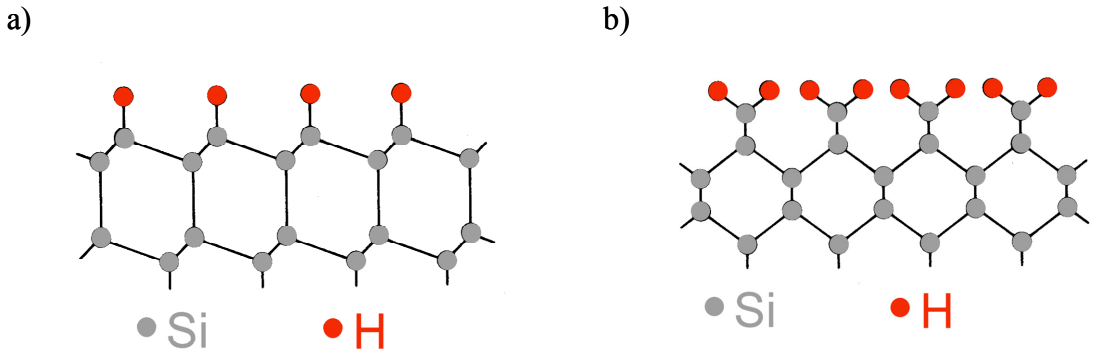

Fig. 2.1: *Schematic representation of (a) Si(111) and (b) Si(100) surfaces from side view.*

Fig. 2.1 shows a sketch of Si(111) and (100) surfaces side views in the ideal case, where Si(111) surface exhibits one dangling bond (i.e., one surface bond possibly bonded to organic molecules or hydrogen) and Si(100) surface reveals 2 dangling bonds. These surfaces have different signatures in IR spectroscopy and of course, different reaction possibilities and/or rates during grafting procedures. Additionally, they behave different with respect to surface passivation by hydrogen or oxide, and maybe also by organic molecules. The Si(100) orientation is widely used in technology due to a better passivation by SiO_2 than for Si(111) surfaces. However, H-terminated Si(111) surfaces are much better passivated than Si(100) surfaces due to the achievement of flat surfaces with less amount of defects.[38]

2.2 Semiconductor surface electronic properties induced by organic molecules

The basic concepts related to the surface electronic properties are of particular importance in the case of heterostructures like organic molecules or/and molecular polymeric layers deposited upon semiconductors or metals. In our case, the electron energetics of organic layers deposited onto Si surfaces was determined by XPS measurements under synchrotron radiation (SXPS). Surface and interface regions from modified semiconductors with organic molecules or layers are crucial for development of organic devices since their modifications lead to surface dipoles, which induces a change in the band bending and affect the work function. The energy band diagram of organically functionalized Si surface will be adopted in this study according to Hunger et al.[39]

The energy band diagram of a functionalized Si surface is shown in Fig. 2.2. The position of the Fermi level at the Si surface can be derived from the position of the binding energy from the bulk Si $2p_{3/2}$ emission, BE(Si $2p_{3/2}$), which is determined by a curve fitting procedure using Voigt line shape and spin-orbit doublet from the measured Si 2p spectra. The binding energy of Si 2p in the volume denoted as $BE^{v}(Si\ 2p_{3/2})$ is a constant ($BE^{v}(Si\ 2p_{3/2})$ = 98.74 eV)[40] and is independent of the surface band bending.

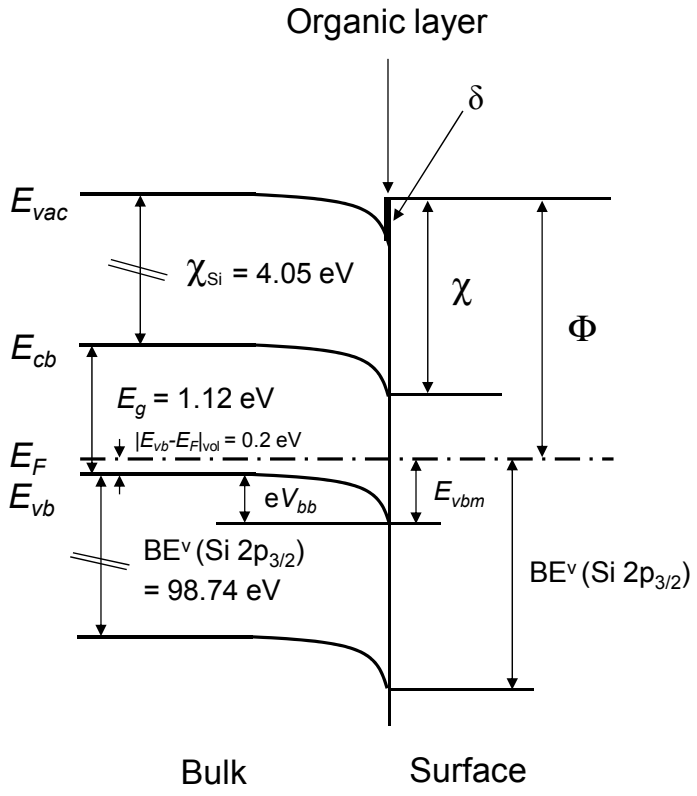

Fig. 2.2: *Energy band diagram of modified p-Si surface with an organic layer.*

The energy between the Fermi energy and the valence band maximum level denoted as E_{vbm} can be then determined from the relation:

$$E_{vbm} = \mathrm{BE}(\mathrm{Si}\ 2p_{3/2}) - \mathrm{BE}^{v}(\mathrm{Si}\ 2p_{3/2}) \tag{2.1}$$

The work function (Φ) is defined as the energy difference between the Fermi level (E_F) and the vacuum level of the semiconductor (E_{vac}), which is equivalent to the energy that needs an electron to get escape from the semiconductor bulk. Thus, the vacuum level of the organic/semiconductor interface could be established with the determination of Φ. Since the position of E_F is located above E_{vbm}, the work function is expressed as:

$$\Phi = E_g - E_{vbm} + \chi \tag{2.2}$$

where E_g is the band gap of Si (E_g = 1.12 eV),[38] and χ is the electron affinity of the surface. The work function (Φ) is a characteristic property of the surface and depends sensitively on the chemical and electronic structures of the organic layers deposited on the solid. For instance, some polar molecules (like halogen or oxygen atoms with a high electron negativity) could be adsorbed on the surface and induce a dipole (i.e., change in surface charge distribution), which opposes the escape of electrons by raising the work function of the sample. This change is detected as an increase in kinetic energy of the electrons at the photoemission secondary electrons cutoff. Experimentally, XPS measurements give a direct measure of the work function of a metal or semiconductor by extrapolation of the secondary electrons cutoff edge, which represents the local vacuum level E_{vac} of the sample. However, Φ can also contain a contribution due to the band bending, in addition to contributions of the chemical potential and surface dipoles. The surface dipole is associated with the dipole moment of the deposited organic molecules. Thus, a shift in work function is not only due to electron affinity, but also to the change in surface band bending.

The band bending is the result of an electrostatic field, which changes the potential of the surface with respect to the bulk and shifts the Fermi level at the semiconductor interface. This induces a change in the work function even without any change of the surface dipole (i.e., electron affinity). All surface electronic levels, from core levels to filled valence levels, empty conduction levels, and $E_{vac(s)}$ follow the band bending. The band bending (eV_{bb}) can be determined from the following expression:

$$eV_{bb} = E_{vbm} - \left| E_g - E_F \right|_{vol} \tag{2.3}$$

The electron affinity (χ) in Eq. (2.4) is defined as the energy required to excite an electron from the bottom of the conduction band minimum (E_{cb}) at the surface to the local vacuum level. The effect of the presence of a surface termination layer or by an adsorbate layer on the surface can be ascertained such that the "intrinsic electron affinity" of Si (χ_{Si}), which is a constant (χ_{Si} = 4.05 eV),[41] is modified by a contribution of a surface dipole (δ) that depends on the charge distribution at the interface and within the adsorbate layer:[5]

$$\chi = \chi_{Si} + \delta \tag{2.4}$$

Finally, the surface dipole (δ) which induces a potential step at the surface is positive ($\delta > 0$) when the electron affinity increases, and negative ($\delta < 0$) when the electron affinity decreases. The surface dipole can be determined from Eqs. (2.2) and (2.4) leading to:

$$\delta = E_{vbm} - E_g + \Phi - \chi_{Si} \tag{2.5}$$

2.3 Mechanism of the electrochemical Grignard grafting route

Presence of water in the electrolyte solution during anodization of silicon leads inevitably to formation of a layer of silicon oxide SiO_x. Therefore, it is crucial to perform anodic treatments of silicon under anhydrous conditions, if oxide formation on Si surface is not desired. Thus, it appears that anhydrous organic solvents are required. Using Grignard compounds (RMgX) for the electrochemical modification of Si surfaces has the advantage that the Grignard compounds (extremely reactive in contact with water) are always in water-free solution. Additionally, the electrochemical treatments have to be performed in an inert atmosphere. Grignard compounds are also especially attractive as precursors because of the availability from several varieties of aliphatic, aromatic and aryl groups.

Grignard solutions are electrolytes containing RMgX molecules, which can be possibly dissociated in the form $R^- MgX^+$, so that in a first step R^- can be oxidized to lead to the formation of radical R• when an anodic current is applied (see Eq. (2.6a)).

$$\begin{aligned} RMgX + h^+ \quad &\rightarrow \quad R\bullet + MgX^+ \\ \text{or } RMgX \quad &\rightarrow \quad R\bullet + MgX^+ + e^- \end{aligned} \tag{2.6a}$$

Then, the alkyl radical R• formed may react by following different pathways: by dimerization (2.6b), recombination by capture of a hydrogen atom from the solvent (2.6c), or even by abstraction of a hydrogen atom from the H-terminated Si surface (2.6d).

$$R\bullet + R\bullet \rightarrow RR \quad (2.6b)$$

$$R\bullet + SolvH \rightarrow RH + Solv\bullet \quad (2.6c)$$

$$\equiv SiH + R\bullet \rightarrow \equiv Si\bullet + RH \text{ (fast)} \quad (2.6d)$$

Moreover, the dangling bonds created at the silicon surface (≡Si•) are expected to be highly reactive and may then react electrochemically with the Grignard compound (2.6e) or with another radical to form a Si–C bond as illustrated in Eq. (2.6f):

$$\equiv Si\bullet + RMgX + h^+ \rightarrow \equiv SiR + MgX^+ \text{ (slow)} \quad (2.6e)$$

$$\equiv Si\bullet + R\bullet \rightarrow \equiv SiR \text{ (slow)} \quad (2.6f)$$

In this grafting mechanism, other cases have been disregarded like the chemical reaction of the dangling bond at the silicon surface (≡Si•) with RMgX compound, which may lead to the formation of another radical, for instance. However, it has been already demonstrated that the scheme presenting here exhibits a better fit with kinetic models proposed.[17] According to the reaction step of the above scheme, the transfer of two elementary charges per attached alkyl group is required. The complete coverage of a Si(111) surface by alkyl groups has been reached if all hydrogen atoms from the H-terminated Si surface were replaced by alkyl groups, i.e., when a charge flow of ~ 240 μC/cm^2 has been applied. Furthermore, creation of halogen radicals (X•) was not taken into account, even if they are well known to be generated in the case of alkylmagnesium iodides.[42]

The chemical reaction route using Grignard electrolytes in the case of alkyl groups have been proposed by Chazaviel and co-workers.[17,18] This electrochemical mechanism has already proved to operate well in the case of alkyl layers.[15,24] However, in the case of alkyne or more complex groups, it seems that this "simple" grafting mechanism is no longer valid,[18] and should be amended by some additional reaction steps during the electrochemical grafting route as will be discussed in the chapter concerning the grafting of acetylene derivatives (see Chap. 6).

Chapter 3

Experimental methods

In this chapter, several experimental methods used for the preparation and the characterizations of the modified Si surfaces obtained are presented. First, infrared spectroscopic ellipsometry (IRSE) measurements have been performed to provide information about the composition and/or chemical structure of the grafted layers. Then, X-ray photoemission spectroscopy method (XPS) has been performed to characterize and determine the chemical composition of the organic/Si interface of the functionalized Si surfaces. Furthermore, photoluminescence (PL) and surface photovoltage (SPV) techniques have also been performed to obtain information about the change in non-radiative surface recombination velocity and the change in surface potential (band bending) created by the grafted organic layers. Finally, complementary information about the morphology and chemical structures of the modified Si surfaces have been obtained by additional surface techniques like scanning electron microscopy (SEM) and Raman spectroscopy, and will be shortly described as well.

3.1 Infrared spectroscopic ellipsometry (IRSE)

Infrared (IR) spectroscopy is one of the most widely used techniques for the determination of molecular structure and for the identification of compounds. IR spectroscopy is a non-destructive method used to examine the chemical species present on surfaces or interfaces, which can be easily performed under atmospheric or nitrogen-purged conditions. Moreover, no specific vacuum conditions are required for the measurements. For these reasons, experimental methods using IR spectroscopy are especially interesting for the characterization of organically modified surfaces. IR spectroscopy has the particularity to operate either in transmission or in reflection modes. Among the several methods using IR spectroscopy technique are e.g., Fourier-Transform Infrared spectroscopy in ATR-mode (FTIR-ATR), Transmission Infrared Spectroscopy (TIRS) or Infrared Spectroscopic Ellipsometry (IRSE) to name a few.[43,44] IRSE will be presented here because this sensitive technique has been mainly used

in this work to identify the presence of the chemical species grafted onto Si surfaces by the determination of the typical vibrational modes observed from the organic molecules. Furthermore, IRSE is an ideal tool for the investigation of organically modified semiconductor since the composition, the molecular orientation, the thicknesses, and the optical constants can be determined by the evaluation of IR ellipsometric spectra.[45,46] A large area for applications in nanotechnology for device bases on organic films is recovered from ferroelectric films of $SrTiO_3$, ZnO, organic silicon, to inorganic materials passing through functional hybrid material to biosensors, and microelectronic devices.[47-50] In-situ measurements have also recently been performed as described in ref. [51] The principal advantage of the IRSE technique is the analysis of thin organic films with thicknesses from a few micrometers down to single molecular monolayer due to its high sensitivity.[47]

3.1.1 Theorie

The principle of the IR spectroscopy is to absorb light radiation and observe vibrational bands from the change in the dipole moment. Ellipsometric spectroscopy measures the change in the polarization state of radiation after reflection (or transmission) from the sample surface. In general, upon reflection from the sample surface, linearly polarized radiation becomes elliptically polarized. The polarization state of the radiation is analyzed with the analyzer. Since the optical properties of the sample are considered isotropic for an organically modified Si substrate within the surface plane of the sample, the polarization state of the reflected radiation can be characterized by the experimental quantities $\tan \Psi$ and Δ. These two independent experimental parameters can permit to assign vibrational bands by the identification of the Kramers-Kronig relations from the determination of specific pair of shapes, i.e., a relation between an IR-absorption band shape observed in $\tan \Psi$ with the related band shape in the corresponding Δ spectrum, which is another advantage of this technique because of the possibility to determine consistent pairs of the absorption and the refractive index (real and imaginary part of the dielectric function, respectively).[52] The measured ellipsometric parameters $\tan \Psi$ and Δ represent the amplitude ratio and the relative phase shift difference between p- and s-polarized components of the reflected waves, respectively. These ellipsometric parameters contain information on those material properties that contribute to the optical response of the sample and have been defined by the quantity ρ, which is the ratio of the complex reflection coefficients r_p and r_s, through the following relation:

$$\rho = \tan\Psi \; e^{i\Delta} = \frac{r_p}{r_s} \tag{3.1}$$

where r_p and r_s are the reflection coefficients of the two orthogonally polarized components from the reflected waves, and tan Ψ the absolute amplitude ratio.

$$\tan\Psi = \frac{|r_p|}{|r_s|} \tag{3.2}$$

The polarized reflectances R_p and R_s oriented perpendicular and parallel with respect to the plane of incidence are given by:

$$R_p = |r_p^2| \quad \text{and} \quad R_s = |r_s^2| \tag{3.3}$$

In the measurements performed in our studies,[46,53] the ellipsometric parameters are determined from the intensity measurements at four azimuthal angles of the polarizer (0°, 90°, 45°, and 135°) at a fixed analyzer position (45°):

$$\cos 2\Psi = \frac{I(90^0) - I(0^0)}{I(90^0) + I(0^0)} \tag{3.4}$$

$$\sin 2\Psi \cos\Delta = \frac{I(90^0) + I(0^0)}{I(90^0) - I(0^0)} \tag{3.5}$$

From these formulae, it is evident that p- and s-polarized reflectance spectra can be included in our measurement scheme when cos 2Ψ is determined. The band shapes observed in IRSE spectra of organic thin films are characteristic for the molecular orientations.

3.1.2 Instrumentation

Infrared ellipsometry measurements were performed with a photometric ellipsometer attached to a Bruker IFS 55 Fourier Transform Interferometer[46,53] using a Mercury-Cadmium-Telluride (MCT) detector with a spectral resolution of 4 cm^{-1} (model KV104-1, Kolmar Technologies, USA). The IRSE measurements were performed at 65° angle of incidence, and the polarization state of the reflected radiation was analyzed using the experimental setup as described in Fig. 3.2 (see ref. [46]).

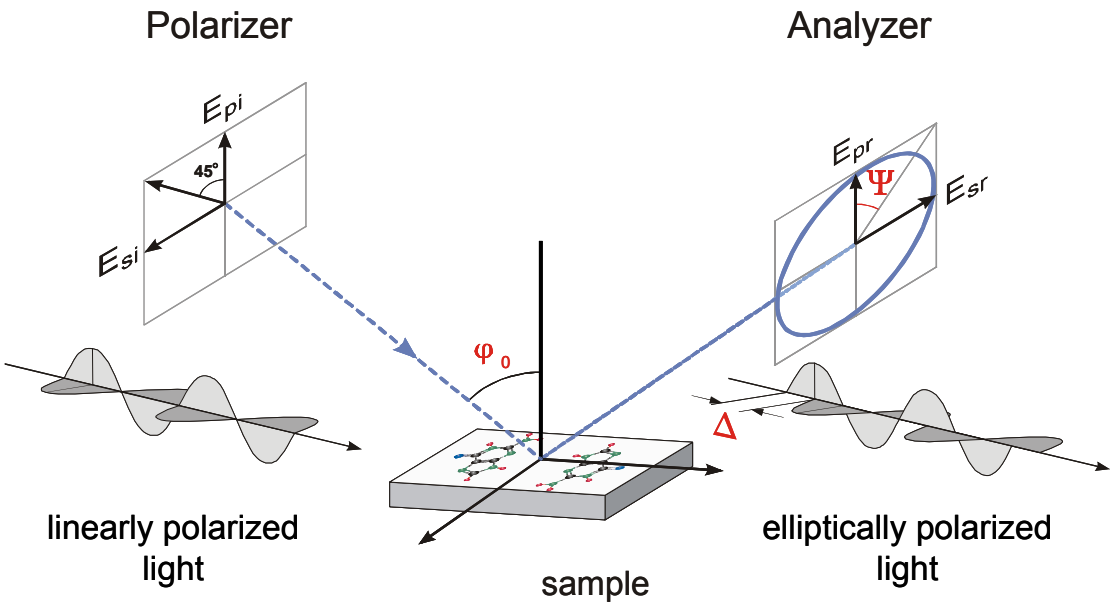

Fig. 3.1: *Principle of the IRSE measurement.*

The setup was purged with dry air. These specific parameters were used for most of the IRSE measurements presented herein. Otherwise, it was specifically noticed in the corresponding text or figure. All IRSE spectra were recorded at the ISAS institute in Berlin. The schematic setup illustrated in Fig. 3.2 shows the path taken by the radiation light. The IR radiation from the Bruker IFS 55 FTIR spectrometer after passing a series of mirrors was linearly polarized after passing through the polarizer. After reflection from the surface sample, the linearly polarized radiation light became generally elliptically polarized. The polarization state of the reflected light was passing through the analyzer and was then focused onto a MCT detector through another series of mirror. The two ellipsometric parameters (tan Ψ and Δ) obtained from the analyzer can be thus determined.

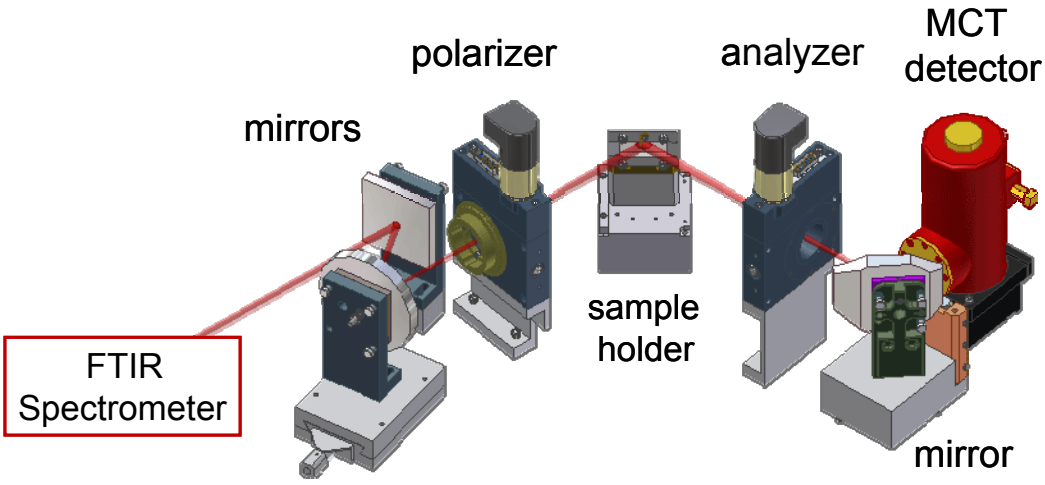

Fig. 3.2: *Ellipsometry setup used in this study.*

3.2 X-ray photoemission spectroscopy (XPS)

Complementary to the IRSE analysis, X-ray photoemission spectroscopy (XPS) measurements were performed to determine the electronic states and chemical analysis of the organic molecules grafted onto Si surfaces. The chemical state of oxidation, the composition and the thickness of the surface layers (organic or Si oxide) have been investigated. Moreover, band diagrams of organically modified Si surfaces have been obtained for different types of molecules by measuring the work function, the position of the bulk Si $2p_{3/2}$ emission, and the assumptions of typical values (e.g., the electron affinity or the position of the bulk Si 2p emission). Most of the XPS measurements presented here were performed with synchrotron radiation in BESSY II synchrotron facility under ultrahigh vacuum (UHV) with a pressure of ~ 5.8 10^{-10} mbar.

3.2.1 Theorie

X-ray photoemission spectroscopy technique is based on the photoelectric effect. For XPS measurements, photons from a monochromatic source radiation could arise from a classical X-ray source like MgKα (hν = 1253.6 eV) or AlKα (hν = 1486.6 eV) anodes or even from a higher energy source like a synchrotron radiation. The synchrotron radiation compared to laboratory sources presents the main advantage that the photon energy can be selected from a continuous energy spectrum over a wide energy range. Moreover, variable polarization, high intensity and brightness, and a narrow photon spot are also accessible with a synchrotron radiation source. The principle of photoemission process consists of the ejection of a photoelectron from inner shell (ionization of atom) under excitation by a monochromatic radiation as depicted in Fig. 3.3. The kinetic energy (E_{kin}) of the ejected inner shell photoelectrons is collected by an electron analyzer and is expressed as:

$$E_{kin} = h\nu - E_{BE} - \phi_s \tag{3.6}$$

where $h\nu$ is the photon energy, E_{BE} represents the binding energy (energy relative to the Fermi level), and ϕ_s is the work function of the spectrometer.

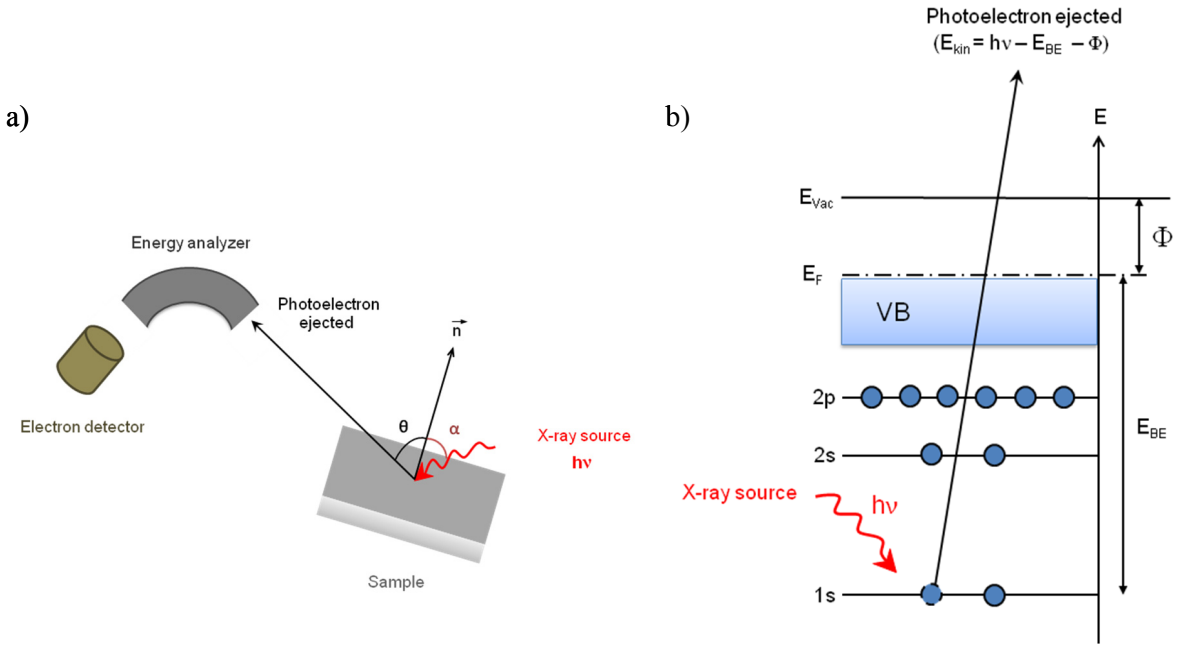

Fig. 3.3: *Schematic representation of (a) an XPS experiment and (b) the corresponding photoemission process. The angle of incidence (emission of the photons) (α) and the takeoff angle (or polar angle) of the photoelectron ejected (θ) are defined with respect to the surface normal. Φ is the work function of the sample and, E_{vac} and E_F are the vacuum energy level and Fermi energy, respectively.*

Fig. 3.4 shows an XP survey spectrum where additional features than the main photo-electron peaks appeared such as X-ray sources satellites (for non-monochromatic X-rays), shake-up and shake-off peaks, and Auger peaks.[54]

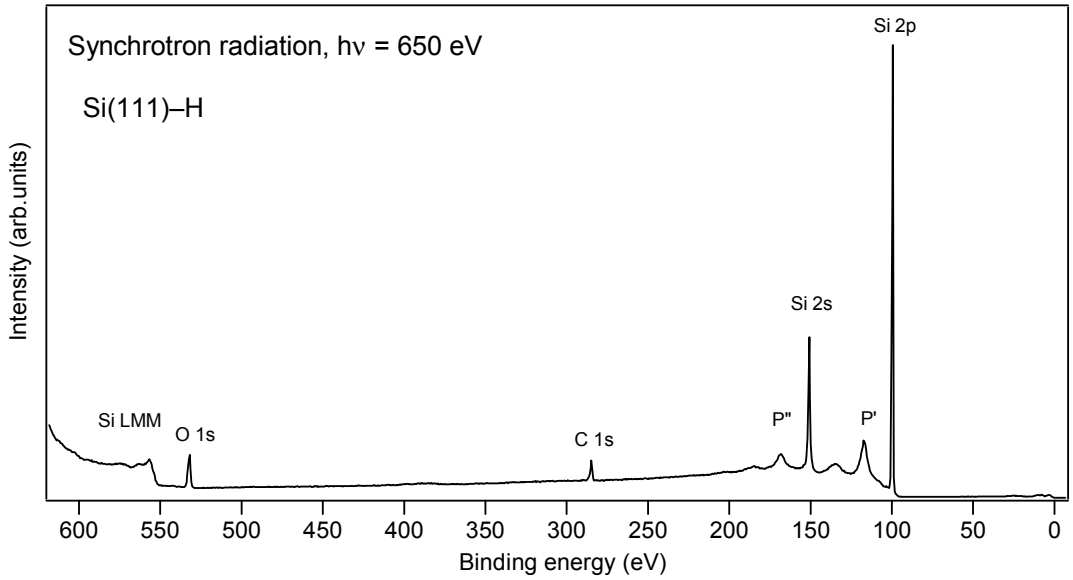

Fig. 3.4: *Survey XP spectrum of a hydrogenated Si(111) surface recorded under synchrotron radiation. Si 2p, Si 2s emissions and respective plasmons noticed P', and P" are observed in the low binding energy region, and C 1s, O 1s and Auger peak Si LMM emissions are distinguished in the higher binding energy range.*

Moreover, in a core level spectrum, usually not only a single emission occurs from the ejection of an electron from the inner shell of a given element because of chemical shift, or orbit-spin coupling, for instance.[55] The molecular environment including oxidation states and bonding can be determined by the electronegativity of the elements present on the surface from the chemical shifts which occur in the core level emission spectra recorded. For instance, a carbon atom bounded to a more electronegative atom (N, O, F, Br, …) will have its valence electronic density rarefied and so, the repulsion field by its inner electrons will be lower. Thus, it will be more difficult to eject one of these electrons since the inner electron binding energy will increase. If this carbon atom is bonded to a less electronegative atom, then the inverse behavior will occur. One important parameter, which has to be taken into account in the XPS measurements, is the *inelastic mean free path* (IMFP), λ. The *inelastic mean free path* can be defined as the distance where an electron can escape from the surface without undergoing energy losses before being inelastically scattered. The "universal" *inelastic electron mean free path,* λ (in Å), is given as function of the electron energy as depicted in Fig. 3.5. In the energy range of ~ 10 to 1000 eV, the escape depth of electrons is in the order of a few Å only.[56] This spectrum shows that in this energy range, due to the short λ (~ 10 Å) only the outermost surface region was probed under surface-sensitive conditions. Furthermore, the photoionization cross section of a material has also to be known since this parameter varies from such factors depending of the elements, and the energy of the photon energy (ionizing radiation). The photoionization cross section, σ, is defined as the likelihood of ionization of an electron from a given orbital in an atom with a given photon energy.

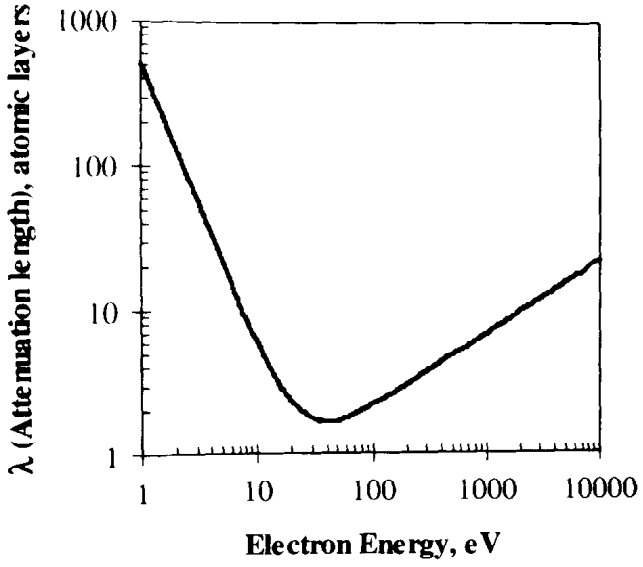

Fig. 3.5: *Universal schematic representation of inelastic mean free path of electron in solid as a function of the electron energy. (taken from ref. [56])*

Quantitative analysis

The energy resolved from the XP spectra of emitted core electrons exhibits peaks at binding energies corresponding to elastically scattered electrons, and an associated background due to inelastically scattered electrons. Thus, for quantitative compositional analysis, a subtraction of background is necessary to determine the elastic photopeaks area. A background subtraction accorded to Shirley[57] or Tougaard[58] has been used. The measured photoelectron intensities produced by the organic film depend on its composition. The intensity of electrons for a given energy observed in a homogeneous material is defined as:

$$dI = F\ \sigma\ n\ \lambda\ T(KE)\exp\left(\frac{-x}{\lambda}\right)dx \tag{3.7}$$

where F is the flux of X-ray photons, σ is the photoionization cross section for the particular transition (in a given shell of a given atom for a given X-ray energy), n is the atomic volume density (number of atoms in a given volume element), λ is the electron mean free path (depends on the kinetic energy of the electron and the nature of the material of which it must travel through), and $T(KE)$ is the transmission function of the analyzer (depending on the kinetic energy). Thus, for a bulk homogeneous material as a silicon material for instance, the intensity of the elastic peak is given by:

$$I^{\infty}_{Si2p} = F\ \sigma\ n\ \lambda_{Si2p}\ T(KE)\exp\left(\frac{-x}{\lambda_{Si2p}}\right)dx \tag{3.8}$$

The closed overlayer model has been chosen for a quantitative estimation of the thickness according to ref. [54] Here, the intensity of the photoemission signal of a substrate has been monitored as a function of the thickness of the overlayer. The thickness of the organic layers deposited (in our case, the emission from C–Si bonds will be used) can be estimated from the relative intensity ratio of C 1s (overlayer) and Si 2p (substrate) from the XP core level emission spectra, I_{C1s}/I_{Si2p}. The substrate and the overlayer photoelectron intensities depend on the overlayer thickness, d. The intensity of the overlayer signal (C 1s) is:

$$I_{C1s} = I^{\infty}_{C1s}\left[1-\exp\left(\frac{-d}{\lambda^{0}_{C1s}}\right)\right] \tag{3.9}$$

and the intensity for the substrate signal (Si 2p) is:

$$I_{Si2p} = I^{\infty}_{Si2p} \exp\left(\frac{-d}{\lambda^{0}_{Si2p}}\right) \tag{3.10}$$

where I^{∞}_{Si2p} is the photoelectron intensity from the substrate without the overlayer, I^{∞}_{C1s} is the photoelectron intensity from the thick overlayer. λ^{0}_{Si2p} and λ^{0}_{C1s} are the electron mean free path of the overlayer (C 1s) and the substrate (Si 2p) signal in the overlayer (o), respectively.

Data analysis

The detailed analysis of the SXP emission spectra acquired under normal emission angle was analyzed using Wavemetrics Igor Pro 4 (macros routine) software. The SXP core level emissions were deconvoluted with a Voigt line shape (combination of Gaussian and Lorentzian functions) using a least-squares fitting procedure after subtraction of a Shirley or Tougaard background.[57,58] For Si 2p and Br 3d core level emissions, the spectra were deconvoluted using spin-orbit doublets of Voigt line shapes with respective branching ratio of 0.5 and 0.67, and spin-orbit splitting of 0.605 and 1.05 eV, respectively.[59] The C 1s core level emission spectra were fitted with four or five peaks.

3.2.2 Instrumentation

SXPS (Synchrotron)

Synchrotron X-ray photoemission spectroscopy (SXPS) experiments were performed at the undulator beamline U49/2-PGM2 from the BESSY II synchrotron facility in Berlin. Photoemission spectra were recorded in normal emission with a Phoibos 150 electron analyzer (SPECS GmbH, Berlin, Germany) with a set of 9 channeltrons at the experimental SoLiAS station[60] using photon energies of 650 and 150 eV (for bulk and surface sensitive information). The SXPS measurements were performed with an overall energy resolution of about 80 meV from the total apparatus (monochromator and analyzer), an angular resolution of + 8°, and under takeoff angle of $\theta = 72°$ with a pass energy of 10 eV. The vacuum of the analysis chamber was in the range of 5.8 10^{-10} mbar. A clean gold foil or an evaporated gold film set at a binding energy of 84.0 eV for the Au $4f_{7/2}$ core level signal was used to calibrate the XPS energy scale using an excitation energy, $h\nu = 150$ eV. The photoemission energy

scale was then referenced to the Fermi energy of the gold sample. For the annealed measurements, the different Si substrates were laid down on a hot metal plate and were annealed at 390 or 430 °C for 30 min. The annealing temperatures performed were accurately determined by a pyrometer as a function of the heater current. The measurement of the work function was performed in normal emission ($\theta = 0°$) under an excitation energy of $h\nu = 150$ eV with a pass energy of 1 eV and with an applied bias voltage of – 6.0 V.

XPS Laboratory

XPS measurements were performed in an ultrahigh vacuum (UHV) chamber with a base pressure of $5\ 10^{-9}$ mbar. Photoemission spectra were excited by a non-monochromated X-ray source equipment with two anodes (AlKα = 1486.6 eV and MgKα = 1253.6 eV), operated at 300 W, and measured by means of a hemispherical electron-energy analyzer with a multi-channel detection system. Photoelectrons were collected at a take-off angle of ~ 75° with respect to the surface normal. However for some samples, a take-off angle of $\theta = 30°$ was also performed to enhance the sensitivity to the surface. The Au $4f_{7/2}$ and Cu $2p_{3/2}$ signals were used as reference to calibrate the XPS energy scale. The information depth reached by the two anodes AlKα and MgKα was ~ 30 and 33.3 Å, respectively.[61]

3.3 Pulsed photoluminescence (PL) and surface photovoltage (SPV) techniques

3.3.1 Theorie of PL

The pulsed photoluminescence (PL) spectroscopy is a method which permits to correlate the chemical and morphological structure of the surface with the surface recombination velocity, when combined to techniques like high-resolution energy electron loss spectroscopy (HREELS), or even, low electron energy diffraction (LEED), for instance.[62] The PL characterization gives a quantitative analysis of the surface defect densities with pulsed laser excitation. The presence of electronic surface states in the forbidden band gap causes the recombination of electron-hole pairs at surface and can act as traps or recombination active centers. The efficiency of interband photoluminescence of crystalline Si (c-Si) at room temperature is limited by non-radiation bulk and surface defects. The pulsed PL yields information about surface (interface) passivation by the changes in the band-to-band recombination related PL due to the PL quenching by the surface recombination active defects at the interface.[63]

Fig. 3.6 depicts the elementary processes at a semiconductor surface under strong illumination. Short light pulses are used to generate electron-hole pairs by absorption of the light by the semiconductor (1). The excess of charge carriers produced diffuse into the bulk. Non-radiative recombination in the bulk (2) or at the surface (3), and a radiative band-to-band recombination (4) also known as photoluminescence (PL) occur. Moreover, Auger recombination appears as well (5). Under high excitation intensity (~ 1 mJ/cm^2), the excess of electrons and holes generated are considered as equal ($\delta n = \delta p$) and reach a concentration value of ~ 10^{18} cm^{-3}. Since the concentration of excess charge carrier is much larger than the equilibrium carrier concentration, the band bending is neglected and the bands at the semiconductor surface are considered flat. For indirect semiconductors, the radiative band-to-band recombination efficiency at room temperature is very low because phonons are involved in the transition process. Thus, it is evident that the corresponding radiative recombination lifetime is very long (more than 10 ms). Moreover, in the case of non-radiative recombination processes, such as Shockley-Read-Hall (SRH) recombination, the recombination processes are usually much faster. Therefore, the recombination is dominated by non-radiative bulk and/or surface recombination processes.

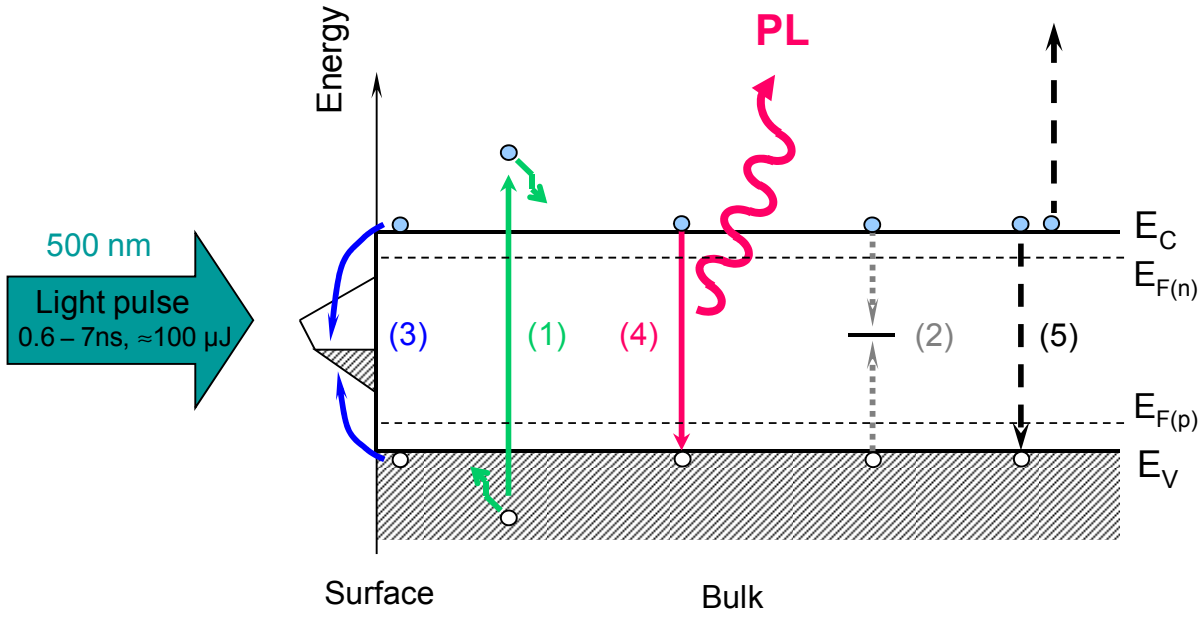

Fig. 3.6: *Elementary processes at a semiconductor surface under strong illumination: (1) light absorption, (2, 3) non-radiative bulk and surface recombination, (4) radiative band-to-band recombination (PL), and (5) Auger recombination.*

However, by considering no change in the bulk lifetime (the excess carriers recombine mainly in non-radiative processes, and thus limit the lifetime of the electron-hole pair to the range in ms), the changes of the non-radiative surface recombination indicate the PL intensity since the quenching of the PL signal contains information about non-radiative recombination. The PL transient and intensity at high excitation level are obtained from the one dimensional kinetic equation as calculated by Timoshenko et al.:[63]

$$\frac{dn}{dt} = D\frac{\partial^2 n}{\partial x^2} + G(x,t) - \frac{n}{\tau_0} - \beta n^2 - \gamma n^3, \tag{3.11}$$

where n is the non-equilibrium carrier density (light induced charge carriers), t is the time, D is the ambipolar diffusion coefficient (D = 15 cm^2/s for c-Si), $G(x,t)$ is the generation rate of non-equilibrium carriers, τ_0 is the carrier lifetime in the bulk, β is the coefficient of interband radiative recombination (3 10^{-15} cm^3/s), and γ is the Auger recombination coefficient (2 10^{-30} cm^6/s).[64]

The relation between the surface recombination velocity (S) and the concentration of non-radiative surface active defects (N_S) is defined by following relation:[63]

$$S = \sigma_s \, \nu_{th} \, N_S \tag{3.12}$$

with σ_s the surface recombination cross section (commonly taken as σ_s = 10^{-15} cm^{-2} for highly efficient recombination active centers, e.g., non-radiative recombination centers like silicon dangling bonds on Si surface),[65] and ν_{th} the thermal velocity of carriers (for a c-Si, ν_{th} = 10^7 cm/s at room temperature). Thus, S is on the order of 100 cm/s for Ns = 10^{10} cm^{-2}. The transient and the integrated PL intensities are respectively given by:

$$I_{PL}(t) = \beta \int_0^d \delta n^2(x,t)dx \tag{3.13}$$

$$I_{PL}^{\text{int}} = \int_0^{t_{eff}} I_{PL}(t)dt = \frac{\beta}{2} n_{eff}^2 \tau_{eff} \tag{3.14}$$

where d is the thickness of the sample, and τ_{eff} is the effective carrier lifetime with $\frac{1}{\tau_{eff}} = \frac{1}{\tau_{bulk}} + \frac{1}{\tau_{surface}}$ (3.15), and since $\tau_{bulk} >> \tau_{surface}$, the equation becomes $\tau_{eff} \approx \tau_{surface}$ and finally,

$$\tau_{surface}^{-1} = \frac{2S}{d} = \frac{2\,\sigma\,\nu\,N_S}{d} \approx I_{PL}^{-1} \tag{3.16}$$

Therefore, the change in the PL amplitude is proportional to the change of the inverse of the non-radiative surface recombination for a given experimental condition.

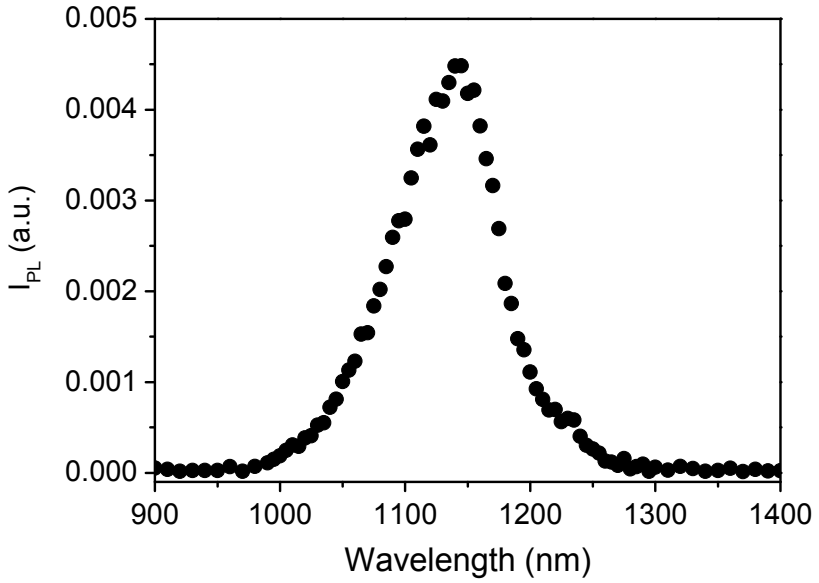

Fig. 3.7: *PL intensity (I_{PL}) spectrum of H-terminated Si(111) surface (laser excitation: 500 nm, 70 µJ per pulse, 0.6 ns pulse width).*

The measured PL transient allows then the experimental determination of the surface non-radiative recombination velocity, *S*. Then, pulsed PL is performed to inspect the surface passivation by the changes in the band-band recombination related PL of Si due to quenching of the PL by surface defects. For instance, a typical PL intensity spectrum response for H-terminated Si(111) surface is shown in Fig. 3.7.

3.3.2 PL experimental setup

The experimental setup used for the PL characterization is depicted in Fig. 3.8. A dye laser pumped by a nitrogen laser was used as excitation light source to emit single pulses at a wavelength of 500 nm (pulse width: 0.6 ns, pulse energy: about 300 µJ cm^{-2}). The PL intensity

from the Si substrate (band gap of c-Si, $E_g = 1.12$ eV, i.e., wavelength is ~ 1150 nm) was recorded by time integration using an InGaAs detector during about 400 µs. The PL signal was connected to a Lock-In amplifier. A computer (PC) controlled the dye laser through a trigger signal given by the lock-in amplifier. The laser beam was focused on the sample by a lens and mirror. The detection of the PL intensity has been performed by 2 possibilities: a) an interference filter was used to measure the PL intensity as a function of time at constant wavelength of 1150 nm (see Fig. 3.8) or b) a prism monochromator (Carl Zeiss Jena) was placed in front of the detector to measure the spectrum of the PL signal. Hereby, a lens was mounted in front of the monochromator to focus the PL signal to the entrance slit of the prism monochromator. Finally, the PL signal was recorded by a Lock-In which gave the signal to the PC.

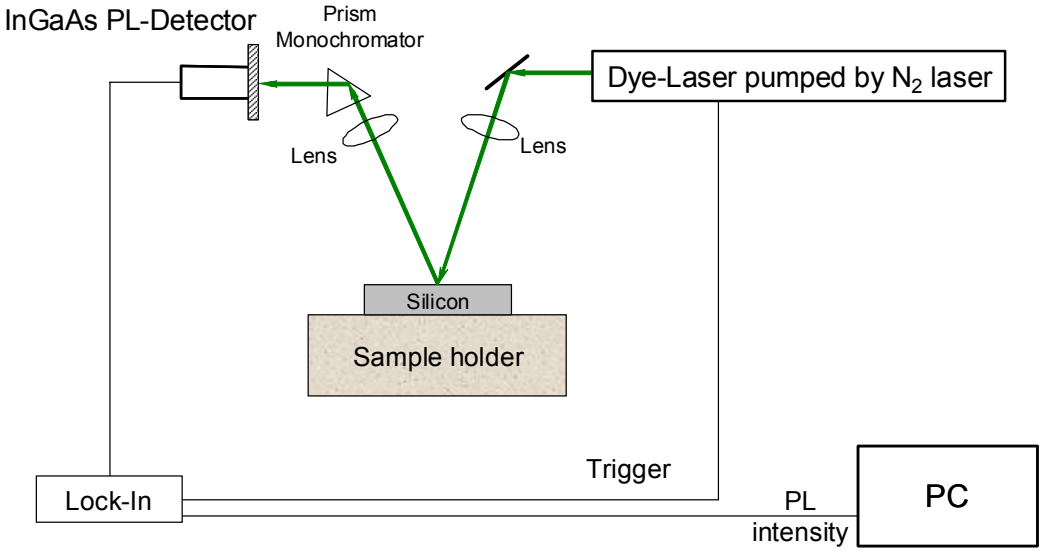

Fig. 3.8: *Experimental setup for PL measurements.*

3.3.3 Theorie of SPV

The pulsed surface photovoltage (SPV) is an attractive method because of its contactless and non-destructive characterization technique to measure the minority carrier lifetime/diffusion length. Thus, low defect densities can be determined as low as 10^9–10^{11} cm^{-3}. An overview of the SPV theory and applications has been published in the literature.[66] The determination of surface band bending can be obtained under in-situ and ex-situ conditions by SPV measurements.[67] In the case of ex-situ SPV technique, the energetic distribution of surface or interface state density $D_{it}(E)$ can be determined by measuring the surface photovoltage, U_{Ph}, as function of the external bias voltages, U_f, as described in ref. [68] Here, a brief summary of this publication. Under illumination at the semiconductor, electron-hole pairs are

generated in both the space charge region (SCR) and in the p-type semiconductor, respectively. The change in band bending is acquired by the spatial separation of excess charge carriers (electrons and holes) generated by a laser light pulse excitation. Three basic mechanisms of charge separation occur: a Dember voltage effect (due to different mobility of excess electrons and holes), a built-in electric field and a preferential trapping of either positive or negative charges. The electron-hole pairs in the SCR are quickly separated by the electric field, where for instance, in a p-type semiconductor electrons drift towards the surface and holes drift towards the bulk. The negative charges in the SCR are partially compensated by the excess positive charges resulting to a decrease in the band bending. The surface photovoltage (U_{Ph}) is defined as the maximum deviation of the band bending in the SCR region from the equilibrium value (initial band bending in the dark) after illumination, leading to the relation:

$$U_{Ph} = \Phi_s - \Phi_s^\circ \tag{3.17}$$

where Φ_s and Φ_s° represent the surface band bending under illumination and in the dark, respectively. The time decay (required to return to the equilibrium) of U_{Ph} provided information about interface recombination behavior (bulk lifetime).[69]

Fig. 3.9 shows the energy band diagram of a p-type semiconductor in the thermal equilibrium (in the dark) and directly after light excitation. The intrinsic Fermi level position is located in the midgap region due to surface states. For a p-type semiconductor, the Fermi level is close to the valence band edge.

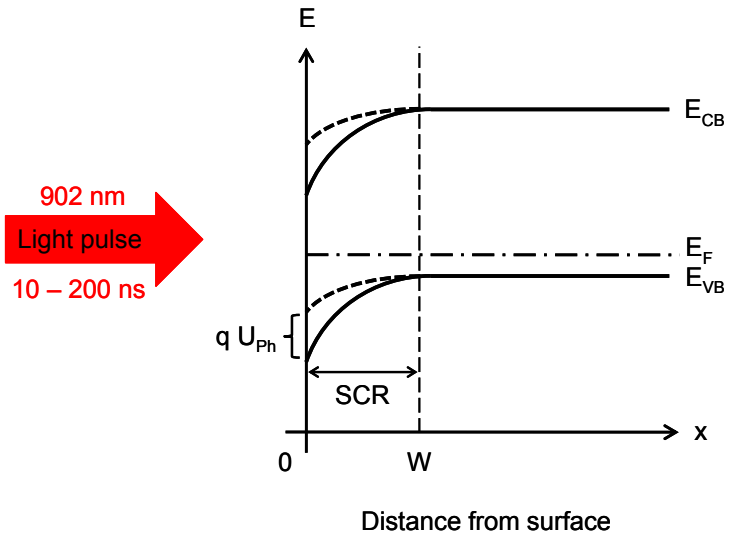

Fig. 3.9: *Principe of photovoltage measurements on a p-type semiconductor surface. Band diagram of a p-type semiconductor surface in the dark (solid curve) and under illumination (dashed curve).*

Under illumination, the Fermi level (in the non-equilibrium case) is splitting into two quasi-Fermi levels (for electrons $E_{F(n)}$ and holes $E_{F(p)}$, respectively) with U_{Ph} equal to the splitting potential. The surface photovoltage is obtained from the change in the band bending after illumination divided by the electron charge. The surface potential and consequently information on the band bending is obtained from the maximum value of the photovoltage pulse. For a p-type semiconductor the sign of U_{Ph} is negative while in the case of n-type semiconductor, a positive sign occurs.

3.3.4 Experimental setup for SPV measurements

The photovoltage transients were excited by single light pulses from a laser diode with a wavelength of 902 nm (pulse width: 100 ns, intensity: 150 µJ cm^{-2}). A parallel-plate capacitor used for the SPV measurements consisted of a semi-transparent conductive electrode (TCO) on top (see Fig. 3.10), a thin mica foil dielectric spacer, the sample and an ohmic electrode at the bottom (for light trapping).

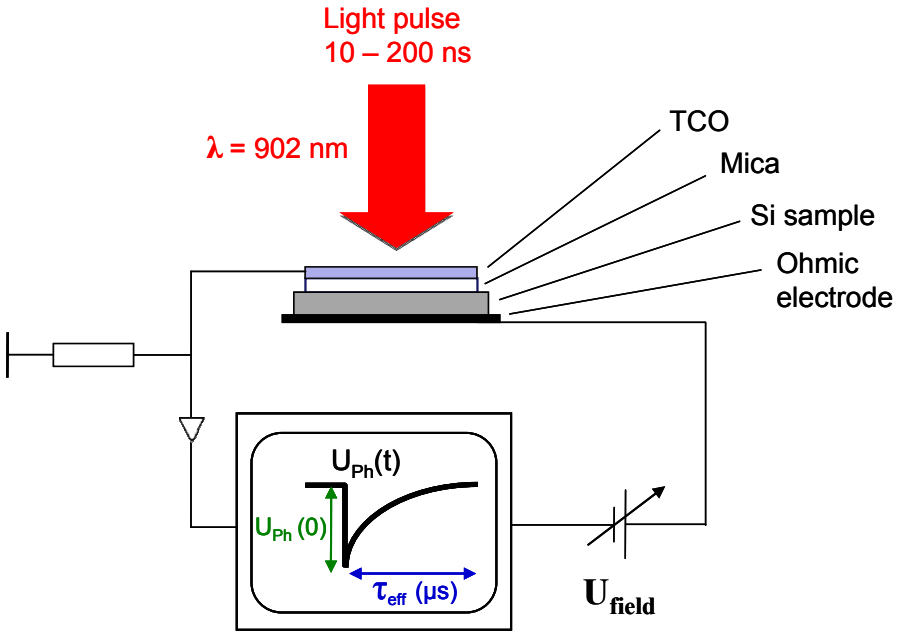

Fig. 3.10: *Schematic sketch of the experimental setup for transient PV measurements on a p-type semiconductor surface with c-Si sample, insulator (Mica spacer) and the conducting TCO electrode.*

U_{Ph} was measured between this parallel-plate capacitor under light illumination and as a function of time. An oscilloscope recorded U_{Ph} via a resistance in the GΩ range and a high impedance buffer with a time resolution of 5 ns. An external bias potential could be applied between the c-Si sample and the TCO electrode.

3.4 Additional techniques for the characterization of the modified surfaces

Additionally to the experimental techniques described above, the investigations about the structure and the morphology of the modified Si surfaces have been completed with different additional surface methods. In this subsection, these surface methods are only shortly described since this thesis is not focused on these experimental methods.

Scanning electron microscopy (SEM) has been performed to obtain complementary information about the morphology and to determine the thickness of some organically modified c-Si surfaces (ethynyl derivatives, polypyrrole, and polythiophene). SEM measurements have been carried out by use of a Hitachi S-4100 SEM microscope with a cold field-emission-cathode where an electron beam was scanned across the Si surfaces. The secondary electrons emitted from the Si substrates were collected by a detector, and the morphology of the surface has been obtained since these secondary electrons are sensitive (weak kinetic energy) to the surface morphology. The information depth of this experimental technique is in the nm range because of the re-absorption of the secondary electrons in the bulk material, and a resolution up to 1.5 nm can be reached. Moreover, energy of the primary electron beam can be continuously varied between 0 and 30 keV. Finally, SEM pictures were obtained with a tilt angle of 30° in relation to the surface to investigate the waste edges of the samples.

Moreover, Raman spectroscopy has been applied to inspect the vibrational modes of the polymeric layers (i.e., polypyrrole and polythiophene) grafted onto Si(111) surfaces. A Raman spectrometer (Dilor, Labram) with He-Ne laser excitation (632.8 nm, about 200 μW on sample surface) was used for the measurements. Raman spectroscopy is based on the change in the molecules polarisability. After excitation with the laser light, the elastically scattered light (Rayleigh scattering) was separated from the excitation beam by a notch-filter and the scattered light (Stokes and anti-Stokes lines) has been collected by a Si-charge coupled device (CCD) after passing a holographic monochromator. Finally, Raman spectra were obtained in the spectral range from 25-4000 cm^{-1} with a resolution of 1 cm^{-1}.

Additional information about the detailed description and theory of these experimental techniques can be found in refs. [70,71]

Chapter 4

Preparation of Si samples

Since the electronic properties of the organic modified Si samples can be drastically influenced by the preparation of the H-terminated Si surfaces (starting substrate), a special attention has been focused on the first step of preparation of the hydrogenated Si samples. Moreover, the grafting of organic molecules onto Si surfaces requires similarly precautions during the electrochemical deposition process or even the rinse procedure. In this chapter, first, the different types and orientations of Si wafer used in this work are presented. Then, the experimental procedures to obtain H-terminated Si surfaces from Si(111), Si(100) and porous Si (PSi) surfaces are described and IRSE characterizations of these surfaces are shown. Furthermore, the electrochemical procedure for the deposition of organic layers onto Si surfaces by a one-step modification route using Grignard solutions is depicted. Finally, the current-potential behaviors of Grignard containing pyrrol and thiophene heterocycles are shown and discussed.

4.1 Preparation and characterization of H-terminated Si surfaces

The quality of H-terminated Si surfaces obtained depends on several parameters like the quality of the Si substrate, the quality of the chemicals used during the preparation process, but also on the careful handling by the experimenter. To work under the best experimental conditions, ultrapure water (Milli-Q) with a resistivity of 18 MΩcm was used for rinsing procedures. All chemicals used for the preparation of H-terminated Si surfaces were made from VLSI grade and were purchased from Aldrich Chemical Corp. Moreover, it is important to mention that all chemical materials (beakers and tongs) were cleaned in hot piranha solution (conc. H_2SO_4:H_2O_2 = 2:1) before starting every hydrogenation process in order to be sure that no contaminants were present on the surfaces. Thereafter, the Si samples were rinsed abundantly with ultrapure water before a further used. Furthermore, a special attention was taken to handle carefully the Si wafer by the extreme edge in order to avoid scratching of the

surface. These scratching could cause severe damage concerning the structural defects and might then influence the chemical and electronic properties. Each Si wafer was cut in small pieces with a diamond pen. As it can be noticed, H-terminated Si surfaces always show hydrophobic characteristic.

Silicon wafers

Four different types of Si wafer were used for the study of organically modified Si surfaces. Three Si wafers were doped with different concentrations of boron leading to p-type Si characteristics while the other one was doped with phosphor and exhibited n-type Si characteristics. Each Si wafer was cut from float zone (FZ) single crystal in order to avoid interstitial oxides and has small amount of defects in the bulk. The four doping concentrations and characteristics from these different Si wafers are summarized below in Tab. 4.1.

Tab. 4.1: *Characteristics of the different Si wafers used in this work.*

Si Wafer (doping)	Orientation	Preparation process	Side polished	Resistivity (Ωcm)
p-doped	<111>	FZ	One	0.5 – 2.63
p-doped	<100>	FZ	One	0.7 – 2
p-doped	<100>	FZ	Double	5 – 10
n-doped	<111>	FZ	One	0.7

4.1.1 H-terminated Si(111) and H-terminated Si(100) surfaces

Preparation

First, the Si samples were placed in a Teflon® beaker and cleaned in 2-isopropanol during 8 min in an ultrasonic bath to take off remnant contaminants (grease, dust particles, foreigner elements...). Afterward, the Si samples were rinsed with plenty of ultrapure water (18 MΩcm), and then immersed in another Teflon® beaker containing hot acid piranha solution (conc. H_2SO_4:H_2O_2 = 2:1) for 15 min at about 100 °C to remove organic residues and form a thin oxide layer. Then, the Si samples were rinsed again with ultrapure water during several minutes and finally, atomically flat and hydrogenated Si(111) surfaces were obtained by dissolving the chemical oxide in 40% NH_4F during 15 min.[72,73] H-terminated Si(111)

surfaces obtained were then rinsed again thoroughly with Milli-Q water and dried under a nitrogen stream, N_2(g). The samples were then immediately transferred into the experimental equipment and thus characterized by the several experimental methods used here (IRSE, XPS, PL and SPV) or into the glove box purged by N_2(g) for further chemical modification with Grignard reagents.

The H-terminated Si(100) surfaces were prepared by the same procedure than used for Si(111) surfaces, but etching by 40% NH_4F solution was replaced by etching in 5% HF solution for 5 min.[74] Afterward, the Si(100) samples were rinsed with copious amounts of Milli-Q H_2O and dried under a N_2(g) flow.

IRSE characterization

Fig. 4.1 shows tan Ψ spectra of fresh H-terminated Si(111) and H-terminated Si(100) surfaces in the Si–H stretching vibrational mode. Atomically flat H-terminated Si(111) surfaces obtained from dipping in 40% NH_4F solution show a strong and sharp peak at 2083 cm^{-1}, which is assigned to Si–H stretching vibrational mode, ν(Si–H).[75] According to previous studies, polarized IR radiation used for the determination of flat H-terminated Si(111) surfaces (obtained through etching in 40% NH_4F solution) has also revealed a sharp peak at 2083 cm^{-1} when the sample is illuminated with a p-polarization light, while in s-polarized light only a small ν(Si–H) signal is observed at 2083 cm^{-1}.[75] The sharp and strong peak observed in p-polarized light indicates that Si–H bonds are perpendicular to the surface, whereas the small peak observed in s-polarized light suggests the increase of small amounts of Si surface atoms, which are present along a terrace step or from defect site on the flat surface. Thus, the strong and sharp peak at 2083 cm^{-1} gives clearly evidence of the achievement of atomically flat H-terminated Si(111) surfaces, and that Si–H bonds are perpendicular to the surface. On the other hand, atomically rough H-terminated Si(100) surfaces obtained through etching in 5% HF solution show a small IR-absorption at 2110 cm^{-1} due to $Si–H_2$ stretching vibrational modes, which are shifted by ~ 27 cm^{-1} with respect to ν(Si–H) on Si(111) surfaces.[76,77]

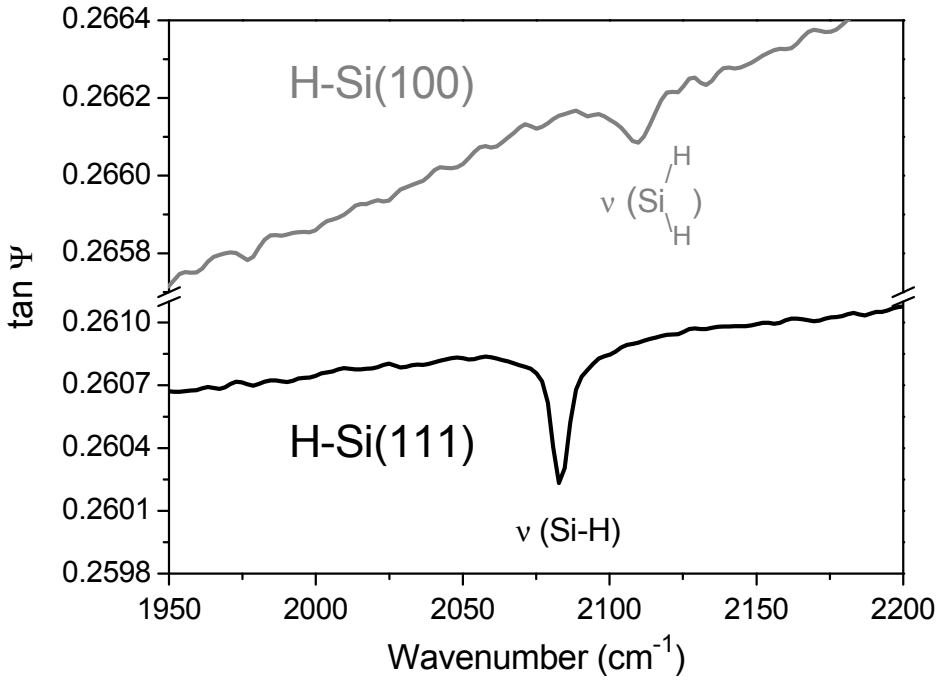

Fig. 4.1: *Tan Ψ of H-terminated Si(111) and H-terminated Si(100) surfaces measured by IRSE spectroscopy.*

4.1.2 H-terminated porous Si surfaces

Preparation

Since a wide range of possible applications concerning porous silicon (PSi) has already been exhibited,[78-80] a considerable effort has to be realized for the understanding and the control of the pores formation mechanism. For this reason, the preparation of H-terminated porous Si surfaces (H-PSi) has also been performed for some organic functionalization to increase the amount of surface species for IRSE measurements. Here, both side polished Si(100) samples were used for the preparation of H-PSi. H-terminated porous Si surfaces were prepared like H-terminated Si(100) surfaces. Afterward, the Si samples were transferred on a sample holder (metal plate), and an electrochemical Teflon® cell with a diameter aperture of about 2 cm^2 was mounted and sealed by a Viton® ring on top of the Si sample. The electrochemical Teflon® cell (opened on the top side) was pressed strongly to the Si sample (to avoid leakage) but carefully (for not breaking the sample up), and the solutions could be easily filled in and out. Indeed, the electrochemical cell was filled with a mixture of 48% HF and ethanol (ratio 1:1) to prepare H-PSi surfaces. An anodic current density of ~ 2 mA/cm^2 for 600 s was applied to the Si sample, and bubbles formed in the mixed solution during the electrochemical

process were blown away by a pipette. A three electrode configuration was used with Au as reference and as a counter electrode, respectively. Finally, after this electrochemical treatment H-PSi samples were obtained and were rinsed rigorously with Milli-Q water followed by drying under N_2(g) stream. The H-PSi samples were then immediately measured by IRSE spectroscopy or transferred into a glove box for further organic modification. The experimental setup for the preparation of H-terminated PSi is shown in Fig. 4.2.

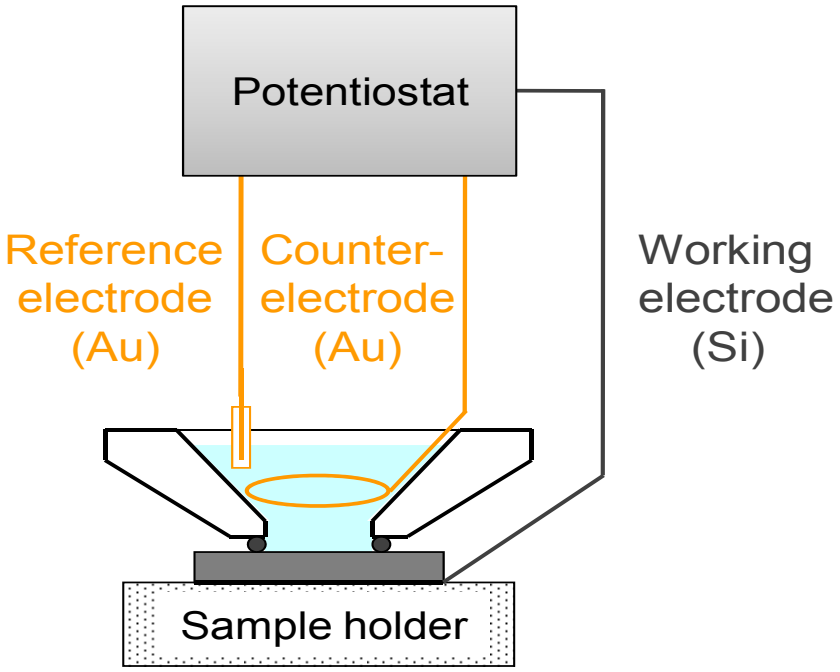

Fig. 4.2: *Experimental setup for the preparation of H-terminated porous Si surfaces.*

IRSE characterization of H-terminated porous Si surface

The tan Ψ spectrum of hydrogenated porous Si surface (H-PSi) is shown in Fig. 4.3. In addition to the MCT detector, a liquid He cooled bolometer has been used here to acquire a better resolution in the lower frequency region. However, the spectrum obtained from the bolometer reveals a peak down feature at ~ 600 cm^{-1} range (Fig. 4.3b), which is an artefact of the detector. In the lower frequency region, tan Ψ spectrum of H-PSi (Fig. 4.3a) shows three prominent absorption peaks due to bending vibrational modes at 636, 669, and 906 cm^{-1}, respectively.

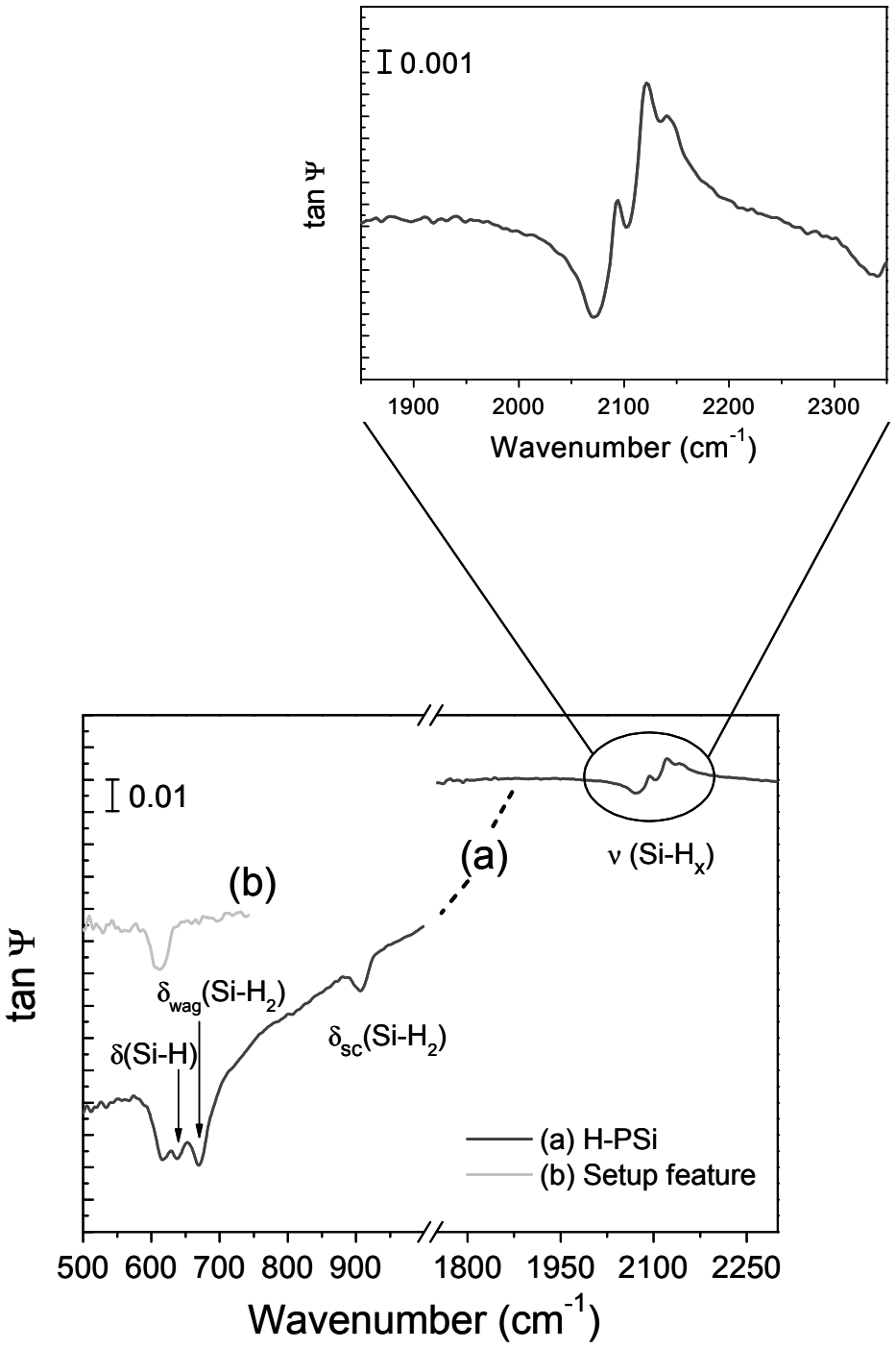

Fig. 4.3: *Tan Ψ spectra of (a) hydrogenated porous Si surface (H-PSi) prepared by an anodic current density of 2 mA/cm^2 for 600 s. The setup feature (b) coming from the bolometer is displayed with the light gray curve.*

The absorption band at 636 cm^{-1} is attributed to Si–H bending mode, δ(Si–H),[81-83] while the other absorption band at 669 cm^{-1} is assigned to the Si–H wagging vibrational mode, δ_{wag} (SiH_2).[82,83] Finally, the absorption band at 906 cm^{-1} is ascribed to the SiH_2 bending scissors vibrational mode, δ_{sc} (SiH_2).[81-83] In addition, another IR-absorption band more associated to the bolometer set-up than a contribution from the H-PSi also appears at 625 cm^{-1}. In

the higher frequencies region, tan Ψ spectrum exhibits three other distinctive absorption bands in the stretching vibrational modes region. These peaks located at 2094, 2121, and 2140 cm^{-1} are assigned to $\nu(Si–H_x)$ stretching vibrational modes with x = 1, 2 and 3, respectively.[81-83] However, neither absorption band at 2200 and 2250 cm^{-1} due to oxide in the Si–Si backbonds $O_y–Si–H_x$ molecular vibrational modes,[84] nor strong broad absorption band in the oxide region (1000-1250 cm^{-1}), which comes from SiO_2 stretching vibrational modes have been observed. The absence of these peaks is a good indication that no oxide species are formed during the preparation of H-PSi surface. Moreover, H-PSi surface obtained here reveals a certain structure of PSi which exhibits a certain anisotropy distribution from SiH_x bonds related to formation of pores.

The direction of the absorption bands in tan Ψ spectra gives information about the direction of the molecular vibrational transition dipole moments.[43] Peak-down features in the low frequencies region suggest that the absorption through the molecular vibrational transition dipole moment are oriented perpendicularly to the surface, while the peak-up features present in the high frequencies region are supposed to have transition dipole moment more tilted to the surface. These observations support the model of PSi, which presents formation of pores in the Si surface. In compliance with other works,[79,85-87] the presence of pores in the Si surface is formed as walls and is perpendicular to the Si surface plane. These perpendicular walls possess a high volume for hydrogen passivation, which is reflected by the presence of the band shapes characteristic from Si–H vibrational modes in the IRSE spectra of PSi.

4.2 Grignard reagents used for the electrochemical modification

All solvents and Grignard reagents used for the electrochemical modification of Si surfaces to obtain organically modified Si surfaces were anhydrous, and have been stored in a glove box under nitrogen atmosphere. All chemicals have been received from Sigma Aldrich and were used as supplied without any further purification. Except pyrrylmagnesium bromide solutions, which were prepared by the chemical group of Dr. Janietz from IAP Golm.

Several Grignard compounds were used for the electrochemical grafting of organic molecules on Si surfaces. To this, three different kinds of molecules containing Grignard reagents were attempted to be grafted onto Si surfaces using this specific electrochemical Grignard method. First, Si samples modified with Grignard containing alkyl (methyl) groups were performed followed by Grignard containing alkynyl (ethynyl) derivatives, and finally, Grignard containing heterocyclic rings like pyrrole and thiophene structures were investigated. A list of all Grignard compounds used in this work can be seen on Tab. 4.2.

Tab. 4.2: *List of all Grignard compounds used in this work (DEE = diethyl ether, THF = tetrahydrofuran).*

Grignard reagent	Name	Concentration (mol/L)	Solvent
CH_3MgBr	Methylmagnesium bromide	3.0	DEE
CH_3MgI	Methylmagnesium iodide	3.0	DEE
CD_3MgI	Methyl-d_3-magnesium iodide	1.0	DEE
$HC{\equiv}CMgBr$	Ethynylmagnesium bromide	0.5	THF
$HC{\equiv}CMgCl$	Ethynylmagnesium chloride	0.5	THF
$CH_3C{\equiv}CMgBr$	Propynylmagnesium bromide	0.5	THF
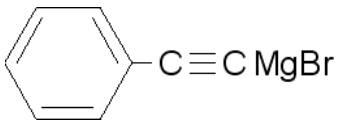	Phenylethynylmagnesium bromide	1.0	THF
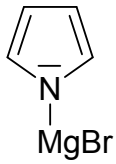	Pyrrylmagnesium bromide	0.1	THF
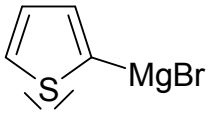	Thiophen-2-yl magnesium bromide	1.0	THF

4.3 Preparation of organically modified Si surfaces

H-terminated Si samples were freshly prepared as described previously in this chapter and were then transferred via an antechamber into a N_2(g)-purged glove box for further electrochemical treatments. However, Grignard reagents are extremely reactive and explosive in contact with oxygen and water; that is the reason why the modification of Si surfaces was performed in a glove box which was permanently purged under a stream of N_2(g), and where an inert controlled atmosphere was constantly present so that concentrations of O_2 and H_2O were below 0.1 ppm. Afterward, the H-terminated Si samples were hanged up with an alligator clip on top of an open parallelepipedic Teflon® cell and can be filled with ~ 5 ml of the Grignard solutions. The electrochemical Teflon® cell and the set-up of the electrochemical treatment are sketched on Fig. 4.4.

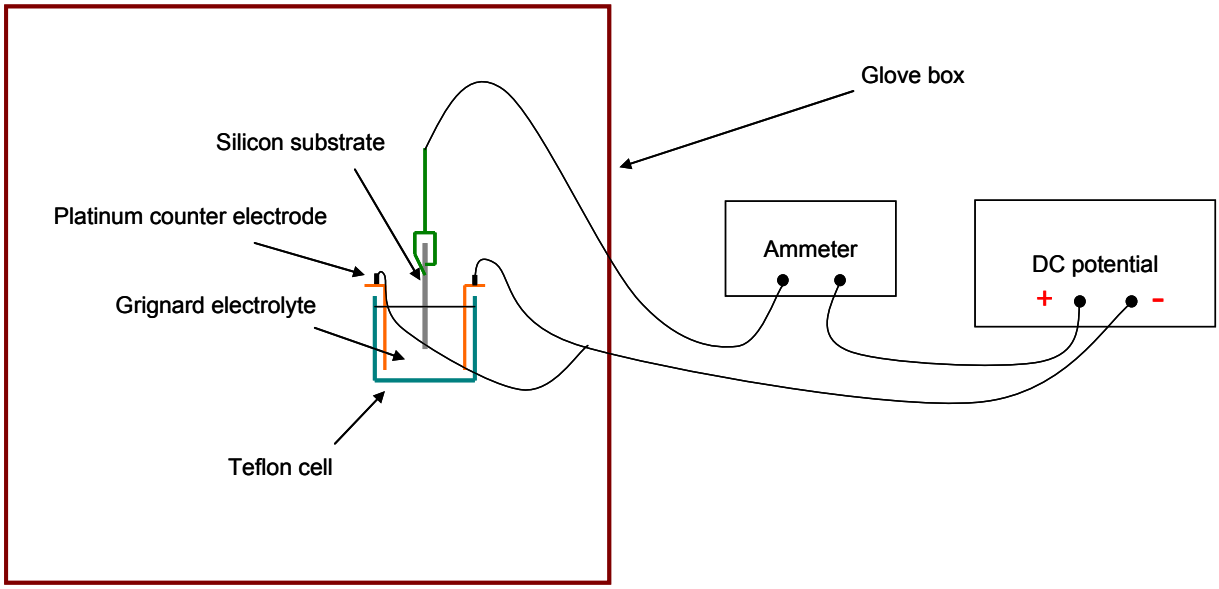

Fig. 4.4: *Setup of the electrochemical treatment for organic modification of silicon substrates.*

The electrochemical modification was performed under galvanostatic conditions in a two-electrode cell equipped with a "U"-shaped platinum (Pt) plate as counter electrode where different anodic treatments were applied to Si electrodes for several minutes depending on the Grignard solutions present in the electrochemical Teflon® cell. Here, the Si substrates served as the working electrode (anode). A current passed through the Si substrates into the Grignard electrolytes and the electrochemical reaction started. The accurate parameters used for the different organic modifications will be indicated timely together with the corresponding Grignard compounds. Modified Si substrates obtained were then removed from the solution and

rinsed successively in anhydrous tetrahydrofuran (THF) or diethyl ether (DEE) (depending on the solvent present in the corresponding Grignard solution), respectively. Finally, the samples were rinsed with bromobutane (BrBu) to eliminate all remnants from residual Grignard compounds. After this, the modified Si samples were taken out from the glove box and rinsed again with pure ethanol (VLSI grade) to remove possible magnesia compounds. In a final step, each modified Si substrate was rinsed with ultrapure water followed by drying under stream of N_2(g).

4.4 Current-potential behavior of Si(111) in pyrrylmagnesium bromide and thiophen-2-yl magnesium bromide solutions

Concerning the grafting from pyrrole and thiophene containing Grignard solutions, cyclovoltammetry (CV) measurements were performed to observe the current behavior on the applied potential for the Si electrode in contact with these electrolytes. Additionally, galvanostatic techniques were also studied. The charge flow could be determined from the following relation:

$$Q = I\ t \tag{4.1}$$

In the following section, current-voltage (Cv) and current-time (Ct) curves will be discussed for pyrrylmagnesium bromide (Pyl-MgBr) and thiophen-2-yl magnesium bromide (Tyl-MgBr), respectively. In these preliminary preparations for the grafting of polypyrroles (PPy) and polythiophenes (PT) onto Si(111) surfaces from Grignard compounds, the corresponding modified Si substrates have been then characterized by XPS measurements (see Chap. 7). Thus, the results obtained here for the H-passivated Si(111) surfaces modified by the different electrochemical treatments applying different charge flows have been called substrates A, B, C, D, and X, Y, Z, for Si substrates modified with Pyl-MgBr and Tyl-MgBr, respectively.

FZ-purified Si wafers (p-doped, (111)-oriented, single-side polished) with a resistivity of 0.5 – 2.63 Ωcm were used for the functionalization by Pyl-MgBr and Tyl-MgBr, respectively. The samples were cut in a manner that the dimension of the Si substrates immersed into the solution was ~ 1 cm^2; except for some samples which have been noticed in text. In case of CV measurements, electrochemical treatments were performed in a three electrode cell configuration with Au wire as reference electrode, Pt plate as counter electrode, and H-terminated Si substrate as working electrode. The setup and the Teflon® cell used have already been presented in Fig. 4.4.

First, electrochemical treatments of p-Si(111) surfaces in Pyl-MgBr solution were performed. Thereby, one cycle of a CV from 0 V to + 1.2 V was applied to H-terminated Si(111) substrate with a scan rate of 100 mV/s (see Fig. 4.5). At the beginning of the scan, the initial value of the current is very small, ~ 0.042 µA. The current starts to increase monotonously from ~ 0.2 V to + 1.2 V reaching a value of ~ 3.35 µA. The current decreases then constantly until ~ 0.4 V in the back scan. A charge flow of ~ 30 µC/cm^2 is calculated. This modified Si substrate is called "A" for the XPS measurements (see Chap. 7).

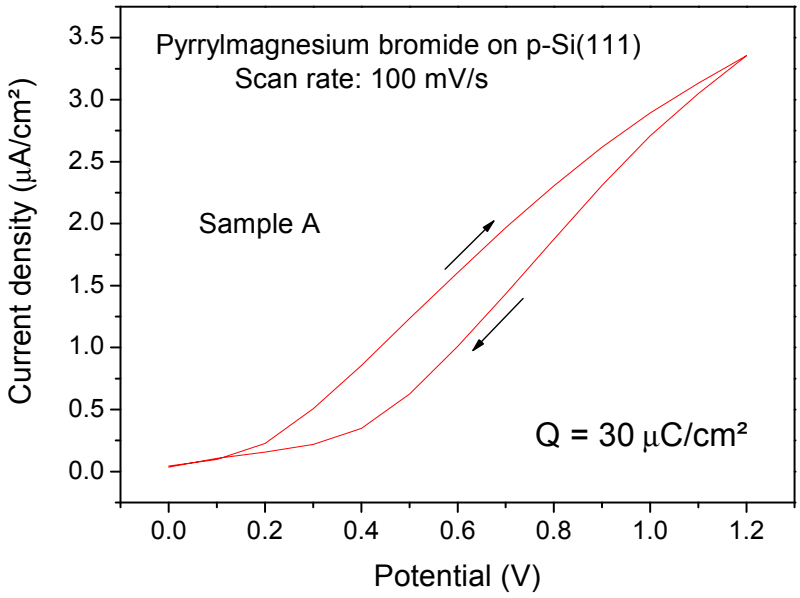

Fig. 4.5: *Cyclic voltammetry of pyrrylmagnesium bromide deposited on p-Si(111) surface. The scan direction is indicated by the arrows and starts from 0 V.*

Then, two different constant potentials in potentiostatic mode were applied to H-terminated Si(111) surfaces for different time of anodization. For one sample, a potential of 1.2 V was applied for 80 s (sample B), whereas a potential of 0.7 V for 300 s (sample C) was supplied to another Si substrate (see Fig. 4.6). Sample B (left panel) starts to decrease from a current density of ~ 1.57 µA/cm^2, while sample C (right panel) starts to decrease with a little bit higher current density of ~ 2.15 µA/cm^2. Fig. 4.6 shows that sample B reaches more rapidly a constant current than sample C, but the change in current density (Δi) is more pronounced for sample C. Thereby, application of potential in sample B was switched off after ~ 80 s, while in the case of sample C, the potential was switched off after ~ 300 s. The integration of the corresponding curves reveals a charge flow of ~ 110 and 230 µC/cm^2, for both modified Si surfaces, respectively.

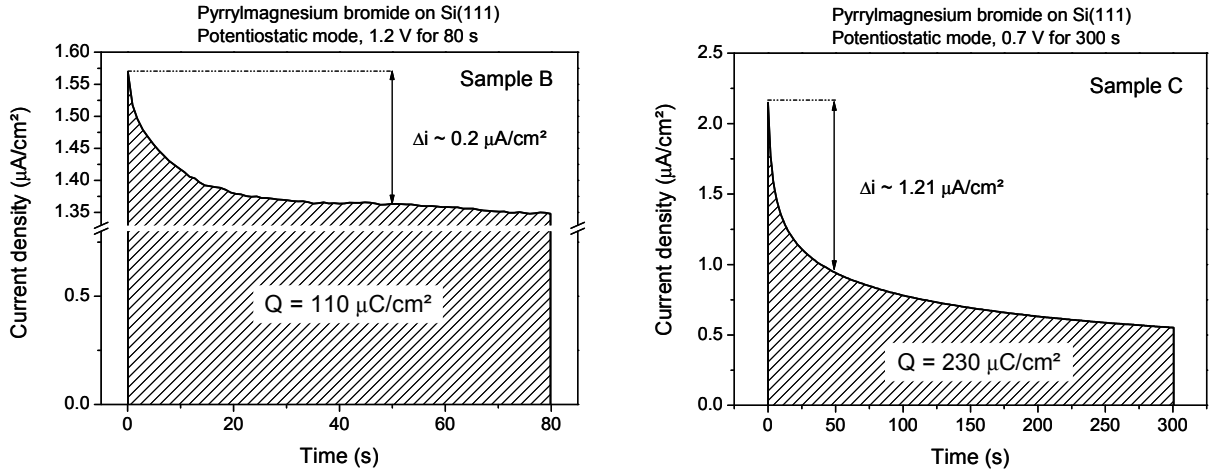

Fig. 4.6: *Potentiostatic mode applied to fresh H-terminated Si(111) surfaces in Pyl-MgBr solution. Dimension of Si substrate in the left panel was ~ 1 cm², while in the right panel it was ~ 2 cm².*

In order to deposit thicker films of polypyrrole using Pyl-MgBr solution, a high anodic current of 0.1 mA/cm² was applied for 20 min (in galvanostatic mode) to a fresh H-terminated Si(111) surface. Fig. 4.7 illustrates the demeanor of the corresponding potential of this anodic treatment. The graph gives evidence that a high potential was applied to the Si electrode to overcome the potential drop in the electrolyte. The increase in potential is quite linear from ~ 24.65 to 29.70 V and points to additional potential drop by the formation of a less conducting surface layer, which increases in thickness with time. Such high potential may also lead to the oxidation of solvent species.

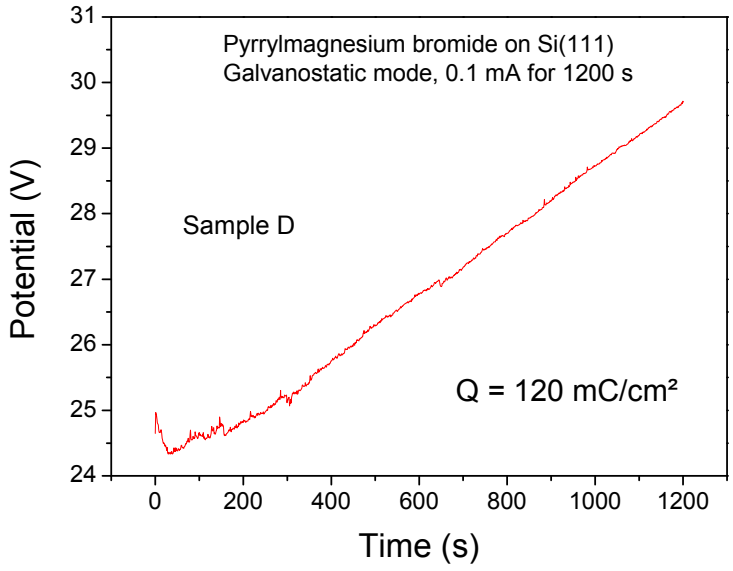

Fig. 4.7: *Potential as function of duration time when an anodic current density of 0.1 mA/cm² was applied to H-terminated Si surface for 1200 s in Pyl-MgBr solution.*

However, the charge flow is calculated to be ~ 120 mC/cm^2. A thick polymeric layer has been achieved after this electrochemical treatment because a brown film was visible with the naked eye. This thick modified Si surface obtained is called sample D. Afterward, the same electrochemical treatments were applied to Tyl-MgBr solution as well. As a consequence, Fig. 4.8 shows a CV from 0 V to + 2.0 V with a scan rate of 100 mV/s of a fresh H-terminated Si(111) surface immersed into Tyl-MgBr solution. The behavior observed for this CV curve is similar to the case of Pyl-MgBr solution. However, it seems that the slope of the curve at the beginning is less inclined than in the case of Pyl-MgBr solution. Moreover, the current density is much higher than for Pyl-MgBr solution at 1.2 V. The current drops faster in the back scan than in the case of sample A because the polymeric surface layer is thicker and blocks the e^- transfer. A charge flow of ~ 550 µC/cm^2 is calculated. The modified Si substrate with Tyl-MgBr solution in such condition is called sample X for the XPS measurements (see Chap. 7).

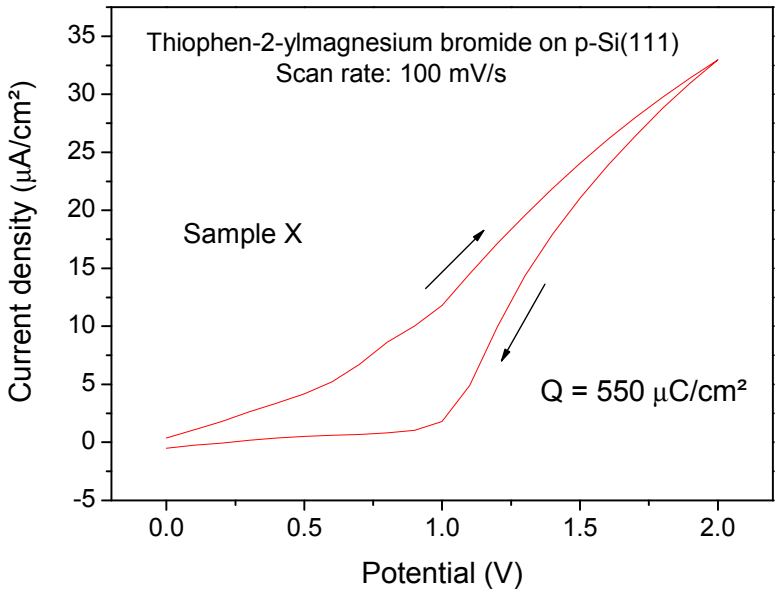

Fig. 4.8: *Cyclic voltammetry of p-Si(111) surface in thiophen-2-yl magnesium bromide solution. Arrows indicate the scan direction starting from 0 V.*

Fig. 4.9 shows the current density-time behavior of p-Si(111) during deposition of Tyl-MgBr solution by applying a potential of 1.0 V. The current decreases rapidly and levels out at ~ 300 s. The corresponding charge flow is calculated to be ~ 460 µC/cm^2 because the area immersed into the Grignard solution was about 2 cm^2. A thick polymeric film has been prepared similarly to the deposition from Pyr-MgBr solution.

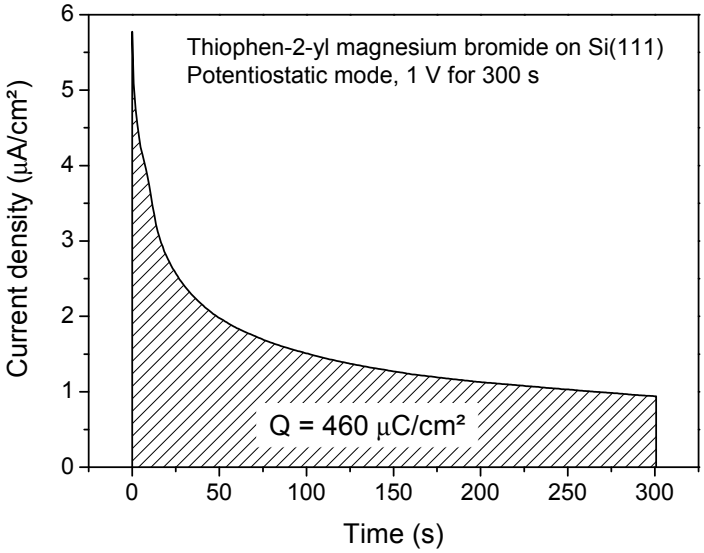

Fig. 4.9: *Deposition from Tyl-MgBr solution onto p-Si(111) surface by applying a constant potential of 1.0 V for 300 s. Dimension of Si electrode immersed in solution was 2 cm^2.*

In addition, an anodic current density of 0.5 mA/cm^2 has been applied in galvanostatic mode for 900 s as depicted in Fig. 4.10. The corresponding potential obtained starts from ~ 12.6 V and reaches a value of ~ 22 V after 900 s.

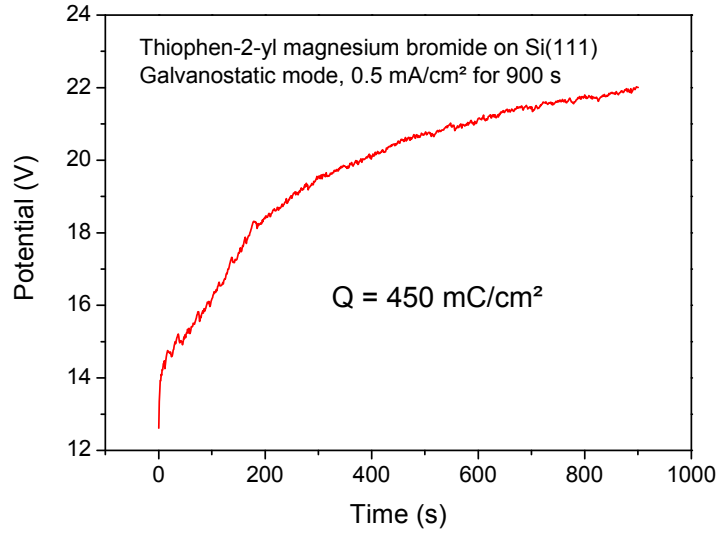

Fig. 4.10: *Potential-time behavior by applying an anodic current density of 0.5 mA/cm^2 to H-terminated Si surface for 900 s in Tyl-MgBr solution.*

In the beginning, the potential of this modified Si surface increases exponentially, whereas the one observed for Si surface treated in Pyl-MgBr solution shows a linear behavior. These trends may arise from the concentration of the solutions and indicate that in case of Si modified in Tyl-MgBr solution the formation of a thin surface layer is faster since the potential tends to reach a constant value after 900 s. Using Pyl-MgBr solution, it seems that even after the same time, the deposition process of the layer is still not finished and continues further.

Chapter 5

Modification by methyl groups: IRSE, SXPS, and PL

Methyl groups are very small molecules and are small enough to fit in each Si atop site from a Si(111) surface.[24] A complete coverage of the surface can be achieved, and can thus show interesting and attractive properties for this kind of surface orientation. For this reason, since the last few years, methylated Si(111) surfaces have been intensively investigated by Lewis' group using the two-step alkylation Grignard method.[19,20,22,88,89] Methylated Si(111) surfaces have already shown to have good passivation properties. However, the two-step alkylation method requires a first step of chlorination followed by a second step of heating or illumination with light in Grignard solutions for several hours.[20,88] Here, in order to avoid such constraints, another grafting method to obtain methylated Si surfaces has been used. The one-step electrochemical Grignard route method has been chosen here to achieve such modified Si surfaces.[17,18,24] This method is totally different from the two-step alkylation method because the radicals created for the grafting of the organic molecules on Si surfaces are generated electrochemically, whereas in the two-step alkylation method, a first step chlorination is necessary to generate the radicals for the grafting process. Moreover, only few minutes are needed to achieve a complete coverage of the Si surfaces with this electrochemical grafting method using Grignard solutions. In this chapter, the grafting of Si surfaces with methyl groups (CH_3 and CD_3) by the Grignard electrochemical route will be discussed. First, these methylated Si(111) surfaces have been investigated with IRSE measurements to check the presence of the methyl groups by typical vibrational modes signatures arisen from the methyl groups on the Si surface. Moreover, the grafting of CH_3 groups have also been performed on other orientations like Si(100) and porous Si surfaces. Then, SXPS measurements on the modified Si(111) surfaces have also been performed under synchrotron radiation in BESSY II to provide quantitative information about the methyl layer grafted onto Si(111) surfaces. In addition, the methylated Si(111) surfaces have been investigated using PL and SPV techniques to afford particularity information about the electronic properties at the organic/silicon interface

like non-radiative recombination active defects and band bending, respectively. Furthermore, the grafting on both p- and n-type Si wafers using these investigations methods has also been compared. Finally, the stability and the robustness of these methylated Si(111) surfaces in ambient atmosphere and under treatment with 5% HF solution have also been investigated with IRSE, SXPS and PL experimental techniques.

5.1 IRSE characterization

Verification of the Grignard process with CH_3 groups

The electrochemical grafting process proposed by Chazalviel and co-workers[17,18] using Grignard electrolytes for organic modification of Si surfaces has been verified by the use of CH_3 groups.

First of all, a hydrogenated Si(111) sample has been just dipped in CH_3MgBr electrolyte for 5 min without any application of current or potential. This experiment has been performed to check that no spontaneous grafting occurred. This Si sample has been compared to another one which has been handled in the same solution by applying an anodic current density of 1 mA/cm^2 for 5 min. The results can be observed in Fig. 5.1. On this figure, tan Ψ spectra of the modified Si(111) surfaces have been referred to a H-terminated Si(111) surface and were plotted in the 1100-1400 cm^{-1} region.

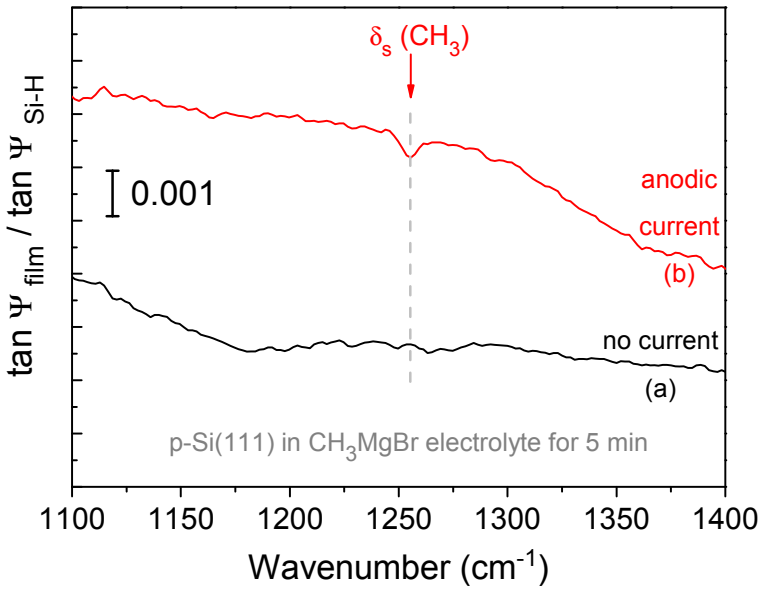

Fig. 5.1: *Tan Ψ spectra of Si(111) surfaces modified in CH_3MgBr electrolyte (a) without a current and (b) with application of an anodic current density of 1 mA/cm^2 for 5 min. The spectra have been shifted for visual convenience.*

It can be clearly seen that no relevant IR-absorption band due to the presence of CH_3 groups appears for the curve corresponding to the Si sample only dipped in the Grignard solution (Fig. 5.1a), while a weak band appears at ~ 1255 cm^{-1} for the Si surface of which an anodic current has been applied in the same solution (Fig. 5.1b). This band is assigned to the symmetric bending vibrational mode of CH_3 groups, δ_s (CH_3), which is also well known as the "umbrella" mode.[24,90,91] No peaks corresponding to the symmetric and asymmetric stretching vibrational modes of CH_2 or/and CH_3 groups at around 2800-3000 cm^{-1} have been observed (not shown here). Obviously, these vibrational modes are too weak to be conspicuous. However, the "umbrella" mode is a strong hint of the binding of methyl groups on the Si surface. Nevertheless, further studies by IRSE measurements have been performed to investigate whether the weak band attributed to δ_s (CH_3) "umbrella" bending vibrational mode was real or just an artefact. Therefore, Δ spectra have been recorded and the protons of the CH_3 groups have been replaced by deuterium atoms to form CD_3 groups. Exchanging H for D atoms is expected to shift the "umbrella" mode to the lower frequencies.[92,93] In the same manner, the Δ spectra should show a deviation like structure if the vibrational modes observed in tan Ψ spectra are real. However, Fig. 5.1 reveals that the application of an anodic current to the Si electrode is needed to initiate the electrochemical Grignard reaction route as mentioned in Chap. 2.

5.1.1 Grafting of CH_3 and CD_3 groups onto p-Si(111) surfaces

Since the grafting of CH_3 molecules has been well achieved using this electrochemical method, another attempt has been performed using a Grignard solution containing also methyl groups but with deuterium atoms instead of hydrogen atoms. Thereby, the "umbrella" bending vibrational mode for CD_3, δ_s (CD_3), is expected to be shifted to a lower energy because of the heavier mass of the deuterium atoms in comparison to hydrogen atoms.

Fig. 5.2 shows tan Ψ spectra of methyl-terminated Si(111) surfaces referenced to H-terminated Si(111) surface. Tan Ψ spectra for both methyl-terminated Si(111) surfaces point out intense upward pointing peaks at 2083 cm^{-1}. These peaks are assigned to the Si–H stretching vibrational mode and correspond to the complete loss of Si–H surface species by the grafting of organic molecules.[94] Simultaneously, weak downward pointing peaks appear at ~ 908 and 1253 cm^{-1}. These peaks are ascribed to the C–D and C–H symmetric bending vibrational modes (also called "umbrella" mode) of CD_3 and CH_3 groups, respectively.[92,93]

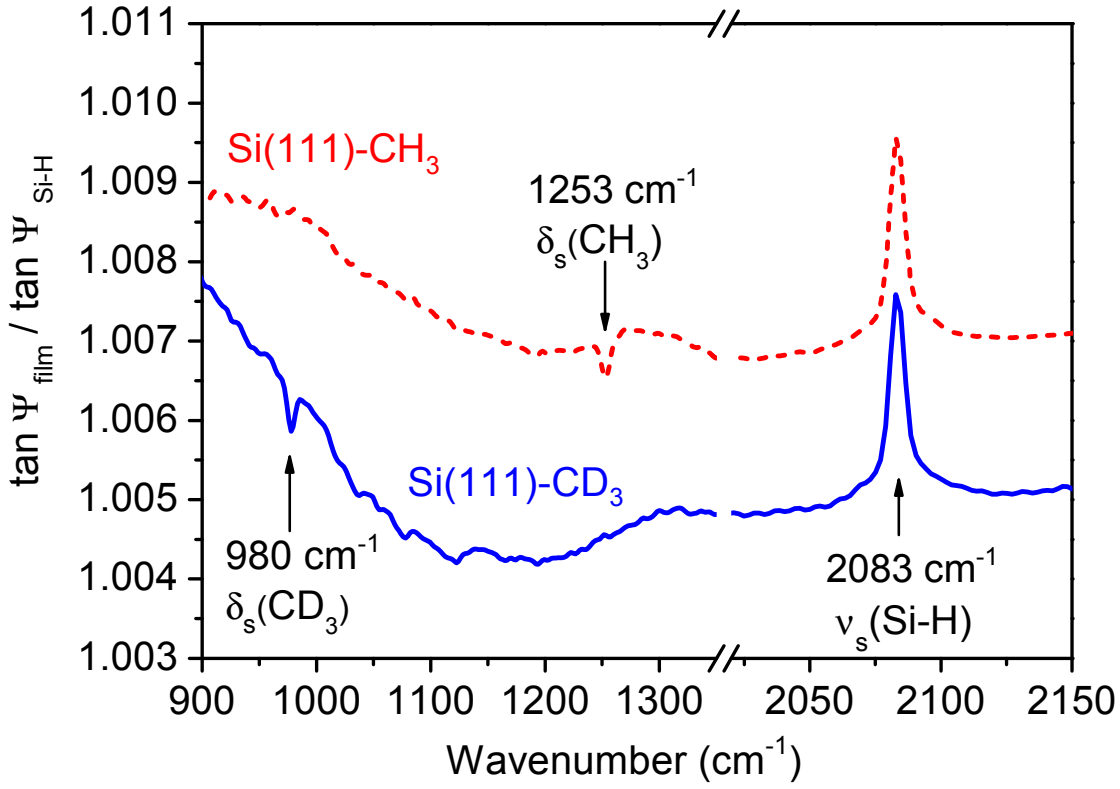

Fig. 5.2: *IRSE spectra of p-Si(111) surface modified by methyl groups, CH_3 (red dashed curve) and CD_3 (blue solid curve), respectively. Tan Ψ of CH_3- and CD_3-modified Si(111) surfaces are referenced to tan Ψ of H-terminated Si(111) surface. Both methyl-terminated Si(111) surfaces have been obtained by the application of 0.5 V for 5 min.*

The shift of the methyl (CH_3 and CD_3) groups on the corresponding spectra indicates the grafting of CH_3 and CD_3 groups onto p-Si(111) surfaces. Since these reliable contributions for the grafting of methyl groups are located near the silicon oxide region, an additional parameter from the IRSE measurements, Δ, has to be also performed in parallel to give evidence of the real presence of these bands.

Complementary parameter, Δ, performed to verify the signals observed by tan Ψ

Fig. 5.3 illustrates tan Ψ and Δ spectra of CH_3- and CD_3-terminated Si(111) surfaces referenced to H-terminated Si(111) surface. The figure is separated into two panels for a better distinction of the optical abrupt change of Δ parameter (bottom panel) in correlation with the appearance of a band feature in the tan Ψ spectra (top panel), respectively.

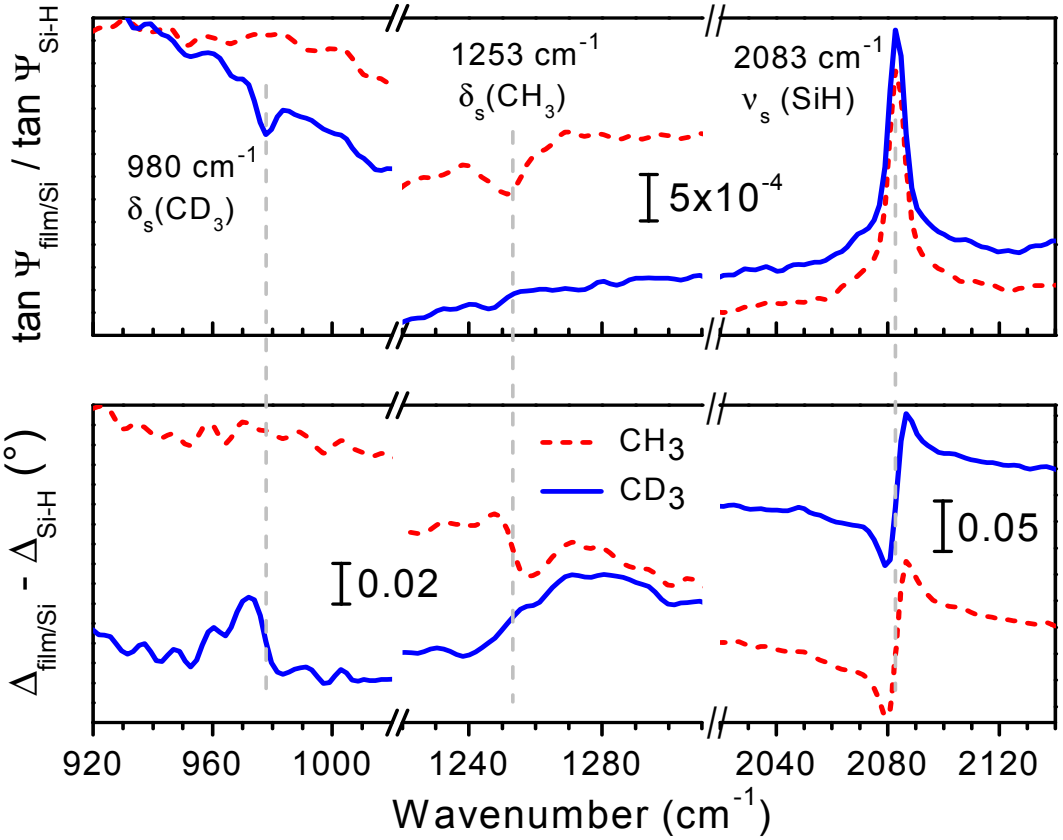

Fig. 5.3: *Correlation between the Kramers-Kronig parameters related tan Ψ and Δ spectra is obtained by IRSE measurements for CH_3- and CD_3-terminated Si(111) surfaces (red dashed and blue solid curves, respectively). The spectra have been referenced to H-terminated Si(111) surface, respectively.*

Methylated Si(111) surfaces obtained by electrochemical modification are depicted in red and blue curves for CH_3 and CD_3 groups, respectively. IRSE measurements clearly reveal a concordance between the typical bands of "umbrella" vibrational mode from methyl groups observed on tan Ψ spectra at 980 and 1253 cm^{-1} for δ_s (CD_3) and δ_s (CH_3), respectively, with an optical abrupt change on the Δ spectra in respect to these bands, respectively. Thus, the direct correlation of change in tan Ψ and Δ characteristic for the "umbrella" mode clearly indicates that these IR-absorption bands are not artefacts. However, since the "umbrella" mode is an obvious hint of the well achievement for the grafting of methyl groups onto Si(111) surfaces, these "umbrella" modes will be discussed and compared in the following subsections.

5.1.2 Influence of different parameters in the change of δ (CH_3)

Fig. 5.4 depicts three tan Ψ spectra of CH_3-terminated Si(111) surfaces of which different charge flows have been applied during the electrochemical grafting to investigate the influence on the grafting process. Thereby, the Si electrode modified by potentiostatic mode (0.5 V, ~ 215.2 mC/cm^2) is illustrated by a dot curve, while the ones modified by galvanostatic mode (0.5 and 1 mA/cm^2, ~ 150 and 300 mC/cm^2) are indicated with the dashed and solid curves, respectively. Each modified Si(111) surface has been obtained after treatment in CH_3MgBr electrolyte for 5 min. As observed on the figure, there is no tremendous difference of the "umbrella" vibrational mode at 1253 cm^{-1} between the different electrochemical treatments which have been modified either by galvanostatic or by potentiostatic mode. However, if an anodic current of 1 mA/cm^2 is applied (solid curve), the "umbrella" mode is slightly shifted to an higher energy at approximately 1255 cm^{-1}, which is the value also observed from other groups.[20,24] The insert in Fig. 5.4 depicts the integrated IR-absorption of the "umbrella" mode plotted as a function of the calculated flown charge (see Tab. 5.1). This investigation shows that the charge flow applied to the Si substrate does not influence the ratio of CH_3 groups grafted onto Si surfaces. These results are consistent with the fact that only ~ 240 μC/cm^2 are required to replace all hydrogen atoms present on H-terminated Si(111) surfaces by CH_3 groups. Moreover, the small intensity difference observed for these bands in the different curves is certainly due to the fact that more or less signal coming from the methyl groups is detected. However no polymerization process may occur with the utilization of methyl groups (since alkyl groups did not possess double or triple bonds). Thus, when the Si electrode has received enough radicals to react with every H atoms from the atop sites of a Si(111) surface, the excess of additional radicals formed do not affect the Si surface. Furthermore, it seems that H-terminated Si(111) surface modified in galvanostatic mode with application of 1 mA/cm^2 for 5 min exhibits a higher integrated IR signal of the "umbrella" band observed.

Further PL studies have also revealed that the charge flow applied to the Si electrode affect the electronic properties in the amount of non-radiative active defects at the interface for these methylated Si surfaces (not shown). Besides, it has been found that the CH_3-terminated Si(111) surfaces of which an anodic current density of 1 mA/cm^2 for 5 min has been applied, present the "best" grafting concerning the non-radiative recombination active defects and for this reason, anodic current density of 1 mA/cm^2 for 5 min has been applied in most of the further experiments.

Tab. 5.1: *The calculated flown charge applied to Si electrodes during the electrochemical grafting process and the corresponding integrated IR signal of the "umbrella" mode.*

Grafting process	Charge applied	IRSE integral of "umbrella" band
Potentiostatic mode 0.5 V for 5 min	215.2 mC/cm^2	3.9 ± 0.39
Galvanostatic mode 0.5 mA/cm^2	150 mC/cm^2	3.3 ± 0.33
Galvanostatic mode 1 mA/cm^2	300 mC/cm^2	3.8 ± 0.38

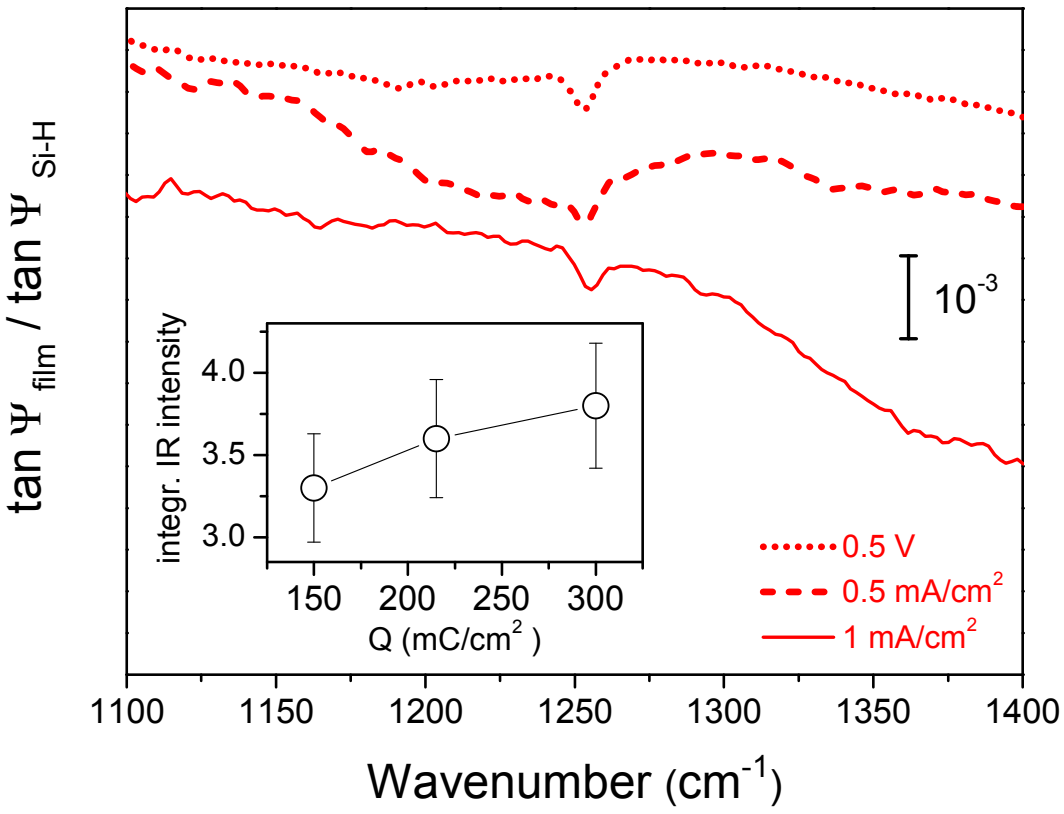

Fig. 5.4: *The "umbrella" bending vibrational mode, δ_s (CH_3) at ~ 1253 cm^{-1} of methylated Si(111) after different charge flow applied for 5 min in CH_3MgBr electrolyte (potentiostatic: ····· 0.5 V; galvanostatic: ----- 0.5 mA/cm^2, —— 1 mA/cm^2). Tan Ψ spectra were referred to H-terminated Si(111) surface. The spectra have been shifted for visual clarity. Insert shows the integrated IR intensities as a function of the applied charge flow.*

5.1.3 Role of halogen atoms during the electrochemical grafting of methyl groups

Fig. 5.5 shows the normalized tan Ψ spectra of CH_3-terminated Si(111) surfaces electrochemically modified with two different Grignard electrolytes (CH_3MgBr and CH_3MgI) that contains different halogen atoms Br and I, respectively. The electrochemical reaction has been performed for both Grignard compounds by applying an anodic current density of 1 mA/cm^2 for 5 min. At first glance, it can be noticed that obviously no prominent difference is observed between the two curves obtained (CH_3MgBr: red; CH_3MgI: blue).

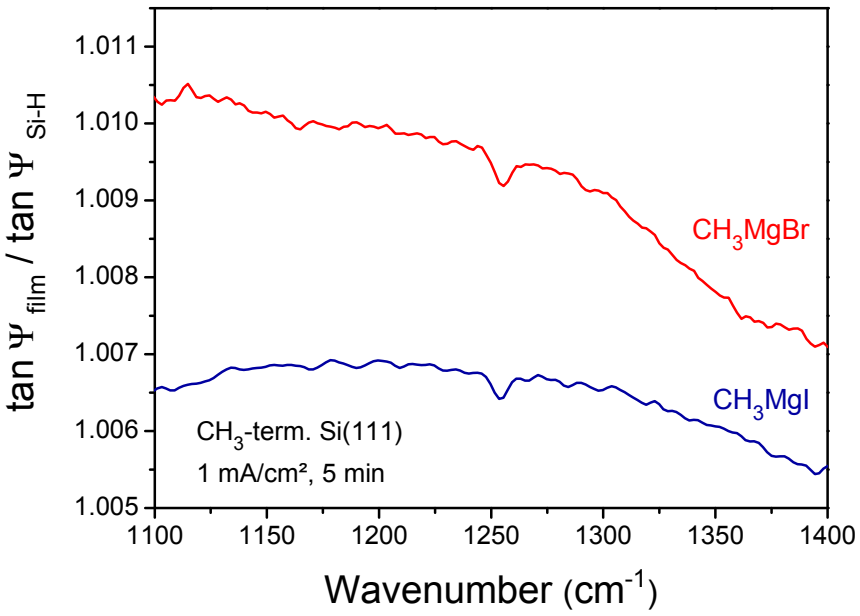

Fig. 5.5: *Normalized tan Ψ spectra of CH_3-terminated Si(111) surfaces modified with different Grignard electrolytes (CH_3MgBr and CH_3MgI) containing Br and I as halogen atoms, respectively. An anodic current density of 1 mA/cm^2 has been applied for 5 min.*

However, regarding more precisely the tan Ψ spectra, one can remark that for the modification in CH_3MgBr electrolyte a higher band assigned to "umbrella" vibrational mode at ~ 1255 cm^{-1} is conspicuous, while for the one treated with CH_3MgI electrolyte the "umbrella" vibrational mode is located at ~ 1253 cm^{-1}. The integral of the corresponding IR-absorption bands determined reveals quite the same area with ~ 10% error due to the weak peak, but also because of the asymmetry of the peak. No prominent difference can be observed with IRSE measurements. Besides, it will be demonstrate on further experiments that halogen influence sorely the grafting process of some molecules (e.g., ethynyl groups), and could by the same manner totally change the chemical, vibrational and electronic properties of the modified Si surface obtained (see Chap. 6).

5.1.4 CH_3-terminated Si(111) surface versus CH_3-terminated Si(100) surface

In this subsection, the comparison between CH_3 groups grafted onto p-Si(111) and p-Si(100) surfaces have been investigated with the Kramers-Kronig related tan Ψ and Δ spectra obtained by IRSE measurements. The aim of this study is to verify whether the grafting Grignard method also works with a Si surface presenting another type of surface orientation; since in technology, Si(100) surface is the most relevant one. H-terminated Si(100) surface shows different surface structure in relation to H-terminated Si(111) surface (2 dangling bonds instead of 1, see Chap. 2), Si–H stretching vibrational mode is known to be shifted from 2083 to 2110 cm^{-1} for H-terminated Si(111) to H-terminated Si(100) surfaces (Fig. 5.6), respectively.[76,77] Thus, CH_3-terminated Si(100) surface is also expected to indicate a shift of the IR-absorption band arising from the "umbrella" bending vibrational mode of CH_3 groups. Fig. 5.6 shows the normalized tan Ψ and Δ spectra of CH_3-terminated Si(111) and Si(100) surfaces, respectively. An anodic current density of 0.5 mA/cm^2 has been applied for 5 min to obtain these CH_3-terminated Si surfaces. On this figure, Si–H peak disappears after electrochemical grafting for both Si surfaces (Fig. 5.6b). Nevertheless, the tan Ψ spectrum obtained from CH_3-terminated Si(111) surface (red curve) shows the band assigned to "umbrella" bending vibrational mode at ~ 1252 cm^{-1}, while a very weak band appears at ~ 1268 cm^{-1} for the CH_3-terminated Si(100) surface (brown curve). This weak band at ~ 1268 cm^{-1} can be related to a real IR-absorption band because an optical change in Δ spectrum is also observed at this wavenumber in tan Ψ spectrum (Fig. 5.6a). Therefore, this weak peak could be assigned to the CH_3 "umbrella" mode of CH_3 groups grafted onto Si(100) surface. The observed shift for the CH_3 "umbrella" vibrational mode from Si(100) to Si(111) surfaces is ~ 16 cm^{-1}. This shift is in the same direction as observed for the Si–H stretch peak from H-terminated Si(111) to Si(100) surfaces and is ~ 27 cm^{-1}. Finally, no specific orientations have been determined in this study concerning the CH_3 groups, nonetheless to obtain such information, computational methods should be performed.

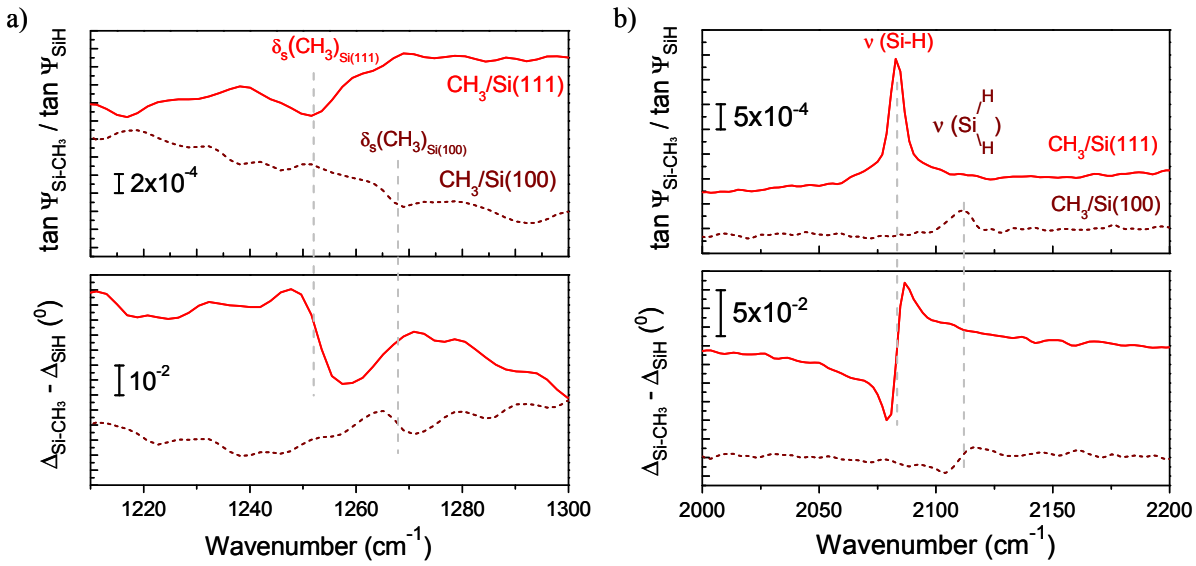

Fig. 5.6: *Kramers-Kronig related tan Ψ and Δ spectra for CH_3-terminated Si(111) and Si(100) surfaces in the (a) CH_3 "umbrella" mode region and in the (b) Si-H symmetric stretching mode region. Please pay attention that the scales on both panels are not similar. The spectra have been shifted for visual convenience.*

5.1.5 Methyl groups grafted on porous Si

Grafting of CH_3 groups onto porous Si (PSi) has not been intensively studied until now. However, this is quite interesting to understand how the grafting of methyl groups onto PSi will be influenced by the initial H-terminated PSi (H-PSi) structure (see Fig. 4.3) in term of the orientation of the bonds which will be formed between the PSi surface and the methyl groups. In addition, more surface area leads to a higher IR signal of the grafted CH_3 species. As already explained in the previous chapter, H-PSi starting surface for the grafting of methyl groups has exhibited anisotropic morphology with very small pore structures.

Methyl-terminated porous Si (MePSi) is obtained using the same electrochemical grafting method than used for the deposition of organic molecules onto H-terminated Si(111) and H-terminated Si(100) surfaces (CH_3MgBr, 0.5 mA/cm^2 for 5 min). Fig. 5.7 shows tan Ψ, Rp and Rs spectra from (a) MePSi, (b) H-PSi, and (c) tan Ψ of MePSi divided by tan Ψ of H-PSi, and (d) tan Ψ of MePSi in a wider spectral region. The binding of CH_3 groups on PSi surface is well observed by typical absorption bands due to CH_3 termination (Fig. 5.7a, c and d). However, absorption bands due to SiH_x groups are also conspicuous in Fig. 5.7d, as indicated in tan Ψ spectrum of MePSi surface. Thereby, after grafting of CH_3 groups onto H-PSi surface, the presence of downward pointing peak features assigned to Si–H bending vibrational modes (at 669 cm^{-1}, δ_{wag}(Si–H) wagging vibrational mode and at 906 cm^{-1}, $\delta(SiH_2)$ scissor vibrational mode) are still distinguishable in the lower spectral range (Fig. 5.7d). Besides for

these corresponding peaks, only a slight number of Si–H surface species are grafted by CH_3 after electrochemical modification. Similarly, the same behavior is also observed in the Si–H stretching vibrational region between 2000-2200 cm^{-1}, where upward pointing peak features are ascribed to Si–H stretching vibrational modes, $\nu(SiH_x)$ (with x = 1, 2, 3). These peaks exhibit a small diminution of intensities as well upon CH_3 modification. This observation could then buttress the assumption that not every Si–H bonds from H-PSi surface has been replaced by CH_3 groups after the electrochemical grafting. Additionally, no prominent SiO_2-related modes have been observed in the oxide range for MePSi surface. On Fig. 5.7 b, CH_2 and CH_3 absorption bands in the 2900-2970 cm^{-1} region are also ubiquitous on H-PSi surface, which indicates the presence of some CH_x-containing contaminants from the atmosphere. On Fig. 5.7d, another absorption band as downward pointing peak appears at 773 cm^{-1} in the lower frequencies region and is attributed to the rocking vibrational mode of CH_3 molecules, $\rho(CH_3)$. In the higher frequency region, distinguishable absorptions bands are also observable as upward pointing peaks in the 2900-2970 cm^{-1} range and are assigned to C–H stretching symmetric and asymmetric vibrational modes of methylene groups, $\nu_{as}(CH_2)$ at 2931 cm^{-1} (due to hydrocarbon contaminants) and methyl groups, $\nu_s(CH_3)$ and $\nu_{as}(CH_3)$ at 2902 and 2969 cm^{-1}, respectively. However, Fig. 5.7c shows tan Ψ spectrum of MePSi divided by the tan Ψ spectrum of HPSi and clearly indicates the disappearance of the CH_2-related absorption band at 2930 cm^{-1}, leaving thus only the true bands originating from the grafted CH_3 groups. Interestingly, no "umbrella" mode, $\delta_s(CH_3)$ is observable at 1253 cm^{-1}, like it was the case for the methylated Si(111) and Si(100) surfaces. Another assumption that MePSi still follows the initial pattern of H-PSi is indicated with the presence of Si–H vibrational modes. This is observed by the IR-absorption bands assigned to the stretching vibrations which appear as upward pointing peak features, while the IR-absorption bands attributed to the bending vibrations appear as downward pointing peak features. Thus, the spectra obtained from the MePSi surface exhibit obviously the preservation of anisotropy of the porous silicon structure from the initial hydrogen passivated PSi surface after electrochemical grafting by the CH_3 groups. Table 5.2 summarizes the IR absorption bands and their assignments. This behavior has not been seen for instance in the case of NB grafted onto porous Si, where the Si–H modes have disappeared totally from the Si surface.[95]

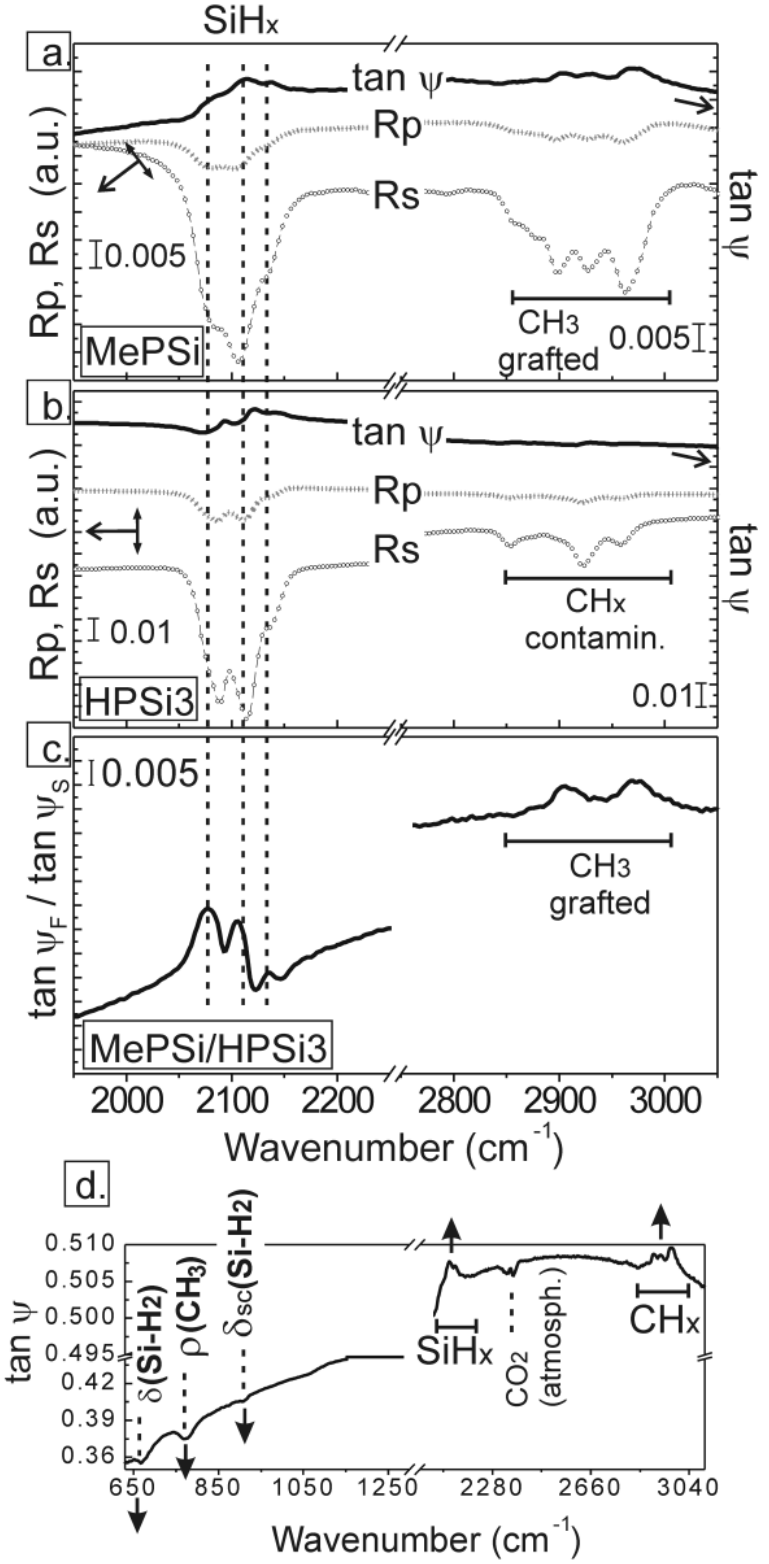

Fig. 5.7: *Tan Ψ and Rp, Rs spectra as obtained from (a) MePSi and (b) H-PSi samples at 65° angle of incidence. The background of Rp has been shifted in respect to Rs by +0.482 in (a) and by +0.534 in (b) for visual convenience, (c) illustrates tan Ψ spectrum of MePSi referenced to tan Ψ spectrum of H-PSi, and (d) depicts tan Ψ spectrum of MePSi in the extended spectral range. The arrows emphasize the directions of the observed absorption bands. ν: stretching; ρ: rocking; δ: bending vibrational modes. Please notice that the right and left sides of the panels (a) and (b) indicate different y-scales.*

Tab. 5.2: *Absorption bands observed from the MePSi spectrum (Fig. 5.7) with the corresponding assignments (δ: bending; ρ: rocking; ν: stretching vibrations).*

Absorption peak position (cm^{-1})	Assignment	Reported absorption peaks (cm^{-1}) [refs.]
669	$\delta_{wag}(Si\text{-}H)$	667 [81]
773	$\rho(C\text{-}H)_{CH3}$	757 [20]
906	$\delta_{sc}(Si\text{-}H_2)$	910 [83,96]
2904	$\nu_s(C\text{-}H)_{CH3}$	2900 [96]
2931	$\nu_{as}(C\text{-}H)_{CH2}$	2928 [20]
2967	$\nu_{as}(C\text{-}H)_{CH3}$	2965 [20,92]

5.2 SXPS characterization

In this section, methylated (CH_3 and CD_3 groups) and H-terminated Si(111) surfaces have been investigated using X-ray photoemission spectroscopy under synchrotron radiation (SXPS). The chemical and electronic properties of these modified Si surfaces have been discussed, also in term of thermal stability. Methyl groups grafted onto Si(111) surfaces have revealed a high stability against the annealing treatment since the C 1s photopeak attributed to carbon atoms bonded to silicon surfaces are still remained on Si surfaces. Only a small amount from the initial contribution of this peak (fresh sample) is reduced. Moreover, after this annealing treatment, the methylated Si samples have also revealed a well-distinguished spin-orbit splitting in the Si 2p core level emission. For the first time, this splitting is well observed for these methyl-terminated Si(111) surfaces of which the contribution arising from the bulk Si 2p emission and the one due to the bondings between silicon surface atoms and carbons atoms from methyl groups are clearly shown. This behavior gives then clear evidence that methyl groups are covalently attached to Si surface atoms. Furthermore, no prominent difference has been observed in the Si 2p and C 1s core level emissions between both methyl-terminated Si(111) surfaces achieved by CH_3 and CD_3 groups. However, methylated Si(111) surfaces grafted with CD_3 molecules seem to present better passivated Si surfaces. Finally, it has been observed that the electronic properties can be strongly influenced by the presence of defects on the surface, as well as the bonding of organic molecules on the surface leading to a surface dipole. For this study, detailed SXPS measurements have been performed

and the results acquired for such modified Si surfaces have been discussed below in terms of change in work function, surface band bending, electron affinity, and surface dipole induced by the presence of organic molecules on the surface. Thus, in order to investigate these electronic properties, a band diagram has been constructed (see Fig. 5.13).

All SXPS measurements have been performed under synchrotron radiation at the undulator beamline U49/2-PGM2 at BESSY II in Berlin. Small dimensions of Si(111) samples, p-doped with a resistivity of 0.05 – 2.63 Ωcm have been used in this work. The Fermi-level position, E_F, relative to the valence band maximum corresponding of this dopant concentration has been determined to be located at (0.20 ± 0.02) eV from the valence band maximum energy, E_{vbm}, for the intrinsic Si(111) surface.[41] After insertion of the fresh modified Si samples into the vacuum system of the SoLiAS experimental station, the Si samples have been first recorded using photon energy, hν, of 150 and 650 eV. Then, the same Si samples have been heated at 390 °C for 30 min. In the case of CH_3-terminated Si(111) surface, a second annealing has also been performed at 430 °C for 30 min.

Comparison between Si 2p emissions under surface and bulk sensitive conditions

Fig. 5.8 displays the high-resolution SXP spectra in the Si 2p core level emission region for a fresh H-, CH_3- and CD_3-terminated Si(111) surfaces. The Si samples are recorded at two different excitation energies, (a) hν = 150 and (b) 650 eV, respectively. At a photon energy of 150 eV, the Si samples are probed under "surface" sensitive condition (escape depth ~ 5.4 Å), while at a photon energy of 650 eV, the spectra are recorded under "bulk" sensitive condition (escape depth ~ 17.5 Å). As expected, for Si surfaces the Si 2p core level spectra reveal a spin-orbit doublet which has been observed for each sample. This splitting corresponds to the spin-orbit doublet of the Si 2p emission and can be decomposed into similarly shaped $2p_{1/2}$ and $2p_{3/2}$ contributions (ΔE_{BE} = 0.605, and 1:2 peak area ratio).[59] Moreover, under surface sensitive condition (hν = 150 eV), the intensities of Si 2p core level emissions are ~ 5 times more intense than under bulk sensitive conditions (hν = 650 eV). Beyond, no photopeaks in the binding energy corresponding to the region of silicon oxide SiO_2 emissions (up to ~ 4 eV above the bulk Si $2p_{3/2}$ peak position) have been detected. This observation clearly indicates that no SiO_2 species have been formed on the Si surfaces.

At an excitation energy of hν = 650 eV, the high resolution Si 2p core level spectra show a small shift of the bulk Si $2p_{3/2}$ peak for CH_3- and CD_3-terminated Si(111) surfaces, respectively, in relation to H-terminated Si surface (Fig. 5.8b). The bulk Si $2p_{3/2}$ peak of H-terminated Si(111) surfaces is located at ~ 99.41 eV and a shift of ~ 0.05 to 0.22 eV

towards the lower binding energy occurs for methylated Si(111) surfaces in comparison to H-terminated Si(111) surfaces. This small shift (< 1 eV) is consistent with the fact that organic molecules have been deposited onto Si(111) surfaces because it is well known that organic modification of Si surfaces leads to a small shift of the bulk Si $2p_{3/2}$ signal.[54,97] The intensity of the Si 2p photopeak decreases from H- to methyl-terminated Si(111) surfaces. The attenuation of Si 2p photopeak has been expected whether methyl groups are grafted on top of the Si surface atoms (or whether chemical bonds are formed between the Si substrate and the carbon of the methyl groups). Moreover, the intensities of the methyl-terminated Si(111) surfaces are quite equivalent, which is consistent with the fact that no more than one monolayer can be achieved for both methylated (CH_3 and CD_3) Si surfaces. However, this attenuation is just a hint that the Si surfaces have sustained a change in the electronic properties of the Si and can not be taken as quantitative conclusion. These shifts in the lower binding energies as related to the bulk component of H-terminated Si(111) surfaces suggest that methyl-terminated Si(111) surfaces are less electronegative. From these shifts, the surface band bending of these modified Si(111) surfaces induced by the organic molecules grafted can be determined. Similarly, the same demeanors are also observed at more surface sensitive information, i.e., at excitation energy hν = 150 eV (Fig. 5.8a). Here again, no oxide or very few amounts of oxide have been detected. However, it seems that the H-terminated Si(111) surfaces indicate a very weak hump in the SiO_2 region. This hump suggests that the fresh H-terminated Si(111) sample has been probably contaminated during the insertion into the vacuum system of the SXPS equipment. Moreover, a very weak feature is also detected in the higher binding energies at about + 1.40 eV from the bulk Si $2p_{3/2}$ peak for both methyl-terminated Si(111) surfaces, respectively. This small feature could be attributed to the contribution from the top layer Si surface atoms attached with halogen atoms according to Terry and co-workers.[98,99] These halogen atoms arose probably from the Grignard solutions and/or during the rinse with bromobutane solution. A change in Si 2p emission line shapes of the methylated and H-terminated Si(111) surfaces suggests that the observed Si 2p photopeaks consist of multiple spin-orbit doublet contributions. These multiple spin-orbit doublets are more prominent for CH_3-terminated Si(111) surfaces. This statement supposes that another component occurs on the Si 2p emission spectra and is shifted to the higher binding energies (about + 0.18 eV) than the bulk component. This indicates that a charge is being transferred from the Si atoms to another element more electronegative. This chemical shift can then points out that the Si atoms from the surface are bounded to carbon atoms from the methyl groups, as expected by their respective electronegativities (1.90 and 2.55, for Si and C atoms, respectively).[100]

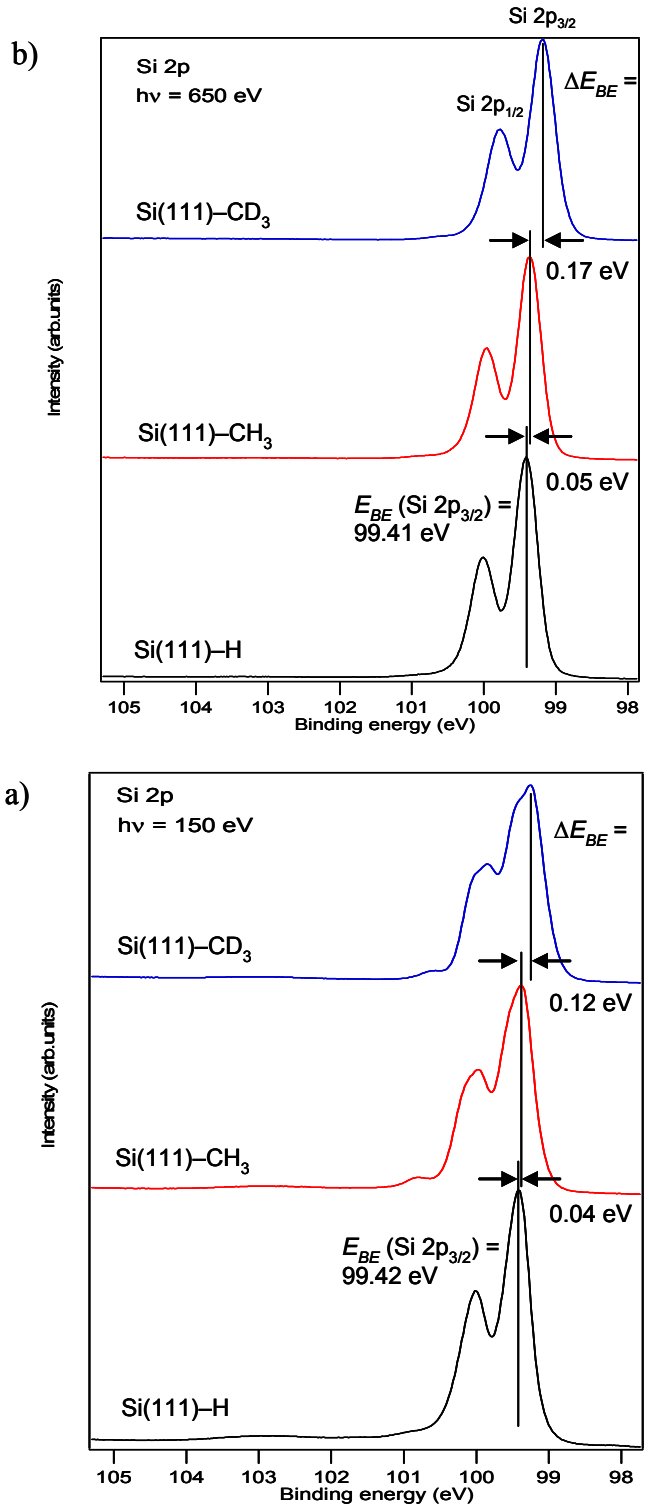

Fig. 5.8: *High resolution Si 2p core level emission spectra from H-, CH_3- and CD_3-terminated Si(111) surfaces have been recorded at photon energies (a) of 150 and (b) 650 eV, respectively. The difference energy between the modified Si(111) samples have been indicated with the arrows.*

However, H-terminated Si(111) surfaces reveal a bulk Si $2p_{3/2}$ peak contribution located at 99.42 eV, and a shift in the lower binding energies of 0.04 and 0.16 eV of the bulk Si $2p_{3/2}$ peak has been observed from H- to CH_3- and CD_3-terminated Si(111) surfaces, respectively.

5.2.1 Successive annealing under different conditions

All core level spectra have been fitted using a least-squares fitting procedure after a Shirley background subtraction. The Si 2p and Br 3d core level spectra have been fitted using spin-orbit doublets of Voigt line shapes. Necessary constraints have been maintained due to the spin-orbit doublet of Si 2p (ΔE_{BE} = 0.605, 1:2 peak area ratio), and Br 3d (ΔE_{BE} = 1.05, 2:3 peak area ratio).[59] C 1s core level spectra have been deconvoluted using singlet Voigt line shapes.

Annealing of the samples has been performed in order to remove adventitious contaminations like aliphatic carbons or other remnant contaminations from the Si surfaces. Moreover, these annealing treatments can also give information about the stability of the bonding formed between Si surface atoms and C atoms from methyl groups.

Fig. 5.9 shows the high resolution of (a) C 1s and (b) Br 3d core level spectra for H-, CH_3- and CD_3-terminated Si(111) surfaces before and after annealing treatments. Each spectrum has been recorded at photon energy of 650 eV. In Fig. 5.9b, the C 1s core level emissions of these modified Si samples reveal several carbon features. Before annealing, the H-terminated Si(111) surface indicates two components. The larger peak at 284.76 eV is attributed to the emission from adventitious aliphatic carbons bonded to other carbon or hydrogen atoms. This component can be then indicative of C–C, C–H, and/or C=C bondings.[54,97] These remnant carbon contaminants arise probably during the transfer to the experimental setup. A weak hump shifted to the higher binding energy by + 1.0 eV at 285.76 eV is also observed and is probably due to carbons bonded to the silicon back bonds oxide. After annealing, the component corresponding to the aliphatic carbons is strongly reduced by ~ 70% and the hump at higher binding energy totally disappeared. In the case of the methylated Si surfaces, C 1s core level emissions show more peak features. The similar contribution components than H-terminated Si surface are also observed, but are shifted to the higher binding energies in relation to the H-terminated Si(111) surface by about + 0.37 and + 0.58 eV, i.e., at 285.13 and 285.34 eV for CD_3- and CH_3-terminated Si(111) surfaces, respectively. These shifts in the higher binding energy from H- to CD_3- and CH_3-terminated Si(111) surfaces has also been noticed for alkyl chains grafted onto Si(111) surfaces according to Jaeckel et al.[101] Besides, these peak components reveal more aliphatic contamination carbons present in the case of CH_3-terminated Si(111) surfaces. A weak feature appears like in H-terminated Si surfaces and is shifted by about + 1 eV from the respective position of the aliphatic carbon components for both methyl-terminated Si(111) surfaces. Here, these components are certainly due to carbon

atoms from adventitious remnant contaminants bonded to Br or O atoms coming from the rinse process or during the Grignard grafting process. In the case of CH_3-terminated Si(111) surfaces, another component shifted to around + 4.08 eV occurs at 289.42 eV. This feature is most likely due to the satellite of the principal peak[102,103] or could be certainly due to contaminants from carboxylic groups (C=O) (electronegativity of oxygen, O is 3.44).[97,104,105] These carboxylic groups are probably arisen from the breaking of DEE molecules from the solvent contains in the Grignard solutions. The predominant C 1s photoelectron peak observed at 283.98 and 284.04 eV, respectively, for both CD_3- and CH_3-terminated Si(111) surfaces is assigned to C bonded to Si atoms, C–Si bonds.[88,101,106,107] This chemical shift by ~ 1 eV which occurs in the lower binding energy in relation to the adventitious aliphatic carbons reveals that the C atoms from this emission are bonded to a less electronegative element. This is in that case Si atoms because only the Si element which possesses this property is present. As compared to the aliphatic peak component, more C bonded to Si atoms are observed since the C–Si peak emission reveals ~ 20 to 70% more contribution from this component than the corresponding aliphatic components for CH_3- and CD_3-terminated Si(111) surfaces, respectively. These demeanors reveal then a better achievement of methyl-terminated Si(111) surfaces by CD_3 groups in relation to CH_3 groups. After the annealing treatments, most of the aliphatic carbons have been desorbed from the Si surfaces by ~ 50 and 80% for CH_3- and CD_3-terminated Si(111) surfaces, respectively. However, a second annealing at a higher temperature of 430 °C for 30 min is necessary in the case of CH_3-terminated Si(111) surfaces to mainly remove these adsorbed aliphatic carbon contaminants and to obtain then a quite similar C 1s emission shape as compared to the CD_3-terminated Si(111) surfaces. Albeit the desorbtion of the aliphatic carbons occurs after the annealing treatment, no prominent changes in the shape and in the intensity of C–Si contribution have been observed. However, for the CD_3-terminated Si(111) surfaces, ~ 5% of the C–Si component has been "desorbed" and a small shift about + 0.04 eV to the higher binding energies occurred, which leads to the same energy position than the C–Si emission of the peak from CH_3-terminated Si(111) surfaces. In the case of CH_3-terminated Si(111) surfaces, all remnant adventitious adsorbates have been desorbed, after the second annealing treatment. The C–Si component emission of the peak from CH_3-terminated Si(111) surfaces has not been affected, but a small feature at ~ 283.5 eV appeared. This small shoulder is most likely due to the formation of silicon carbide, SiC, after the annealing treatments.[97,108,109] However, these results reveal that the C atoms from the methyl groups bonded to Si surfaces are stable up to 430 °C. This demenaor is in good agreement with the desorbtion of alkyl chains grafted onto Si surfaces of which a thermal treatment has been applied.[110] Since the annealed Si surfaces present less contami-

nant on their surfaces, the discussions and the fitting of the C 1s and Si 2p emissions from the annealed methylated Si surfaces will be presented in the following subsection.

High resolution Br 3d core level spectra for both methylated Si surfaces are shown in Fig. 5.9a. Br atoms are not detected on H-terminated Si(111) surfaces. The Br 3d core level spectra have been fitted (not shown here) and two different oxidation states have been found with respect to the necessary constraints from the Br 3d spin-orbit doublet contribution.[59] The first spin-orbit doublet peak appears at ~ 69.55 eV and is attributed to Br bonded to Si atoms, whereas a second spin-orbit doublet peak shifted to about + 1.05 eV to the higher binding energies at ~ 70.60 eV has been assigned to Br bonded to C atoms coming from remnant adventitious carbons. This shift is consistent with the literature.[97,111] The two spin-orbit doublet pair components are then overlapped. The attribution of these peaks has been done with respect to the electronegativities of these elements. C (2.55) is more electronegative than Si (1.90) so that the contribution from Br–C spin doublet emission should be shifted to higher binding energy than the component arising from Br–Si bonds. In the case of CH_3-terminated Si(111) surfaces, the Br–Si spin-orbit doublet emission at ~ 69.55 eV decreases successively by about 50 and 75% from the first to the second annealing process, respectively, in relation to the initial peak, while almost all the Br–C component disappears already after the first annealing. This demeanor is consistent with the observation deduced from the C 1s core level emissions. In the case of the CD_3-terminated Si(111) surfaces, the peak due to Br atoms can only come from the rinse solution (bromobutane) because the Grignard solution used for the grafting of CD_3 groups contains iodine atoms instead of bromine atoms. This suggests strongly that some remnant contaminants can also come from the rinse process. This behavior is observed by the high amount of Br–C components on this surface. However, surprisingly it seems that the CD_3-terminated Si(111) surfaces are more reactive in contact with bromobutane solution as compared to CH_3-terminated Si(111) surfaces because more contribution from Br–C bonds occurred. After annealed the Si sample terminated by CD_3 groups, more Br–Si bonds seem to occur since the intensity of the corresponding peak is increased. This phenomenon suggests that during the annealing treatment, Br–C bonds have been probably cracked, and thus some of the Br atoms have reacted with the Si surface atoms. Moreover, in correlation with the C 1s core level emissions, the peak related to possible C–Br bonds also totally disappear after the annealing process.

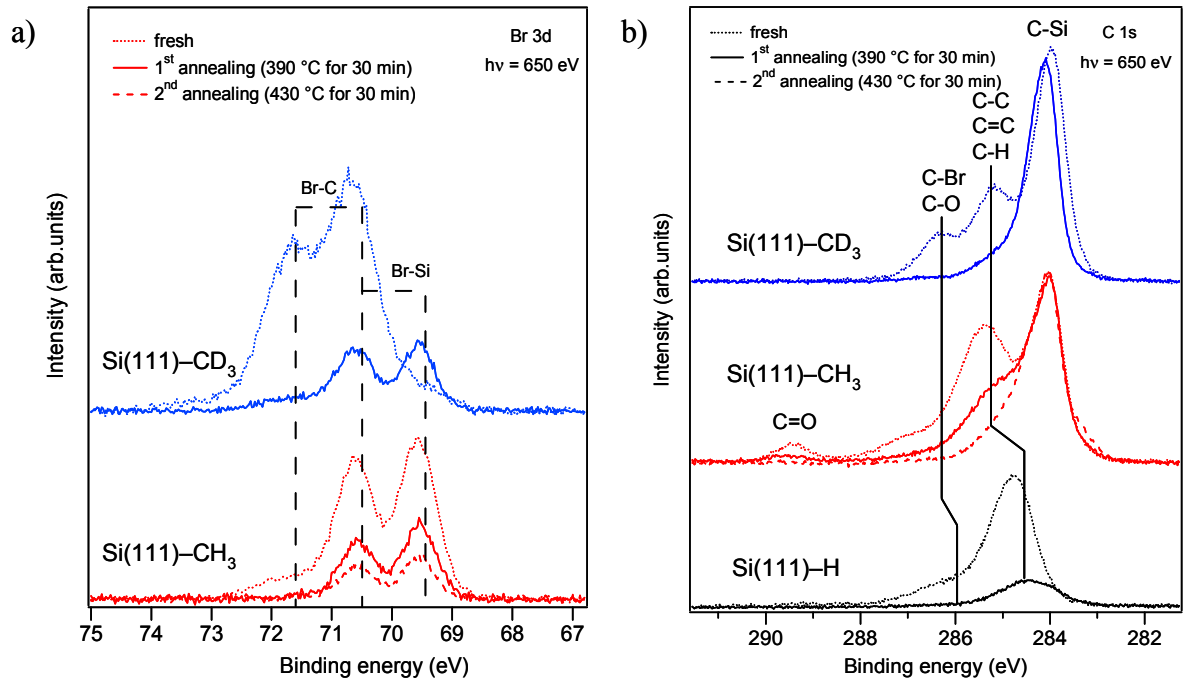

Fig. 5.9: *XP core level emissions of (a) Br 3d and (b) C 1s recorded at hν = 650 eV for H-, CH_3- and CD_3-terminated Si(111) surfaces, respectively, before and after annealing processes. Note that the intensity is in arbitrary units so that the graphs are not shown in the same count per seconds (cps) intensity regime (it means that the real intensity are not relative here and cannot be compared directly).*

Fig. 5.10 depicts the high resolution Si 2p core level spectra of H-, CH_3- and CD_3-terminated Si(111) surfaces before and after annealing procedures. The SXPS measurements have been performed at photon energy of 150 eV to be in surface sensitive conditions. As already explained above, the line shape emissions of the spectra related to methyl- and H-terminated Si surfaces change. Moreover, the change in the line shape emissions are more pronounced after annealing of the Si samples. These demeanors indicate then that molecules are grafted onto Si surfaces since a shift occurs between the H-terminated Si(111) surface and the methylated Si(111) surfaces. Furthermore, the change in the line shape emission could also arise from the change in the Si surfaces after the annealing procedure, which could be related to the desorbtion of contaminant carbons. For H-terminated Si surfaces, the Si 2p core level spectra shows a decrease in intensity, which is probably correlated to the loss of the hydrogen bonded on the silicon by the irradiation of this surface by synchrotron radiation. However, very few amounts of oxidation states from Si (Si^{1+}, Si^{2+},Si^{3+}, and Si^{4+})[112,113] seems to appear after annealing. For CH_3-terminated Si(111) surfaces, the intensity of the bulk Si $2p_{3/2}$ photopeak does not reveal a prominent change in relation to the H-terminated Si(111) surfaces. Conversely, the shape line changes and reveals a structure more pronounced of which two Si spin-orbit doublet emissions from the bulk silicon component (Si°) and also

from the Si atop atoms bonded to C atoms from the CH_3 groups could be guessed. Again, this separation is more evident after a second annealing. However, apparition of very small amounts of oxides occurs as also observed for H-terminated Si(111) surfaces. In the case of the modified Si(111) surface terminated by CD_3 groups, a very well-defined structure is revealed by the Si 2p core level spectra. Here, the two Si spin-orbit doublet contributions are extraordinary well-separated. A shift of + 0.27 eV is observed between the bulk Si° emission and the Si emission from the Si-C bonds.[98]

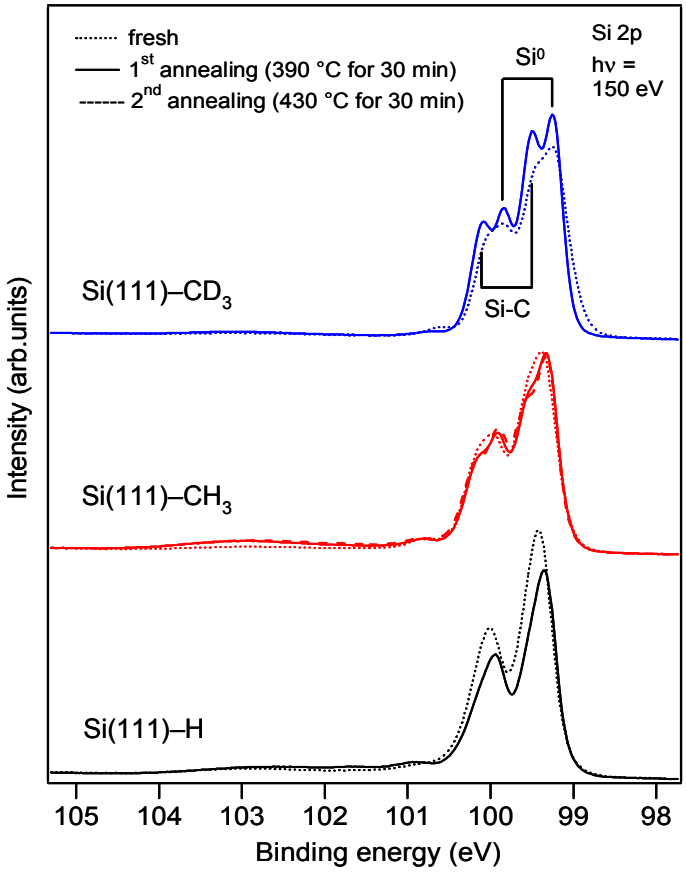

Fig. 5.10: *High resolution of Si 2p core level emissions of the fresh and annealed H-, CH_3- and CD_3-terminated Si(111) surfaces, respectively, taken at photon energy of hν = 150 eV (surface sensitive condition).*

Additionally, no oxide is observed after annealing in contrast to the SXPS measurements of the other Si surfaces. Moreover, an increase of ~ 15% in the bulk Si 2p emission has been observed. This increase is consistently related to the desorbtion of the adventitious species observed in the high resolution core level emission of C 1s, and Br 3d spectra, respectively. This well-separated splitting of these two Si spin-orbit doublet contributions is a hint of the well grafting of CD_3 groups onto Si(111) surface. This well-defined splitting is observed for the first time for this kind of electrochemical grafting onto Si(111) surfaces according to the

accessible literature. However, a splitting of a H-terminated Si(111) has been already reported in refs. [114,115] This phenomenon has been possibly observed due to the high resolution of the experimental setup performed under synchrotron radiation, but it is also due to the careful and meticulous manipulations of the Si surfaces during the grafting process.

5.2.2 Deconvolution of C 1s core level emission

Fig. 5.11 shows the C 1s core level spectrum of a methylated Si(111) surface terminated with CD_3 groups after annealing and recorded with a photon energy of 650 eV. As suggested before, this spectrum should present only the component arose from Si bonded to C atoms from the methyl groups. However, the C 1s photopeak recorded presents an asymmetry towards the higher binding energies. The C 1s core level emission reveals thus a multiple peaks fine vibrational structure and is then deconvoluted into four components as recently reported by Hunger et al.[88] for the same system obtained with a two-step procedure on n-type Si surfaces. These C-related signal component found are labeled as C^n (n = 0, 1, 2, 3), and are assigned to C atoms from the methyl groups bonded to Si atoms (C^0), the vibrational losses of the C–H stretching vibrations from the methyl groups (C^1, C^2), and the contaminations from remnant aliphatic carbons (C^3), respectively. The first component C^0 at the lower binding energy at ~ 284.06 eV corresponds to the adiabatic peak attributed to C–Si bonds. The C^1 and C^2 components were identified to come from satellite peaks that have the same initial state origin as C^0, i.e., Si bonded to C atoms from the methyl groups in the first and second excited states of C–H stretching vibrational modes by vibrational losses of the final state. Since the final state losses lead to an equidistant shift of these two excited states in the higher binding energy[88,116] in relation to C^0, the fitting procedure realized here has been adjusted to couple the binding energy shifts of C^1 and C^2 together ($\Delta E_{B2} = 2\,\Delta E_{B1}$, where ΔE_{B1} is the shift in binding energy between C^0 and C^1). Moreover, according to [88], ΔE_{B1} has been fixed at 0.38 eV and the components C^1 and C^2 have been then shifted by + 0.38 and + 0.76 eV, i.e., at 284.44 and 284.82 eV, respectively, in relation to C^0 emission. With these fixed parameters, the fitting from the components coming from the C 1s emission of the modified Si sample presented here is in good concordance with the previous results reported in ref. [88] for CH_3-terminated n-Si(111) surface. The last component C^3, at a higher binding energy of 285.33 eV (+ 1.27 eV), is ascribed to remnant contaminations from aliphatic carbons. Here again, this chemical shift determined is in well accordance with ref. [88] After annealing this sample, this component is reduced by ~ 90% from the initial peak and has a relative intensity of ~ 6% in relation to C^0. The parameters obtained from the fitting results are found to be well correlated

with the values reported in ref. [88], which indicates that a clean methylated Si(111) surface have also been achieved in this work. Moreover, the observation of the vibrational mode emissions C^1 and C^2 on Si(111) surfaces gives clear evidence of the extraordinary cleanliness achieved for the preparation of CD_3-terminated Si(111) surfaces by the one-step electrochemical Grignard grafting route.

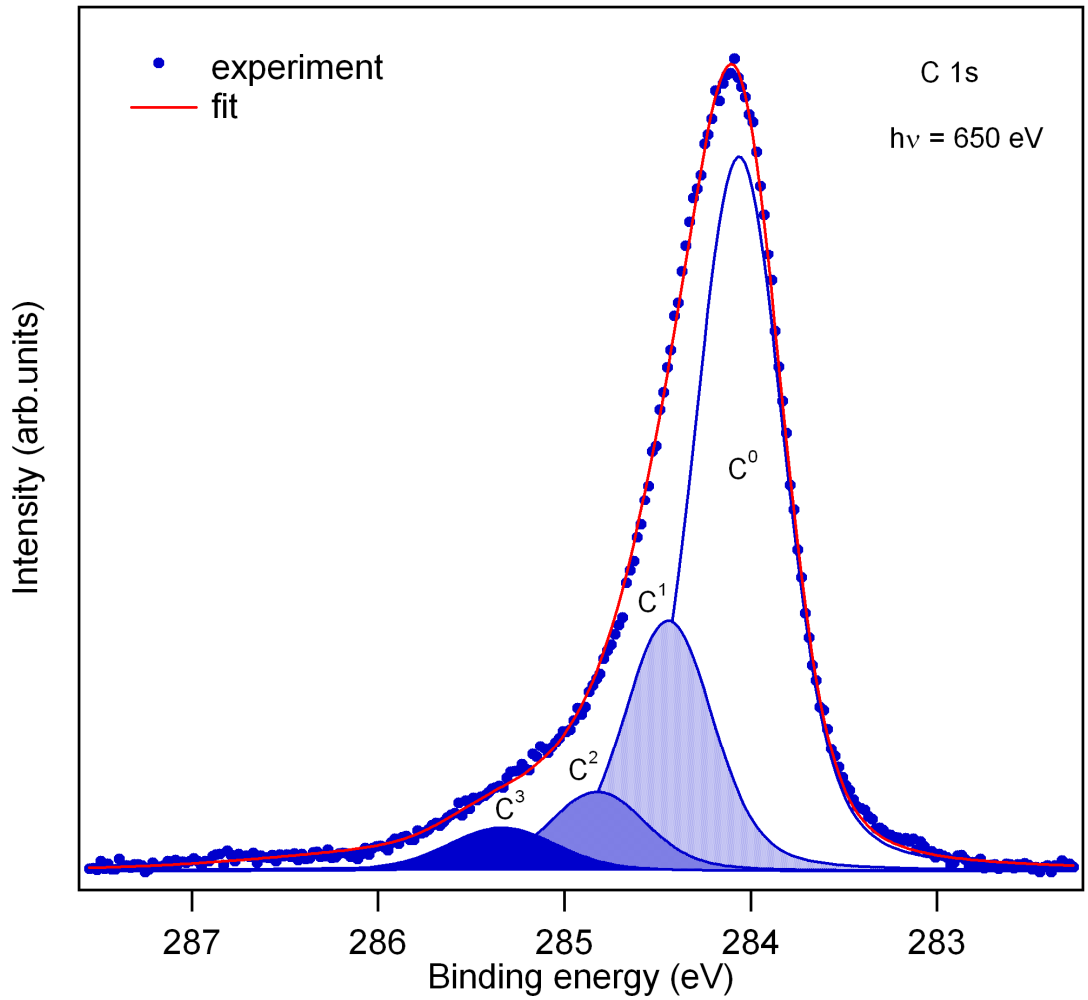

Fig. 5.11: *High resolution of C 1s core level emission of CD_3-terminated Si(111) surface after annealing. The SXP spectrum has been recorded with photon energy of 650 eV. The dots correspond to the raw data and the solid line represents the fitting curve result obtained. Component C^0: carbon from the methyl groups bonded to silicon atoms; C^1, C^2: first and second C–H vibrational stretching features from methyl groups bonded to silicon; C^3: adventitious aliphatic carbons.*

5.2.3 Deconvolution of Si 2p core level emission

Fig. 5.12 depicts the high resolution Si 2p core level emission spectrum of the Si(111) surface terminated with CD_3 groups after annealing at 390 °C for 30 min. This spectrum has been collected under surface sensitive conditions with a photon energy of 150 eV, which produces an inelastic electron mean free path λ of ~ 4 Å. The bulk Si 2p signal and the peak emission expected from the silicon bonded to carbons from methyl groups are well distinguished even without any fitting procedure. This observation gives then already a clear hint of the cleanliness achieved for this modified Si sample since this splitting is sorely prominent. However, a fitting procedure has been done to obtain quantitative information. After a Shirley background subtraction, a fitting procedure has been realized using split-orbit doublets of Voigt line shapes with the necessary constraints maintained due to the spin-orbit doublet splitting of Si 2p (ΔE_{BE} = 0.605, 1:2 branching area ratio). Si 2p spectrum has been deconvoluted and reveals four components. Surprisingly, more than two features have been determined. The bulk Si $2p_{3/2}$ emission component has been founded at a binding energy of 99.23 eV whereas the Si $2p_{3/2}$ emission component attributed to Si bonded to C atoms from the methyl groups is chemically shifted by + 0.27 eV towards the higher binding energy at ~ 99.50 eV in relation to the bulk Si $2p_{3/2}$ signal. This chemical shift is in compliance with a methylated Si surface prepared by the two-step alkylation method.[88] Moreover, due to the electronegativities of the Si and C, the chemical shift observed clearly exhibits the polarity of the bondings, where the Si atoms are more positively charged. The Lorentzian width for both components has been fixed at 0.039 eV. Furthermore, the two other features observed have also been chemically shifted towards the higher binding energy at + 0.81 eV (~ 100.04 eV) and + 3.32 eV (~ 102.55 eV) in relation to the bulk Si $2p_{3/2}$ emission, respectively. The component at ~ 100.04 eV has been assigned to Si bonded to Br atoms. The adventitious Br atoms arise evidently from the rinse process since the corresponding Grignard solution contains only iodide ions (methyl-d_3-magnesium iodide). The chemical shift of + 0.81 eV shows a similar energetically shift compared to chlorinated Si(111) surface.[98,99] The other chemical shift at about + 3.32 eV has been ascribed to silicon oxide concentration from Si^{4+} oxidation state, but probably also from Si^{3+} in smaller quantity.[112,113] Moreover, it is well known that oxidation states of Si are shifted successively towards higher binding energies by about + 1.0 eV in relation to the bulk Si $2p_{3/2}$ emission (Si^0). Thus, possible features from the first oxidation state of the silicon (Si^{1+}) could be also overlapped with the signal which arises from the Si–Br component. However, these chemical shifts observed towards higher binding energies are consistent with the respective electronegativies of Si, Br, and O atoms (1.90, 2.96, and 3.44, respectively). No

investigations in the small range of the silicon oxide have been done to determine exactly the amount of the different oxidation states from the silicon oxide. However, according to the fit, a ratio of ~ 94% from the emission of Si–C component is determined in relation with the relative intensity of the bulk Si^0 emission. In the case of the Si emissions arising from the Si–Br component signal and from the residual surface oxide concentration, only ~ 5% and ~ 1% of the relative intensity from the bulk Si^0 emission have been found. These observations indicate then clearly the high surface quality of the grafted CD_3 groups onto Si(111) surfaces by the electrochemical grafting method using Grignard solutions.

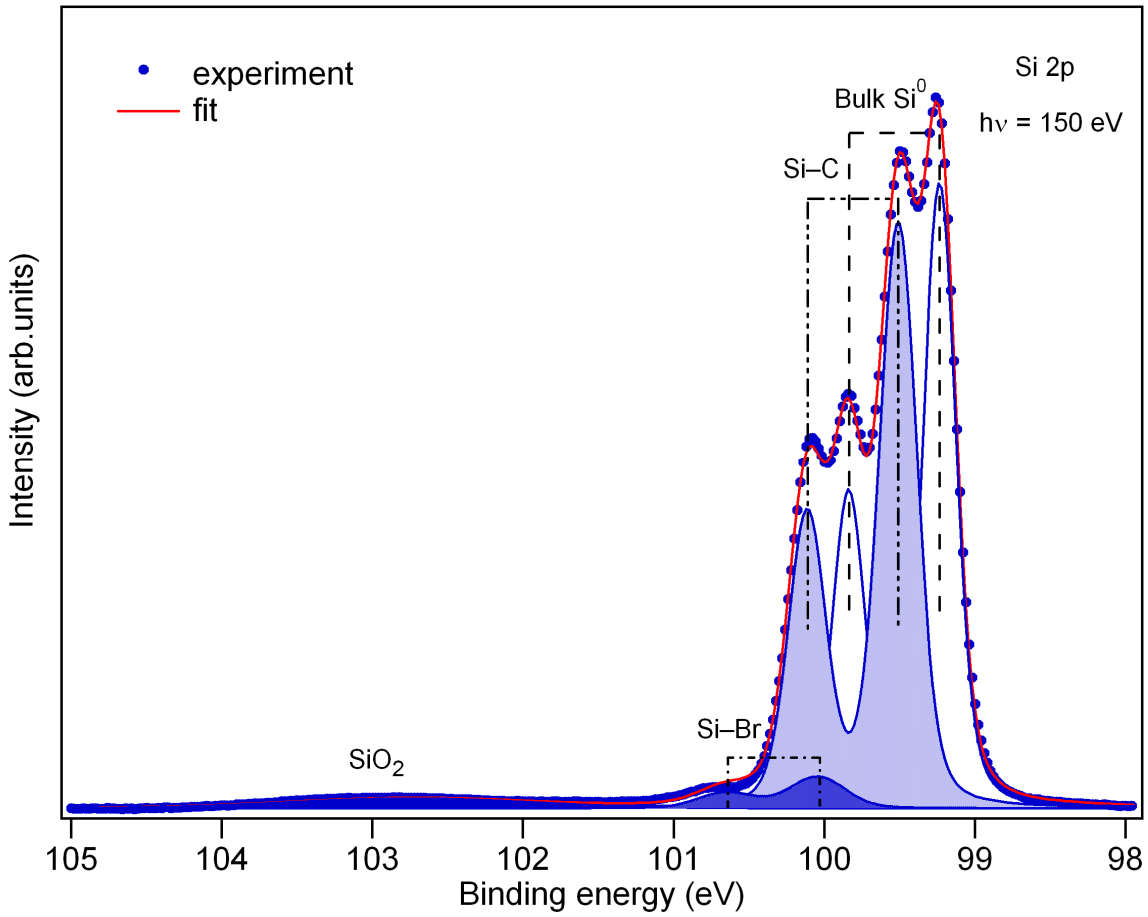

Fig. 5.12: *High resolution Si 2p core level emission of CD_3-terminated Si(111) surface after annealing, has been recorded at an excitation energy of 150 eV (surface sensitive condition). The fitting has been obtained after a Shirley background subtraction and has been deconvoluted into spin-orbit doublets of Voigt line shapes. The dots represent the raw data and the solid line corresponds to the fitting curve obtained.*

5.2.4 Construction of the energy band diagrams

Fig. 5.13 illustrates the surface energy band diagrams of the H-terminated Si(111) surface in comparison with the methyl-terminated Si(111) surface after the annealing process. Each fresh Si sample has been first measured and then annealed at ~ 390 °C for 30 min. Only the Si(111) surface modified with CH_3 groups has been sustained a second annealing at ~ 430 °C for 30 min. No pronounced changes occur in the surface electronic properties between the two successive annealing in the case of CH_3-terminated Si(111) surfaces. Moreover, CH_3- and CD_3-terminated Si(111) surfaces present the same electronic properties after annealing. Arbitrary, only the energy band diagrams of H and CD_3-terminated Si(111) surfaces have been constructed by following the physical explanations given in Chap. 2.

However, the steps for the determination of the electronic properties shown here have been shortly summarized. First, the work function, Φ, has been determined by the extrapolation of the secondary electrons cutoff edge from these Si samples (not shown). Then, the surface band bending, eV_{bb}, has been established from the position of the binding energy of the bulk Si $2p_{3/2}$ signal (relative to the Fermi energy) acquired from the curve fitting of the Si 2p core level emission spectra recorded at hν = 650 eV (bulk sensitive condition). For this determination, the binding energy of the Si 2p signal in the bulk with respect to the valence band maximum is assumed to be 98.74 eV,[40] and knowing the doping of the Si wafer, the position of the Fermi energy has been established. Moreover, taking into account the energy band gap of the Si (E_g = 1.12 eV) and the electron affinity of the bulk silicon as χ_{Si} = 4.05 eV,[41] the energy band diagram can be constructed and thereby, the electron affinity, χ, and the surface dipole, δ, as well can be then easily determined. The parameters obtained from these measurements are reported in Tab. 5.3.

From the electronic properties determined, a trend has been observed for the modified Si samples measured before and after annealing, respectively. For the fresh samples, the position of the bulk Si $2p_{3/2}$ emission seems to shift to the lower binding energies from H-, to CH_3 and CD_3-terminated Si(111) surfaces. This demeanor reveals then also a decrease of the band bending which goes to the flat band conditions direction from H- to methyl-terminated Si(111) surfaces. However, the CD_3-terminated Si(111) surface seems to possess the better chemical passivated Si surface because the lower band bending (0.25 eV) occurs as compared to the other modified Si surfaces (0.42 to 0.48 eV). In the ideal case for a surface, the flat band conditions appear when every surface states of a surface have been totally passivated chemically and then no band bending occurs. Moreover, the work function, the electron affinity and the surface dipole are also decreasing from the H-, to CH_3- and CD_3-terminated

Si(111) surfaces, respectively. The corresponding Φ found for these modified Si surfaces are 4.40, 4.05, and 4.07 eV, respectively, which is in compliance with previous studies.[88,117] The work function reveals a higher barrier for the electrons of slightly above ~ 0.33 eV in the case of H-terminated Si(111) surfaces as compared to methyl-terminated Si surfaces. A negative surface dipole has been found for each Si sample: – 0.09, – 0.48, and – 0.58 eV for H-, CH_3-, and CD_3-terminated Si(111) surfaces, respectively. Here, a difference about 0.10 eV is observed between the two methylated Si surfaces, which is in the range of the uncertainty error for the determination of these parameters. However, this could also certainly arise from the presence of different adventitious species still present on the Si surfaces (i.e., more Br atoms on CD_3-modified Si(111) surfaces, for instance). After annealing these samples, H-terminated Si(111) surfaces show no prominent change in the band bending. However, an important increase in the work function (+ 0.18 eV), electron affinity (+ 0.11 eV), and surface dipole (+ 0.11 eV) is observed.[118] In the case of CH_3-terminated Si(111) surfaces, no tremendous difference appears between the first and the second annealing step. However, in comparison to the fresh CH_3-terminated Si surfaces a tendency towards the flat band conditions is observed (– 0.07 eV), while for the electron affinity and the surface dipole only a small increase appeared (+ 0.03 eV after the second annealing). An increase of + 0.10 eV for the work function is already observed after the first annealing step. In the case of CD_3-terminated Si(111) surfaces, here again, an increase in the work function, electron affinity, and surface dipole occurs in relation to the fresh modified Si sample. In that case, higher increase of the band bending by + 0.07 eV is observed. The change in band bending, surface dipole and work function are probably due to the desorbtion of the adventitious Br atoms with the removal of the remnant aliphatic carbons from the Si surface. However, the electronic properties of the two type (CH_3 and CD_3) of methylated Si(111) surfaces after the annealing step are well correlated. An error of about ± 0.02 eV is observed for both annealed surfaces, except the work function where a difference of about ± 0.10 eV appears. However, this difference could also arise from the uncertainty error from the value determined for the work function.

According to the C 1s and Si 2p core level emissions recorded, these two annealed methylated Si surfaces have shown similar line shapes and behaviors which are well correlated here with the surface electronic properties deduced from the SXPS measurements.

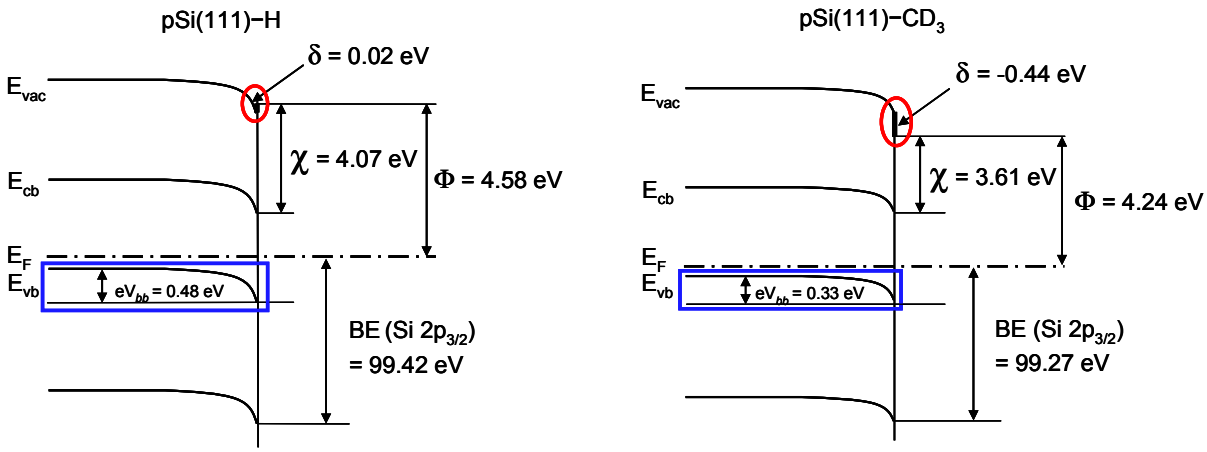

Fig. 5.13: *Energy band diagrams of H- and CD_3-terminated Si(111) surfaces after annealing at 390 °C for 30 min.*

Tab. 5.3: *Surface electronic properties of H-, and CH_3-, and CD_3-terminated Si(111) surfaces before and after annealing as determined from SXPS measurements.*

R=	Binding energy, Si $2p_{3/2}$ (eV)	Surface band bending, eV_{bb} (eV)	Work function, Φ (eV)	Electron affinity, χ (eV)	Surface dipole, δ (eV)
–H	99.41	0.47	4.40	3.96	-0.09
–H (annealed)	99.42	0.48	4.58	4.07	0.02
$–CH_3$	99.36	0.42	4.05	3.57	-0.48
$–CH_3$ (1^{st} annealing)	99.29	0.35	4.14	3.57	-0.48
$–CH_3$ (2^{nd} annealing)	99.29	0.35	4.15	3.60	-0.45
$–CD_3$	99.19	0.25	4.07	3.47	-0.58
$–CD_3$ (annealed)	99.27	0.33	4.24	3.61	-0.44
incertitude	± 0.05	± 0.05	± 0.10	± 0.15	± 0.15

1^{st} annealing: 390 °C for 30 min; 2^{nd} annealing: 430 °C for 30 min; Si $2p_{3/2}$ at hv = 650 eV.

5.3 PL characterization

In this section, non-radiative recombination active defects at the interface have been investigated for H-, CH_3-, and CD_3-terminated Si(111) surfaces. The PL intensity (I_{PL}) for these surfaces has been measured since I_{PL} is inversely related to the amount of non-radiative recombination active defects at the interface (see Chap. 3). Thereby, the study of I_{PL} gives information about the passivation of the modified Si surfaces obtained. Methyl groups (CH_3 and CD_3) have been well grafted onto Si(111) surfaces as shown previously by IRSE and SXPS measurements. Nevertheless, the results obtained so far for these modified Si(111) surfaces do not give any information about the electronic (passivation) properties of these layers at the Si interfaces. Therefore, PL investigations have been performed to observe the changes in the amount of non-radiative recombination active defects at the interfaces of these methyl-terminated Si(111) surfaces in relation with H-terminated Si(111) surfaces.

Comparison between H-, CH_3- and CD_3-terminated Si(111) surfaces

Fig. 5.14 shows the I_{PL} spectra of H-, CH_3-, and CD_3-terminated Si(111) surfaces, respectively. I_{PL} is the highest for H-terminated Si(111) surfaces (which corresponds to the lowest number of non-radiative recombination active defects at the interface). However, the methylated Si surfaces have only twice less I_{PL} in relation to H-terminated Si(111) surfaces. This behavior points out to a well passivated interface even for this type of surface modification. Likewise, a ratio intensity of ~ 30% is observed between CH_3- and CD_3-terminated Si(111) surfaces. Obviously, the modification of Si surfaces with CD_3 groups seems to present a better passivation than those modified with CH_3 groups. This demeanor is consistent with the SXPS results found out in the previous section of which the CD_3-terminated Si(111) surfaces have shown to possess a better splitting between the bulk and the surface contributions from Si surface (Si° and Si-CD_3, respectively) than the CH_3-terminated Si(111) surfaces. In the case of CH_3-terminated Si(111) surfaces, a second annealing has been necessary to observe in Si 2p core level spectra a splitting similar of those obtained by CD_3-terminated Si(111) surfaces. The I_{PL} of each Si(111) surfaces is centered at ~ 1140 nm, which corresponds to the band gap of the Si (E_g = 1.12 eV). Moreover, a slight shift in the higher wavelength (~ 10-15 nm) is noticed for the signals corresponding to methyl-terminated Si(111) surfaces in relation to H-terminated Si(111) surfaces.

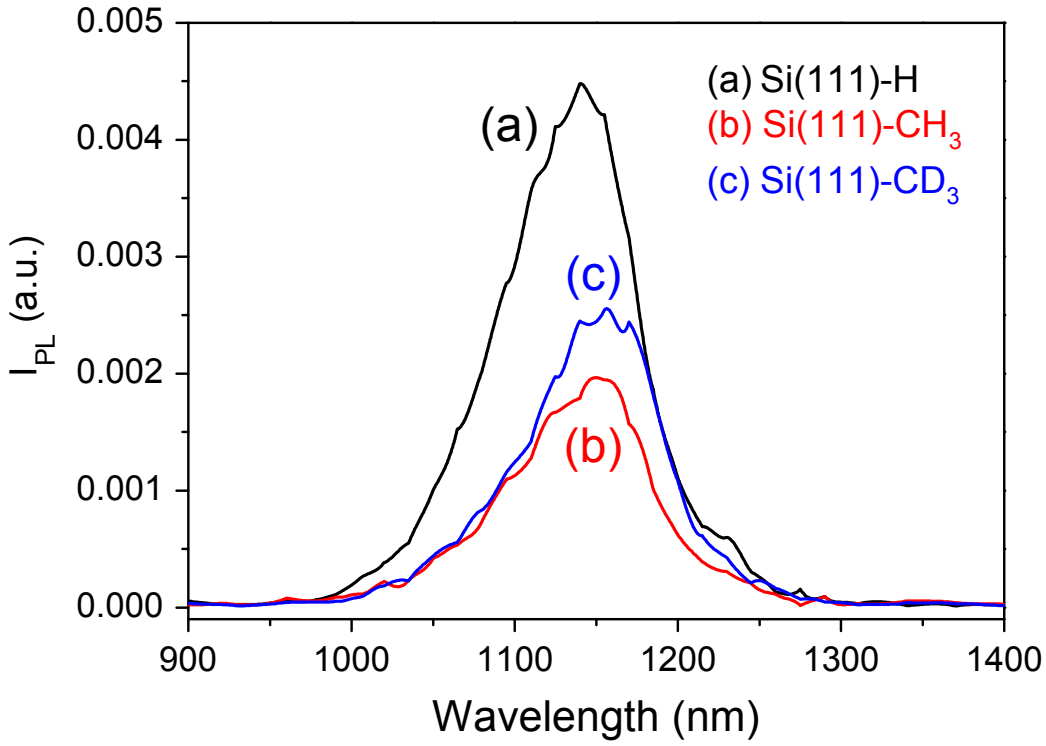

Fig. 5.14: *I_{PL} of (a) H-terminated, (b) CH_3-terminated and (c) CD_3-terminated Si(111) surfaces (excitation : 500 nm, 70 µJ per pulse, 0.6 ns pulse width).*

5.4 n-Si(111) surfaces modified by methyl groups

The electrochemical grafting of methyl groups on p-type Si surfaces has been successfully achieved following the electrochemical Grignard route. The same experiments have also been attempted on n-type Si(111) surfaces. The grafting of methyl groups on n-Si(111) surface is interesting in the development of a-Si/c-Si structure solar cells, for instance, where methyl layers could play the role of a buffer layer to enhance the passivation of the a-Si(p)/c-Si(n) interfaces.

Since n-type Si wafers possess an intrinsically majority of electrons in relation to holes, a halogen lamp (white light, 60 W) has been used during the electrochemical process to enlighten the Si electrodes. The light creates photo-induced holes for the electrochemical reaction with the Grignard solution.

5.4.1 IRSE measurements

Fig. 5.15 displays tan Ψ and Δ spectra obtained by IRSE measurements for n-Si(111) surfaces (a) oxidized in ambient air and a CH_3-terminated Si(111) surface which has been modified in CH_3MgI solutions, and (b) CH_3- and CD_3-terminated Si(111) surfaces which have been respectively modified in CH_3MgBr and CD_3MgI solutions. An anodic current density of 1 mA/cm^2 has been applied for each Si surface in the respective Grignard solutions. As expected the oxidized Si surface (Fig. 5.15a, black curve) reveals a large band at ~ 1212 cm^{-1} and is ascribed to SiO_x surface species.[119] The methylated Si surface (Fig. 5.15a, red curve) shows no band in the oxide region but a weak band at 1254 cm^{-1} due to the "umbrella" mode $\delta_s(CH_3)$ is well seen like for methylated p-Si(111) surfaces. Fig. 5.15a shows also the Δ spectra of these samples which exhibit an abrupt change only when a band occurs in the respective tan Ψ spectrum. This correlation gives a clear evidence of the omnipresence of silicon oxide and the real band corresponding to the CH_3 "umbrella" mode at ~ 1254 cm^{-1} for the respective modified Si surfaces. Moreover in both cases, the peak at 2083 cm^{-1} assigned to the symmetric vibrational mode of Si–H, ν_s (Si–H), is reflected by upward pointing peak feature. This indicates that the H atoms initially present on the surface have totally disappeared from the Si surfaces leaving place to oxide formation or methyl groups, respectively. Finally, all these results and more particularly the presence of the "umbrella" vibrational mode, $\delta_s(CH_3)$, is the better hint of the presence of methyl groups on Si surfaces and reveals the well achievement of methyl-terminated Si(111) surfaces even on n-type Si(111) wafers.

Nevertheless after having discovered that CH_3 groups can also be grafted onto n-Si(111) surfaces, the electrochemical grafting of CD_3 groups onto n-Si(111) surfaces has also been performed to observe and verify the typical shift expected between the "umbrella" vibrational modes, $\delta_s(CH_3)$ and $\delta_s(CD_3)$, for both CH_3- and CD_3-teminated Si(111) surfaces (Fig. 5.15b). Similarly, not only the methyl groups (CH_3- and CD_3) grafted onto p-Si(111) surfaces, but also methylated Si(111) surfaces obtained with n-type Si(111) surfaces show the presence of a downward pointing peak in the tan Ψ spectra. These downward pointing peaks at 975 and 1255 cm^{-1} are attributed to the "umbrella" vibrational mode of CD_3 and CH_3 groups, $\delta_s(CD_3)$ and $\delta_s(CH_3)$, for both methyl-terminated Si(111) surfaces, respectively. These bands are also well related to an abrupt change in the corresponding Δ spectra, which confirms the well grafting of these methyl groups onto n-Si(111) surfaces. In the same manner, it is noticed that the upward pointing peak at 2083 cm^{-1} corresponding to ν_s (Si-H) disappears.

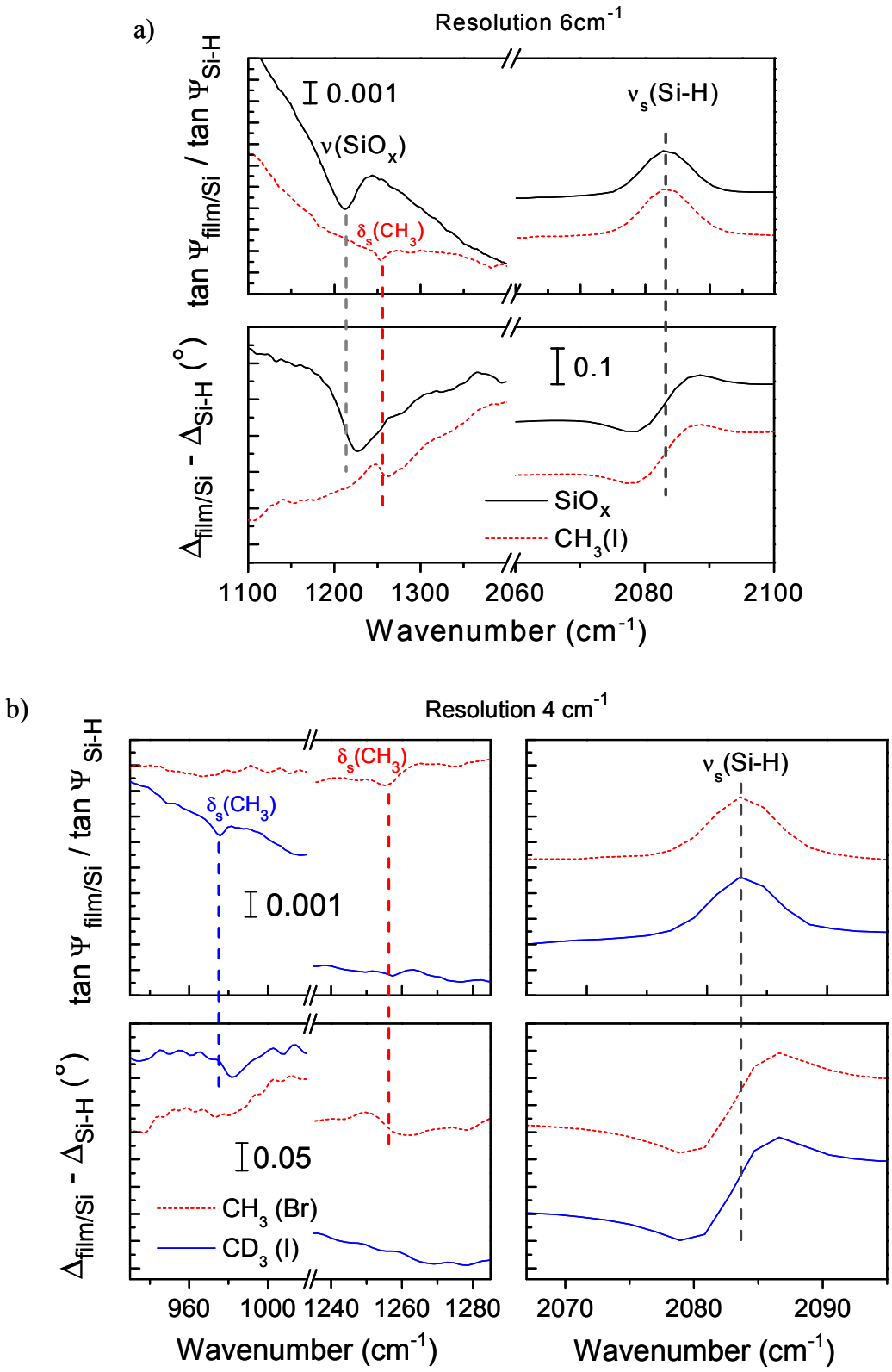

Fig. 5.15: *Tan Ψ and Δ spectra of (a) CH_3-terminated and oxidized n-Si(111) surfaces, and of (b) CH_3- and CD_3-terminated n-Si(111) surfaces, respectively. All spectra have been referenced to a H-terminated Si(111) surface.*

5.4.2 Comparison between n- and p-Si(111) surfaces using SXPS

The Si $2p_{3/2}$ peaks from n- and p-Si(111) surfaces exhibit the same trend for both H- and CD_3-terminated Si(111) surfaces, respectively. First, a shift is revealed after annealing the different Si surfaces at 390 °C for 30 min in relation with the same Si substrates non-annealed. A shift of about – 0.05 eV towards the lower binding energies for H-terminated Si(111) surfaces is observed, while in the case of CD_3-terminated Si(111) surfaces a shift of about + 0.03 eV is measured in the higher binding energies, for both n- and p-Si(111) type, respectively (not shown here).

However, Fig. 5.16 depicts the SXP spectra of Si 2p core level emissions in the case of H-terminated Si(111) and CD_3-terminated Si(111) surfaces after annealing of both n- and p-type Si(111) surfaces, respectively. A shift towards the lower binding energies at about + 0.30 eV is observed between n- and p-type H-terminated Si(111) surfaces. This shift is consistent with the E_F level of both p- and n-type Si.[120] Moreover, another shift about – 0.08 eV is also noticed between H-terminated Si(111) and CD_3-terminated Si(111) surfaces for both type of doped Si wafers, respectively. The shift of the bulk Si $2p_{3/2}$ emissions from H-terminated Si(111) to CD_3-terminated Si(111) surfaces is consistent with the fact that organic molecules have been grafted onto Si surfaces and thus modify the electronic structure of theses surfaces (organic molecules/Si interfaces). However, the shift which occurs for both type Si is in the same direction (towards the lower binding energy). This behavior is not clear until now since the shift of the CD_3-terminated n-Si(111) surfaces is expected to be towards the higher binding energy in relation to the H-terminated n-Si(111) surfaces. Thus, further investigations have to be performed with other organic molecules to understand this interesting phenomenon. Furthermore, no amount of SiO_2 at ~ 104 eV is observed for both H-terminated Si(111) surfaces. In the case of both CD_3-terminated Si(111) surfaces, a very tiny hump arises out of the background at ~ 104 eV. This suggests that very few amounts of SiO_2 have grown after the modification of Si(111) surfaces. However, these amounts are very small as related to the formation of SiO_2 with a thickness of 2 nm. Amazingly, these Si 2p core level spectra for both methylated Si(111) surfaces obtained by the grafting of CD_3 molecules on Si(111) surfaces show a well-defined splitting between the contribution for Si 2p from the bulk Si° and the Si–C bonds formed from the CD_3 groups. Nevertheless, this splitting is more significant for p-type than for n-type CD_3-terminated Si(111) surfaces and is a result of a clean and a well modified Si(111) surfaces terminated with CD_3 groups.

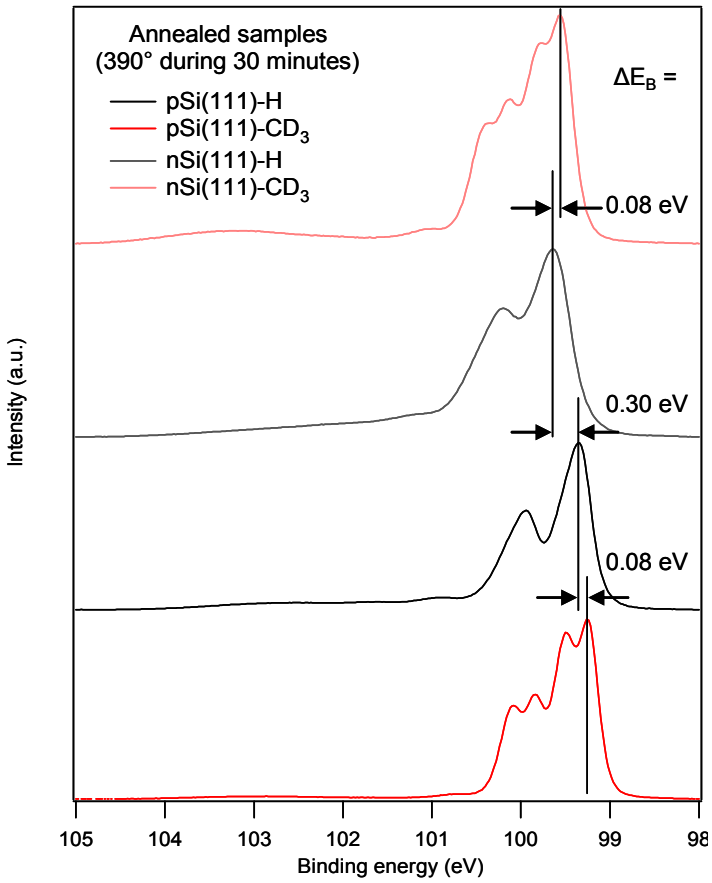

Fig. 5.16: *SXP spectra of Si 2p core level emission from H- and CD_3-terminated Si surfaces for both n- and p-Si(111) substrates. Each spectrum has been recorded with photon energy of 150 eV (surface sensitive condition).*

5.4.3 Comparison between n- and p-Si(111) surfaces using SPV

The change in band bending of organically modified Si surfaces can be easily observed with SPV measurements as illustrated in Fig. 5.17. The measurements have been performed with the application of a short laser pulse (λ_{ex} = 902 nm, pulse width 150 ns) after 4 µs of pre-polarization under a potential of 20 and 200 mV for methylated (CH_3 and CD_3 groups) and H-terminated Si(111) surfaces, respectively. A short transient has been applied in order to observe the shape and to determine the accurate value of the photovoltage response, U_{Ph}, from these Si surfaces. Thus, the change in band bending can be determined by the change observed in the photovoltage response since these two physical "magnitudes" are proportional. For this, n- and p-doped Si(111) wafers have been investigated after organically modification of the Si samples to verify the direction change of the band bending due to the different doping of the Si wafers used. Fig. 5.17 depicts the change occurred between H- and the methyl-terminated Si(111) surfaces for (a) p-type and (b) n-type Si(111) wafers, respectively.

In the case of p-doped Si(111) surfaces, H-terminated Si(111) sample exhibits a photovoltage response at $U_{Ph} \approx -483.6$ mV. This observation is consistent with previous values reported in the same energy range for H-terminated Si(111) surfaces, but with a small deviation due to the different doping of Si wafers studied. The methylated Si surfaces modified in CD_3MgI and CH_3MgBr solutions reveal a smaller U_{Ph} at around -9.5 mV and -23.3 mV, respectively, in relation to H-terminated Si(111) surface. The change in U_{Ph} between the H-terminated and the methylated Si surfaces by more than a factor 10 gives rise to the presence of methyl groups on the modified Si(111) surfaces. Since a smaller band bending is observed for both CH_3- and CD_3-terminated Si(111) surfaces in comparison to H-terminated Si(111) surface, these modified Si surfaces indicate a smaller depletion, which can be interpreted as an easier charge transfer between the methyl groups and the p-type Si substrate. Moreover, these smaller band bending reveal a better electronic passivation since more surface gap states are recovered, which indicates a direction to the flat band conditions. Furthermore, a difference of U_{Ph} about 13 mV occurs between CH_3- and CD_3-terminated Si(111) surfaces. This is certainly due to the presence of some remnant adventitious species on the surface (aliphatic carbons, Br or I atoms,…) which can strongly change the band bending at the Si surface. However, the results observed here is consistent with those obtained from SXPS and PL measurements, which have also revealed a “higher” efficiency in the case of Si surfaces modified in CD_3MgI solution.

In the case of n-doped Si(111) surfaces, an expected change in U_{Ph} in the other direction occurs. The H-terminated Si(111) surface reveals a value at $U_{Ph} \approx 80.7$ mV while methylated Si surfaces modified in CH_3MgBr and CD_3MgI solutions lead to an U_{Ph} of about 192.5 mV and 266.8 mV, respectively. The increase of the band bending due to the presence of these molecules is consistent with the fact that methyl groups are electron donator molecules. On n-type Si surfaces, the electron transfer from the methyl groups to the Si surface results to a higher band bending, i.e., to a stronger depletion in the space charge region near the surface, in relation to H-terminated Si(111) surface. However, here again, CD_3-terminated Si(111) surface indicates a “higher” efficiency of charge transfer since a difference of U_{Ph} about + 74 mV occurs between methylated Si surfaces modified in CH_3MgBr and CD_3MgI solutions, respectively.

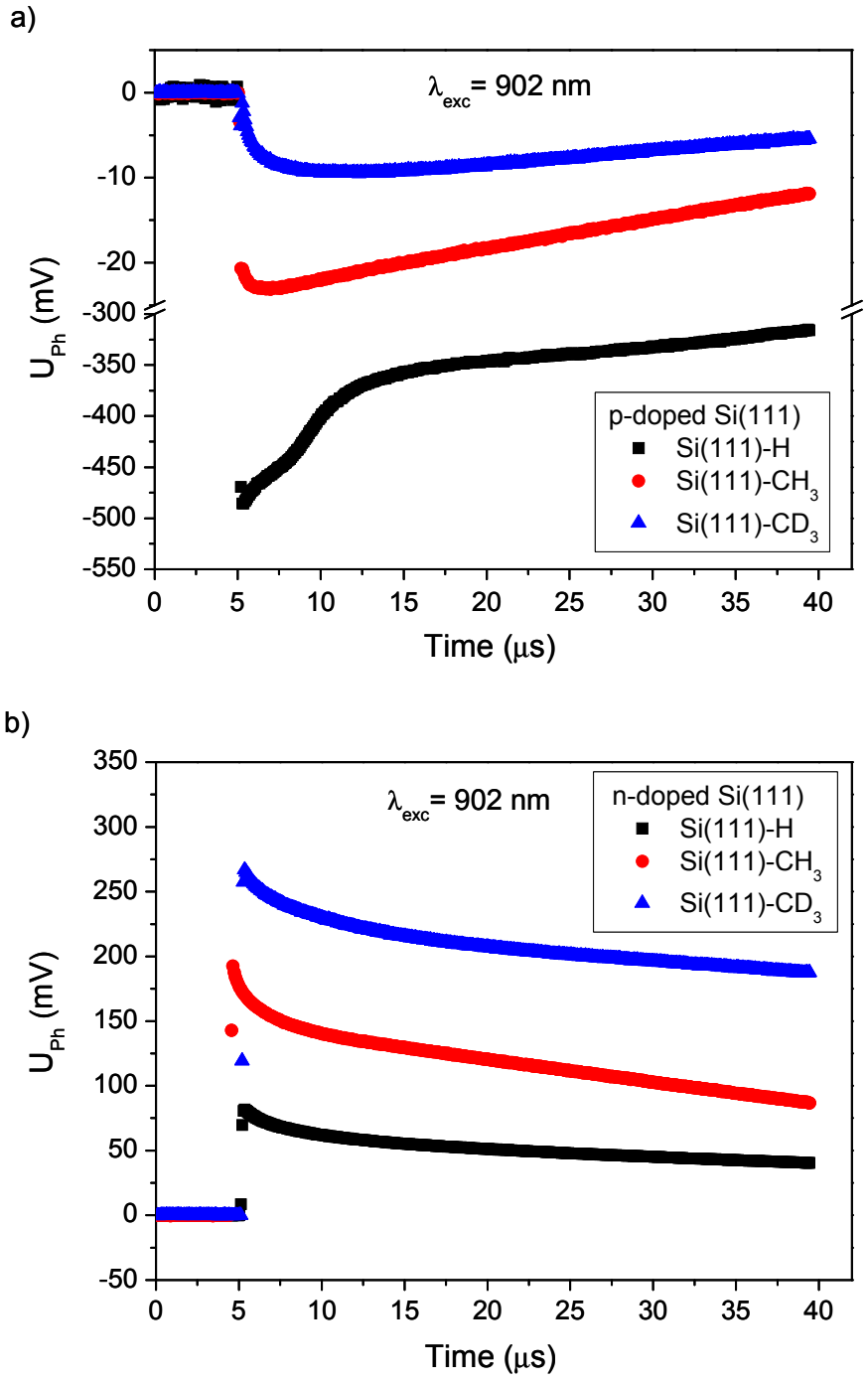

Fig. 5.17: *SPV transients of methylated (CH_3 and CD_3 groups) and H-terminated Si(111) surfaces on (a) p-Si(111), and (b) n-Si(111) substrates recorded after 4 µs under a potential of 20 mV and 200 mV, respectively. The methylated surfaces have been electrochemically prepared from methylmagnesium bromide and methyl-d_3-magnesium iodide Grignard solutions.*

5.5 Stability of methylated Si(111) surfaces

Hydrogenated Si(111) surfaces are known to possess low interface state densities ($D_{it} \cong 5\ 10^{10}\ cm^{-2}\ eV^{-1}$).[121] Unfortunately, these passivated Si surfaces degrade rapidly in ambient atmosphere (after just some hours or even few minutes). Thus, an alternative way to avoid this demeanor, is to protect the Si surface by the creation of an organic surface layer.[22] For this purpose, methyl groups are chosen as potential organic layer since methyl groups present the specific particularity to have a van der Waals diameter of ~ 2 Å. These molecules are small enough to fit in all atop Si surface atoms (atomic distance between adjacent Si surface sites is 3.8 Å). For this reason, the stability and robustness of methylated Si(111) surfaces have been investigated with IRSE, SXPS and PL experimental techniques. In this section, the stability of methylated Si(111) surfaces in ambient atmosphere has been compared to the H-terminated Si(111) surfaces by IRSE characterizations for a period of 22 days and after several months as well. Additionally, methylated Si(111) surfaces have been investigated with SXPS and PL techniques during a period of 12 days and 1 year, respectively.

5.5.1 IRSE investigations

Stability of CH_3-terminated Si(111) surfaces against oxidation in ambient air

Fig. 5.18 shows (a) the evolution of normalized tan Ψ spectra of H- and CH_3-terminated Si(111) surfaces in the 1000-1350 cm^{-1} range, and (b) tan Ψ spectra of H-terminated Si(111) surfaces in the 1800-2220 cm^{-1} region, up to 22 days of oxidation in ambient air. In Fig. 5.18a, each spectrum has been referenced to the fresh H-terminated Si(111) surface. The two tan Ψ of the fresh Si surfaces: H-, and CH_3-terminated Si(111) surfaces have been used as Si substrates reference for both modified surfaces, respectively. The IRSE study reveals that the $\delta_s(CH_3)$ "umbrella" mode at 1253 cm^{-1} is still conspicuous after 22 days in ambient air in the case of CH_3-terminated Si(111) surfaces. Moreover, no protuberant peak in the oxide region is observable for this modified surface even after 22 days of exposure in ambient air. Only a weak hump at ~ 1200 cm^{-1} could be suggested. On the contrary, in the case of H-terminated Si(111) surfaces, the peak related to Si–H at 2083 cm^{-1} decreases rapidly in 4 days whereas the peak related to SiO_x clearly appears after 12 days.

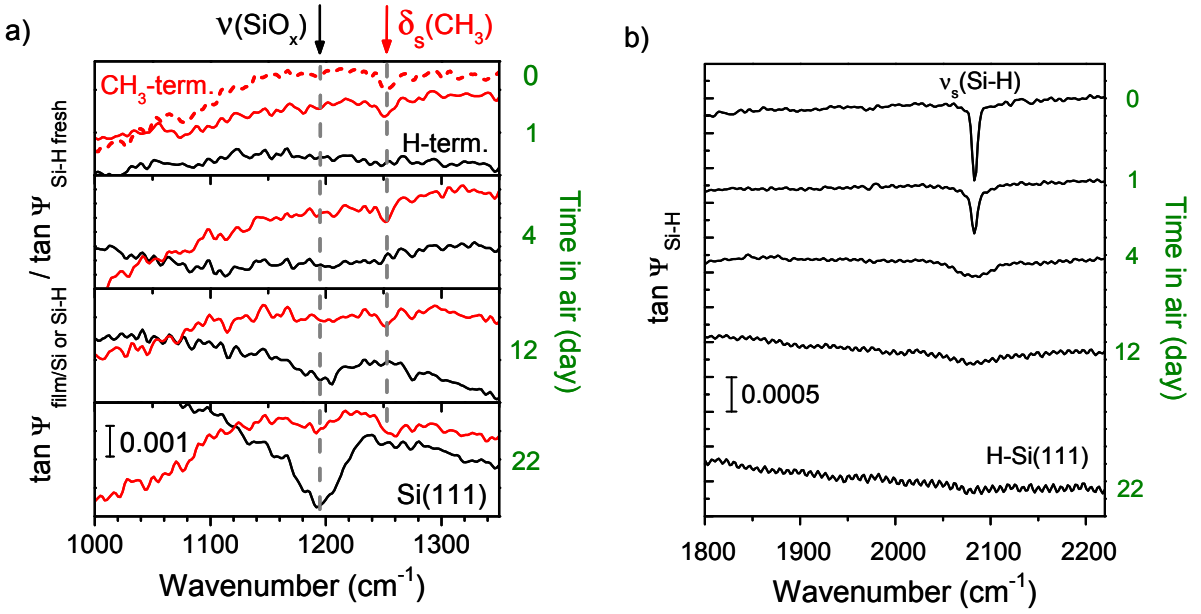

Fig. 5.18: *(a) tan Ψ spectra during the oxidation process of H-Si(111) and CH_3-Si(111) surfaces (black and red curves, respectively) in ambient air up to 22 days (---, fresh methylated Si surface); (b) oxidation of H-Si(111) surface in the ν(Si-H) regime. The spectra were shifted for visual convenience.*

This behavior is quite uncommon since H-terminated Si(111) surfaces are well known to oxidize more rapidly (normally after already some hours in ambient atmosphere). However, the humidity of the laboratory room where the samples were laid down has not been measured. Obviously, an intermediate Si–OH or Si–O–Si–H (silicon backbond oxide) layer is formed and is stable for a longer time period. However, in the case of H-terminated Si(111) surfaces after 22 days, a prominent peak is observable in the 1100-1250 cm^{-1} range and is assigned to an amount of ~ 1 nm (3 ML) of silicon oxide (SiO_2).

Fig. 5.19 compares the CH_3- and H-terminated Si(111) surfaces stayed for a period of 5 months in ambient atmosphere with a fresh CH_3-terminated Si(111) surface. As expected in the case of H-terminated Si(111) surfaces, a tremendous peak centered at 1218 cm^{-1} occurs due to the formation of silicon oxide, SiO_2. Moreover, two weak peaks are also observed at 1095 and 1108 cm^{-1}, respectively, and are certainly due to other vibrational modes from SiO_2. CH_3-terminated Si(111) surfaces did not reveal any band centered at 1218 cm^{-1} corresponding to SiO_2 vibrational modes. However, a weak hump located in the 1060-1190 cm^{-1} region appears for the CH_3-terminated Si(111) surface exposed to ambient atmosphere for 5 months. Both CH_3-terminated Si(111) surfaces exhibit a weak band at 1253 cm^{-1} assigned to δ_s (CH_3) symmetric "umbrella" vibrational mode of CH_3 groups. However, the absorption band due to δ_s (CH_3) seems to be slightly reduced after 5 months in ambient air but was still present.

These results suggest that CH_3-terminated Si(111) surfaces are much better passivated against oxidation in ambient air than H-terminated Si(111) surfaces.

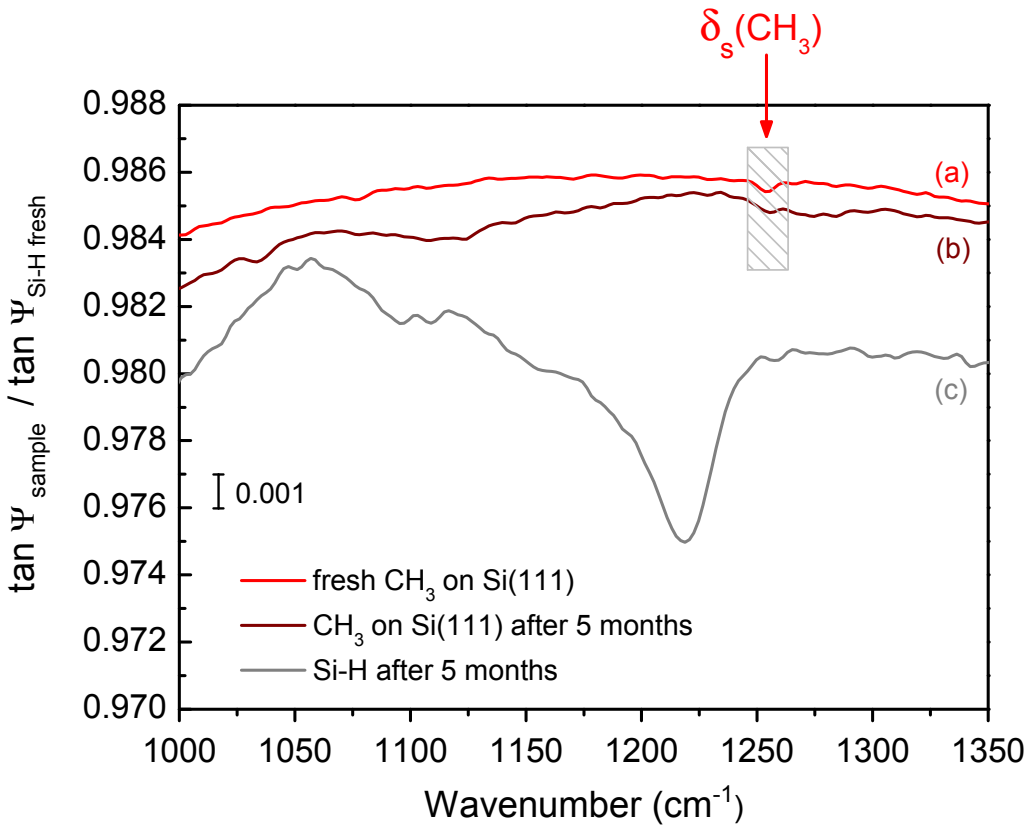

Fig. 5.19: *Tan Ψ spectra of (a) freshly CH_3-terminated, (b, c) CH_3- and H-terminated si(111) surfaces after 5 months in ambient atmosphere. Each spectrum has been referenced to a fresh H-terminated Si(111) surface and has been shifted for better clarity.*

Effect of the pulsed laser on Si(111) surfaces

The effect of the pulsed laser used in the PL equipment to characterize CH_3-terminated Si(111) surfaces will be discussed and compared to the PL measurements performed on H-terminated Si(111) surfaces.

Fig. 5.20 shows tan Ψ spectra of (a) a fresh H-terminated Si(111) surface, (b) a H-terminated Si(111) surface after 5 months in ambient atmosphere, and (c) a H-terminated Si(111) surface which has been investigated with PL (laser-irradiated) up to 45 days. In the case of samples (b) and (c), the presence of Si–H peak located at 2081 cm^{-1} is not seen anymore. However, Si–H peak is present for the freshly prepared H-terminated Si(111) surface (not shown here). The disappearance of this peak is consistent with the growth of oxide on the Si surfaces leading to a higher amount of non-radiative recombination centers which quenches the PL intensity. Besides in the case of sample (b), vibrational bands in the SiO_2 region are

observed and are totally different from the bands which are observed in the case of sample (c). Obviously, different type of oxide species are formed when a pulsed laser has been used to investigate H-terminated Si(111) surfaces. In the case of sample (c) more vibrational structural changes are indicated in comparison to sample (b).

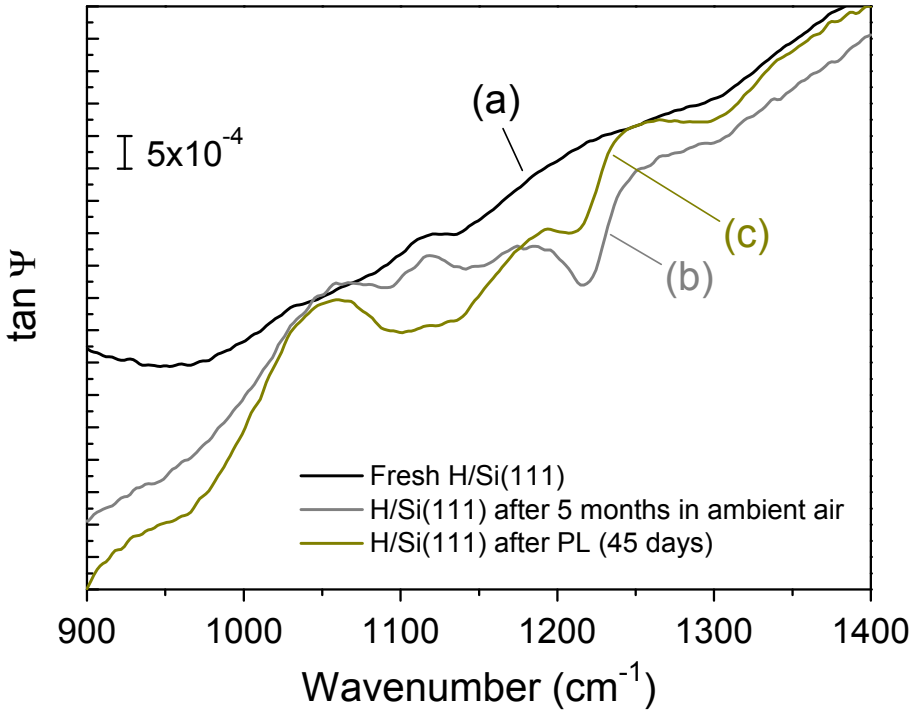

Fig. 5.20: *Tan Ψ spectra of (a) fresh H-terminated Si(111) surface, and (b, c) H-terminated Si(111) surfaces after 5 months in ambient air and after PL irradiation, respectively.*

Besides in the case of sample (b), two pronounced bands at 1091 and 1216 cm^{-1}, and two slight shoulders at 1143 and 1301 cm^{-1} are observed, while the sample (c) exhibits a very huge hump centered at 1115 cm^{-1} (which has recovered the two separated peaks observed in the sample (b)), a weak band at 1216 cm^{-1} (weaker than the sample (b)), and a small shoulder at 1301 cm^{-1} (bigger than the sample (b)) as well. Therefore, it seems that the oxidation mechanism which occurred for these two different H-terminated Si(111) surfaces did not follow the same process.

Fig. 5.21 depicts several CH_3-terminated Si(111) surfaces treated in the same manner than the H-terminated Si(111) surfaces in Fig 5.20. The laser processing leads to oxide formation, even on the CH_3-terminated Si(111) surfaces. Obviously, the oxidation of CH_3-terminated Si(111) surfaces is much less pronounced than for the H-terminated one. However, the CH_3-terminated Si(111) surface exposed to PL measurements for a period of 45 days reveals a

higher amount of silicon oxide than the CH_3-terminated Si(111) surface which has been stored for 5 months in ambient air. Thus, this demeanor gives entirely evidence that pulsed laser used in the PL measurements plays a role (affect and damage the Si surfaces measured) in the rapid growth of the silicon oxide formation.

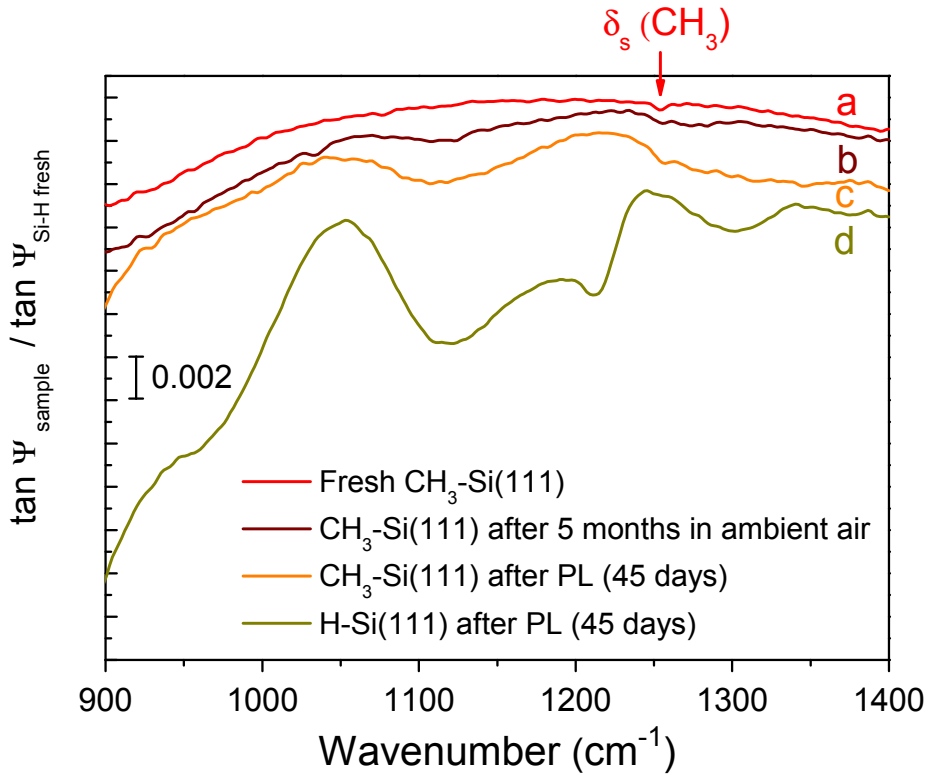

Fig. 5.21: *Referenced tan Ψ spectra of (a) freshly prepared CH_3-terminated Si(111) surface, (b, c) after oxidation in ambient air for 5 months and during PL treatment, respectively, and (d) H-terminated (111) surface after PL treatment. All spectra have been normalized to tan Ψ spectrum of a fresh H-terminated Si(111) surface.*

Another important role that CH_3-terminated Si(111) surfaces revealed, is that even after storing the Si sample for 5 months in ambient air (Fig. 5.21b), δ_s (CH_3) "umbrella" vibrational mode is still distinguishable. Moreover, very few oxide amounts are observable in that case. These results indicate a very good stability of the methylated Si(111) surface prepared. Furthermore, in comparison to the H-terminated Si(111) surface which has also been characterized by PL measurements (Fig. 5.21d), it is well shown that the CH_3 groups strongly protect the Si surfaces against oxidation (see the tremendous difference between CH_3- and H-terminated Si(111) surfaces exposed to PL measurements, Fig. 5.21). Additionally as remark, CD_3-terminated Si(111) surface which has also been sustained by the same PL measurements shows no distinct difference to the results obtained for the CH_3-terminated Si(111) surface illustrated here (not shown).

Treatment in 5% HF solution reveals the robustness of CH_3-terminated Si(111) surfaces

The aim of this experiment is to discover whether methyl groups are still anchored to Si(111) surfaces after treatment in 5% HF solution (Fig. 5.22), like it was already observed in the case of aryl groups deposited on Si(100) surfaces.[122] The same CH_3-terminated Si(111) surface has been characterized by IRSE measurements after treatment in 5% HF solution for different time periods. The fresh CH_3-terminated Si(111) surface (red curve) has been first performed by IRSE, then the Si sample has been dipped in 5% HF solution for 5 min (violet curve), and measured again by IRSE. Finally, this same Si sample has been again dipped for 25 min in the same solution (purple curve). No IR absorption due to SiO_2 is visible in the 1000-1200 cm^{-1} region for the fresh CH_3-Si(111) surface.

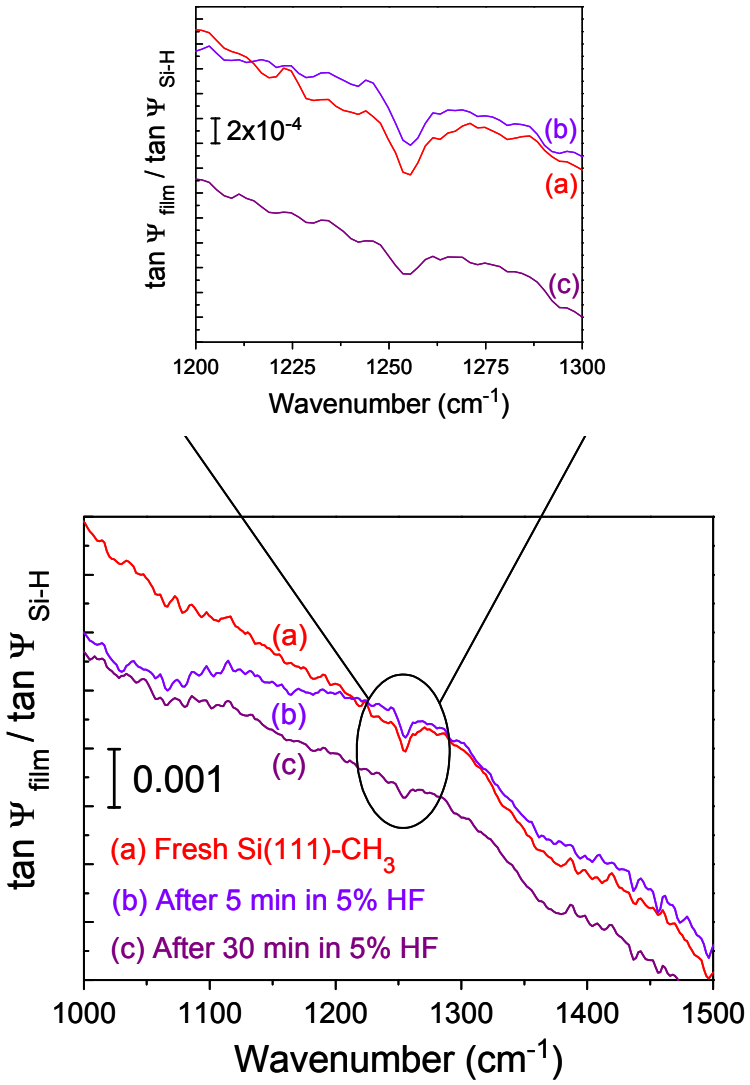

Fig. 5.22: *Referenced tan Ψ spectra of (a) a fresh CH_3-terminated Si(111) surface, (b, c) dipped in 5% HF solution for 5 and additional 25 min, respectively. Each spectrum has been referenced to tan Ψ spectra of H-terminated Si(111) surface.*

Furthermore, the band corresponding to δ_s (CH_3) "umbrella" vibrational mode is well observed at ~ 1255 cm^{-1}. Likewise, no bands in the SiO_2 are revealed when the sample is dipped in 5% HF solution for 5 and 30 min, respectively. This demeanor shows clearly that CH_3 groups protect strongly the Si(111) surfaces towards oxidation in the etching solution, which is also a hint of the robustness of CH_3 groups. However, even if the "umbrella" vibrational mode δ_s (CH_3) is still present, it tends to decrease slowly after treatments in 5% HF (see top panel on Fig. 5.22). A probable explanation of this decrease can be that HF solution not only etches SiO_2 on the Si surface but also attacks Si after a longer time period, and consequently some methyl groups are dissolved together with the Si atoms. However, this figure reflects the robustness of methylated Si(111) surfaces in presence of 5% HF solution even after 30 min of etching.

Another sample which has been stored in ambient air for ~ 407 days (~ 13 months) has also been etched in 5% HF solution and the respective tan Ψ spectra in the CH_3 "umbrella" mode region have been plotted in Fig. 5.23. Surprisingly, the peak at 1253 cm^{-1} assigned to the symmetric bending vibrational mode of CH_3 groups is still ubiquitous after a period of more than one year in ambient air and only a slight IR-absorption band due to SiO_2 is visible. Thus, the same treatment in 5% HF solution has also been performed for this "older" CH_3-terminated Si(111) surface. Astonishingly, here again the δ_s (CH_3) "umbrella" vibrational mode located at 1253 cm^{-1} is still visible even after 30 min in 5% HF solution. This behavior indicates the robustness of these methyl layers against oxidation and HF dipping, and gives a hint that these methyl groups are well attached to Si(111) surfaces. Moreover, the δ_s (CH_3) signal is not slowly decreased like it has been illustrated in the case of the fresh CH_3-terminated Si(111) surface after 30 min in 5% HF solution.

After treatment in 5% HF solution for 5 min, the broad band attributed to silicon oxide in the 1000-1200 cm^{-1} region does not disappear at all. Nevertheless, after additional treatment for 25 min in 5% HF solution this band totally disappears. However, some additional features in the 1260-1300 cm^{-1} range grow up after ~ 407 days in ambient air and seem to disappear when the sample is treated in 5% HF solution for 5 min. But these peaks reappear after the treatment in 5% HF solution for additional 25 min. Until now, the origin of these additional peaks is still not clear. Further attempts have to be realized to understand the origin of these features.

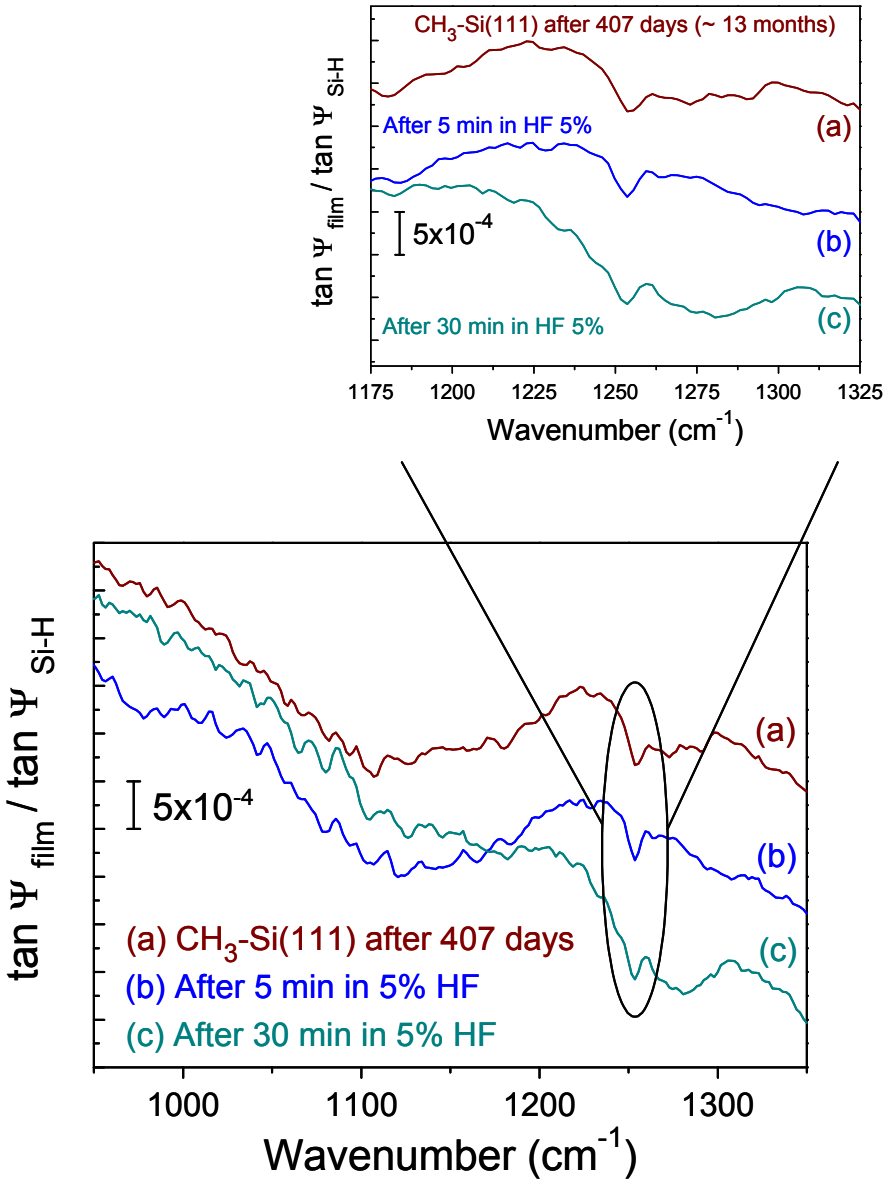

Fig. 5.23: *Referenced tan Ψ spectra of CH_3-terminated Si(111) surfaces: (a) after 407 days in ambient atmosphere, (b, c) after subsequent 5% HF-dip for 5 and additional 25 min, respectively. Each spectrum has been normalized to tan Ψ spectra of H-terminated Si(111) surface.*

5.5.2 SXPS measurements

The stability of H- and CH_3-terminated Si(111) surfaces have also been compared by SXPS measurements. For this, a Si sample has been prepared following the common process already explained in Chap. 4 with treatment in 40% NH_4F concentrated solution in order to obtain flat H-terminated Si(111) surfaces, while another Si sample has been obtained after an additional electrochemical treatment under anodic current density of 1 mA/cm^2 for 5 min in a

Grignard solution containing methyl groups (CH_3MgBr solution). After the preparation of the samples, the Si samples have been directly transferred to the SoLiAS analysis chamber at the synchrotron BESSY II for SXPS measurements. For the investigations of these Si surfaces in ambient air as function of the time, the procedure performed for the measurements are as followed: the fresh Si samples are first transferred into the analysis chamber under UHV conditions and are measured. Then, they are taking out from the SXPS equipment and have been laid in ambient atmosphere for the period of time required. Afterward, the samples have been transferred again in the UHV chamber for the next measurements. The Si samples have also been transferred into a nitrogen-purged glove box from time to time in order to wait for the next SXPS measurements.

The SXP core level spectra of Si 2p, C 1s, and Br 3d obtained from this series of measurements are shown in Fig. 5.24. High resolution Si 2p and Br 3d core level emissions have been collected at photon energy of 150 eV to be under surface sensitive conditions, whereas C 1s core level emission has been performed with photon energy of 650 eV. The both H- and CH_3-terminated Si(111) surfaces freshly prepared do not reveal the formation of SiO_x species since no peak at around + 3.5 eV towards higher binding energies than the bulk Si $2p_{3/2}$ signal, labeled as Si^0, has been observed. However, after half a day (~ 14 h) exposed in ambient air the former H-terminated Si(111) surface displays a prominent peak due to SiO_x. This statement reveals the fast growth of the silicon oxide on this surface. The area of this peak seems then to increase slowly, while the area of Si^0 decreased strongly by ~ 40% after 14 h and after 25 h as well. Then, the decrease is slightly less pronounced but still continues. Between 2 and 4 days, the amount of oxide signals becomes more intense than the Si^0 peak signal area. Obviously, CH_3-terminated Si(111) surface exhibits a lower formation rate of SiO_x than H-terminated Si(111) surface as observed from the SiO_x peak area for these modified Si surfaces. Moreover, the Si^0 peak of the CH_3-terminated Si(111) surface continuously decreases by ~ 10% from the fresh sample until 2 days of measurements, and then a stronger decrease by ~ 50% occurs from 2 until 4 days of oxidation. After 4 days, the Si^0 peak position is shifted to lower binding energy. As observed on Fig. 5.24, this peak area is still more prominent in comparison to the growth of SiO_x species.

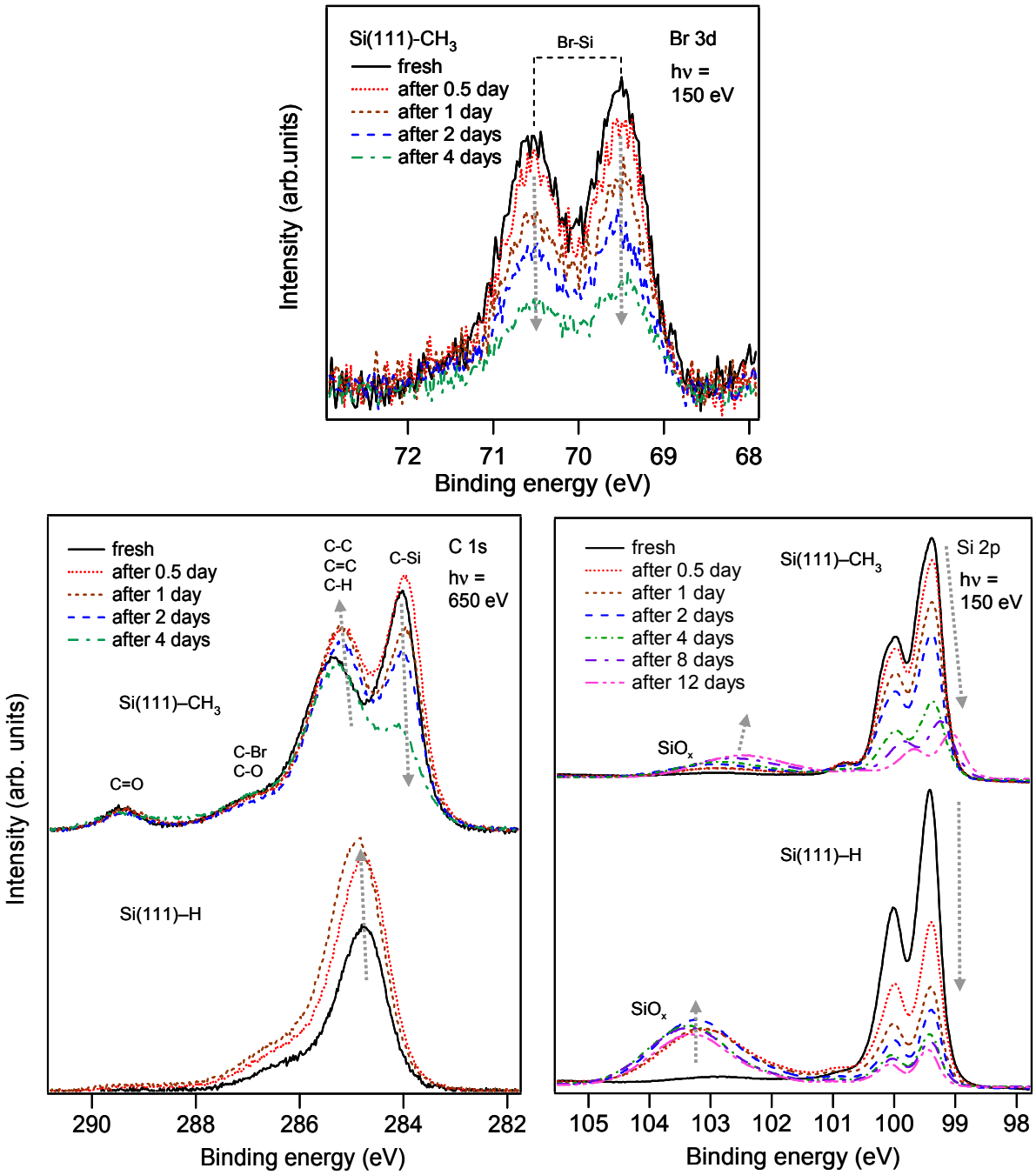

Fig. 5.24: *High-resolution of Si 2p, C 1s and Br 3d core level emissions from H- and CH_3-terminated Si(111) surfaces performed under synchrotron radiation (hν = 150 eV for Si 2p and Br 3d emissions, and 650 eV for C 1s emission, respectively). The Si 2p emission spectra are shown up to 12 days, whereas Br 3d and C 1s emissions are illustrated until 4 days in ambient air.*

Additionally, C 1s and Br 3d core level spectra show the different type of C and Br atoms present on the surface. Fig. 5.24 indicates also the omnipresence of Br atoms on the CH_3 modified Si surfaces. The different features in the C 1s core level emissions have been already explained (see subsection 5.2.1). The more intense emission at ~ 283.97 eV is attributed to Si atoms bonded to C atoms from the CH_3 groups, whereas the peak at ~ 285.30 eV is assigned

to adventitious aliphatic carbons. The weak shoulder at ~ 286.81 eV is ascribed to C bonded to O or Br atoms, obviously due to the rinse procedure after the electrochemical grafting process. The weak peak at 289.47 eV is probably due to C double bonded to O atoms and could be ascribed to C=O because of the high chemical shift observed towards the higher binding energies or to the satellite π-π^*.[102,103] These attributions have been done with respect to the electronegativities of the element (C: 2.55 and O: 3.44, respectively). The C 1s photopeak recorded for H-terminated Si(111) surface exhibits no emission from C bonded to Si or Br atoms. This behavior is consistent with the fact that this surface has not been in contact with the bromobutane solution and has not also been treated with Grignard solutions. The C 1s photopeak spectra observed for H-terminated Si(111) surfaces show only emissions from aliphatic remnant carbons (C–H, C–C, or C=C bonds) at ~ 284.77 eV and a weak hump at ~ 286.41 eV assigned to C bonded to O atoms (C–O bonds). However, the C 1s emission corresponding to the aliphatic carbon atoms increases slightly for both surfaces, while the C 1s emission due to the C–Si bonds from CH_3 groups decreases slowly with the time, but is still visible even after 12 days in ambient air. Surprisingly, a shift towards lower binding energies occurs. Furthermore, the peak emissions of C–Si bonds and aliphatic carbon atoms observed after 1 day of measurement have approximately the same intensity. So, the presence of aliphatic carbons seems to adhere easily to the surface by physisorbtion. The high resolution of Br 3d core level spectra of CH_3-terminated Si(111) surface reveal that more Br bonded to Si atoms (Br–Si) are present as Br bonded to C atoms (or others atoms) since main part of the signals arise from Br–Si bonds. However, the diminution of this peak could also arise from the "coverage" of the aliphatic carbons, but it is supposed here that this diminution is more probably due to the irradiation of the Si samples by synchrotron radiation since high energy is necessary to break these bondings. These assumptions will be discussed in more details together with the following figures and also by means of the PL characterization of these modified Si surfaces in relation to the H-terminated Si(111) surface.

Since silicon oxide species in different oxidation states appear from about + 1.5 to + 3.5 eV towards higher binding energies than the bulk Si $2p_{3/2}$ emission, Si^0, the corresponding peak intensity ratio is obtained from the integral of this area between 101.2 to 106.1 eV. The peak area corresponds to the coverage of Si^{1+}, Si^{2+}, Si^{3+}, and Si^{4+} oxide species on the surface. Moreover, since the SiO_x:Si 2p peak area ratio is independent of the photoionization cross-section of all the species present on the surface, the determination of the fraction of equivalent monolayers of silicon oxide, SiO_2 can be easily estimated.

Fig. 5.25 depicts the SiO_x:Si 2p peak area ratio as determined from data of Fig. 5.24 for H- and CH_3-terminated Si(111) surfaces collected at excitation energy of hν = 150 eV and 650 eV, respectively, for an extended exposed period time of up to 12 days in ambient air.

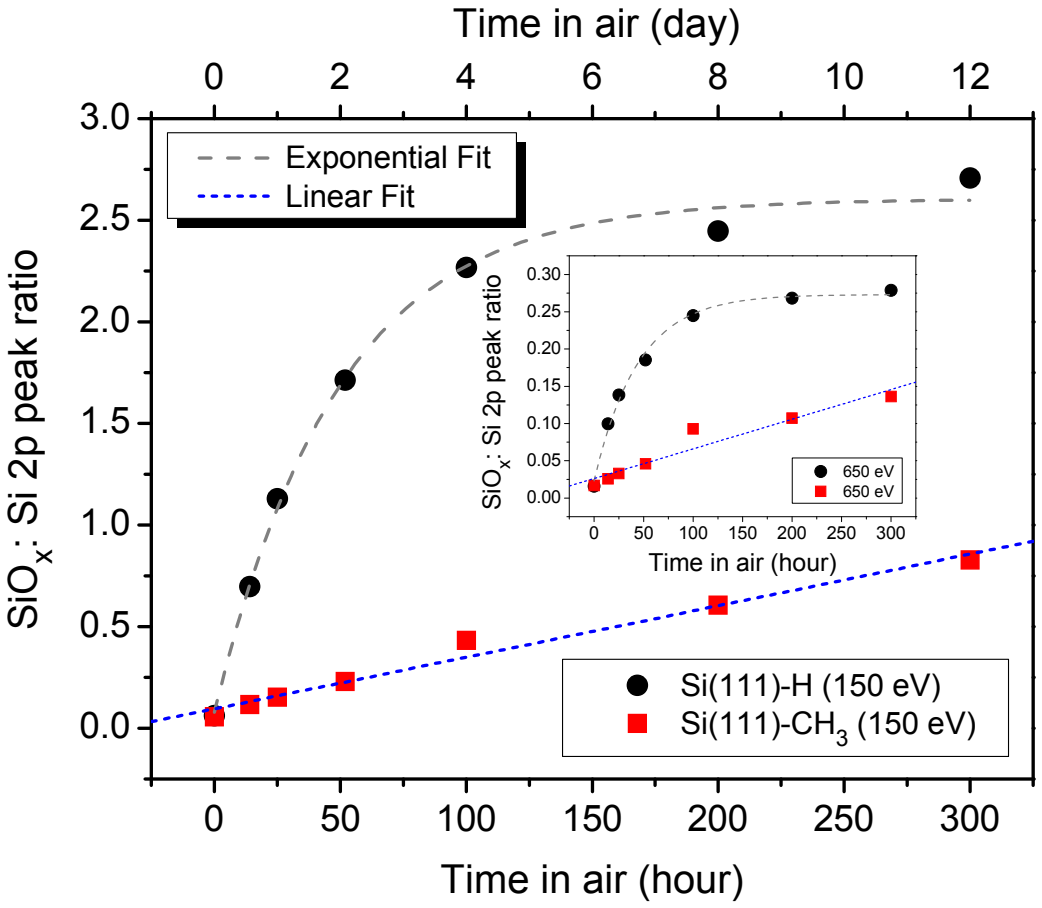

Fig. 5.25: *Ratio of the oxidized Si 2p peak area, SiO_x, to the bulk Si 2p peak area for H- and CH_3-terminated Si(111) surfaces exposed to ambient air up to 12 days as calculated from the spectra in Fig. 5.24, respectively (hν = 150 eV, insert: hν = 650 eV).*

The SiO_x:Si 2p peak area ratio corresponds to the measured ratio of oxidized (SiO_x) to un-oxidized Si surface (Si^0). The ratio calculated is used to determine the monolayer equivalents of SiO_2 present on the Si surfaces. The same trend occurred between the two excitation energies carried out and a factor ~ 10 is observed from 150 to 650 eV since lower excitation energy is more surface sensitive. The ratio of H-terminated Si(111) surfaces increases rapidly compared to CH_3-terminated Si(111) surface. The increase from the H-passivated Si(111) surfaces follow an exponential tendency while the CH_3-terminated Si(111) surfaces reveal a linear trend with a small slope. However, after about 100 h (~ 4 days) in ambient air, the CH_3-terminated Si(111) surfaces exhibit only ~ 20 and 40% from the SiO_x present on the H-terminated Si(111) surface at hν = 150 and 650 eV, respectively. Finally, after approximate-

ly 288 h (~ 12 days), ~ 30 and 50% of SiO_x has been determined on CH_3-terminated surface as compared to H-terminated Si surface at hν = 150 and 650 eV, respectively. A good correlation is observed between the SiO_x:Si 2p peak area ratio calculated from the Si 2p emission spectra recorded at the two different excitation energies, which is not surprising. However, under surface sensitive condition (hν = 150 eV) a higher difference in the amount of oxide has been observed between the two modified Si surfaces.

The evolution of the surface band bending of H- and CH_3-terminated Si(111) surfaces established from the determination of the bulk Si $2p_{3/2}$ emission peak from the Si 2p core level spectra performed at hν = 150 eV is depicted in Fig. 5.26. A fresh H-terminated Si(111) surface exhibits a surface band bending eV_{bb} of ~ 0.48 eV, which is higher than the one observed for a fresh CH_3-terminated Si(111) surfaces of ~ 0.44 eV. No prominent change occurred in the surface band bending for the H-terminated Si(111) surface, even after 12 days in ambient air.

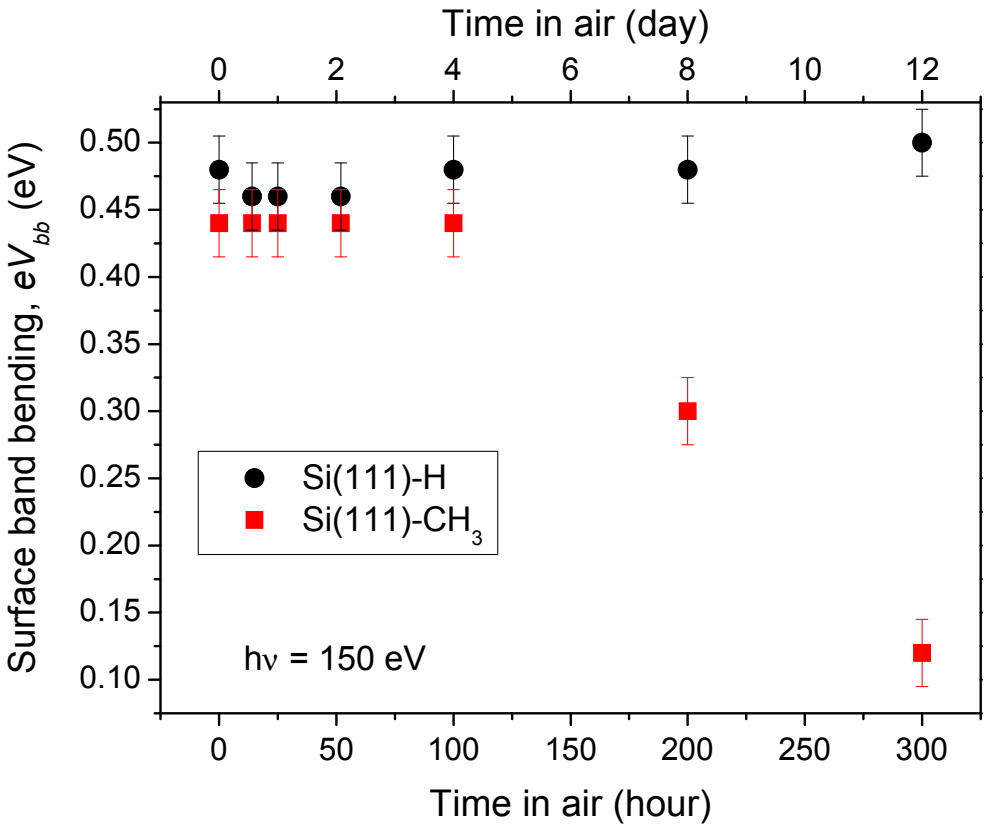

Fig. 5.26: *Surface band bending of H- and CH_3-terminated Si(111) surfaces as determined from the position of the bulk Si $2p_{3/2}$ photoemission (fig. 5.24). The evolution of the surface band bending is shown for an extended time period of 12 days in ambient air.*

In the case of CH_3-terminated Si(111) surfaces, no change in surface band bending is observed until 4 days in ambient air. However, after this time period a tremendous continuous decrease appears up to ~ 0.12 eV after 12 days in ambient air. This behavior shows a change in the CH_3-modified Si(111) surfaces and is probably due to the beginning of the total loss of Br atoms present on the surface. The total removal of these atoms which present a high electronegativity strongly modified the surface band bending of this CH_3-modified Si surface.

Fig. 5.27 depicts the change in work function, Φ, and electron affinity, χ, of H- and CH_3-terminated Si(111) surfaces in relation with their irradiation time in ambient air. The fresh H-terminated Si(111) surface reveals a higher Φ and χ than the fresh methylated one. A tendency occurs for both Si surfaces: for H-terminated Si(111) surface, Φ and χ exhibit almost no tremendous change and stay at ~ 4.40 eV and ~ 3.96 eV, respectively, even after 12 days in ambient air. In the case of CH_3-terminated Si(111) surface, Φ increases continuously from 4.05 to 4.48 eV in the first 8 days and ends at ~ 4.41 eV, which is similar to the Φ of H-terminated Si(111) surface after 12 days in ambient atmosphere. A fresh sample of methyl-terminated Si(111) surface indicates an χ of 3.57 eV. For this modified Si surface, χ seems to follow also the same tendency of the respective Φ of this surface and increases to 3.87 eV after 4 days and stays constant until 8 days. However, χ decreases between 8 and 12 days to 3.62 eV. The results obtained here indicate clearly that Φ and χ seem not to be affected by the presence or formation of silicon oxide on H-terminated Si(111) surface even after 12 days in ambient air. However, this observation is consistent with the fact, that the H-terminated Si(111) surface has been already oxidized after 1 day in ambient air. Therefore, the changes after this time period are directly correlated to the surface atoms. This demeanor exhibits also that H-terminated Si(111) surface oxidized sustains no change in relation with the irradiation of the synchrotron radiation, while it is not the case for the methylated Si surface. For CH_3-terminated Si(111) surface, the increase of Φ and χ are well correlated with the slow increase of oxide formation on this modified Si surface, but also from the continuous desorbtion of the Br adventitious atoms bonded to Si atop atoms surface as revealed by the Br 3d emission discussed above (see Fig. 5.24). No more Br atoms are still present on the methylated surface after 8 and 12 days, so that χ decreases also strongly like the band bending observed in Fig. 5.26, while the Φ seems to rejoin the same Φ value of the H-terminated Si(111) surface oxidized after 12 days. However, there are only suppositions since unfortunately no Br 3d emission spectra have been recorded after 4 days, but these assumptions are well supported by the PL measurements show in the next subsection (see Fig. 5.30). The synchrotron radiation seems to modify the surface electronic properties of the methylated surfaces.

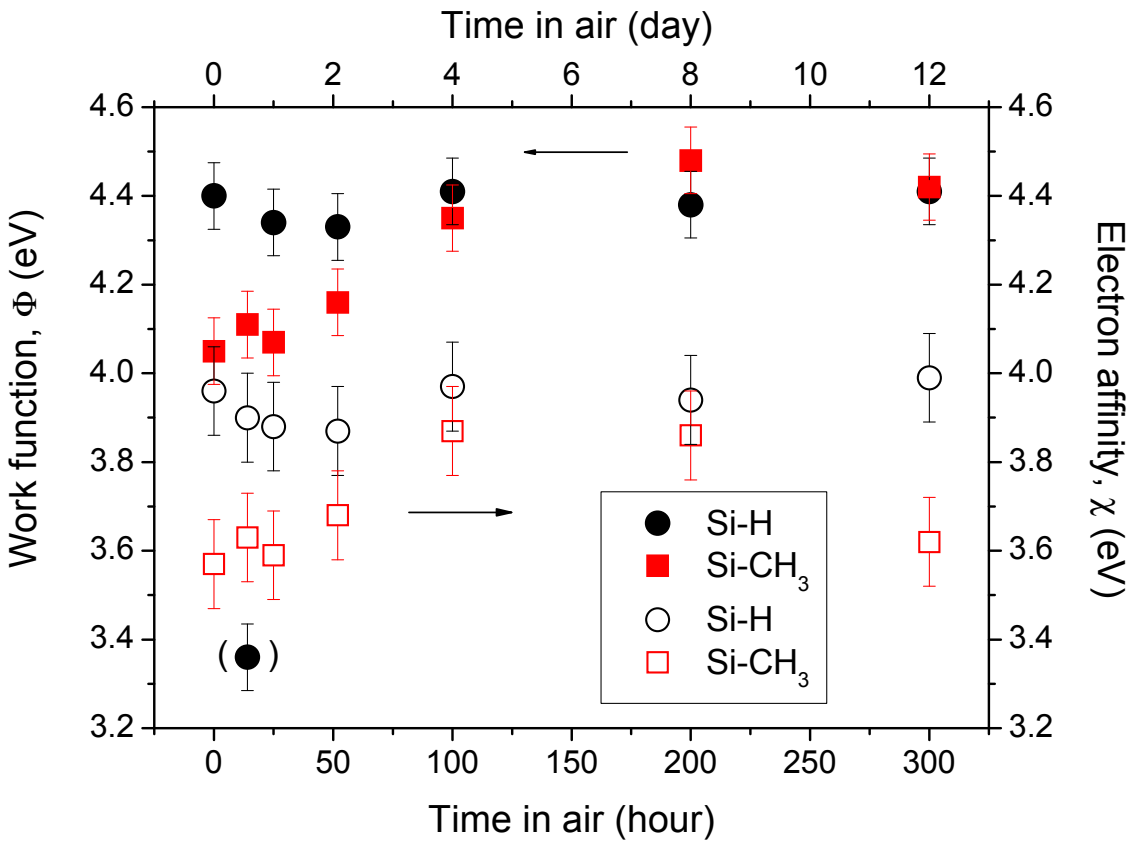

Fig. 5.27: *Work function, Φ, and electron affinity, χ, for H- and CH_3-terminated Si(111) surfaces as function of the time in ambient air as calculated from SXPS measurements.*

5.5.3 PL characterization

H-terminated Si(111) surfaces prepared in 5% HF and 40% NH_4F solutions

First, different preparation of H-terminated Si(111) surfaces have been compared by photoluminescence (PL) technique. The H-terminated Si(111) surfaces have been obtained by chemical treatments in two different etching solutions: 5% HF hydrogen fluoride and 40% NH_4F ammonium fluoride concentrated solutions, respectively. Fig. 5.28 displays the PL intensity response (I_{PL}) of theses H-terminated Si(111) surfaces. The H-terminated Si(111) surface obtained by treatment in 40% NH_4F solution reveals an about twice higher I_{PL} as compared to the I_{PL} obtained from H-terminated Si(111) surface treated in 5% HF solution. The maximum value of I_{PL} is observed at ~ 1142 nm (which corresponds to the band gap of Si, E_g = 1.12 eV (≅ 1150 nm)). It is well known that H-terminated Si(111) surfaces prepared in 40% NH_4F solution lead to atomically flat surfaces and establish less numbers of defects than H-terminated Si(111) surfaces prepared in 5% HF solution.[123]

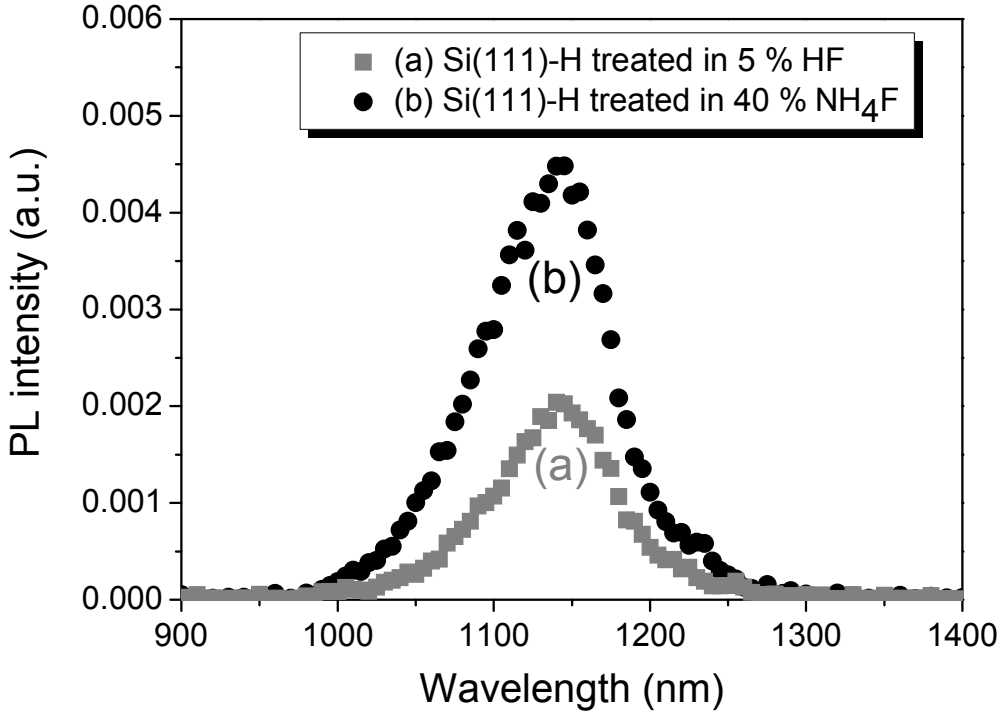

Fig. 5.28: *I_{PL} spectra of H-terminated Si(111) surfaces prepared in (a) 5% HF and (b) 40% NH_4F solutions, respectively.*

The oxidation process of H-terminated Si(111) surfaces has also been investigated by PL technique as function of time stored (700 h, ~ 29 days) in ambient atmosphere. The results obtained are summarized in Fig. 5.29 (bottom panel). The I_{PL} of both H-terminated Si(111) surfaces decreases with increasing of time. However, the surface treated in 5% HF solution decreases from a lower I_{PL} as already indicated in Fig. 5.28. The H-terminated Si(111) surface modified in 40% NH_4F solution tends to reach more rapidly a lower I_{PL} signal than the one which has been treated in 5% HF solution pointing to a less hindered diffusion effect during the oxidation process. The I_{PL} of both surfaces decreases very rapidly and stays approximately at a low PL intensity after ~ 8 h exposed in ambient air. Nevertheless, it seems that H-terminated Si(111) surface prepared with 5% HF solution presents a higher PL signal after 24 h stored in ambient air, but finally after ~ 680 hours (~ 28 days), both curves are rejoined. This behavior suggests that after this time duration, the Si surfaces present the same growth non-radiative recombination active centers since their PL signals are equivalent.

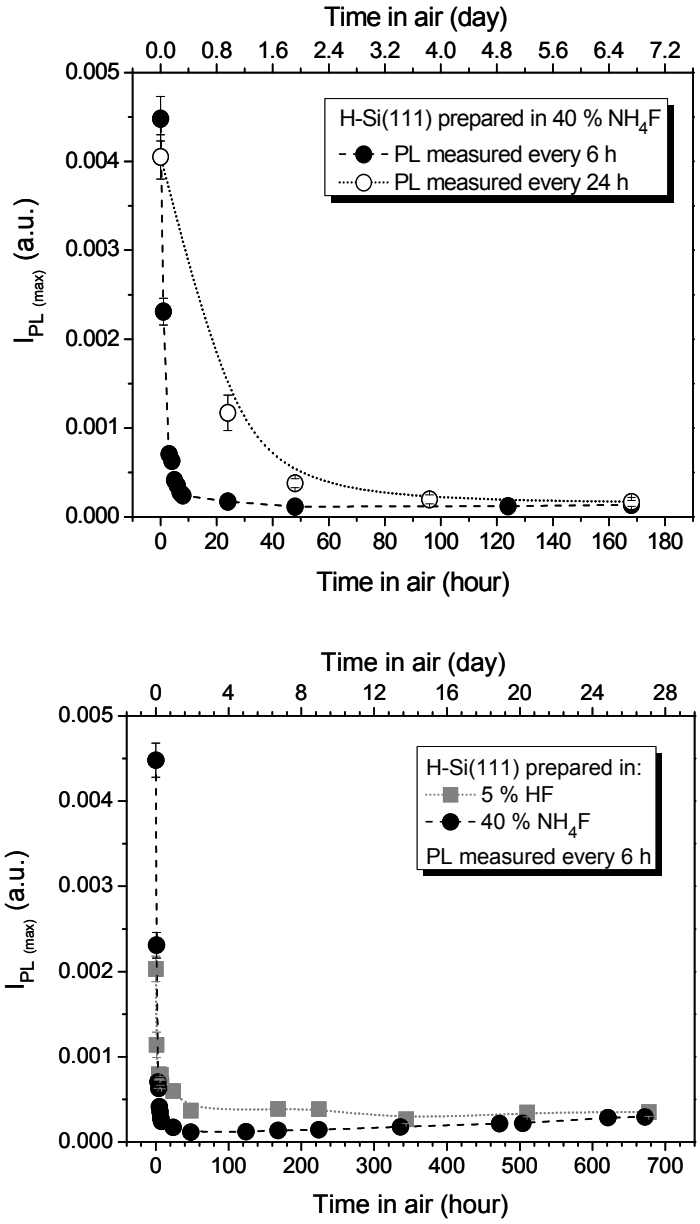

Fig. 5.29: *Bottom: I_{PL} of H-terminated Si(111) surfaces prepared in 5% HF and 40% NH_4F solutions, respectively, as function of time. Top: I_{PL} of H-terminated Si(111) prepared with 40% NH_4F solution measured every 6 or 24 hours by the pulsed laser irradiation.*

Furthermore, an additional curve belonging to another H-terminated Si(111) surface treated in 40% NH_4F solution has been added to show the lower degradation of Si surfaces when H-terminated Si(111) surface has been measured after every 24 h instead of every 6 h by the use of pulsed laser from PL equipment (Fig. 5.29, top panel). On the top panel of Fig. 5.29, the H-terminated Si(111) surface measured after 6, 12, 18 and 24 h until 168 h (black full circle) indicates a more drastically abrupt of the I_{PL} signal than the other one (black empty circle) of which the measurements were performed only every 24 h. In the later case, the PL decay is less pronounced. This behavior gives clearly evidence that the Si surfaces more exposed to PL measurements are more promptly damaged by the pulsed laser of the PL

setup. Moreover, the decrease of I_{PL} signal is an indication of the creation of defects which occurs on the Si surfaces. Consequently, the irradiation arising from the pulsed laser is suggested to deteriorate the Si surface and leads to damage Si surfaces (where defects are created). The defects created could then react more rapidly with contaminants coming from the atmosphere, i.e., oxidation.[124]

Comparison between H-, CH_3- and CD_3-terminated Si(111) surfaces

I_{PL} has also been measured for methylated Si(111) surfaces to inspect whether this demeanor occurs also on such modified Si(111) surfaces. Fig. 5.30 illustrates the evolution of CH_3- and CD_3-terminated Si(111) surfaces measured with PL technique. Methylated Si(111) surfaces are obtained by the application of an anodic current of 1 mA/cm^2 for 5 min in CH_3MgBr and CD_3MgI solutions for both Si(111) surfaces, respectively. H-terminated Si(111) surface is also added to the figure for a direct comparison. Two series of methylation have been prepared at different days.

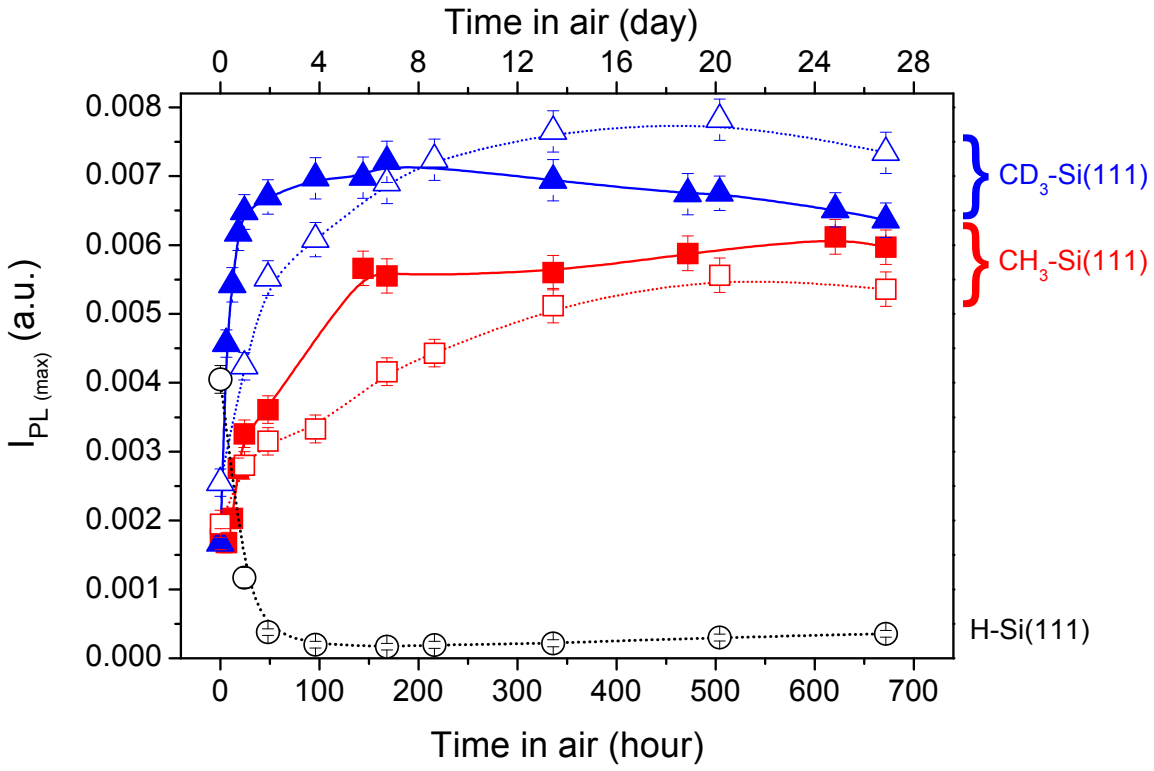

Fig. 5.30: *I_{PL} as function of time of methyl-terminated Si(111) surfaces of two different series, respectively. Anodic current of 1 mA/cm^2 for 5 min has been applied for both Si(111) surfaces in the respective Grignard solutions (CH_3MgBr, and CD_3MgI). I_{PL} of a H-terminated Si(111) surface prepared in 40% NH_4F solution (black empty dots) has been added for comparison. The solid lines are added as guide to the eyes.*

In contrast to H-terminated Si(111) surfaces, the behavior of I_{PL} is completely different. For each methylated Si(111) surface, I_{PL} starts at lower level than the one obtained for H-terminated Si(111) surface but then they increase drastically. CD_3-terminated Si(111) surfaces (blue triangles) exhibit a faster increase in I_{PL} and a slightly higher maximum I_{PL} value than CH_3-terminated Si(111) surfaces (red squares) after ~ 10 h of exposure to ambient air.

The experiments have been continued for a longer duration time of ~ 275 days to observe the behavior of these methylated Si(111) surfaces as function of the time exposed to ambient atmosphere. Fig. 5.31 illustrates the evolution of I_{PL} for CH_3-, CD_3-, and H-terminated Si(111) surfaces as function of long time exposure to air. Surprisingly, the strong increase in I_{PL} up to 21 days (see also Fig. 5.30) is followed by a strong decrease in I_{PL} up to 57 days of exposure to ambient air. After this time period, the corresponding curves seem to reveal a constant I_{PL} even up to 278 days for both CH_3- and CD_3-terminated Si(111) surfaces, which is much higher than for H-terminated Si(111) surfaces. The increase of I_{PL} signal for both methylated Si(111) surfaces suggests that these surfaces could present some remnant contaminants (which are certainly arisen from contaminations due to the rinse process or from atmosphere like aliphatic carbons, Br atoms coming from the Grignard solvent…). These contaminants could probably affect the PL response since a surface charge pushes a charge carrier away from the surface, and therefore the recombination process of electrons and holes is suppressed. A higher PL signal is then supposed for these methylated Si(111) surfaces since I_{PL} is inversely proportional to the number of non-radiative recombination active defects at the interface. Finally, after 21 days the decrease of the I_{PL} signals suggests a diminution of the contaminants present on the surface due to the irradiation of the substrates by the pulsed laser. After reaching the initial value of the fresh samples (after about 50 days), the I_{PL} continues to decrease very slowly and stays quite constant. The constant behavior of these modified Si surface reveals the good stability and passivation of these substrates as function of time. Moreover, CD_3-terminated Si(111) surface present a slightly higher I_{PL} as compared to CH_3-terminated Si(111) surface. This demeanor suggests that the Si(111) surfaces modified with CD_3 groups exhibit a “cleaner” and a better passivated Si surface prepared with less contaminants present on the substrate, as already shown by SXPS and SPV measurements (see Figs. 5.10 and 5.17).

In the case of H-terminated Si(111) surfaces, I_{PL} already decreases dramatically after 4 h. Similarly to the methylated Si(111) substrates, a weak hump is also observable after about 30 days. In this case, the weak hump occurs here is supposed to arise from the formation of a first “symmetric” backbonds Si–O–Si layer which contains less asymmetry than a layer

without order. Since this kind of surface reveals less “defects”, it is then obvious to observe a small increase in the PL response.

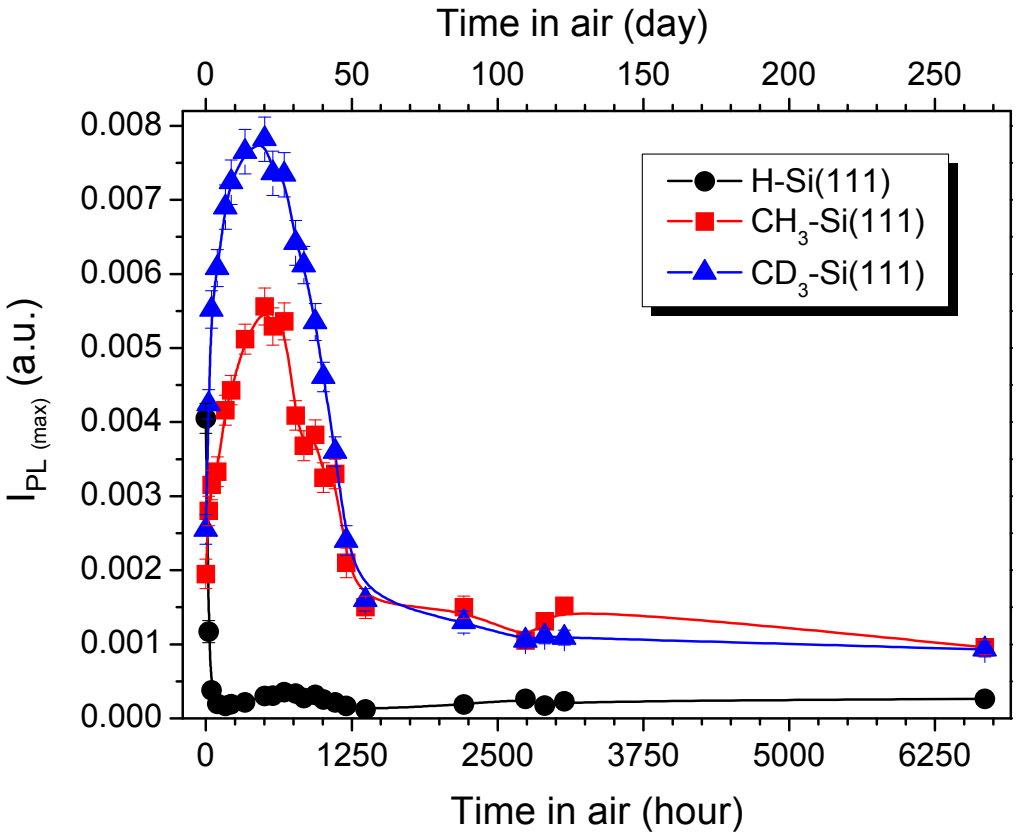

Fig. 5.31: *I_{PL} of H-, CH_3-, and CD_3-terminated Si(111) surfaces in ambient air. Methylated Si(111) surfaces have been prepared using CH_3MgBr and CD_3MgI solutions, respectively, with the application of an anodic current density of 1 mA/cm^2 for 5 min. H-terminated Si(111) surface has been prepared in 40% NH_4F solution. The lines are added to guide the eyes.*

Finally, the experiments performed here reveal the benefit of the grafting of methyl groups onto Si surfaces as shown by the higher value of I_{PL} response constant even after 278 days. This I_{PL} value is half of the fresh methylated Si samples. This statement indicates that only twice higher amount of defects at the interface occurs even after this long time in ambient air. Moreover, these methyl layers give rise to protect remarkably the Si surfaces since the I_{PL} response from H-terminated Si(111) surfaces are revealed in the range of the extinction level of Si surfaces (complete formation of SiO_2) after already ~ 57 days in ambient atmosphere. The methylated Si(111) surfaces reveal then a good passivation of the modified Si(111) surfaces, conversely to H-terminated Si(111) surfaces which have been already oxidized after some hours.

5.6 Conclusion

The organic modification of Si surfaces by methyl groups (CH_3 and CD_3) with the one-step electrochemical grafting method using Grignard solutions has been well achieved as revealed by IRSE, SXPS, PL, and SPV measurements. The methylated Si surfaces have been performed on both p- and n-type Si wafers, but also for different orientations like Si(111), Si(100) and porous Si surfaces. These methylated Si(111) surfaces exhibit clearly a much better passivation for longer time (up to several months) in ambient atmosphere in relation to H-terminated Si(111) surfaces as observed by IRSE, SXPS and PL techniques. Moreover, IRSE and SXPS investigations exhibit a very low oxidation probability for the methylated Si(111) surfaces. Other tremendous properties have also been observed for these methyl-terminated Si(111) surfaces like a thermal stability up to 430 °C, but also a good resistivity against 5% HF etching solution for ~ 30 min. These statements clearly indicate that the covalent Si–C bonds formed at the Si surface are robust and protect strongly the Si surface against external attacks.

Furthermore, SXPS measurements reveal a well-defined spin-orbit doublet splitting of the Si 2p core level emission for these methyl groups grafted onto Si(111) surfaces of which the emission contributions from the bulk (Si^0) and from the surface (Si–C bonds) have been well distinguished. This well-separated splitting is clearly observed for the first time in the case of methylated Si(111) surfaces prepared using the one-step electrochemical Grignard route. This observation and the vibrational losses of C–H stretching vibrational modes in the C 1s core level emission obtained for a monolayer coverage by methyl groups reflect the well-ordered surface structure for these modified Si(111) surfaces. The presence of some adventitious remnant contaminations from aliphatic carbons, Br and O atoms has also been detected in the near surface region. However, after the annealing process, most of these contaminations are desorbed and the total overlayer thickness of the methylated Si(111) surfaces is found to be ~ 3 Å. Since the van der Waals radii of a methyl group is ~ 2 Å, it is clear that the Si(111) surfaces have been covered by only one monolayer of methyl groups. The electronic properties determined from SXPS measurements for the methylated Si(111) surfaces reveal a lower work function, and band bending by ~ 0.44 and 0.15 eV, respectively, than H-terminated Si(111) surfaces. These electronic properties indicate that the methylated Si(111) surfaces are better passivated and possess an easier charge transfer between the methyl layer and the Si surface than in the case of H-terminated Si(111) surfaces. Moreover, as expected, after the annealing process both CH_3- and CD_3-terminated Si(111) surfaces present the same surface electronic properties.

The “umbrella” vibrational mode characteristic from methyl groups observed for the methyl-terminated Si(111) surfaces by IRSE measurements gives rise to the sensitivity of this spectroscopic method down to a monolayer. Moreover, as expected, a shift of the “umbrella” mode from CH_3 to CD_3 groups occurs for these modified Si(111) surfaces. However, no stretching vibrational modes have been observed for the methylated Si(111) surfaces. On the contrary, the grafting of methyl groups on porous Si reveals distinctively these stretching vibrations. This is observed by the presence of more methyl groups grafted to this surface due to the structure of the porous Si, which presents a higher surface density. In that case, the rocking vibrational mode of the methyl groups has also been observed.

In addition, PL measurements reveal that methylated Si(111) surfaces are faster oxidized during the laser irradiation of the PL setup, and IRSE spectra reveal a different type of oxide layer as observed for wet-chemically prepared oxides. However, the benefit of the grafting of methyl groups onto Si surfaces has been revealed by PL measurements since the methylated Si(111) surfaces show better passivation properties than H-terminated Si(111) surfaces for a long time period in ambient atmosphere. It was shown that only twice higher amount of defects at the interface occurred in the case of methylated Si(111) surfaces (as compared to the fresh modified Si samples) even after more than 9 months (~ 278 days) in ambient atmosphere, whereas H-terminated Si(111) surfaces already oxidized after some hours. This demeanor gives clearly evidence that these methyl layers protect remarkably the Si surfaces against oxidation.

Finally, the results obtained from SXPS, PL and SPV measurements reveal better electronic properties (passivation, band banding, defects at the interface…) for CD_3-terminated Si(111) surfaces in comparison to CH_3-terminated Si(111) surfaces.

Chapter 6

Modification by ethynyl derivatives

In the previous chapter, the electrochemical route for the grafting of organic molecules using Grignard solutions has been well performed for CH_3 groups as shown by IRSE, SXPS, PL, and SPV measurements. These CH_3-terminated Si surfaces have revealed a better passivation of Si(111) surfaces in comparison to H-terminated Si(111) surface prepared with 40% NH_4F solution. However, CH_3 groups lead to inactive surface properties due to the non-functionality of the alkyl chain. Therefore, covalent grafting of reactive triple bonds by ethynyl derivatives (−C≡C−H, −C≡C−CH_3 and −C≡C−phenyl) onto H-terminated Si(111) surfaces has been performed by anodic treatment in the respective Grignard electrolytes. The modified Si surfaces have been investigated using IRSE and SXPS methods. These two techniques are complementary to obtain information about the presence of the typical bond vibrations arising from the organic films and the type of chemical bonds at the interface, respectively. In addition, SEM, PL, and SPV measurements have also been performed in order to get information on the morphology, the non-radiative recombination behavior of active defects at the interface, and the band bending created by surface dipole induced by the grafting of organic molecules onto Si surfaces. All ethynyl derivatives tend to form ultrathin polymeric layers at high charge flow. The thickest layer of about 20 nm has been observed for ethynyl-MgCl, whereas the MgBr derivatives with bigger side groups (CH_3 and C_6H_5 instead of H) led to approximately 10 nm thick layers. Exchanging the Cl for Br in the ethynyl Grignard reagent leads to very thin layers, even under the same high current conditions. Thus, it is obvious that the type of halogenide ion plays an important role during the electrochemical grafting via Grignard compounds. The electrochemical mechanism pathway is discussed for the different organic molecules studied here. First, the deposition of "thick" layers of ethynyl derivatives onto Si(111) surfaces has been investigated by IRSE technique after using a high charge flow (450 mC/cm^2). Then, the grafting of "thin" layers (in term of monolayers) onto Si surfaces has also been investigated by SXPS measurements after using a lower charge flow (24 mC/cm^2). Additionally, SEM, ex-situ PL, and SPV techniques have also been performed

for the “thick” layers formed onto Si surfaces. Finally, the results obtained from these different experimental methods and the electronic properties determined from SXP measurements are discussed.

6.1 IRSE characterization

IRSE has been used to inspect the vibrational fingerprint of the surface species after grafting of ethynyl derivatives onto Si(111) surfaces. For this, high anodic current density of 0.5 mA/cm^2 for 15 min (charge flow ~ 450 mC/cm^2) has been applied to the Si substrates for each Grignard solution. The IRSE spectra obtained after organic modification of H-terminated Si(111) surfaces in ethynylmagnesium chloride (HC≡C−MgCl), propynylmagnesium bromide (CH_3−C≡C−MgBr), and phenylethynylmagnesium bromide (C_6H_5−C≡C−MgBr) solutions have been depicted in Fig. 6.1, respectively. These spectra have been collected using a MCT detector with a resolution of 4 cm^{-1}. In addition, the spectrum of the Si surface modified by the ethynylmagnesium bromide (HC≡C−MgBr) compound has been recorded with a Kolmar detector at 6 cm^{-1} resolution in the high wavenumber region (2700-3400 cm^{-1}) to obtain a better S/N ratio and has been added to the figure. The IRSE spectrum (Fig. 6.1a’) reflects low efficiency of grafting using this Grignard reagent as compared to the one containing chloride ions (Fig. 6.1a), even under the same electrochemical condition. Each spectrum has been normalized to the fresh H-terminated Si(111) surface. The upward pointing peak at ~ 2083 cm^{-1} in all spectra indicates the loss of Si−H surfaces species after the grafting process and reveals the organic modification of the Si surfaces. A layer visible to the naked eye (blue) is observed after electrochemical treatment in HC≡C−MgCl, which indicates the formation of a polymeric layer. This finding is supported by the strong increase in IR-absorption ~ 2900 cm^{-1} due to symmetric and asymmetric stretching modes of CH_2 as compared to the other ethynyl derivatives[14] (see Fig. 6.1a). However, this demeanor is in contrast with the anodic grafting of HC≡C−MgBr where no specific color has been noticed. This probably led to a very thin layer even under the same conditions as already reported by Fellah et al.[18] It is then evident that the halogen atoms present in the Grignard compounds play an important role in the grafting process. However, an attack of intermediate radicals on the −C≡C−H species (which have been grafted onto the Si surface) has been recently supposed[14] leading to C−C, C=C and C≡C bonds in a polymeric layer as also observed by the IRSE spectra in Fig. 6.1a. The absorption peak at 3300 cm^{-1} appears only for the Si(111) surface modified in HC≡C−MgCl. This weak and broad peak is assigned to the C−H stretching mode of the acetylenic CH groups in the −C≡CH unit.[125] The IR-absorptions at 2870 and 2958 cm^{-1} are

attributed to the symmetric and asymmetric stretching modes, ν_s and ν_{as}, of CH_2 groups from adventitious contaminations and the layer itself, respectively. The stretching vibration of the ethynyl groups ($\nu_{C\equiv C}$) at 2046 cm^{-1},[18,90,126] is more distinguishable for the surface modification by HC≡C−MgCl compared to the other ethynyl derivatives due to a thicker polymeric layer. A weak band also appears at 1725 cm^{-1}. This IR-band is attributed to C=O stretching vibrational mode and obviously arises from THF molecules (solvent of the Grignard compound) which seem to be incorporated in the layer.[14,127]

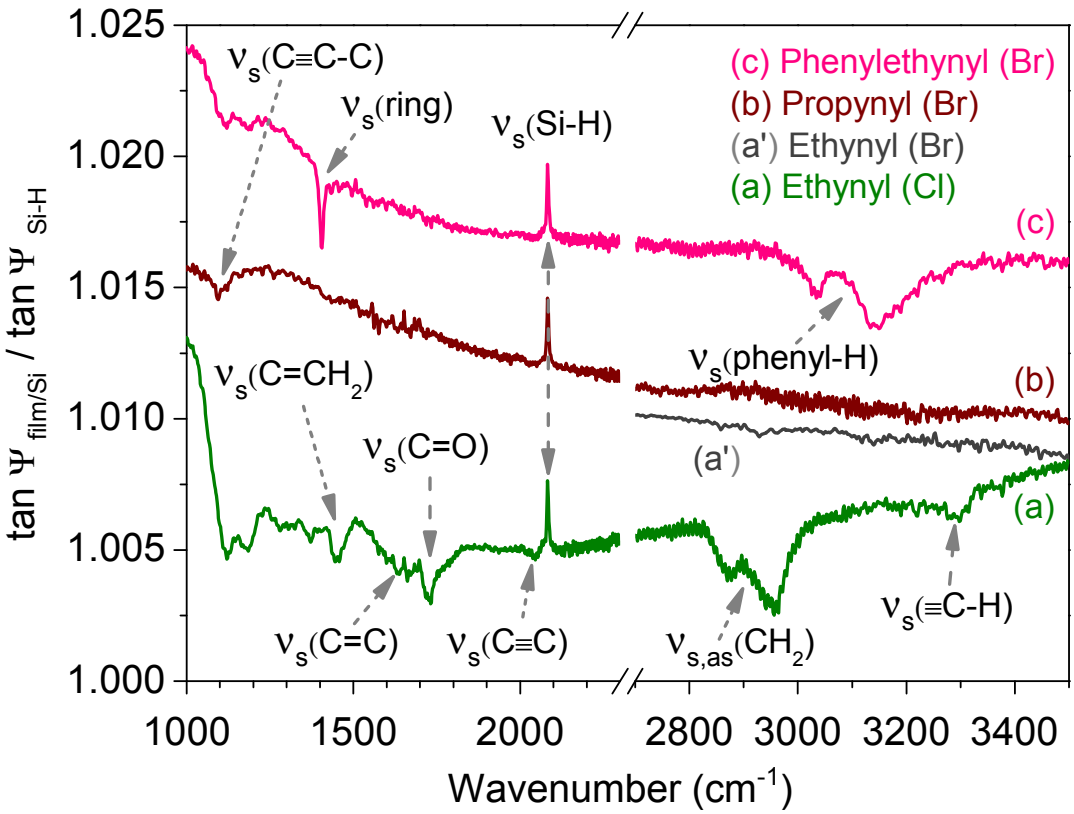

Fig. 6.1: *Tan Ψ spectra after anodic treatment in (a) H−C≡C−MgCl, (b) CH_3−C≡C−MgBr, and (c) C_6H_5−C≡C−MgBr normalised to the tan Ψ spectrum of the H-terminated Si(111) surface. A current density of 0.5 mA/cm^2 has been applied to the Si substrate for each Grignard solution for 900 s (~ 450 mC/cm^2). Spectrum (a') has been recorded for a longer time period with a Kolmar detector (resolution of 6 cm^{-1}) to obtain a better S/N ratio.*

Two other peaks appear at 1450 and 1650 cm^{-1} in this IR spectrum, which are ascribed to the symmetric vibrational modes of C=CH_2 and C=C groups, respectively.[43,46] However, in case of electrochemical treatment with HC≡C−MgBr solution, only a very weak IR-absorption in the C–H stretching modes region of CH_2 groups and no IR-absorption due to the C−H stretching mode of the acetylenic CH groups have been observed. These demeanors reveal clearly that the coverage of the Si substrates using HC≡C−MgBr was less efficient as compared to the one obtained by HC≡C−MgCl compound. The grafting of CH_3−C≡C−MgBr

onto Si(111) surfaces leads to a weak absorption peak in the 1000-1200 cm^{-1} region and can be assigned to the −C≡C−C reflection of the stretching vibrational mode,[128] as denoted in Fig. 6.1b. In the case of Si(111) surface modified in C_6H_5−C≡C−MgBr solution, the presence of IR-absorption bands in the 3000-3200 cm^{-1} region are attributed to aromatic CH bond vibrations. Moreover, an intense and narrow IR-absorption band occurs at 1405 cm^{-1} and is assigned to the ring stretching vibration. The presence of these vibrational modes clearly confirms the grafting of C_6H_5−C≡C− onto the Si surface (Fig. 6.1c).

Furthermore, the modification of Si(111) surfaces with ethynyl derivatives has also been performed by application of a lower current density of about 0.02 mA/cm^2 for 1200 s (~ 24 mC/cm^2). Unfortunately, the typical vibrational modes from ethynyl derivatives have not been detected by IRSE (contrary to the CH_3 groups grafted onto Si(111) surfaces) when a lower charge flow has been applied. The non-observation of these vibrations is probably due to the grafting of a very thin layer and/or to a very small IR-sensitivity. However, these Si substrates have been investigated by SXPS measurements. The results obtained from these measurements are described in the following section.

6.2 SXPS characterization

SXPS has been performed to inspect the chemical environment of modified Si surfaces obtained by ethynyl derivatives. The detailed analysis of the chemical shifts from Si 2p, C 1s and Br 3d core level emissions permits to determine different kind of chemical species present on Si surfaces after the electrochemical modification. Moreover, a better understanding of the electrochemical grafting mechanism can be also established by the application of different charge flows during the grafting process as revealed below for the grafting from HC≡C−MgBr coumpound. For the “thick” organic layers used in IRSE measurements, no signal from the Si 2p emission spectra has been detected at hν = 650 eV because the organic overlayer thicknesses were larger than the information depth of the X-ray photon energy at 650 eV (which is equivalent to an inelastic mean free path (IMFP) of ~ 18 Å). Therefore, the current density has been strongly reduced to suppress the polymerization effect observed at higher charge flow, especially for HC≡C−MgCl. Thus, a lower charge flow has been applied to Si surfaces during the electrochemical grafting of ethynyl derivatives compounds (HC≡C−MgCl, CH_3−C≡C−MgBr and C_6H_5−C≡C−MgBr) by applying an anodic current density of 0.02 mA/cm^2 for 20 min (~ 24 mC/cm^2). The high resolution SXP spectra have been performed at photon energy hν = 150 eV (surface sensitive condition) and hν = 650 eV (bulk sensitive condition).

6.2.1 Different charge flows applied to HC≡C−MgBr solution

Different charge flows of 60 mC/cm^2, 24 mC/cm^2, and 2.4 mC/cm^2 have been respectively applied during the electrochemical grafting of Si(111) surfaces in HC≡C−MgBr solution in order to determine the best parameter for the grafting process. Fig. 6.2 shows the high resolution SXP spectra of (a) Si 2p, (b) C 1s, and (c) Br 3d core level emissions of modified Si(111) surfaces using HC≡C− molecules from HC≡C−MgBr compound. Each spectrum has been collected with an excitation energy of hν = 650 eV.

The Si 2p emission spectra reveal no chemical shift between the bulk Si $2p_{3/2}$ peak from the Si substrates modified by 60 mC/cm² and 24 mC/cm² at 99.37 eV (the position of the bulk Si $2p_{3/2}$ peak from the fresh H-terminated Si(111) surface is located at 99.41 eV, see Chap. 5 subsection 5.2). However, for the Si substrate treated under a charge flow of 2.4 mC/cm^2, a chemical shift of approximately + 0.10 eV towards the higher binding energy occurs. These demeanors indicate that when a high anodic current density is applied (> 2.4 mC/cm^2), the resulting band bending from these modified Si surfaces gets smaller compared to the H-terminated Si(111) surface. However, the highest intensity of the bulk Si $2p_{3/2}$ signal is observed for the Si substrate treated by 24 mC/cm^2. The intensity of the bulk Si $2p_{3/2}$ signal is reduced by ~ 20 and 30% after treatment by 2.4 and 60 mC/cm^2, respectively. Moreover, a weak hump occurs in the 101-104 eV region and is attributed to the different oxidation states of silicon oxide species (Si^{n+}, with n = 1, 2, 3 or 4). Indeed, more silicon oxide species are observed in case of the Si surface modified with the highest charge flow (~ 6% at 60 mC/cm^2, ~ 3% at 2.4 and 24 mC/cm^2, respectively).

The high resolution C 1s (Fig. 6.2b) and Br 3d (Fig. 6.2c) core level spectra of these modified Si samples reveal a higher amount of C and Br atoms in case of the Si surface treated with the higher charge flow (60 mC/cm^2). This behavior is consistent with the lower intensity of Si 2p signal observed from this modified Si surface. Moreover, more contaminations have been observed from this substrate as revealed by the presence of adventitious remnant carbon and bromine atoms on the modified Si surface. The similar line shape of C 1s and Br 3d emissions suggest the presence of identical C and Br species on each modified Si substrates. However, to determine quantitatively the amount of each species, the C 1s and Br 3d emission spectra have been fitted with a series of Voigt line shapes after a Tougaard background subtraction. In the case of Br 3d emission spectra, a spin-orbit doublet stripping has been maintained (ΔE = 1.05 eV, 2:3 peak area ratio).[59] For the C 1s emission spectra, the fitting

indicates a peak at ~ 284.65 eV and is attributed to adventitious aliphatic carbon atoms.[129] This peak is more prominent in the case of the Si modified by the highest charge flow (60 mC/cm^2) and decreases with reduced charge flow by about 30 and 20% (for 24 and 2.4 mC/cm^2), respectively. A peak towards the lower binding energy at ~ 283.80 eV is observed from the fitting procedure. This weak peak is assigned to C-bonded to Si atoms, C–Si bonds, due to the electronegativities of the elements present on the surface.[130] About 3%, 6%, and 2% of C–Si bonds have been determined in relation to the total intensity of the corresponding C 1s signal when the charge flow applied is decreasing. Moreover, another emission towards the higher binding energy at ~ 285.90 eV is also distinguishable as a pronounced shoulder of the main peak (aliphatic carbons). This peak is ascribed to the mixture of C bonded to O and Br atoms, respectively. Thus, the highest amount of these kinds of C species is observed for the higher charge flow applied and decreases with reduced charge flow by ~ 45 and 60% respectively. The Br 3d emission spectra reveal two different species of Br atoms on these modified Si surfaces. The Br 3d spin-orbit doublet emission at ~ 69.25 eV is attributed to Br-bonded to Si atoms, whereas the emission at ~ 70.3 eV is ascribed to Br-bonded to C atoms.[111] These attributions have been done with respect to the electronegativities of Si, C, and Br atoms (1.90, 2.55, and 2.96, respectively). The Si substrate with the higher charge flow applied (60 mC/cm^2) shows clearly the higher amount of Br–Si and Br–C bonds. The amount of these bonds is strongly reduced by a reduction of the charge flow (for 24 and 2.4 mC/cm^2) by ~ 40 and 80% for the Br–Si bonds and ~ 70% for Br–C bonds, respectively. Thus, from all these observations, the Si substrate modified by 24 mC/cm^2 clearly shows the smallest amount of contamination by adventitious carbons and also the highest amount of C–Si bonds grafted, even if more Br–Si bonds have been observed as compared to the lowest current flow applied (2.4 mC/cm^2).

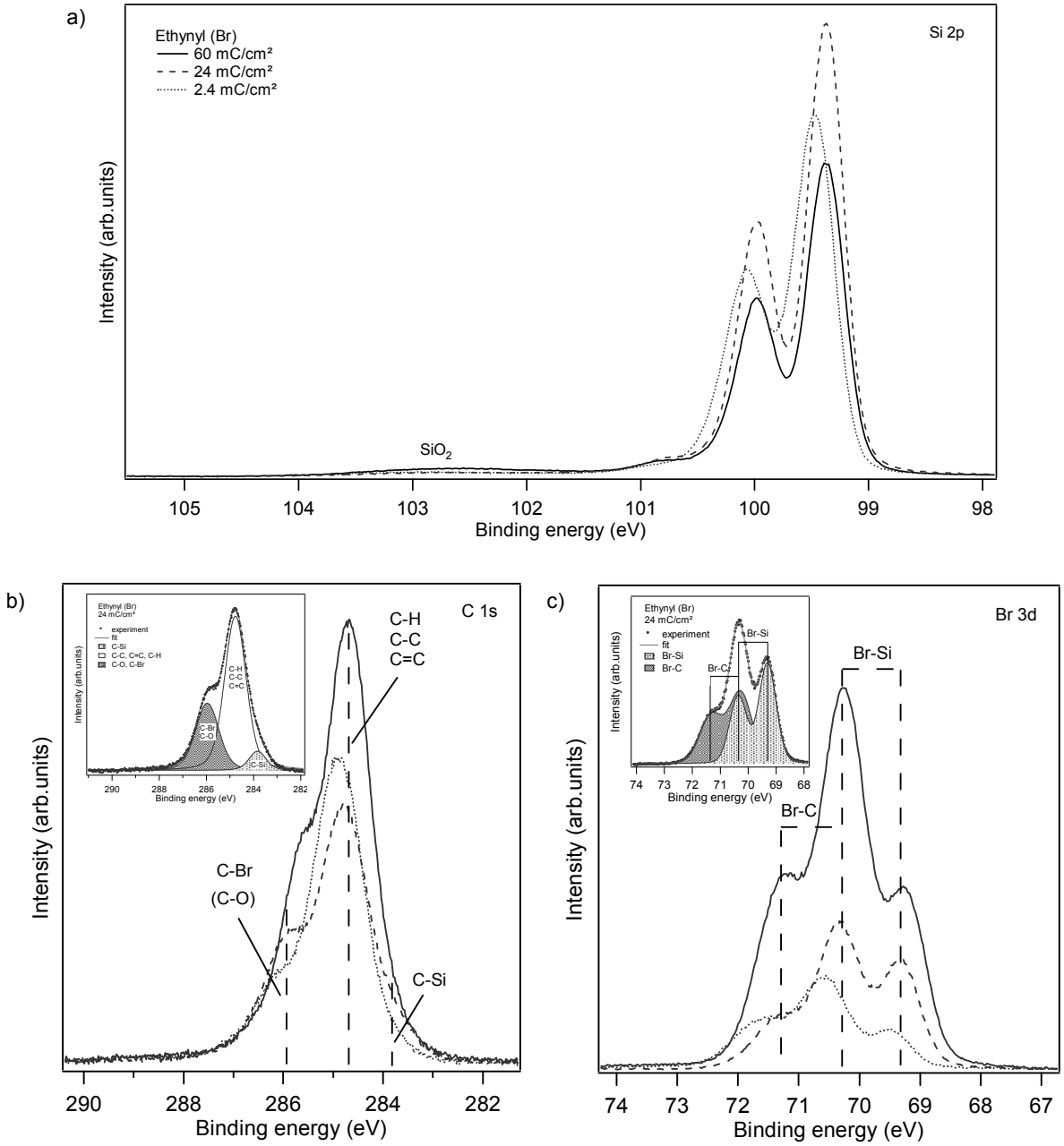

Fig. 6.2: *High resolution SXP spectra of (a) Si 2p, (b) C 1s and (c) Br 3d emissions from Si(111) modified in HC≡C−MgBr Grignard solution by application of different charge flow. The spectra have been recorded at photon energy hν = 650 eV under synchrotron radiation.*

6.2.2 Grafting of H−C≡C−, CH_3−C≡C− and C_6H_5−C≡C−

Fig. 6.3 displays the SXP survey spectra recorded at E_{ex} = 650 eV of a fresh H-terminated Si(111) surface, and after electrochemical modification in methyl-d_3-magnesium bromide and in phenylethynylmagnesium bromide solutions, respectively. For each Si substrate, several peaks are observed and are attributed to Si 2p (99.4 eV), Si 2s (150.9 eV), C 1s (284.5 eV), and O 1s (531.9 eV) emissions. Peaks labeled P' and P" observed at (17.5 ± 0.5) eV in higher

binding energy than Si 2p and Si 2s emissions are assigned to plasmon loss features from these Si emissions, respectively. The peak at 556.7 eV is a result of the Si LMM Auger emission. The C 1s and O 1 s emissions observed in the spectrum of the H-terminated Si(111) surface are probably due to adsorbed contaminations that arise from the exposure of the ambient environment before transfer to the SXP analyzer chamber. However, in case of phenylethynyl-terminated Si sample, C 1s and O 1s emissions show higher intensities, which indicates the presence of a thicker organic layer obtained. Moreover, peaks ascribed to Br 3d (70.4 eV) and Br 3p (183.2 eV) have also been observed and give clear evidence of the presence of Br contaminations coming from the electrochemical process (MgBr solution). The presence of the higher O 1s emission for this modified Si surface will be discussed later.

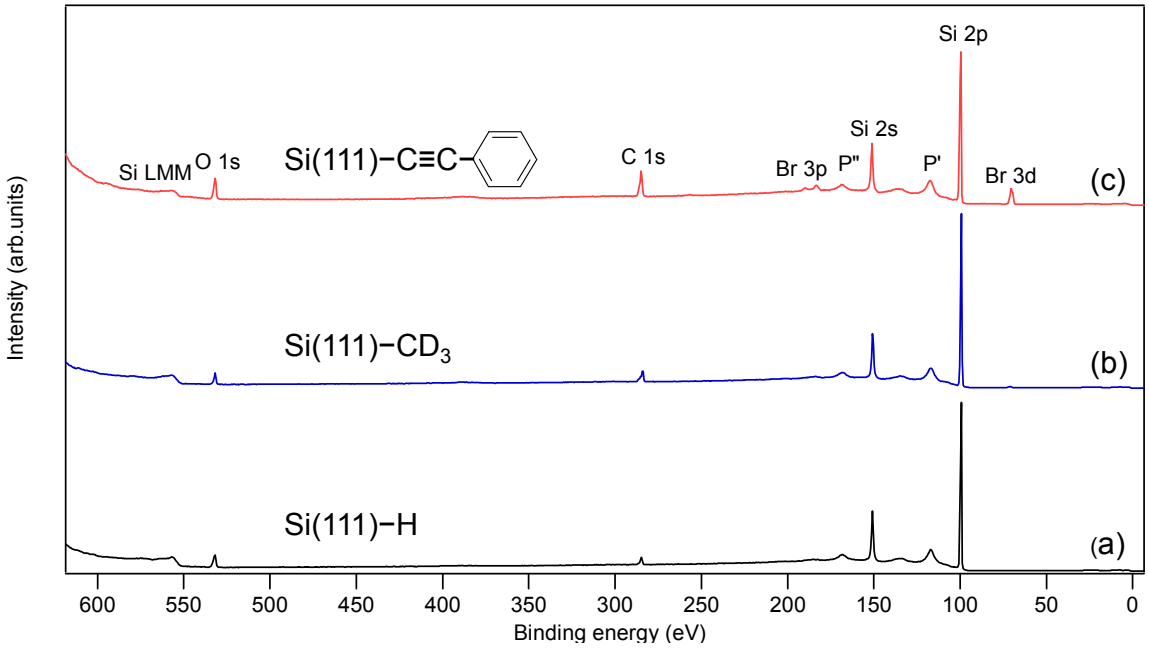

Fig. 6.3: *SXPS survey scans of (a) H-, (b) CD_3- and (c) phenylethynyl-terminated Si(111) surfaces excited with a photon energy of 650 eV. Peaks labelled P' and P" correspond to well-defined surface plasmon emissions from Si 2p and Si 2s emissions, respectively. Note that Br 3d and Br 3p core level emissions are visible in the case of phenylethynyl-terminated Si(111) surface. The spectra have been shifted for visual convenience.*

As shown in the previous subsection, a charge flow of 24 mC/cm^2 applied to Si substrate has presented the "best" parameter for the grafting of ethynyl groups. Therefore, for the SXPS measurements, such charge flow has been chosen for the grafting of the other ethynyl derivatives. Fig. 6.4 presents high resolution SXP spectra in the C 1s and Si 2p core level region after electrochemical modification in (a) HC≡C−MgCl, (b) CH_3−C≡C−MgBr, and (c) C_6H_5−C≡C−MgBr solutions collected at an excitation energy of hν = 650 and 150 eV, respec-

tively. The SXP data of the methylated Si(111) surface (d) is shown for comparison because CH_3-terminated Si(111) surface represents an ideally passivated and highly ordered Si surface.[13] All spectra have been analysed by deconvolution after a Shirley subtraction of the background and fitted by a series of Voigt line shapes as shown in Fig. 6.4. For the Si 2p emission, the constraint due to the spin-orbit doublet of Si 2p has been maintained ($\Delta E = 0.605$, 1:2 peak area ratio). The Si 2p core level spectra have been deconvoluted into several features from different contributions to obtain quantitative information. The CH_3-terminated Si(111) surface reveal a spin-orbit doublet of the Si $2p_{3/2}$ signal from the bulk Si (Si°) and are well seen at ~ 99.26 and 99.84 eV, respectively. Another prominent spin-orbit doublet can be well distinguished at ~ 99.5 and 100.08 eV, respectively. The chemical shift observed for this spin-orbit doublet in relation with Si° peak is attributed to Si−C signatures from the methyl groups.[130] The shift of the doublet Si 2p peak of the Si surfaces modified by ethynyl derivatives with respect to Si(111)−H surface (not shown here) by 0.3-1.0 eV presents clear evidence of the organic grafting onto Si surfaces where Si−C covalent bonds were formed (with an expected chemical shift of < 1 eV).[59] Moreover, no pronounced contributions related to SiO_x species have been detected in the 101-104 eV energy range, even under these surface sensitive conditions ($h\nu = 150$ eV). The chemical shift of the Si atoms bonded to ethynyl groups has been observed in the higher binding energies, indicating that the Si is positively charged as expected by the difference in the electronegativities of Si (1.90) and C (2.55), respectively. Furthermore, the SXP spectra of Si 2p from these modified Si surfaces show a weak peak located at 100.66-100.75 eV, which may be responsible for Si–O–Si (Si^{1+}), Si−OH (Si^{+3}) and/or Si−Br(Cl) bonds. This contribution has an intensity ~ 5 times higher for the CH_3−C≡C- and C_6H_5−C≡C-modified Si(111) surfaces as compared to the H−C≡C-modified Si(111) surface. This result leads to the assumption that these modified Si(111) surfaces have a higher contamination level by silicon back bonds, −OH and/or halogen atoms after the electrochemical grafting from Grignard compounds. The C 1s peaks from the modified Si surfaces have been deconvoluted into three main contributions. For comparison, the C 1s peak from the methyl-terminated Si(111) surface is also shown (Fig. 6.4d) and points out only one contribution at ~ 284.1 eV, which is attributed to Si−C bonds.[98,101] This statement leads to the conclusion that this methylated Si(111) surface has no other contaminations. In the case of ethynyl derivatives modified Si surfaces, the component peak corresponding to Si−C bonds is slightly shifted to a lower binding energy of ~ 283.7 eV.[88,130] Two other contributions at higher binding energies at ~ 284.6 and 286.1(286.3) eV are assigned to aliphatic and adventitious contamination carbons C−C (C=C, C−H) and carbon bonded to halogen and/or oxygen atoms C−Br(Cl), C–O, respectively.[131,132] In the case of phenylethynyl

(Fig. 6.4c), the C 1s peak emission corresponding to the adventitious carbons at 284.6 eV is ~ 30% higher in intensity than the C 1s peak from propynyl- and ethynyl-modified Si surfaces. This observation is quite obvious, considering that the phenyl-ring from the C_6H_5−C≡C−MgBr solution contains more carbons than the CH_3−C≡C−MgBr and H−C≡C−MgCl solutions.

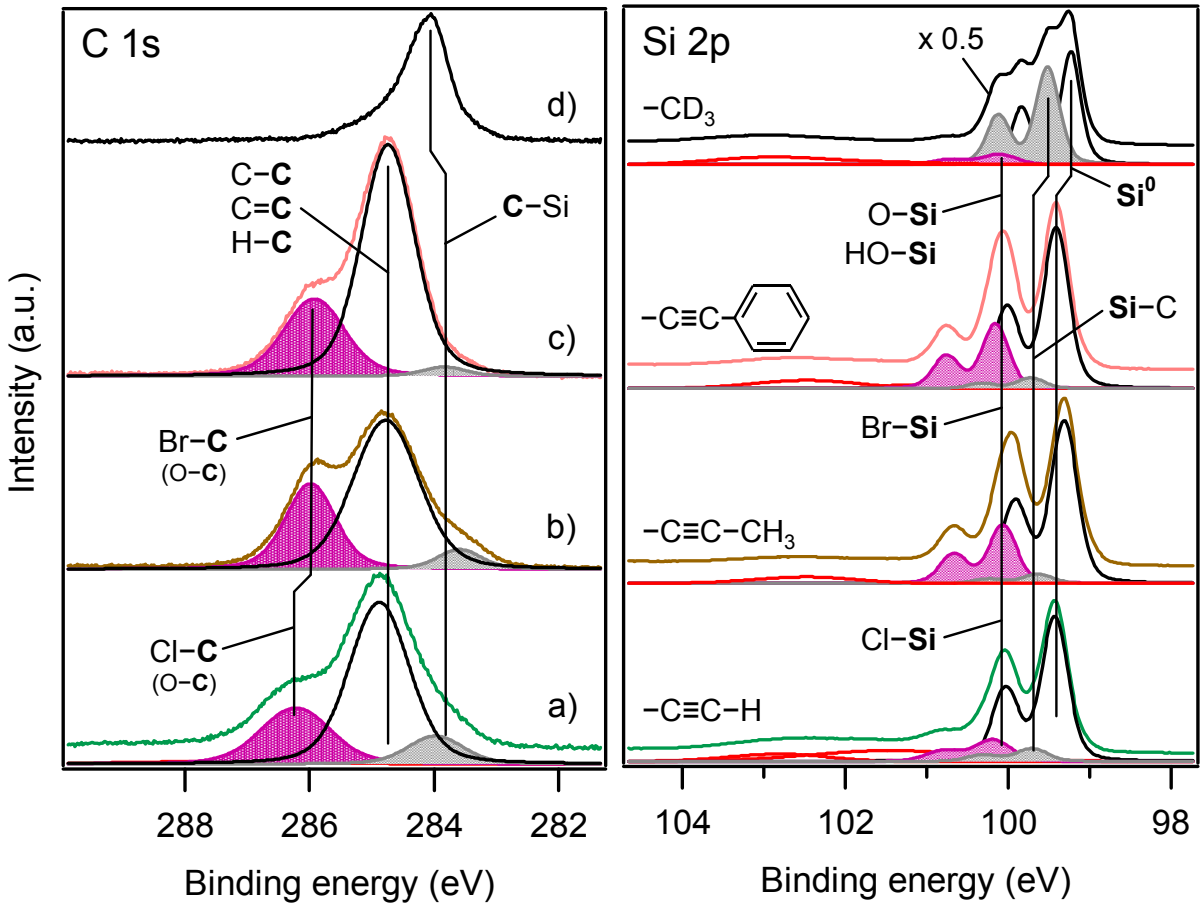

Fig. 6.4: *High resolution SXP spectra in the C 1s (left) and Si 2p (right) region after organic modification in (a) HC≡C−MgCl, (b) CH_3−C≡C−MgBr, and (c) C_6H_5−C≡C−MgBr solutions recorded with an photon energy of hv = 650 and 150 eV, respectively. A current density of 0.02 mA/cm^2 has been applied to the Si samples for each Grignard solution for 1200 s (~ 24 mC/cm^2). SXP data for the methylated Si(111) surface (d) is shown for comparison. Peaks have been fitted with a Gaussian-Lorentzian sum function after a Shirley background subtraction.*

6.3 SEM imaging of "thick" polymeric layers

Scanning electron microscopy (SEM) has been performed to reveal the surface morphology and the thickness of the polymeric layer obtained on Si surfaces after the electrochemical deposition. The Si substrates have been treated in (a) HC≡C−MgCl, (b) CH_3−C≡C−MgBr, and (c) C_6H_5−C≡C−MgBr by applying an anodic current density of 0.5 mA/cm^2 for 900 s (~ 450 mC/cm^2) to obtain the formation of "thick" polymeric layers. The SEM micrographs of such organic layers on Si surfaces are shown in Fig. 6.5 under a tilt angle of 30°. A thickness of ~ 10, 12, and 20 nm have been determined for the "thick" organic layers obtained after electrochemical modification in C_6H_5−C≡C−MgBr, CH_3−C≡C−MgBr, and HC≡C−MgCl solutions, respectively.

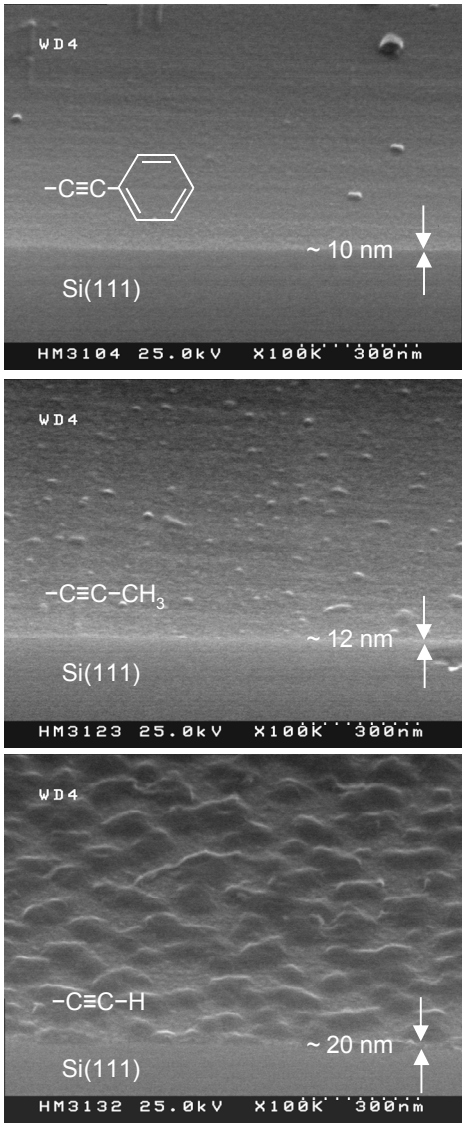

Fig. 6.5: *SEM micrographs of modified Si(111) surfaces electrochemically treated in (a) HC≡C−MgCl, (b) CH_3−C≡C−MgBr, and (c) C_6H_5−C≡C−MgBr solutions using a current density of 0.5 mA/cm^2 for 900 s (~ 450 mC/cm^2) and recorded under a tilt angle of 30°.*

Depending on the thickness, the Si substrates modified in $C_6H_5-C\equiv C-MgBr$ solution were colourless, the one modified in $CH_3-C\equiv C-MgBr$ started to reveal a blue colour, and the thicker layer prepared from $HC\equiv C-MgCl$ was completely blue as observed with the naked eye. Recently, thick polymeric layers up to 870 nm thickness have been observed at high charge flow. Furthermore, the SEM micrographs indicate different structures on the surfaces for the different type of polymers formed. Surprisingly, a regular "wave" like structure is observed in the case of the layer deposited from $HC\equiv C-MgCl$ solution, while the surfaces were smooth for polymeric layers prepared from $CH_3-C\equiv C-MgBr$ and $C_6H_5-C\equiv C-MgBr$ solutions. However, no layer could be observed for the deposition from $HC\equiv C-MgBr$ solution by SEM techniques even after application of the same charge flow.

6.4 PL and SPV characterizations

Photoluminescence (PL) and surface photovoltage (SPV) measurements have been performed to obtain information about non-radiative recombination active defects and band bending created at the organic/silicon interfaces. For these investigations, fresh H-terminated Si(111) surfaces electrochemically modified in (a) $H-C\equiv C-MgCl$, (b) $CH_3-C\equiv C-MgBr$, (c) $C_6H_5-C\equiv C-MgBr$, and (d) $H-C\equiv C-MgBr$ solutions have been prepared, respectively. A current density of 0.5 mA/cm^2 for 900 s (~ 450 mC/cm^2) was applied to the Si electrodes during the anodic treatment. The results obtained are presented in Figs. 6.6 and 6.7 for the PL and SPV characterizations, respectively.

Fig. 6.6 illustrates the PL intensity (I_{PL}) spectra of the modified Si(111) surfaces using a pulsed dye laser at 500 nm excitation wavelength. The $CH_3-C\equiv C$-terminated Si surface (Fig. 6.6b) shows the highest I_{PL} as compared to Si surfaces modified with the other ethynyl derivatives. I_{PL} of the Si surface treated in $H-C\equiv C-MgBr$ solution is reduced by ~ 40% in relation to the $CH_3-C\equiv C$-terminated one. Moreover, a strong decrease by ~ 90 and 95% in I_{PL} is observed for the Si samples treated in $C_6H_5-C\equiv C-MgBr$ and $H-C\equiv C-MgCl$ solutions, respectively. Surprisingly, the Si surfaces modified in the two ethynyl-Grignard compounds containing different halogen atoms, Cl (Fig. 6.6a) and Br (Fig. 6.6d), respectively, reveal totally different electronic properties. The increase in I_{PL} of Si modified with $H-C\equiv C-MgBr$ is probably due to the presence of tremendous adventitious Br contaminations. This demeanor is consistent with the SXP results of the Si substrate modified by a charge flow of 60 mC/cm^2, where a high amount of Br contaminations has been revealed. For a higher charge flow applied to the substrate like in this case, a higher amount of Br contaminations is expected.

Furthermore, another point has to be taken into account: the thickness of these samples. According to SEM measurements, no thickness can be evaluated in the case of the Si surface modified in H−C≡C−MgBr, while a thickness of ~ 20 nm has been found in the case of the sample modified in H−C≡C−MgCl solution. It has been found that for C_6H_5-C≡C−MgBr, the increase in charge flow from 24 to 450 mC/cm^2 decreases strongly the presence of Br–Si bonds (not shown here). With this observation and the assumption that a similar behavior could also occurs in the case of modification in CH_3-C≡C−MgBr solution, less Br contaminations are also expected. Thus, in the case of CH_3-C≡C-terminated Si surface, even if the Si substrate is contaminated with Br species, it has been supposed that this surface also led to less pronounced non-radiative recombination at the interface due to fewer amount of defects at the interface.

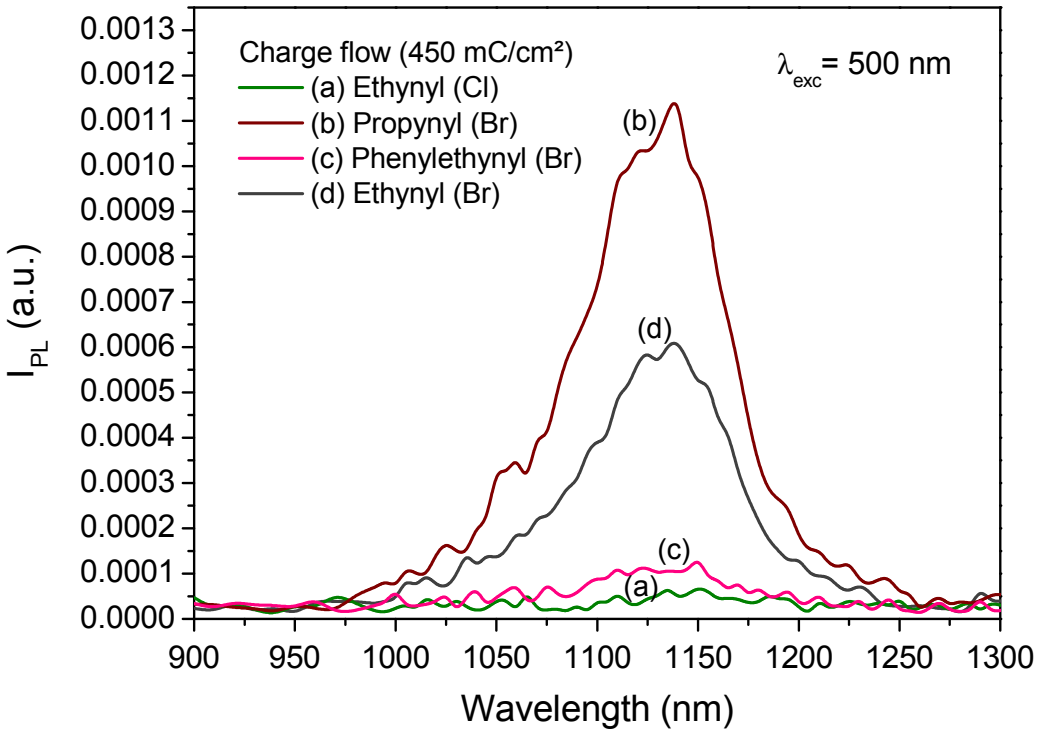

Fig. 6.6: *PL intensity spectra of modified Si(111) surfaces, I_{PL}, after anodic treatment in (a) H−C≡C−MgCl, (b) CH_3−C≡C−MgBr, (c) C_6H_5−C≡C−MgBr, and (d) H−C≡C−MgBr. Current density of 0.5 mA/cm^2 for 900 s (~ 450 mC/cm^2) has been applied to the Si substrates for each Grignard solution.*

Fig. 6.7 shows the SPV measurements performed with the application of a short laser pulse (λ_{ex} = 902 nm, pulse width 150 ns) after 4 µs of pre-polarization at a potential of 200 mV for the modified Si surfaces obtained after electrochemical modification in (a) H−C≡C−MgCl, (b) CH_3−C≡C−MgBr, (c) C_6H_5−C≡C−MgBr, and (d) H−C≡C−MgBr solu-

tions. A current density of 0.5 mA/cm^2 for 900 s (~ 450 mC/cm^2) has been applied to each Si substrate. The change in the photovoltage response, U_{Ph}, is proportional to a change in the band bending of the Si substrate. The typical H-terminated Si(111) sample exhibits a value of $U_{Ph} \approx -484$ mV. The Si substrates modified in $CH_3-C\equiv C-MgBr$ and $H-C\equiv C-MgBr$ solutions lead to an U_{Ph} of approximately – 542 mV and – 560 mV, respectively, whereas in the case of $H-C\equiv C-MgCl$ and $C_6H_5-C\equiv C-MgBr$ solutions, a higher U_{Ph} is observed about − 683 mV and – 694 mV, respectively. A change in the band bending seems to be higher in case of treatment in $H-C\equiv C-MgCl$ and $C_6H_5-C\equiv C-MgBr$ solutions. For the electrochemical modification in $CH_3-C\equiv C-MgBr$ and $H-C\equiv C-MgBr$ solutions, the demeanors observed here is in correlation with the PL intensity response (I_{PL}) obtained. A weaker depletion in the space charge region (smaller band bending) reveals a better passivation of the surface gap states, i.e., leading to fewer amounts of surfaces states/traps. Obviously, a small change in U_{Ph} (~ 60 mV in comparison to H-terminated Si surface) has been related to the higher values of I_{PL}. Moreover, one can see that the return of U_{Ph} to the equilibrium static value at longer times is reached much more rapidly in the case of $H-C\equiv C-MgCl$. Here again, halogen atoms play an important role in the electronic properties of the modified Si surfaces and particularly, in the surface band bending as revealed by these measurements.

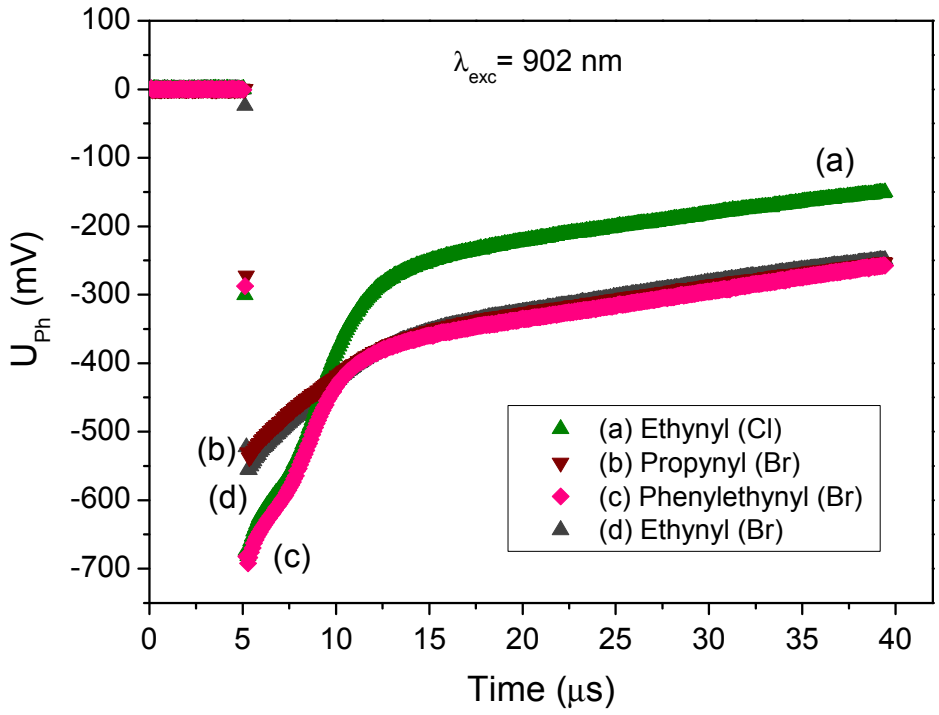

Fig. 6.7: *SPV transients of organically modified Si(111) surfaces electrochemically prepared in (a) HC≡C−MgCl, (b) $CH_3-C\equiv C-MgBr$, (c) $C_6H_5-C\equiv C-MgBr$, (d) HC≡C−MgBr solutions, recorded after 4 µs of pre-polarization at a potential of 200 mV. A current density of 0.5 mA/cm^2 for 900 s (~ 450 mC/cm^2) was applied for each Si samples during the electrochemical treatment.*

6.5 Determination of the chemical composition and thickness

The total coverage in terms of monolayer (ML) and the total overlayer thickness in Å has been estimated from the atomic concentration of the different species present on the Si surface as determined from the SXP spectra shown in Fig. 6.4. The total overlayer thickness has been estimated from the closed overlayer model[54] using the mathematical relations given in Chap. 3. Annealed CH_3-terminated Si(111) surface shows only one emission from C–Si bonds, so that this Si sample is considered to represent an ideal complete modification of all atop Si atoms surface. The measured peak intensities are related to the C 1s emission signal of Si(111) terminated with a CH_3–monolayer and knowing that one monolayer corresponds to an atom surface density of $N_{Si(111)} = 7.8 \times 10^{14}$ cm^{-2}.

Fig. 6.8 exhibits the atomic concentration in % on the modified Si surfaces and the layer thickness in monolayer (ML) and Å, respectively, as obtained from the SXPS measurements (Fig. 6.4). The coverage of the ethynyl derivatives is ~ 5 ML (~ 2 ML for $-CH_3$). Some SiO_x species present at the interface have been reflected by the O 2s and Si 2p suboxide signals.

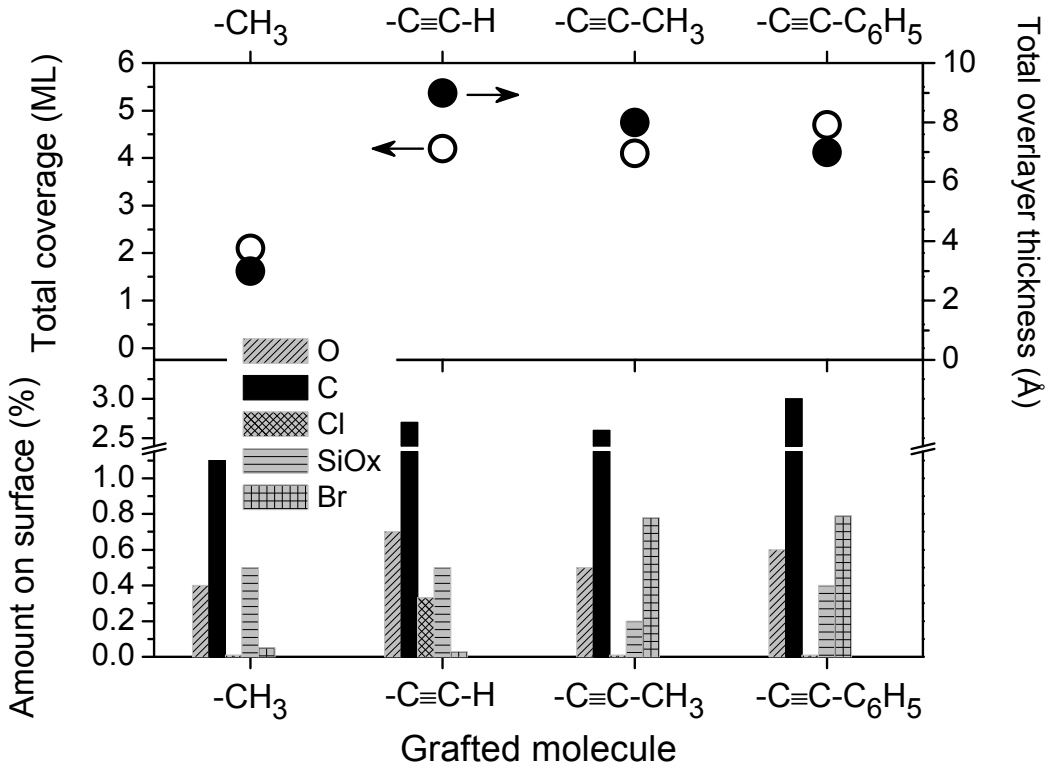

Fig. 6.8: *Atomic concentration of O, C, Cl, SiO_X and Br on the modified Si surfaces (bottom) and the layer thickness in monolayer (ML) and Å, respectively (top), as obtained from the SXPS measurements (see Fig. 6.4). One monolayer corresponds to a Si(111) surface atom density of $N_{Si(111)} = 7.8 \times 10^{14}$ cm^{-2}. The measured peak intensities have been related to the C 1s emission signal of Si(111) terminated with a CH_3-monolayer.*

However, the O 2s emission signal is mainly due to remnant adventitious contaminations. The amount of Br atoms on the Si surface (mainly as Si−Br and C−Br, see Fig. 6.4) from the Br-containing Grignard compounds is twice of the amount of Cl atoms from the Cl-containing Grignard compound. Moreover, in the case of CH_3−C≡C- and C_6H_5−C≡C-modified Si surfaces, the amount of Si−Br bonds at the interface measured is much higher than Si−Cl bonds for Si surface modified with H−C≡C−MgCl as can be seen in Fig. 6.4. This result points to a higher amount of Br at the interface and therefore to a lower reaction rate of Si−Br than for Si−Cl intermediates and/or to a higher hindrance by the bigger $-CH_3$ and $-C_6H_5$ groups during the grafting process. The layer thickness is similar for all ethynyl-Grignard solutions after a charge flow of ~ 24 mC/cm^2 (i = 0.02 mA/cm^2 for 1200 s) as revealed in Fig. 6.8.

6.6 Grafting mechanism for ethynyl derivatives

The presence of Si− and C−halogen (Br, Cl), and Si−C bonds on the modified surfaces lead to the assumption that the Grignard compounds not only react via oxidation of the Br(Cl)Mg−C bond like in the ideal case (reaction scheme I), but also via oxidation of the C≡C bond (reaction scheme IIa) and reactions via halogen atoms with the Si surface (reaction scheme IIb):

I)
$$R{-}C{\equiv}C{-}MgX + h^+ \rightarrow R{-}C{\equiv}C\bullet + MgX^+ \quad (6.1a)$$
$$\equiv Si{-}H + R{-}C{\equiv}C\bullet \rightarrow \equiv Si\bullet + R{-}C{\equiv}C{-}H \quad (6.1b)$$
$$\equiv Si\bullet + R{-}C{\equiv}C{-}MgX + h^+ \rightarrow \equiv Si{-}C{\equiv}C{-}R + MgX^+ \quad (6.1c)$$

II)
$$R{-}C{\equiv}C{-}MgX + h^+ \rightarrow R{-}C{\equiv}C\bullet + MgX^+ \quad (6.2a)$$
$$\equiv Si{-}H + R{-}C{\equiv}C\bullet \rightarrow \equiv Si\bullet + R{-}C{\equiv}C{-}H \quad (6.2b)$$
a)
$$R{-}C{\equiv}C{-}MgX + R{-}C{\equiv}C\bullet \rightarrow R{-}C{\equiv}C{-}X + R{-}C{\equiv}C{-}Mg\bullet \quad (6.2c)$$
$$\equiv Si\bullet + R{-}C{\equiv}C{-}X \rightarrow \equiv Si{-}C(R){=}C\bullet{-}X \quad (6.2d)$$
$$\equiv Si{-}C(R){=}C\bullet{-}X + H{-}source \rightarrow \equiv Si{-}C(R){=}CHX + source\bullet \quad (6.2e)$$
b)
$$\equiv Si\bullet + R{-}C{\equiv}C{-}MgX \rightarrow \equiv Si{-}X + R{-}C{\equiv}C{-}Mg\bullet \quad (6.2f)$$
c)
$$\equiv Si{-}X + R{-}C{\equiv}C{-}MgX \rightarrow \equiv Si{-}C{\equiv}C{-}R + MgX_2 \quad (6.2g)$$

where X = Br, Cl and source = solvent or Si−H.

Typically, the Si−X surface species will react with the Grignard compound (IIc). However, reaction via (IIa) will lead to a steric hindrance of further reaction of neighboured Si−X species formed via (IIb) and therefore the amount of Si−Br at the interface increases with respect to Si−Cl for grafting of the smaller ethynyl group by the MgCl compound. A smaller amount of halogen has been observed in the case of H−C≡C-, while the same amount of halogen has been detected for CH_3−C≡C- and C_6H_5−C≡C-, respectively. This phenomenon probably arises from the covalent atom radii of the different halogen atoms (X = Cl in H−C≡C−MgX and X = Br in CH_3−C≡C− and C_6H_5−C≡C−MgX solutions, respectively) present in the Grignard compounds. Br atoms have a bigger atomic radius than Cl atoms and, thus, obviously block the reaction (steric hindrance). Subsequently, Cl atoms present in the Grignard solution favor the polymerization process at higher charge flow, as observed for HC≡C−MgCl, where the thickness was twice as compared to CH_3−C≡C- and C_6H_5−C≡C-modified Si surfaces after using the same charge flow (see Fig. 6.5). The formation of these thin polymeric layers is supposed to arise via oxidation of the C≡C bonds, as well as from reactions via halogen atoms with the Si surface and not only via oxidation of the Br(Cl)Mg−C bond from Grignard compound like it was the case for alkyl groups (methyl groups).

6.7 Discussion of the surface electronic properties

The surface electronic properties obtained from the SXPS measurements are summarized in Tab. 6.1 for the Si surfaces modified in H−C≡C−MgBr solution with different charge flow and for the other ethynyl derivatives, respectively. The work function (Φ) is determined from the extrapolation of the secondary electron cutoff edge (see Chap. 2). The chemical shift of the bulk Si $2p_{3/2}$ peak emission (Si^0) observed in the Si 2p emission spectra give an indication about the surface band bending which occurs on the Si surface after the modification by organic molecules. The surface band bending (eV_{bb}), the electron affinity (χ), and the surface dipole (δ) are obtained by the assumption that the binding energy of the Si 2p signal in the bulk with respect to the valence band maximum is 98.74 eV,[40] and that the electron affinity of the bulk silicon (χ_{Si}) is taken as χ_{Si} = 4.05 eV.[41] More details about the determination of these values have been already explained in Chap. 2.

Tab. 6.1 summarizes the surface electronic properties determined from the Si surfaces treated in H−C≡C−MgBr solution with different charge flow. The higher eV_{bb} (~ 0.53 eV) of about + 0.10 eV occurs in the case of less flown charge of 2.4 mC/cm^2 in relation to the other ones (Si substrates anodized with 60 mC/cm^2 and 24 mC/cm^2, eV_{bb} ~ 0.43 eV, respectively).

However, for this sample the lowest Φ is observed (~ 4.31 eV). The increase in charge flow (from 24 to 60 mC/cm^2) shows a parallel increase of Φ from 4.47 to 4.69 eV, respectively. Additionally, χ and δ increase also since they are correlated together by the relation $\delta = \chi - \chi_{Si}$. So that the charge flow increases from 2.4 to 24 and 60 mC/cm^2 and δ increases from – 0.12 to + 0.16 eV, respectively. The tremendous change by about + 0.23 eV between the sample modified with 24 and 60 mC/cm^2 is supposed to arise predominantly from the presence of a higher amount of Br atoms in that case. The assumption of these polar atoms present on the surface could drastically change the work function by an increase. In the same way, the contribution of the surface dipoles predominantly due to Br atoms could be also affected, so that the real contribution of the surface dipoles build from the Grignard solution are also reduced.

Tab. 6.1: *Electronic properties of Si(111) surfaces modified by ethynyl derivatives via Grignard compounds (H- and CD_3-terminated Si(111) surfaces have been added for comparison).*

R=	Binding energy, Si $2p_{3/2}$ (eV)	Surface band bending, eV_{bb} (eV)	Work function, Φ (eV)	Electron affinity, χ (eV)	Surface dipole, δ (eV)
–H (annealed)	99.42	0.48	4.58	4.07	0.02
−C≡C−H (Br) (60 mC/cm²)	99.37	0.43	4.69	4.21	+0.16
−C≡C−H (Br) (24 mC/cm²)	99.37	0.43	4.47	3.98	-0.07
−C≡C−H (Br) (2.4 mC/cm²)	99.47	0.53	4.31	3.93	-0.12
$–CD_3$ (annealed)	99.27	0.33	4.24	3.61	-0.44
−C≡C−H (Cl)	99.42	0.48	4.40	3.96	-0.09
$−C≡C−CH_3$	99.29	0.35	4.51	3.97	-0.08
$−C≡C−C_6H_5$	99.53	0.59	4.64	4.19	+0.14
incertitude	± 0.05	± 0.05	± 0.10	± 0.15	± 0.15

For more explanations about the determination of these values, please see chapter 2

Additionally, the surface electronic properties obtained from the Si surfaces electrochemically modified in H−C≡C−MgCl, CH_3−C≡C−MgBr, and C_6H_5−C≡C−MgBr solutions by a lower charge flow of 24 mC/cm^2 (0.02 mA/cm^2 for 1200 s) are also summarized in Tab. 6.1. For comparison, H- and CD_3-terminated Si surfaces are added to Tab. 6.1. In the case of Si surface modified in C_6H_5−C≡C−MgBr solution, a work function of 4.64 eV and a surface dipole of + 0.14 eV have been determined. These values are quite similar to the Si surface obtained from the modification in H−C≡C−MgBr when a charge flow of 60 mC/cm^2 has been applied because these two modified surfaces exhibit the highest amount of adventitious Br atom contamination (as shown on the respective SXP spectra, Figs. 6.2 and 6.4, respectively). The occurrence of the higher Φ and δ for these modified Si surfaces is in good agreement with the dipole effect contribution of Br atoms on the Si surface. In the case of CH_3−C≡C-modified Si surface, about the same amount of Br atoms is observed in relation to C_6H_5−C≡C−MgBr. However, more than twice of the amount of C–Si bonds has been established (see Fig. 6.4) in the case of CH_3−C≡C-modified Si surface. This CH_3−C≡C-modified Si surface reveals then a "better" achievement for the grafting of these molecules. Moreover, a surface band bending of ~ 0.35 eV has been found for this Si substrate, which is quite equivalent to the annealed CH_3-terminated Si(111) surface. This behavior clearly indicates the grafting of molecules using this Grignard compound.

In addition as remark, the Si substrate modified in CH_3−C≡C−MgBr solution with a higher current flow of about 450 mC/cm^2 starts to reveal a blue colour and the morphology structure of this Si substrate changes to a "wave" like structure as compared to the one modified in H−C≡C−MgCl solution. Besides, for the Si substrate modified in H−C≡C−MgCl, the work function, the surface band bending and the surface dipole are quite identical to the fresh H-terminated Si(111) surface. The similarity of the electronic properties observed lets suppose the achievement of a well passivated Si surface in comparison to the other ethynyl derivatives. Moreover, these observations are consistent with the amount of more than 40% of C–Si bonds than in the case of CH_3−C≡C-modified Si surface. A homogenous surface layer has also been observed by the SEM micrograph with a thickness of ~ 20 nm (see Fig. 6.5). However, it has been shown that the ethynyl compounds and derivatives reveal a surface dipole of about (− 0.09 ± 0.03) eV, when the Si substrate was not presenting a large amount of Br atoms (like in the case of C_6H_5−C≡C− (using 24 mC/cm^2) and H−C≡C− (using 60 mC/cm^2)).

6.7.1 Comparison of the surface band bending determined by two different techniques

Fig. 6.9 shows the comparison of the band bending of different molecules electrochemically grafted onto Si(111) surfaces revealed from SPV and SXPS measurements, respectively. The band bending determined from SPV measurements is noticed as U_{Ph}, whereas the surface band bending established from SXPS measurements is represented as eV_{bb}. Thin organic layers of ethynyl derivatives (24 mC/cm^2) have been used for the evaluation of eV_{bb}, whereas U_{Ph} has been measured for the thicker layers of ethynyl derivatives obtained (450 mC/cm^2). However, no light absorption occurred for the thicker layers because λ_{ex} is 902 nm in this case. Therefore, U_{Ph} and eV_{bb} are responsible for the organic/Si interface. This plot shows a linear trend between U_{Ph} and eV_{bb} for the modified Si surfaces.

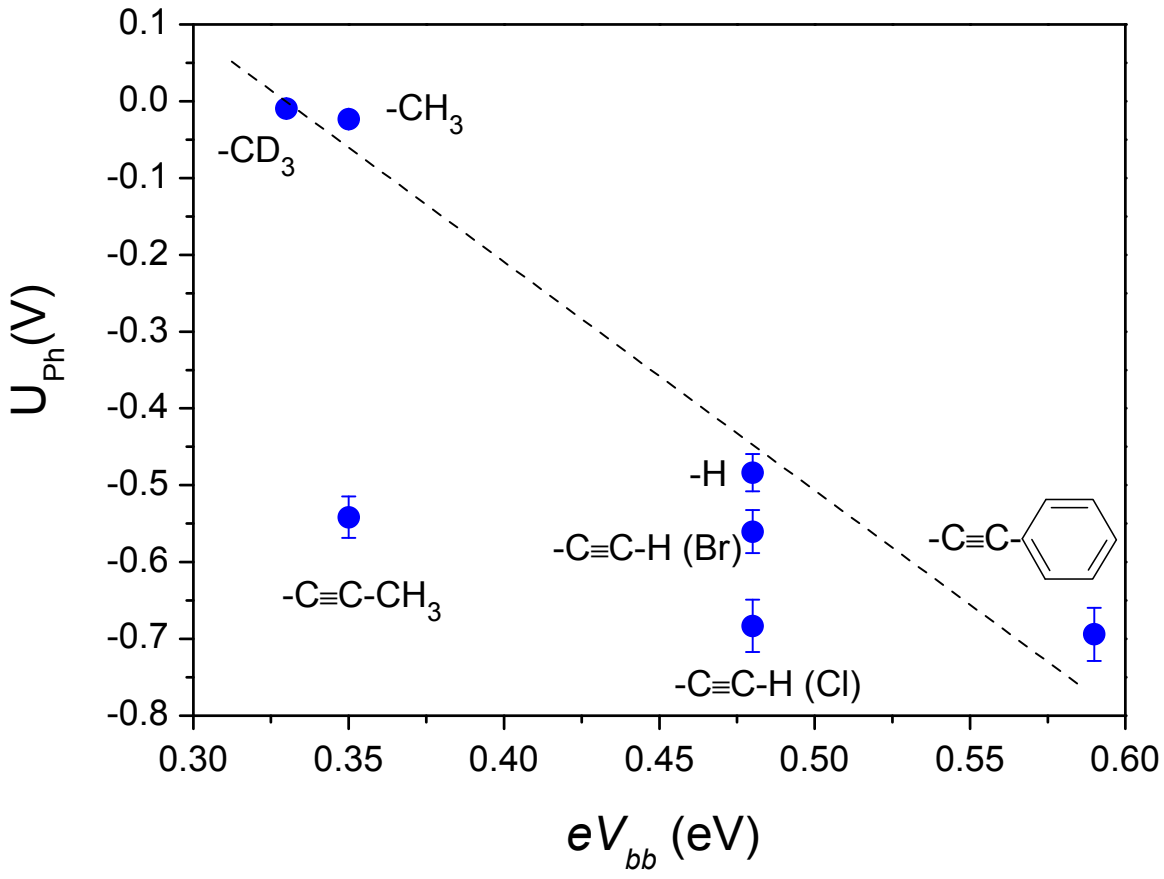

Fig. 6.9: *Photopotential (U_{Ph}) measured by SPV method as a function of the surface band bending (eV_{bb}) ascertained from SXPS measurements from Si modified electrochemically in CH_3MgBr, CD_3MgI, $H{-}C{\equiv}C{-}MgBr$, $H{-}C{\equiv}C{-}MgCl$, $CH_3{-}C{\equiv}C{-}MgBr$, and $C_6H_5{-}C{\equiv}C{-}MgBr$ solutions. H-terminated Si(111) surface is also added to the figure for comparison.*

In the case of electrochemical modification in H−C≡C−MgCl and CH_3−C≡C−MgBr solutions, a higher discrepancy occurs and seems to arise from the probably incorporation of some other charged species (i.e., Br and Cl atoms), which can influence the dipole of the organic molecules and then lead to an "effective dipole" on the surface. However, the CH_3- and CH_3−C≡C-terminated Si surfaces show the lowest eV_{bb}. This indicates an easier charge transfer between these organic molecules and the p-type Si substrate because a lower barrier has been observed (smaller depletion than in the case of the other molecules). Therefore, the smaller reduction of the band bending (in relation to H-terminated Si surface) implies a better electronic passivation because more surface gap states were recovered. This statement indicates a direction to the flat band conditions. As compared to U_{Ph}, every ethynyl derivatives show a band bending (depletion) similar to that of H-terminated Si surface. In the case of CH_3−C≡C-terminated Si surface, it seems that the difference of the charge contribution from the adsorbate layer is totally different for the samples prepared at "low" or "high" charge flow. However, for H-, CH_3- and CD_3-terminated Si surfaces, it is consistent that eV_{bb} and U_{Ph} are similar because the surfaces have been prepared under the same conditions, so that they present the same density and energy distribution of the surface charge. Additionally, these measurements reveal that both SPV and SXPS experimental methods lead to similar trends, although they are completely different techniques.

6.7.2 Surface band bending versus surface dipole and work function

Fig. 6.10 illustrates the surface band bending (eV_{bb}) and the photopotential (U_{Ph}) as function of (a) the surface dipole, δ, and (b) the work function, Φ, of Si surfaces electrochemically modified in CH_3MgBr, CD_3MgI, H−C≡C−MgBr, H−C≡C−MgCl, CH_3−C≡C−MgBr, C_6H_5−C≡C−MgBr solutions, respectively. For comparison, the values for H-terminated Si(111) surface has also been added to the figure. As explained above, eV_{bb} and U_{Ph} represent both the band bending of the surface. However, eV_{bb} and U_{Ph} have been obtained from two different techniques, from SXPS and SPV measurements, respectively. A linear tendency is observed between eV_{bb} and U_{Ph} as function of δ, and Φ, respectively, for the different modified Si surfaces. The surface modified with methyl groups (CH_3 and CD_3 molecules, respectively) reveals the lower Φ and eV_{bb} for this series of molecules. The methylated Si surfaces exhibits a good concordance for eV_{bb} and U_{Ph} in relation to δ, while in comparison with Φ, a shift of ~ 0.09 eV appears (see Fig. 6.10b).

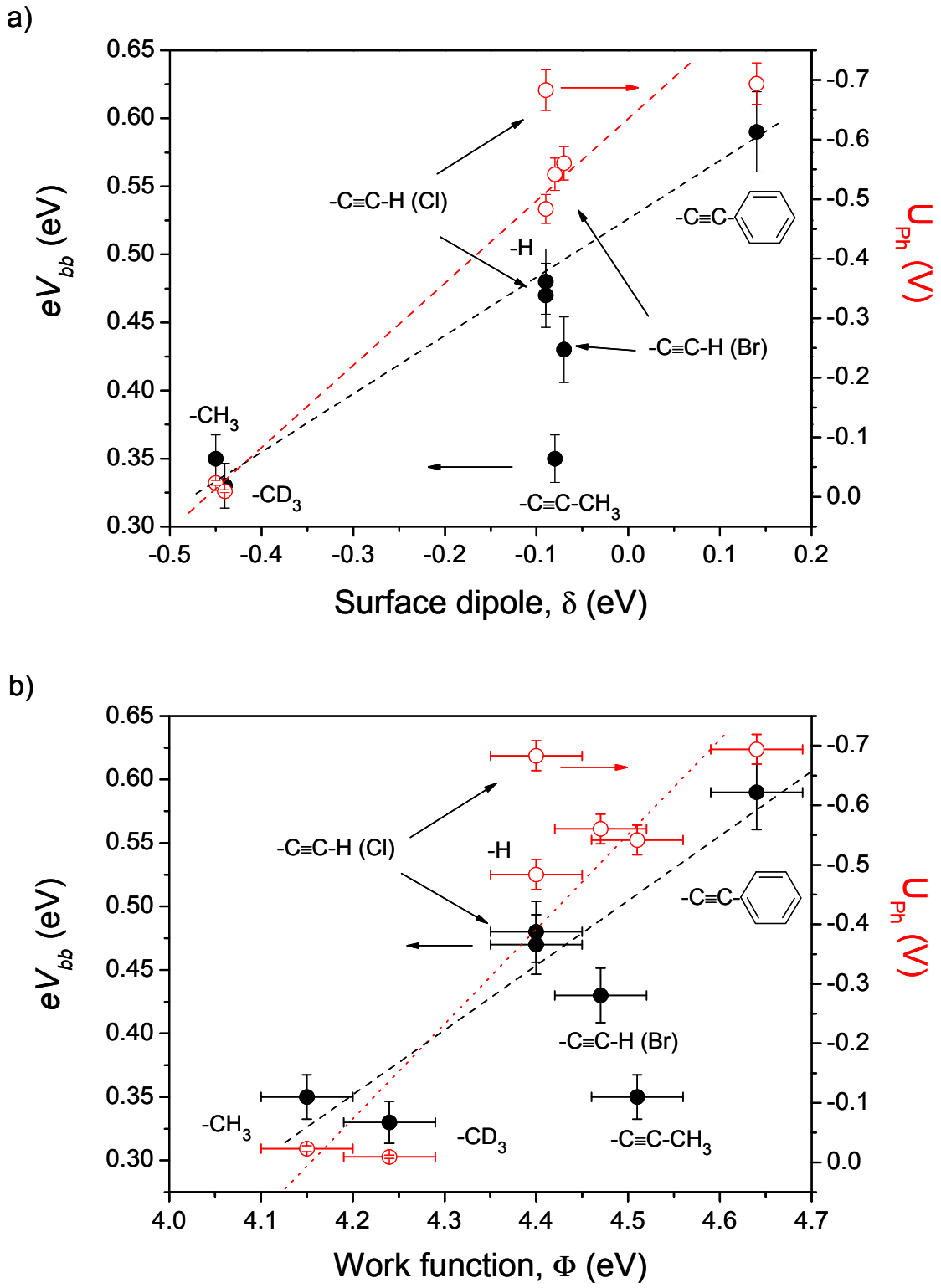

Fig. 6.10: *Surface band bending (eV_{bb}) and photopotential (U_{Ph}) versus (a) surface dipole, δ, and (b) work function, Φ, of H-, CH_3- and ethynyl derivatives-terminated Si(111) surfaces. For comparison, the value of H-terminated Si(111) surface has also been added.*

A general increase in the linear trend is observed in the case of ethynyl derivatives. The bigger the end group of the ethynyl (from H to C_6H_5, i.e., presenting more electrons), the more the increase of eV_{bb} and U_{Ph} with respect to δ, and even to Φ. This behavior is consistent

with the fact that a change in the band bending (eV_{bb} or U_{Ph}) leads to a change in Φ of the modified Si surfaces. However, Si surfaces modified with −H, −C≡C−H, and −C≡C−CH_3 present a similar value of δ (~ 0.10 eV), which implies that the environment (i.e., electronic distribution) at the interface is rather identical. Nevertheless, different Φ are determined for these modified Si surfaces, and an increase also appears with the bigger end group of ethynyl derivatives (from 4.40 to 4.51 eV, for −C≡C−H and −C≡C−CH_3, respectively). Moreover, in the case of Si modified with C_6H_5−C≡C−MgBr solution, (which possess the "more" electron donator molecules due to C≡C added to the phenyl ring) a net drop appears in eV_{bb} and U_{Ph} but also in δ, and Φ, respectively. Finally, the observed linear trend is consistent with the "donator" behavior of the molecular electrons, where the electron density is displaced to the Si surface.[133] Ethynyl derivatives present intrinsically more electrons (because of the C≡C bonds in these molecules) than methyl groups, and result in a higher band bending, i.e., a stronger depletion in the space charge region near the surface. This is consistent with the fact that electron donating molecules display electrons to the p-Si surface, which increases the depletion near the surface, and finally, more electron transfer occurs in this direction. However, the C≡C bonds have an important electronic negative charge near the surface, if we consider that the grafting is performed via the radicals of these molecules, which attracts strongly electrons. This phenomenon results to a higher Φ (with C≡C bonds and with increase the end group of these ethynyl derivatives) on the surface, which impedes the escape of an electron from the bulk Si to the surface due to the presence of a high barrier level. Because the lower band bending occurs for methyl groups, a weaker depletion should also occur on the surface as compared to the other molecules. This suggests also that the surface gap states were more recovered by the molecules, which implies the most efficient passivation of the surface due to the lower band bending, but also a better charge transfer between the molecules and the surface.

6.7.3 Correlation between the work function and the surface dipole

The work function is a material constant and can be influenced by surface dipoles, i.e., by electron affinity which shifts the reference level (the vacuum level). As discussed above, the relation between the band bending and the work function or the surface dipole reveals a linear trend. This linear trend shows clearly that these physical magnitudes are correlated. However, until now, no relation between Φ and δ has been shown for the organically modified Si surfaces.

Fig. 6.11 depicts the behavior between the work function and the surface dipole of electrochemically modified Si(111) surfaces in CH_3MgBr, CD_3MgI, H−C≡C−MgBr, H−C≡C−MgCl, CH_3−C≡C−MgBr, C_6H_5−C≡C−MgBr electrolytes as obtained from SXPS measurements. For comparison, the values of the annealed Si(111) samples modified in CH_3MgBr, CD_3MgI, H−C≡C−MgBr solutions and H-terminated Si(111) surfaces have been added to the figure. This figure reveals a well linear trend for both annealed and non-annealed Si(111) samples. This demeanor confirms that a change in the contribution of the dipole moments coming from the deposited organic molecules on the surface also change the work function of the Si surface. Therefore, it seems that an "effective" dipole moment, which is attributed to the dipole contributions of the individual adsorbate molecules (due to their ordering), gives rise to a macroscopic electrostatic surface dipole. The difference between Φ and δ for the annealed and non-annealed Si surfaces arises from the loss of contaminants after annealing process. A tendancy also appears for these modified surfaces. It can be observed that after annealing the Si samples, Φ and δ increase, respectively.

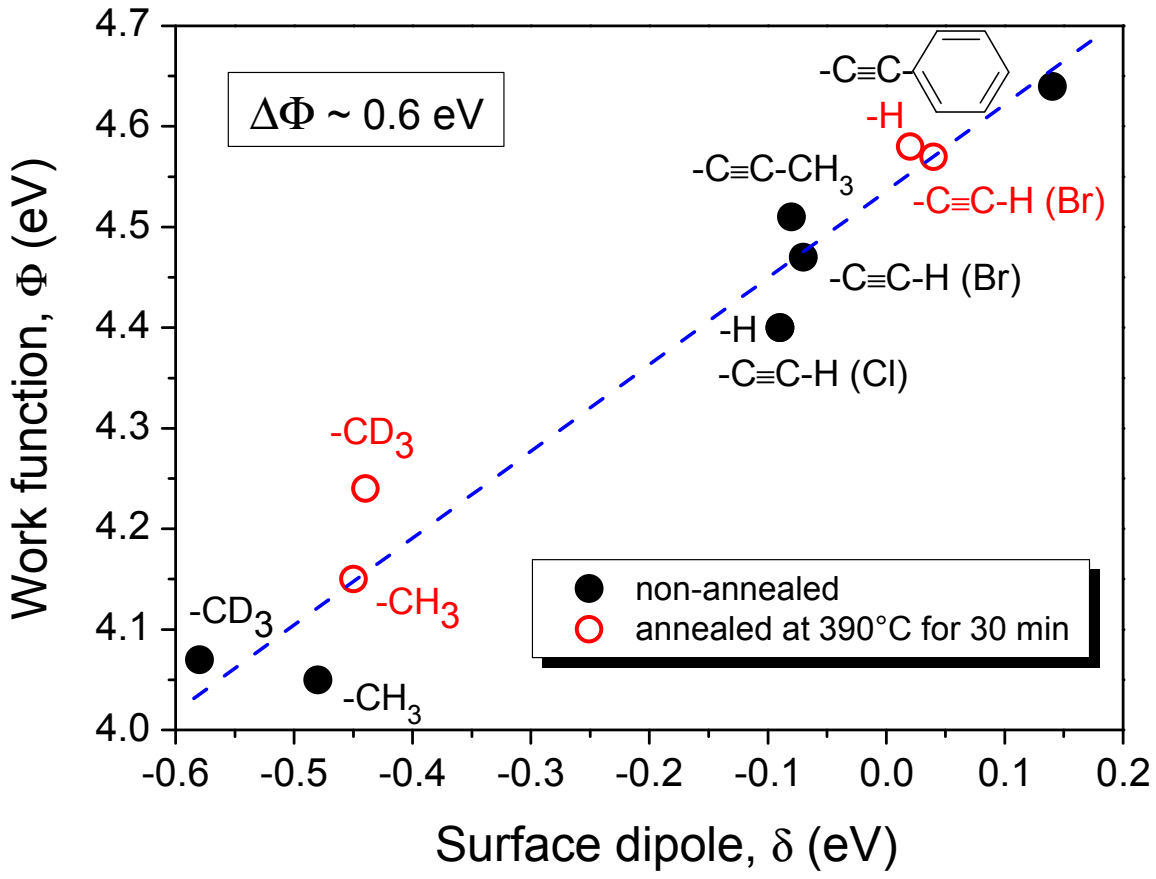

Fig. 6.11: *Work function, Φ, as a function of the surface dipole, δ, of modified Si(111) surfaces. The samples have been obtained after electrochemical treatment in CH_3MgBr, CD_3MgI, H−C≡C−MgBr, H−C≡C−MgCl, CH_3−C≡C−MgBr, C_6H_5−C≡C−MgBr solutions. The H-terminated Si(111) surface has been prepared as usual in 40% NH_4F concentrated solution.*

6.8 Conclusion

The electrochemical grafting of ethynyl derivatives onto Si(111) surfaces in a one-step reaction using an anodic Grignard electrochemical route has been characterized by several techniques such as IRSE, SXPS, SEM, PL, and SPV measurements. This electrochemical grafting method points out the possibility to control the grafting of such ultrathin organic layers onto Si(111) surfaces by varying the charge flow applied. Typical thicknesses ranging from ~ 8 Å (~ 5 ML) to ~ 20 nm have been established during the application of an anodic charge flow between 24 mC/cm^2 and 450 mC/cm^2, respectively. Moreover, the efficiency of the grafting process obviously depends on the type of halogen atoms present in the Grignard electrolyte as used for ethynyl-termination of Si(111) surfaces. However, at low charge flow of ~ 24 mC/cm^2, no tremendous differences in the measured SXP spectra are observed. Besides, the electronic surface properties established from SXPS measurements were quite similar. Nevertheless, at a higher charge flow applied (450 mC/cm^2), the ethynyl-terminated Si(111) surfaces show totally different electronic properties (thicknesses, defects at interface, band bending, morphology…) as revealed by IRSE, PL, and SPV investigations, but also SEM micrographs. In the case of the other ethynyl derivatives (propynyl- and phenylethynyl-MgBr), IRSE-spectra have indicated the presence of the molecules (by several typical IR-absorption of specific vibrational modes from these molecules) and polymerization at higher charge flow. SXP core level spectra have given clear evidence of the grafting of ethynyl derivatives onto Si(111) surfaces by the presence of the peak emission at ~ 283.7 eV attributed to Si−C bonds as observed in C 1s core level spectra. For each surface, a thickness of ~ 5 ML (~ 8 Å) has been ascertained. However, Si(111) surfaces modified in H−C≡C−MgCl shows higher “efficiency” of Si−C bond formation and a less pronounced contaminations from halogen and aliphatic carbon atoms, respectively. Moreover, the efficiency of the grafting process decreases with the bigger the end group of the ethynyl derivatives, and the surface electronic properties obtained from SXPS measurements revealed a linear trend between the band bending, the working function and the surface dipole established for these molecules. Additionally, H- and CH_3-terminated Si(111) surfaces have also been compared with these modified Si surfaces. A linear tendency is also observed and it has been shown that the band bending and the surface dipole are contributed independently to the change in the work function. An increase in the electron donator ability of the molecules leads to an increase in the surface dipole, the band bending and the work function of the grafted molecules, respectively. This behavior indicates clearly the molecular effect of the deposited organic layer, which results from a change of both surface dipole (electron affinity or dipole moment) and band

bending (charge transfer), i.e., controlled by the work function. Therefore, controlled electronic properties can be obtained using such electrochemical grafting treatment and can be used as a potential tool for new Si-based molecular electronic devices. Moreover, a correlation between two different techniques for the band bending determination has been confirmed. Finally, the grafting of H−C≡C- onto Si(111) surface from H−C≡C−MgCl electrolyte at high charge flow leads to the formation of a thick and uniform polymeric layer via reaction of the C≡C bond resulting in a thickness up to ~ 20 nm. In the case of CH_3−C≡C−MgBr and C_6H_5−C≡C−MgBr, the formation of a polymeric layer has also been obtained, but with a thinner thickness of only ~ 10 nm, when using the same experimental conditions. The smallest ethynyl derivative Grignard compound H−C≡C−MgCl induced an enhanced film thickness as observed by SXPS and SEM measurements. The formation of these thin polymeric layers is supposed to arise via oxidation of the C≡C bonds and reactions via halogen atoms with the Si surface, and not only via oxidation of the Br(Cl)Mg−C bond from Grignard compound as it was the case for the methyl containing Grignard solutions.

Chapter 7

Polymerization from pyrrole and thiophene Grignard compounds

Conducting polymers like polypyrrole and polythiophene are especially attractive molecules showing remarkable electrical conductivity and thermal stability in their oxidized forms. Such heterocyclic polymers contain a π-conjugated like-structure and offer a unique combination of electrical, mechanical and optical properties, which makes them attractive for a variety of technological applications including Schottky diodes, corrosion protections, lithium-ion batteries, light emitting diodes, organic electronics, and photovoltaics, to mention but a few.[134-137] The deposition of such molecules onto hydrogenated Si(111) surfaces is then becoming very interesting and exciting for both, fundamental understanding and technological applications of electronic devices.[138,139] To obtain such organic/Si heterostructures, the direct deposition of covalently bonded polypyrrole and polythiophene onto Si(111) surfaces has been attempted electrochemically using Grignard solutions and without the need of any adhesion promoter molecules.[140] This electrochemical method for the grafting of organic layers has been intensively studied and has revealed covalent Si–C bonds for methyl groups and ethynyl derivatives, as described in the previous chapters. In this chapter, several characterization methods like IRSE, Raman, and XP spectroscopies have been performed to provide information about the vibrational and chemical properties of such modified Si surfaces. Additionally, SEM measurements have also been performed to determine the morphology and the thickness of the polymeric layers formed on Si(111) surfaces. For these investigations, pyrrylmagnesium bromide solutions have been prepared by the chemical group of Dr. Janietz (IAP Golm) since no Grignard reagent containing pyrrole structure is available in chemical industry, while thiophen-2-yl magnesium bromide solutions have been purchased by Sigma Aldrich. The first results acquired are very promising and exciting for further potential applications of such organic/Si heterostructures.

7.1 Formation of polymeric films: the case of polypyrrole

7.1.1 IRSE and Raman characterizations

IRSE and Raman spectroscopy have been performed to give evidence of the deposition and formation of polymeric layers of polypyrrole (PPy) and polythiophene (PT) onto Si(111) surfaces by the typical vibrations of specific chemical groups present on the surface. Some vibrational modes coming from the specific groups of PPy and PT can present either active vibrational mode in IR spectra and at the same time non-active vibrational mode in Raman spectra or active vibrational modes in both, IR and Raman spectra, respectively (e.g., see Fig. 7.1). These demeanors arise typically from the properties of these molecules.

Fig. 7.1 shows the tan Ψ (top panel) and Raman (bottom panel) spectra of Si(111) surfaces modified in pyrrylmagnesium bromide solution, respectively. An anodic current density of 0.1 mA/cm^2 for 1200 s has been supplied in galvanostatic mode to obtain such modified Si(111) surfaces. The measured tan Ψ spectrum of the film has been referenced to the tan Ψ spectrum of H-terminated Si(111) surface. The spectra are shown in the 900-2200 cm^{-1} region. A positive peak appears at 2083 cm^{-1} in the tan Ψ spectrum normalized and is assigned to the total loss of Si–H symmetric stretching vibrational mode, ν_s(Si–H). In addition, several downward pointing peaks are also distinguishable. Two features reveal the presence of ring structures as observed by the IR-absorption bands at ~ 949 and 1147 cm^{-1}, respectively. These absorption bands are attributed to the C–H asymmetric ring deformation, δ_{as}(C–H) and ring breathing of pyrrole, respectively, according to ref. [141] The broad IR-absorption band at ~ 1205 cm^{-1} is assumed to belong to the electronic-like absorption of C–N stretching chains,[142] from C–H in plane symmetric deformation vibration, or from doping state of PPy.[143] However, no distinct bands are observed in the Raman spectrum for these features, which supposes that these vibrations are not Raman active. The IR-absorption band in the 1420-1440 cm^{-1} is assumed to correspond to the C–N asymmetric stretching vibrational mode, ν_{as}(C–N).[144] The Raman spectrum indicates the same feature, which suggests that this band is also Raman active. Another prominent band active in both IR and Raman spectra is observed at ~ 1601 cm^{-1} and is ascribed to the C=C symmetric vibrational mode of the ring structure, ν_s(C=C).[140] Moreover, the Raman spectrum reveals a hump at ~ 1317 cm^{-1} and can be attributed to the C–C stretching vibration in plane, ν(C–C).[140] Nevertheless, the weak feature observed at ~ 1715 cm^{-1} attributed to the C=O stretching vibrational mode, ν(C=O) reveals the presence of carboxyl groups on the surface.[128] These carboxyl groups arise probably

from the chemical reaction resulting from the breaking of THF molecules during the electrochemical deposition. However, as expected, this figure gives clearly evidence of the presence of PPy molecules directly deposited on Si(111) surfaces. As remark, a brown polymeric film of PPy has been visible with the naked eye immediately after the electrochemical deposition, which is another indication of the well deposition of PPy on Si(111) surfaces.

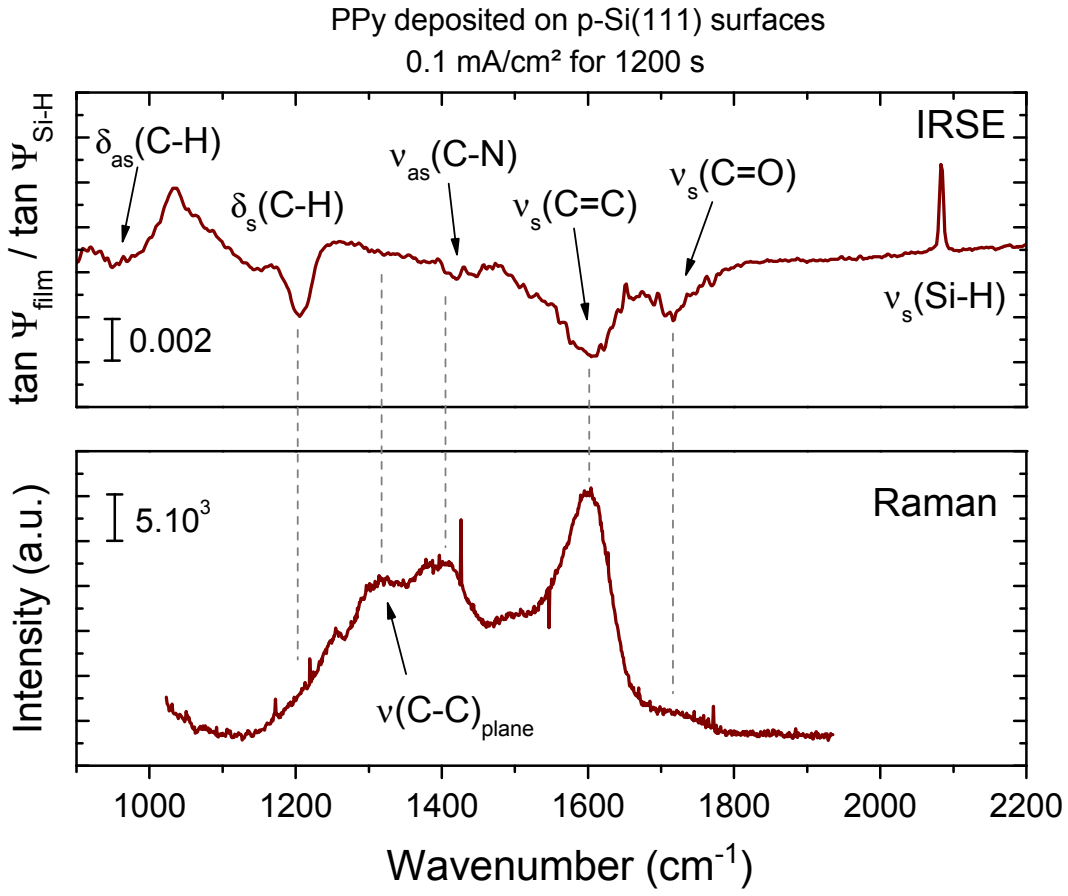

Fig. 7.1: *Deposition of polypyrrole on Si(111) surface by electrochemical Grignard route. A current density (0.1 mA/cm² for 1200 s) has been applied in galvanostatic mode. The top panel depicts IRSE characterization, while the bottom panel illustrates Raman characterization in the 900-2200 cm⁻¹ region, respectively.*

Fig. 7.2 shows the tan Ψ spectrum of PPy deposited onto Si(111) surfaces using a lower current density of 0.1 mA/cm^2 for 900 s. This spectrum is referenced to tan Ψ of H-terminated Si(111) surface. The tan Ψ spectrum is shown in the higher energy region between 2000-3500 cm^{-1}. Here again, the total loss of the stretching vibrational mode of Si–H at 2083 cm^{-1} is observed due to the deposition process. The contaminations from the ambient atmosphere are detected at ~ 2324-2350 cm^{-1} and are assigned to the vibrational mode of CO_2 molecules. The weak broad IR-absorption band ~ 2850-2980 cm^{-1} is attributed to the symmetric and asymmetric stretching vibrational modes of methylene and methyl groups, indicat-

ing the presence of some adventitious CH_2 and/or CH_3 groups after the deposition. These contaminants are probably arisen from the atmosphere during the exposure to ambient air. However, two prominent and characteristic bands of PPy on Si surface are well resolved. The broad and strong peak in the 3000-3280 cm^{-1} region is ascribed to C–H stretching vibrations and the weaker broad band at ~ 3422 cm^{-1} is typically due to the N–H stretching vibrational mode, ν(N–H).[144] In this spectrum, these two peaks are well separated, which it was not the case for other PPy/semiconductor systems.[145,146]

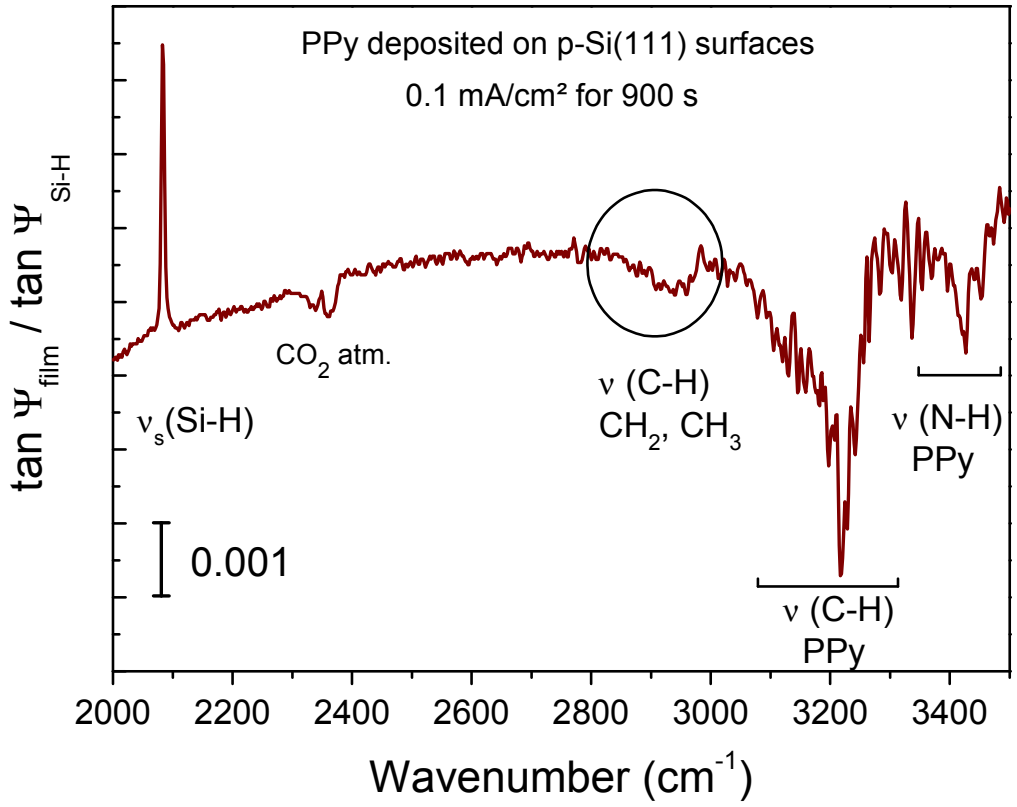

Fig. 7.2: *Tan Ψ spectrum of polypyrrole electrochemically deposited on Si(111) surface by application of a current density of 0.1 mA/cm² for 900 s in pyrrylmagnesium bromide solution in the 2000-3600 cm^{-1} region, referenced to tan Ψ spectrum of H-terminated Si(111) surface.*

7.1.2 SEM imaging

Fig. 7.3 shows two SEM micrographs of the modified Si surfaces after electrochemical deposition of PPy onto Si(111) surface in pyrrylmagnesium bromide solution. These two modified Si samples have been obtained by the application of an anodic current density of 0.1 mA/cm^2 for (a) 1200 s (~ 120 mC/cm^2) and (b) 900 s (~ 90 mC/cm^2). The polymeric PPy films deposited on Si(111) surfaces reveal ultrathin polymeric layers (~ 30 nm), homogenous, and adhesive properties, for both modified Si(111) surfaces, as observed on the SEM micro-

graphs. A hint of the good stability of these PPy films deposited onto Si(111) surfaces in ambient air is revealed with the hydrophilic properties of these films even after being exposed in ambient atmosphere during ~ 2 and 10 months, respectively. Moreover, PPy films prepared from pyrrole in aqueous or non aqueous solutions have been shown to be more inhomogeneous.[141]

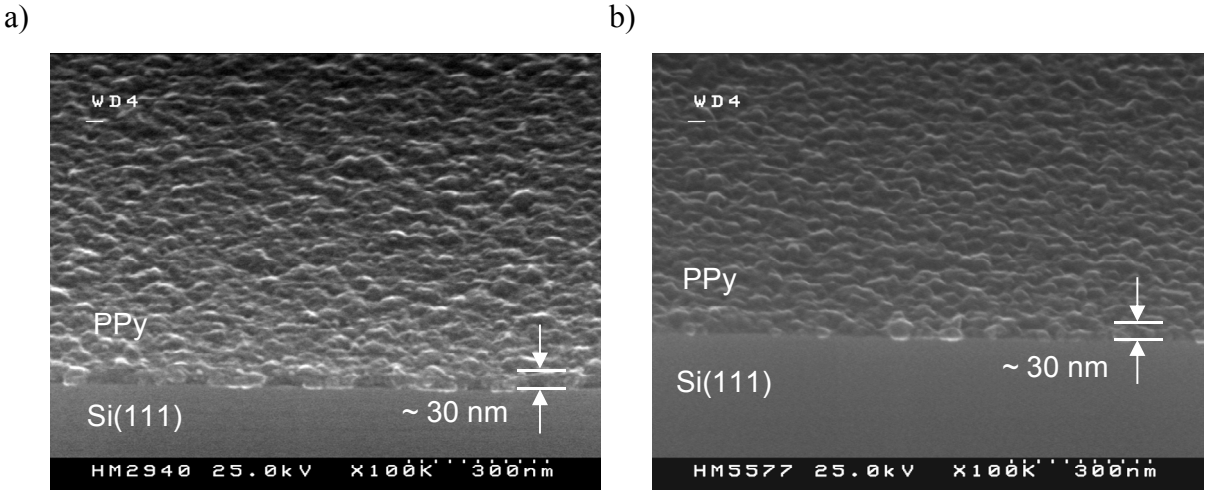

Fig. 7.3: *SEM micrographs of PPy deposited onto Si(111) surface obtained by the application of different current density: 0.1 mA/cm^2 for (a) 1200 s and (b) 900 s, respectively, in galvanostatic mode using a pyrrylmagnesium bromide compound. As result, a brown polymeric film has been observed with the naked eye for both modified Si samples. These modified Si surfaces by PPy molecules have been stored in ambient air for approximately 2 and 10 months, respectively, before being recorded.*

7.1.3 XPS investigations

XPS measurements have been performed to differentiate the chemical environment of organic species present on the Si surface after deposition and formation of polymeric layer of polypyrrole and polythiophene onto Si(111) surfaces by different electrochemical treatments applied to the Si electrode.

XP survey spectra

Fig. 7.4 displays the survey XP spectra of PPy electrochemically deposited onto p-Si(111) surfaces in pyrrylmagnesium bromide solution with the different experimental conditions summarized in Chap. 4 (or see Tab. 7.1). The four substrates called samples A, B, C, and D are shown. The attempt to prepare thin polymeric film onto Si surfaces has been performed by the application of low amount of flown charge (30 to 230 μC/cm^2, see Tab. 7.1) by cyclo-

voltammetry measurement (0 – 1.2 V for 1 CV, sample A) or in potentiostatic mode (1.2 V for 80 s, and 0.7 V for 300 s, samples B and C, respectively), respectively. For the deposition of a "thicker" polymeric film, a charge flow of 120 mC/cm^2 has been applied in galvanostatic mode (0.1 mA/cm^2 for 1200 s, sample D). Due to the tremendous difference of charge flow applied to the Si electrodes during the electrochemical deposition, different polymeric films of PPy are expected. In case of the deposition of thin polymeric films, samples A, B, and C depict almost the same peak contributions. Only some peaks show different intensities. Peaks attributed to Si 2p and Si 2s at ~ 99.73 and 150.78 eV, respectively, are observed for each modified Si surface. As could be noticed on these spectra, Si 2p and Si 2s intensities increase and decrease in common. An increasing trend occurs for these peak intensities from galvanostatic mode to potentiostatic mode (samples: D < A < B < C). The smallest Si peak intensity is observed in the case of sample D. This behavior is attributed to the result of a thicker polymeric layer. The presence of Br, C, and O atoms are also detected by the Br 3p, C 1s, and O 1s peak emissions at ~ 184.31, 284.90, and 532.62 eV, respectively. Interestingly, the C 1s peak intensities increase in the opposite direction (samples: C < B < A < D) of the Si peak intensities. As expected, these demeanors seem to indicate the deposition of different polymeric thicknesses of PPy films on Si(111) surfaces. Moreover, two other emissions are also observed at ~ 498.10 and 577.16 eV, respectively. These peaks are attributed to adventitious contaminations from the sample holder: Cr 2p, and Zn LMM Auger emissions, respectively. Additionally, XP spectrum from sample D reveals an emission at ~ 400 eV and is ascribed to N 1s peak emission. The occurrence of this emission clearly indicates the formation of a thick polymeric film because N 1s peak contribution can not arise from the rinsing procedure or from the ambient atmosphere. A high amount of C atoms and a slight amount of Si atoms are also noticed. Moreover, the polymeric film obtained revealed hydrophilic properties and has light brown colour. These observations give rise to the formation of a thick polymeric film of PPy on Si(111) surface, which is also consistent with the higher charge flow applied to this Si sample.

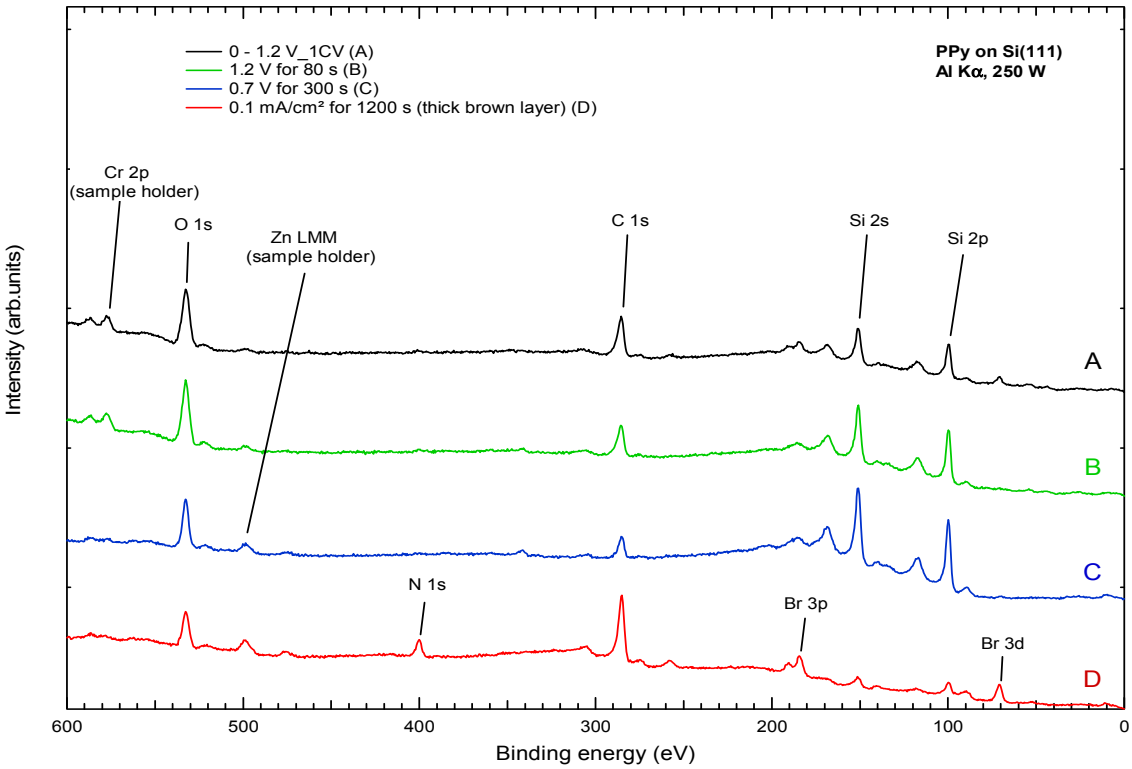

Fig. 7.4: *XP survey spectra of PPy electrochemically deposited on p-Si(111) surfaces from pyrrylmagnesium bromide solution. AlKα excitation energy (hν = 1486.6 eV) has been operated with a power of 250 W. (A) 1 CV: 0 – 1.2 V, (B,C) 1.2 V for 80 s, and 0.7 V for 300 s, and (D) 0.1 mA/cm^2 for 1200 s. The spectra are shifted for visual convenience.*

XP spectra in the 130 – 220 eV region

Fig. 7.5 shows the XP spectra of PPy deposited on Si(111) surfaces from samples A, B, C, and D in the 130 – 220 eV region. Each sample has been recorded in normal (90°) emission (solid curve), while in the case of samples A and B, additional spectra have been recorded under emission of 30° (dashed curve) in relation to the surface to be more in surface sensitive conditions. The peaks observed at ~ 150.80 and 168.40 eV are attributed to Si 2s core level and their plasmon emissions, respectively. These peak intensities are more pronounced in the case of sample C (blue solid curve) and decrease for the other samples (from samples: B_{30} to A_{30} and A), respectively, and more especially for sample D where a thick polymeric film has been expected (red solid curve).

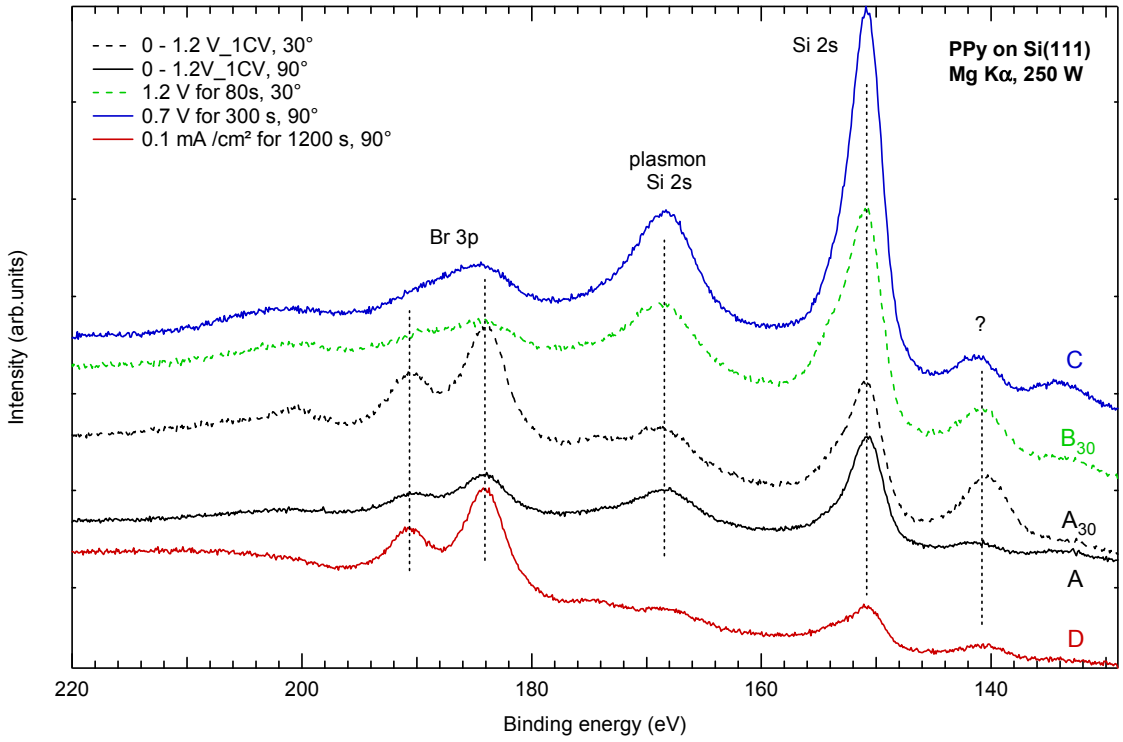

Fig. 7.5: *XP spectra of PPy deposited on Si(111) surfaces in Pyl-MgBr solution with the application of different electrochemical methods (see Tab. 7.1). MgKα (hν = 1253.6 eV) has been used as excitation energy with a power of 250 W.*

No significant difference between Si 2s peaks recorded under emission of 90° and 30° is observed for sample A (black solid and dashed curves, respectively). Nevertheless, Br 3p emission at ~ 184.02 eV is more prominent in case of measurement under emission of 30° (more surface sensitive than 90° because more signal from the overlayer is probed), which indicates that Br atoms are more present at the surface. Moreover, a small hump at ~ 140.48 eV is also observed under emission of 30°, while it was not the case in normal emission. However, this peak is observable for each sample, but only a weak intensity appears in the case of sample D. This feature has not been attributed for the moment, but it is still on going to understand the origin of this contribution. For samples D and A_{30}, the peak corresponding to Br 3p emission is more prominent than for the other samples.

N 1s core level spectra

Fig. 7.6 presents the N 1s core level spectra for the same samples discussed above, under the same energy excitation (AlKα, hν = 1486.6 eV). The N 1s peak observed at ~ 400.16 eV is visible for each sample. However, this peak is noticeably more prominent for sample D (red curve, thick film). Evidently as expected, a thicker film formed should possess more N atoms

than the other ones. This behavior is quite consistent with the charge flow applied to these different Si samples. As compared to sample D, a weak N 1s emission occurs for samples A and C, ~ 13 and 5%, respectively, while sample B reveals ~ 23% from the total integral peak intensity of the thicker film (sample D). It is then obvious that the better parameter to form thin polymeric layer of PPy on Si(111) surfaces can be achieved by application of the parameter used to prepare sample B. However, the peaks clearly show the presence of N atoms for each sample, and the XP core level spectra of N 1s emission seem to exhibit only one contribution.

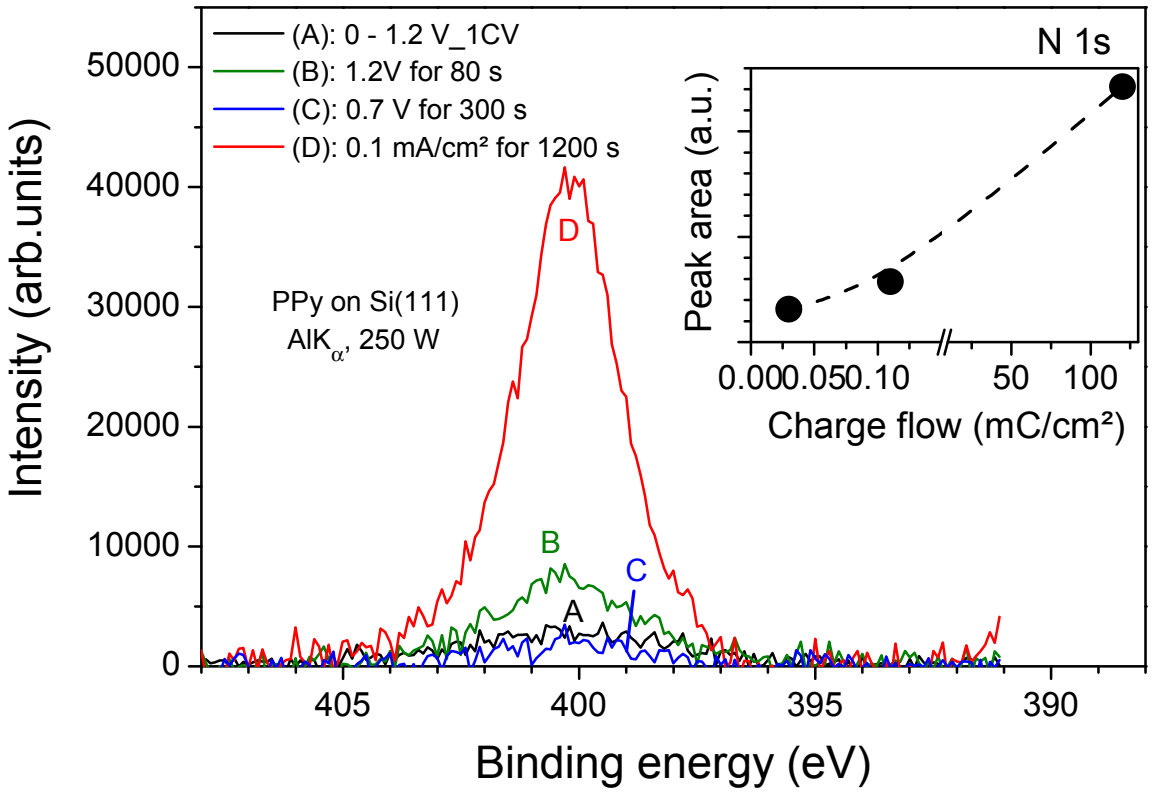

Fig. 7.6: *High resolution of N 1s core level spectra from the deposition of PPy on Si(111) surfaces. AlKα as excitation energy of 1486.6 eV was applied with a power of 250 W. Insert shows N 1s peak area as a function of charge flow.*

Nevertheless, to determine how these N atoms are bonded with the Si(111) surface and the different contributions of N 1s peak emission (N–Si, N–C, N–O, N–H...), the same experiments should have to be performed under synchrotron radiation. (These experiments are planned to be performed in the future)

Tab. 7.1: *Peak intensities determined from the different charge flow in the case of PPy electrochemically grafted onto Si(111) surfaces.*

Sample	Ref	A	B	C	D
Treatment in Grignard	Si(111) NH_4F-dip (40%)	1 scan from 0 → 1.2 V	Potentiostatic 1.2 V for 80 s	Potentiostatic 0.7 V for 300 s	Galvanostatic 0.1 mA/cm^2 for 1200 s
Charge (μC/cm^2)	XXX	30	110	230	120 10^3
Peak integral intensity (a.u.)	XXX	15 732	28 710	7167	121 215

7.2 Formation of polymeric films: the case of polythiophene

7.2.1 IRSE characterization

Fig. 7.7 depicts tan Ψ spectrum of polythiophene deposited onto Si(111) surfaces by electrochemical Grignard route, referred to an H-terminated Si(111) surface. A current density of 0.1 mA/cm^2 for 900 s (~ 90 mC/cm^2) has been applied to the Si substrate immersed in thiophen-2-yl magnesium bromide solution to obtain the modified Si(111) surfaces. The total loss of every Si–H atom sites is revealed by a strong and sharp upward pointing peak at 2083 cm^{-1} attributed to the symmetric stretching vibration of Si–H. This result can be considered as a hint of the modification of the surface. At the same time, several downward pointing peak features appear. For instance, the C–H out of plane deformation vibration is assigned to the peaks observed at ~ 1082 cm^{-1} and 1216 cm^{-1}, respectively.[147] The IR-absorption band at 1415 cm^{-1} is ascribed to C=C stretching vibrations. Contaminations due to the ambient atmosphere are revealed with the C–H symmetric and asymmetric stretching vibrational modes of adventitious CH_2 and/or CH_3 groups in the 2800-3000 cm^{-1} stretching region. Moreover, another contamination of the modified surface is revealed by the presence of the peak at 1715 cm^{-1} and is ascribed to the C=O stretching vibrational mode, ν(C=O) from the carboxyl groups.[127] This feature arises certainly from the THF solvent containing in Grignard solution (Grignard solution is diluted in THF). In the higher energy range (3000-3300 cm^{-1}), a strong

and broad IR-absorption band appears due to C–H bonds of the polythiophene. The different vibrational modes observed in this experiment clearly reveal the presence of polythiophene structure on the modified Si surface.

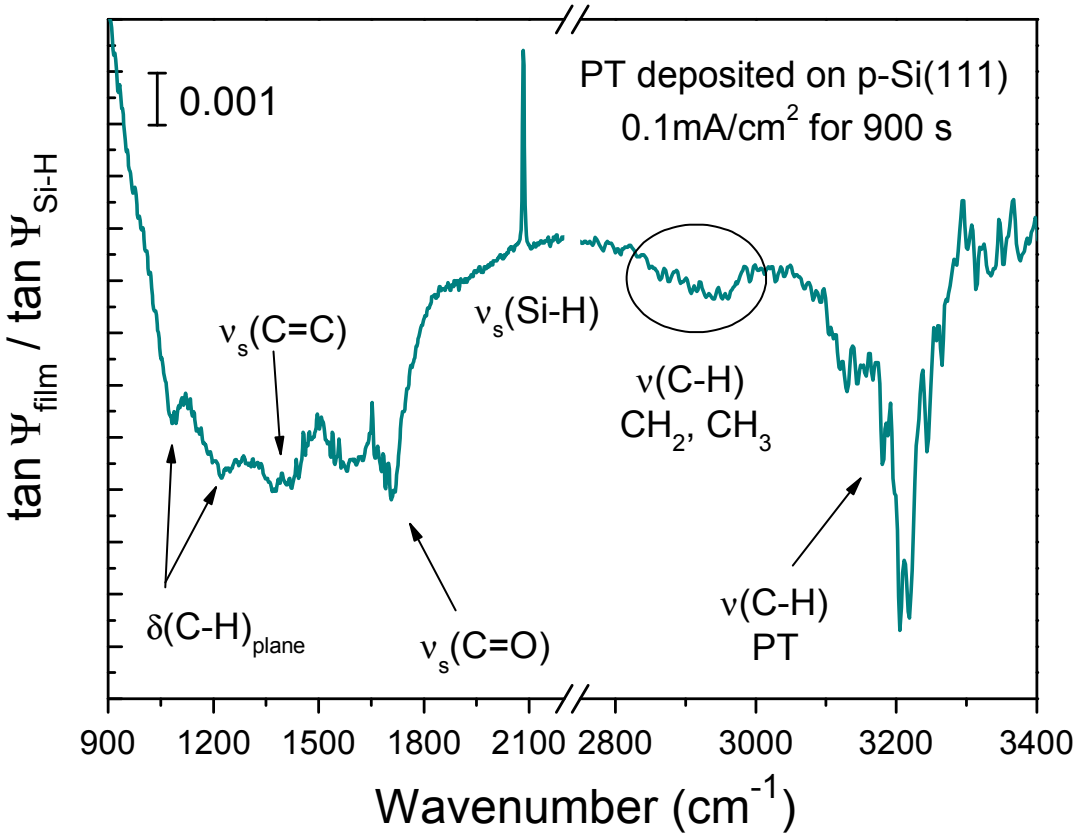

Fig. 7.7: *Tan Ψ spectrum of polythiophene electrochemically deposited on Si(111) surface by application of an anodic current (0.1 mA/cm² for 900 s) in thiophen-2-yl magnesium bromide solution, referenced to H-terminated Si(111) surface. A brown polymeric layer of ~ 26 nm thickness has been observed with the naked eye.*

7.2.2 SEM imaging

Two different charge flows have been applied for the deposition of polythiophene on Si(111) surfaces from thiophen-2-yl magnesium bromide solution, leading to two different thicknesses. SEM measurements have been performed for these two modified Si surfaces as shown in Fig. 7.8. For a lower current density applied of (a) 0.1 mA/cm² for 900 s (~ 90 mC/cm²), a brown polymeric film is obtained, whereas for a higher current density applied of (b) 0.5 mA/cm² for 900 s (~ 450 mC/cm²), a blue polymeric film is observed with the naked eye, respectively. From the SEM measurements, the layer thicknesses are determined to be ~ 26 and 100 nm for both modified Si surfaces, respectively. The thicknesses cal-

culated are quite consistent with the films color observed with the naked eye, but also with the charge flow applied. For the deposition of PT onto Si(111) surfaces, it has been found that the thicknesses of polymeric PT films could be well controlled with the charge flow supplied. The polymeric PT films obtained show hydrophobic properties. This behavior is another indication of the well deposition of polythiophene films onto Si(111) surface. The polymeric PT films deposited onto Si(111) surfaces also reveal the formation of ultrathin, homogenous, and adhesive polymeric layers as observed on the SEM micrographs.

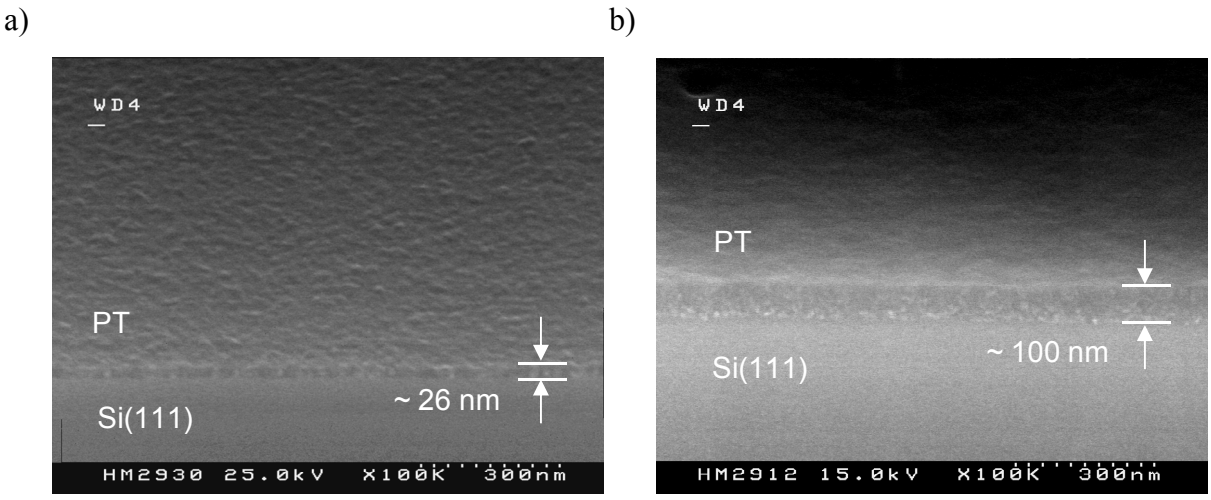

Fig. 7.8: *SEM micrographs of PT deposited onto Si(111) surfaces using thiophen-2-yl magnesium bromide electrolyte in galvanostatic mode, (a) 0.1 mA/cm^2 for 900 s (~ 90 mC/cm^2) and (b) 0.5 mA/cm^2 for 900 s (~ 450 mC/cm^2). The PT modified Si surfaces have been stored in ambient air for about 2 months before being recorded by SEM technique.*

To test the adhesion of such electrochemically deposited polymeric layers (PPy and PT), an ultrasonic treatment in 2-isopropanol for 8 min has been performed. The polymeric films were still observable on the Si substrates. This evidently indicates that the polymeric films are well anchored to Si surfaces, and proves that a strong interaction occurs between the polymeric layers and the Si surfaces. This is a hint that the polymeric films have been covalently bonded to the Si surfaces with this electrochemical grafting method. However to determine how the molecules have been anchored to Si surfaces (with C, N, or S atoms), SXPS characterizations have to be performed in the future using synchrotron radiation.

7.2.3 XPS investigations

XP survey spectra

Fig. 7.9 shows the XP survey spectra of PT grafted onto Si(111) surface by different electrochemical treatments in thiophen-2-yl magnesium bromide solution. The electrochemical techniques used here for the preparation of the samples are summarized in Chap. 4 (or see Tab. 7.2). AlKα has been applied as excitation energy (hν = 1486.6 eV) with a power of 250 W. The XP survey presents the spectra from the three different samples called X, Y, and Z. The samples X and Y of which "thin" layer films deposited (black and blue solid curves, respectively) are expected clearly show the peaks occurring from Si 2s, Si 2p, O 1s, and C 1s emissions at ~ 99.73, 150.78, 284.78, and 532.24 eV, respectively. The Si 2p and Si 2s peak emmisions are going together. The sample Y indicates higher Si 2p and Si 2s peaks than the sample X, while for the sample Z, nor Si 2p neither Si 2s emissions are detected. In the case of sample Z, the highest C 1s emission is observed. However, no conclusion can be made from the different contribution intensities of C 1s peaks because these contributions could arise either from thiophene aromatic ring or even from adventitious aliphatic carbons coming from contaminations (rinse, atmosphere...). However, the trend occurs here is in accordance with the number of C atoms expected in the case of a thicker polymeric film formed on Si(111) surfaces. Additionally, for this sample, two other peaks are well distinguished and are attributed to S 2p and S 2s emissions at ~ 164.92 and 228.07 eV, respectively. These peaks are typically characteristic from the presence of S atoms on Si surface because S atoms could only arise from the thiophene molecules. For the two thinner samples (X and Y), the presence of S 2p emission has been very difficult to determine due to the overlapping with the Si 2s plasmon region. To be certain that this peak is observable in this region a quantitative analysis in the S 2s core level spectra has to be performed using synchrotron radiation. However, these peaks observed for the sample Z is a good indication of the well deposition of a thick polymeric layer on the Si surface**.** Surprisingly, at the same time the peak of O 1s emission at ~ 532.24 eV decreases from a factor of three from the samples modified with CV to galvanostatic mode (X (black) > Y (blue) > Z (red)). Moreover, to get more information about the different carbon and sulfur contributions, but also about the bondings present on the Si surface, C 1s, S 2p and S 2s core level spectra have to be performed under synchrotron radiation (These experiments are planned for the near future).

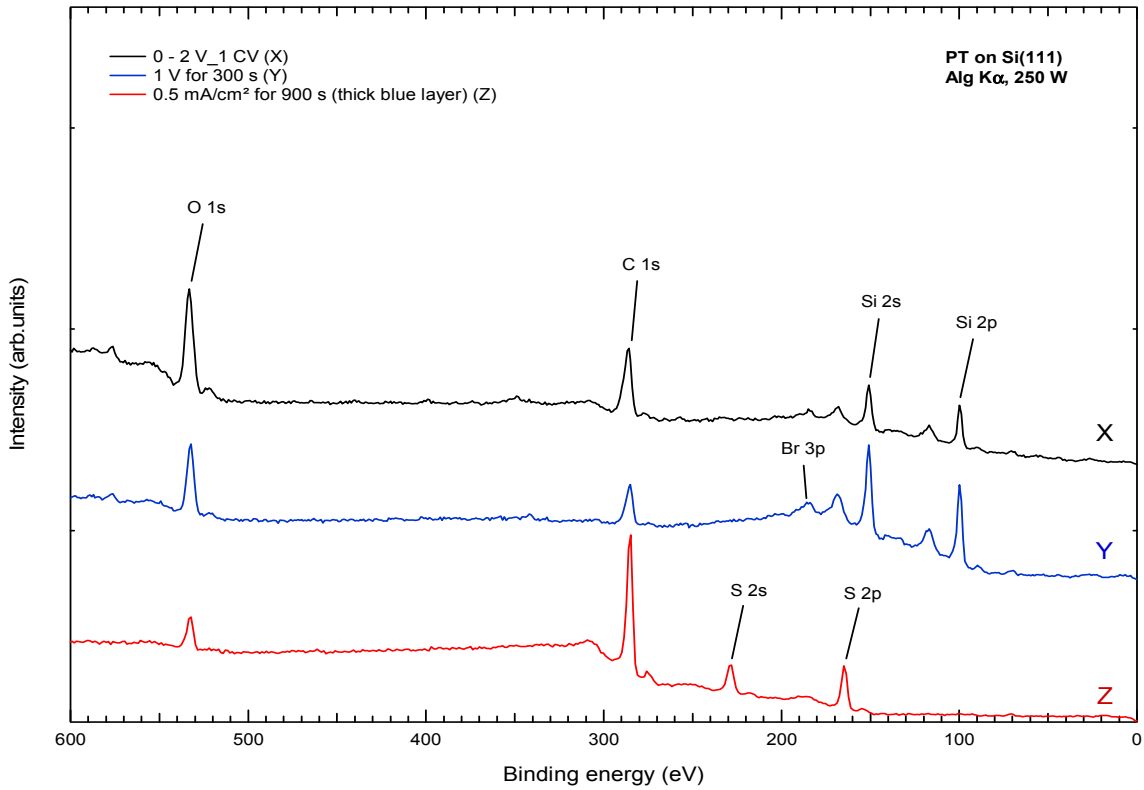

Fig. 7.9: *XP survey spectra of Si(111) surface modified electrochemically by Grignard containing thiophene structure. (X) 1 CV between 0 – 2 V, (Y) 1 V for 300 s, and (Z) 0.5 mA/cm^2 for 300 s. XP measurements have been performed using AlgKα excitation energy (hv = 1486.6 eV) with a power of 250 W.*

XP spectra in the 130 – 220 eV region

Fig. 7.10 illustrates XP spectra of PT deposited onto Si(111) surface in the 130 – 240 eV region. The spectra from the samples described above are depicted on this figure. The preparation conditions are summarized in Tab. 7.2. Sample X is recorded at 30° emission angle (black solid curve), while sample Y is performed at two emission angle: 30° (surface sensitive) during 100 scans (blue dashed curve) and at normal emission angle, 90° (perpendicular to the surface) during 3 scans (blue solid curve), respectively. Sample Z is recorded at normal emission angle. For samples X and Y, the two prominent peaks observed at ~ 150.94 and 168.50 eV are attributed to Si 2s emissions and Si 2s plasmon emissions, respectively. Si 2s emission seems to be more intense in case of the emission recorded at 90°.

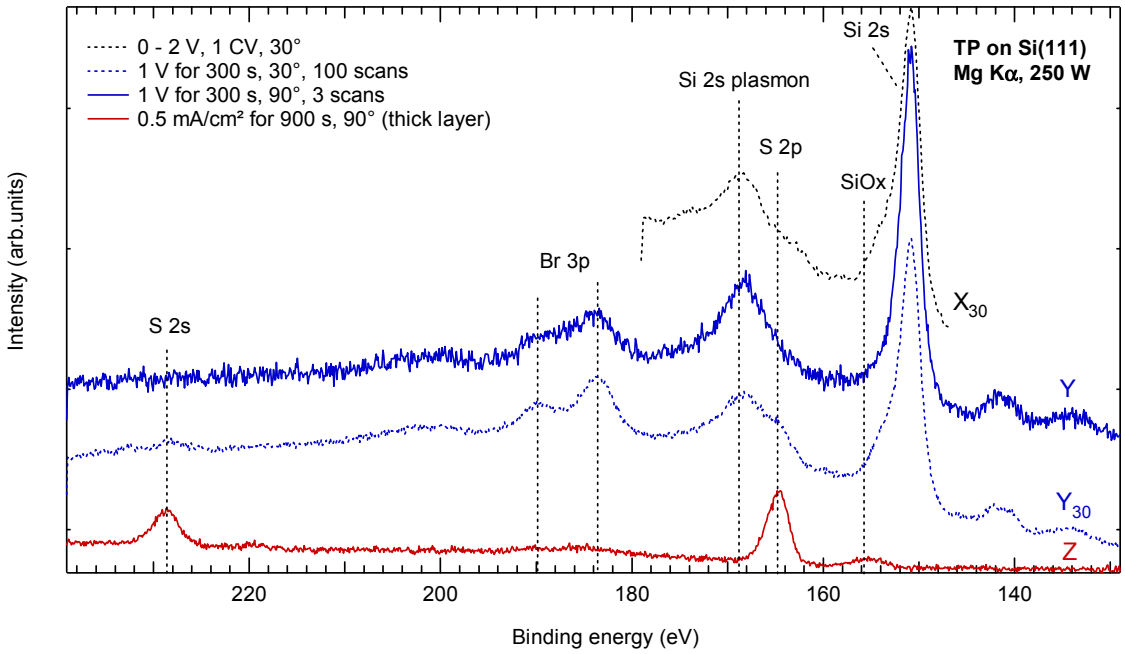

Fig. 7.10: *XP spectra of polythiophene modified Si surfaces in the 130 – 240 eV region. MgKα (hv = 1253.6 eV) was used here as excitation source operating with a power of 250 W.*

In the case of sample Z, these emissions cannot be observed due to the "thicker" polymeric film formed (information depth: ~ 30 Å), however a weak hump at ~ 155.19 eV attributed to SiO_x appears. The sample Z reveals only two prominent emissions at ~ 164.60 and 228.46 eV, which are assigned to S 2p and S 2s emissions, respectively. These two emissions give rise to the deposition of a thicker polymeric PT film. In the case of samples X and Y, only a shoulder at ~ 164.40 eV is distinguishable and is ascribed to S 2s emission. Nevertheless, an overlapping with the Si 2s plasmon emission could occurs because this shoulder is located in the region of this plamon. However, this shoulder is more visible for the samples recorded at 30° emission angle (dashed curves). Moreover, this S 2p emission seems to exhibit the same intensities for both "thin" layer samples (X and Y, respectively). Additionally, a weak hump at ~ 228.46 eV attributed to S 2s emission seems to arise for sample Y recorded at 30° emission. This observation clearly indicates the presence of S atoms on this Si sample. Nevertheless, a doublet emission peaks attributed to Br 3p emission also appears at ~ 183.52 and 189.62 eV, respectively. This suggests a contamination of the Si surface by Br atoms in the case of the "thin" polymeric layers deposited onto Si surface.

Tab. 7.2: *Charge flow applied in relation with the electrochemical treatments*

Sample	Ref	X	Y	Z
Treatment in Grignard: Thiophen-2-yl magnesium bromide	Si(111) NH_4F-dip (40%)	1 scan from 0 → 2 V	Potentiostatic 1 V for 300 s	Galvanostatic 0.5 mA/cm^2 for 900 s
Charge (μC/cm^2)	XXX	550	460	450 10^3

7.3 Conclusion

Grignard reagents containing pyrrole and thiophene structures like pyrrylmagnesium and thiophen-2-yl magnesium bromide solutions have been used for the grafting of organic molecules on Si(111) surfaces using the Grignard electrochemical route. The deposition of polypyrrole and polythiophene onto Si(111) surfaces using an one-step modification for the electrochemical grafting has been attempted for the first time in this work. The results obtained give clear evidence of a strong interaction between the organic layers and the Si surface. The organically modified Si surfaces characterized with IRSE, XPS, Raman and SEM experimental techniques have well demonstrated that thicknesses of polymeric layers obtained could be controlled by the application of charge flow. IRSE and Raman measurements reveal the presence of such polymeric layers on Si(111) surfaces by the typical vibrational modes observed from these polymers. Moreover, several information concerning the active and non-active vibrational mode of these peaks have been determined by investigations of both IRSE and Raman spectroscopies. SEM micrographs reveal different thicknesses obtained depending on the charge flow applied. For a charge flow applied of ~ 90 to 120 mC/cm^2 during the electrochemical deposition of PPy onto Si surfaces, a brown polymeric film (~ 30 nm) has been observed with the naked eye. In the case of electrochemical deposition of PT onto Si(111) surfaces, a brown (~ 26 nm) to blue (~ 100 nm) polymeric film has been seen with the naked eye as well, when a charge flow has been applied from 90 to 450 mC/cm^2, respectively. Homogeneous, ultrathin, and adhesive polymeric films have been obtained for both polymers, as observed by SEM micrographs. However, polythiophene and polypyrrole films reveal a

smooth but a “wave” like-structure, respectively. XPS investigations show clearly the presence of polypyrrole and polythiophene onto Si(111) surfaces. Moreover, in the case of the “thick” polymeric layers (> 10^3 μC/cm^2), emissions from N 1s and S 2s or S 2p core level have been more prominent. Finally, polymeric PPy films have shown hydrophilic properties, whereas polymeric PT films have shown hydrophobic properties.

Chapter 8

Concluding remarks

Silicon (Si) is used for a wide range of applications such as solar cells, microelectronics, biochips, and so on. For many of these devices, Si wafers with a (100) surface orientation are used because of a better passivation by SiO_2 than for a (111) surface orientation. On the other hand, a hydrogenated Si(111) surface reveals a better passivated surface than a (100) surface orientation due to the achievement of flat surfaces with less amount of defects. However, H-terminated Si(111) surface is not stable in ambient air and oxidizes within some hours or even minutes.

This thesis addresses new types of organic/Si hybrid systems with respect to the surface passivation. In particular, the influence of organic molecules on surface passivation and the resulting electronic properties have been discussed. Therefore, electrochemical grafting of methyl groups (CH_3 and CD_3), different ethynyl derivatives (H–C≡C-, CH_3–C≡C-, and C_6H_5–C≡C-), as well as pyrrole and thiophene heterocycles from Grignard solutions on p-type Si(111) surfaces has been intensively studied.

This work shows that organically modified Si surfaces using the electrochemical Grignard route are much better passivated with respect to stability with low recombination velocities as measured by photoluminescence (PL) technique. Infrared spectroscopic ellipsometry (IRSE) and synchrotron X-ray photoemission spectroscopy (SXPS) investigations exhibit a very low oxidation probability for methylated Si surfaces. In the case of methyl groups (CH_3 and CD_3), stability up to several months has been observed in ambient air as compared to a standard H-terminated Si(111) surface as measured by SXPS, IRSE and PL methods. In previous SXPS studies, the spin-orbit doublet splitting of the Si 2p core level emission has already been observed in the case of H-terminated Si(111) surfaces. In this thesis, SXPS measurements reveal a well-separated spin-orbit doublet splitting of the Si 2p core level emission for methyl groups grafted onto Si(111) surfaces, which is observed for the first time for this type of organic layer. This observation and the vibrational losses of C–H stretching vibrational modes in the C 1s core level emission observed for a monolayer coverage by methyl groups reflect the

well-ordered surface structure for the methylated Si(111) surfaces. Moreover, the “umbrella” vibrational mode that is characteristic for methyl groups has been observed as well for the methylated Si(111) surfaces using IRSE measurements. This result demonstrates the sensitivity of the IRSE method, which allows the detection of a single monolayer of methyl groups on the Si(111) surface. The electronic properties determined from SXPS measurements for the methylated Si(111) surfaces reveal a shift in work function and in band bending of about + 0.44 and + 0.15 eV, respectively, compared to H-terminated Si(111) surface. Additionally, during PL measurements it was found that the modified Si substrates oxidize faster due to the laser irradiation with the excitation laser. However, IRSE spectra reveal the formation of a different type of oxide layer as observed for wet-chemically prepared oxides.

Grafting of ethynyl derivatives leads to polymerization and at least to ultrathin polymeric layers on Si as a result of the electrochemical or subsequent radical oxidation of the C≡C bond leading to the formation of C–C and C=C bonds. However, these layers are homogeneous and well bonded to Si. The “smoothest” surface layer is observed for a polymeric layer prepared from a phenyl-ethynyl compound whereas the “roughest” layer is observed for the smallest ethynyl compound, i.e., the bigger the end group, the thinner and smoother the polymeric layer. Moreover, it has been revealed that the grafting of ethynyl derivatives is influenced by the type of halogen atom present in the Grignard precursor. The smaller the halogen atom is, the thicker is the polymeric layer. However, ultrathin polymeric layers formed by Br containing Grignard compounds compared to Cl containing compounds led to the lowest recombination velocity at the polymeric/Si interface according to PL measurements. In the case of grafting from ethynyl derivatives, the reaction pathway has been expanded by including the halogen atoms in different side reactions. A shift of about + 0.24 and + 0.11 eV in work function and band bending, respectively, has been observed after grafting of these molecules. These electronic properties depend linearly on the surface dipole, which increases with the electron donator ability of the organic molecules as observed from SXPS measurements. Additionally, CH_3- and CH_3–C≡C-terminated Si surfaces show the lowest band bending, which indicates an easier charge transfer between these organic molecules and the p-type Si substrate.

Polymeric layers formed from pyrrylmagnesium bromide and thiophen-2-yl magnesium bromide lead to homogeneous, adhesive and ultrathin layers which are strongly bonded to the Si surface. For the first time, polypyrrole films have been deposited from the pyrrylmagnesium bromide in absolute non-aqueous conditions using this new type of Grignard compound. These polymeric layers exhibit better bonding onto Si surfaces than polypyrrole films deposited from aqueous solutions.

Finally, organic modification of Si surfaces using the electrochemical Grignard grafting method reveals different grafting mechanisms depending on the chemical groups used. In the case of methyl groups, a monolayer is achieved and the observation of a spin-orbit doublet splitting reflects the well-ordered surface structure of such modified surfaces. Moreover, these methylated Si(111) surfaces show a longer time passivation (up to several months) as compared to H-terminated Si(111) surface. In the case of ethynyl derivatives, as well as pyrrole and thiophene containing in Grignard solutions, the formation of polymers has been obtained and the thicknesses have been shown to vary depending on the charge flow applied. For all these molecules, a linear tendency occurs and reveals that an increase in the electron donator ability of the molecules leads to an increase in the work function, the band bending, and the surface dipole of the grafted molecules, respectively. This linear tendency shows that controlled electronic properties can be obtained using such electrochemical grafting treatment and can be used as a potential tool for new Si-based molecular electronic devices.

Bibliography

[1] DiBenedetto, S. A.; Paci, I.; Facchetti, A.; Marks, T. J. and Ratner, M. A.: High-Capacitance Organic Nanodielectrics: Effective Medium Models of their Response, *J. Phys. Chem. B* **2006**, *110*, p. 22394-22399.

[2] Letizia, J. A.; Salata, M. R.; Tribout, C. M.; Facchetti, A.; Ratner, M. A. and Marks, T. J.: n-Channel Polymers by Design: Optimizing the Interplay of Solubilizing Substituents, Crystal Packing, and Field-Effect Transistor Characteristics in Polymeric Bithiophene-Imide Semiconductors, *J. Am. Chem. Soc.* **2008**, *130*, p. 9679-9694.

[3] Mayer, T.; Hunger, R.; Klein, A. and Jaegermann, W.: Engineering the Line Up of Electronic Energy Levels at Inorganic-Organic Semiconductor Interfaces by Variation of Surface Termination and by Substitution, *Phys. Status Solidi* **2008**, *245*, p. 1838-1848.

[4] Smits, E. C. P.; Mathijssen, S. G. J.; Hal, P. A. v.; Setayesh, S.; Geuns, T. C. T.; Mutsaers, K. A. H. A.; Cantatore, E.; Wondergem, H. J.; Werzer, O.; Resel, R.; Kemerink, M.; Kirchmeyer, S.; Muzafarov, A. M.; Ponomarenko, S. A.; Boer, B. d.; Blom, P. W. M. and Leeuw, D. M. d.: Bottom-Up Organic Integrated Circuits, *Nature* **2008**, *455*, p. 956-959.

[5] Vilan, A.; Shanzer, A. and Cahen, D.: Molecular Control Over Au/GaAs Diodes, *Nature* **2000**, *404*, p. 166-168.

[6] Bent, S. F.: Organic Functionalization of Group IV Semiconductor Surfaces: Principles, Examples, Applications, and Prospects, *Surf. Sci.* **2002**, *500*, p. 879-903.

[7] Böer, K. W.: *Survey of Semiconductor Physics: Barriers, Junctions, Surfaces and Devices (vol. 2)*, Van Nostrand Reinhold, New York, **1992**.

[8] Buriak, J. M.: Organometallic Chemistry on Silicon Surfaces: Formation of Functional Monolayers Bound Through Si-C Bonds, *Chem. Commun.* **1999**, *12*, p. 1051-1060.

[9] Buriak, J. M.: Organometallic Chemistry on Silicon and Germanium Surfaces, *Chem. Rev.* **2002**, *102*, p. 1271-1308.

[10] Tao, F. and Xu, G. Q.: Attachment Chemistry of Organic Molecules on Si(111)-7×7, *Accounts Chem. Res.* **2004**, *37*, p. 882-893.

[11] Wayner, D. D. M. and Wolkow, R. A.: Organic Modification of Hydrogen Terminated Silicon Surfaces, *J. Chem. Soc., Perkin Trans. 2* **2002**, p. 23-34.

[12] Linford, M. R.; Fenter, P.; Eisenberger, P. M. and Chidsey, C. E. D.: Alkyls Monolyers on Silicon Prepared From 1-Alkenes and Hydrogen-Terminated Silicon, *J. Am. Chem. Soc.* **1995**, *117*, p. 3145-3155.

[13] Webb, L. J. and Lewis, N. S.: Comparison of the Electrical Properties and Chemical Stability of Crystalline Silicon(111) Surfaces Alkylated Using Grignard Reagents or Olefins with Lewis Acid Catalysts, *J. Phys. Chem. B* **2003**, *107*, p. 5404-5412.

[14] Fellah, S.; Amiar, A.; Ozanam, F.; Chazalviel, J.-N.; Vigneron, J.; Etcheberry, A. and Stchakovsky, M.: Grafting and Polymer Formation on Silicon From Unsaturated Grignards: II. Aliphatic Precursors, *J. Phys. Chem. B* **2007**, *111*, p. 1310-1317.

[15] Fellah, S.; Boukherroub, R.; Ozanam, F. and Chazalviel, J.-N.: Hidden Electrochemistry in the Thermal Grafting of Silicon Surfaces From Grignard Reagents, *Langmuir* **2004**, *20*, p. 6359-6364.

[16] Fellah, S.; Ozanam, F.; Chazalviel, J.-N.; Vigneron, J.; Etcheberry, A. and Stchakovsky, M.: Grafting and Polymer Formation on Silicon From Unsaturated Grignards: I - Aromatic Precursors, *J. Phys. Chem. B* **2006**, *110*, p. 1665-1672.

[17] Fellah, S.; Teyssot, A.; Ozanam, F.; Chazalviel, J.-N.; Vigneron, J. and Etcheberry, A.: Kinetics of Electrochemical Derivatization of the Silicon Surfaces by Grignards, *Langmuir* **2002**, *18*, p. 5851-5860.

[18] Teyssot, A.; Fidélis, A.; Fellah, S.; Ozanam, F. and Chazalviel, J.-N.: Anodic Grafting of Organic Groups on the Silicon Surface, *Electrochim. Acta* **2002**, *47*, p. 2565-2571.

[19] Bansal, A.; Li, X.; Lauermann, I.; Lewis, N. S.; Yi, S. I. and Weinberg, W. H.: Alkylation of Si Surfaces Using a Two-Step Halogenation/Grignard Route, *J. Am. Chem. Soc.* **1996**, *118*, p. 7225-7226.

[20] Webb, L. J.; Rivillon, S.; Michalak, D. J.; Chabal, Y. J. and Lewis, N. S.: Transmission Infrared Spectroscopy of Methyl- and Ethyl-Terminated Silicon(111) Surfaces, *J. Phys. Chem. B* **2006**, *110*, p. 7349-7356.

[21] Bansal, A.; Li, X.; Yi, S. I.; Weinberg, W. H. and Lewis, N. S.: Spectroscopic Studies of the Modification of Crystalline Si(111) Surfaces with Covalently-Attached Alkyl Chains Using a Chlorination/Alkylation Method, *J. Phys. Chem. B* **2001**, *105*, p. 10266-10277.

[22] Royea, W. J.; Juang, A. and Lewis, N. S.: Preparation of Air-Stable, Low Recombination Velocity Si(111) Surfaces Through Alkyl Termination, *Appl. Phys. Lett.* **2000**, *77*, p. 1988-1990.

[23] Lifshits, V. G.; Saranin, A. A. and Zotov, A. V.: *Surface Phases on Silicon: Preparation, Structures, and Properties*, John Wiley & Sons, New York, **1994**.

[24] Fidélis, A.; Ozanam, F. and Chazalviel, J.-N.: Fully Methylated Atomically Flat (111) Silicon Surface, *Surf. Sci. Lett.* **2000**, *444*, p. L7-L10.

[25] Nemanick, E. J.; Hurley, P. T.; Brunschwig, B. S. and Lewis, N. S.: Chemical and Electrical Passivation of Silicon (111) Surfaces through Functionalization with Sterically Hindered Alkyl Groups, *J. Phys. Chem. B* **2006**, *110*, p. 14800-140808.

[26] Sieval, A. B.; Hout, B. v. d.; Zuilhof, H. and Sudhölter, E. J. R.: Molecular Modeling of Alkyl Monolayers on the Si(111) Surface, *Langmuir* **2000**, *16*, p. 2987-2990.

[27] Yuan, S.-L.; Cai, Z.-T. and Jiang, Y.-S.: Molecular Simulation Study of Alkyl Monolayers on the Si(111) Surface, *New J. Chem.* **2003**, *27*, p. 626-633.

[28] Lin, Z.; Strother, T.; Cai, W.; Cao, X. P.; Smith, L. M. and Hammers, R. J.: DNA Attachment and Hybridization at the Silicon (100) Surface, *Langmuir* **2002**, *18*, p. 788-796.

[29] Pike, A. R.; Lie, L. H.; Eagling, R. A.; Ryder, L. C.; Patole, S. N.; Connolly, B. A.; Horrocks, B. R. and Houlton, A.: DNA On Silicon Devices: On-Chip Synthesis, Hybridization, and Charge Transfer, *Angew. Chem. Int. Edit.* **2002**, *41*, p. 615-617.

[30] Ciampi, S.; Böcking, T.; Kilian, K. A.; James, M.; Harper, J. B. and Gooding, J. J.: Functionalization of Acetylene-Terminated Monolayers on Si(100) Surfaces: A click Chemistry Approach, *Langmuir* **2007**, *23*, p. 9320-9329.

[31] Allongue, P.; Delamar, M.; Desbat, B.; Fagebaume, O.; Hitmi, R.; Pinson, J. and Savéant, J.-M.: Covalent Modification of Carbon Surfaces by Aryl Radicals Generated from the Electrochemical Reduction of Diazonium Salts, *J. Am. Chem. Soc.* **1997**, *119*, p. 201-207.

[32] Stewart, M. P.; Maya, F.; Kosynkin, D. V.; Dirk, S. M.; Stapleton, J. J.; McGuiness, C. L.; Allara, D. L. and Tour, J. M.: Direct Covalent Grafting of Conjugated Molecules onto Si, GaAs, and Pd Surfaces From Aryldiazonium Salts, *J. Am. Chem. Soc.* **2004**, *126*, p. 370-378.

[33] Allongue, P.; Villeneuve, C. H. d.; Cherouvrier, G.; Cortès, R. and Bernard, M.-C.: Phenyl Layers on H-Si(111) by Electrochemical Reduction of Diazonium Salts: Monolayer versus Multilayer Formation, *J. Electroanal. Chem.* **2003**, *550-551*, p. 161-174.

[34] Hartig, P.; Dittrich, T. and Rappich, J.: Surface Dipole Formation and Non-Radiative Recombination at p-Si(111) Surfaces During Electrochemical Deposition of Organic Layers, *J. Electroanal. Chem.* **2002**, *524-525*, p. 120-126.

[35] Hartig, P.; Rappich, J. and Dittrich, T.: Engineering of Si Surfaces by Electrochemical Grafting of p-Nitrobenzene Molecules, *Appl. Phys. Lett.* **2002**, *80*, p. 67-69.

[36] Rappich, J.; Merson, A.; Roodenko, K.; Dittrich, T.; Gensch, M.; Hinrichs, K. and Shapira, Y.: Electronic Properties of Si Surfaces and Side Reactions During Electrochemical Grafting of Phenyl Layers, *J. Phys. Chem. B* **2006**, *110*, p. 1332-1337.

[37] Takakusagi, S.; Miyasaka, T. and Uosaki, K.: Photoanodic Formation of an Organic Monolayer on a Hydrogen-Terminated Si(111) Surface via Si-C Covalent Bond Using a Grignard Reagent and its Application for One-Step Monolayer-Patterning, *J. Electroanal. Chem.* **2007**, *599*, p. 344-348.

[38] Zhang, X. G.: *Electrochemistry of Silicon and its Oxide*, Kluwer Academic/Plenum Publishers, New York, **2001**.

[39] Hunger, R.; Jaegermann, W.; Merson, A.; Shapira, Y.; Pettenkofer, C. and Rappich, J.: Electronic Structure of Methoxy-, Bromo-, Nitrobenzene Grafted onto Si(111), *J. Phys. Chem. B* **2006**, *110*, p. 15432-15441.

[40] Himpsel, F. J.; Hollinger, G. and Pollak, R. A.: Determination of the Fermi-Level Pinning Position at Si(111) Surfaces, *Phys. Rev. B* **1983**, *28*, p. 7014-7018.

[41] Sze, S. M.: *Physics of Semiconductor Devices*, Wiley, New York, **1981**.

[42] Evans, W. V. and Pearson, R.: The Ionic Nature of the Grignard Reagent, *J. Am. Chem. Soc.* **1942**, *64*, p. 2865-2871.

[43] Tolstoy, V. P.; Chernyshova, I. V. and Skryshevsky, V. A.: *Handbook of Infrared Spectroscopy of Ultrathin Films*, Wiley Interscience, New York, **2003**.

[44] Hirschmugl, C. J.: Frontiers in Infrared Spectroscopy at Surfaces and Interfaces, *Surf. Sci.* **2002**, *500*, p. 577-604.

[45] Hinrichs, K.; Gensch, M. and Esser, N.: Analysis of Organic Films and Interfacial Layers by Infrared Spectroscopic Ellipsometry, *Appl. Spectrosc.* **2005**, *59*, p. 272-282.

[46] Röseler, A. and Korte, E. H.: *Handbook of Vibrational Spectroscopy: Infrared Spectroscopic Ellipsometry*, Wiley and Sons, Chichester, **2002**.

[47] Gensch, M.; Roodenko, K.; Hinrichs, K.; Hunger, R.; Güell, A. G.; Merson, A.; Schade, U.; Shapira, Y.; Dittrich, T.; Rappich, J. and Esser, N.: Molecule-Solid Interfaces Studied with Infrared Ellipsometry: Ultrathin Nitrobenzene Films, *J. Vac. Sci. Technol. B* **2005**, *23*, p. 1838-1842.

[48] Güell, A. G.; Roodenko, K.; Yang, F.; Hinrichs, K.; Gensch, M.; Sanz, F. and Rappich, J.: Interface Properties and Passivation of p-Si(111) Surfaces by Electrochemical Organic Layer Deposition, *Mater. Sci. Eng. B-Solid* **2006**, *134*, p. 273-276.

[49] Hinrichs, K.; Gensch, M.; Esser, N.; Schade, U.; Rappich, J.; Kröning, S.; Portwitch, M. and Volkmer, R.: Analysis of Biosensors by Chemically Specific Optical Techniques. Chemiluminescence-Imaging and Infrared Spectroscopic Mapping Ellipsometry, *Anal. Bioanal. Chem.* **2007**, *387*, p. 1823-1829.

[50] Sirenko, A. A.; Bernhard, C.; Golnik, A.; Clark, A. M.; Hao, J.; Si, W. and Xi, X. X.: Soft-Mode Hardening in $TrSiO_3$ Thin Films, *Nature* **2000**, *404*, p. 373-376.

[51] Intelmann, C. M.; Hinrichs, K.; Syritski, V.; Yang, F. and Rappich, J.: Recombination Behaviour at the Ultrathin Polypyrrole Film / Silicon Interface Investigated by In-situ Pulsed Photoluminescence, *Jpn. J. Appl. Phys.* **2008**, *47*, p. 554-557.

[52] Smith, D. Y.: *Handbook of Optical Constants of Solids*, Academic Press, New York, **1985**.

[53] Röseler, A.: IR Spectroscopic Ellipsometry: Instrumentation and Results, *Thin Solid Films* **1993**, *234*, p. 307-313.

[54] Briggs, D. and Seah, M. P.: *Practical Surface Analysis by Auger and X-ray Photoelectron Spectroscopy*, 1st. ed., J. Wiley and Sons, Chichester, U.K., **1983**.

[55] Nalwa, H. S.: *Experimental Methods in the Physical Sciences (vol. 38)*, Press, Academic, Ed, Advances in Surface Science, Advances in Surface Science, San Diego, **2001**.

[56] Feldman, L. C. and Mayer, J. W.: *Fundamentals of Surface and Thin Films Analysis*, North-Holland, New York, **1986**.

[57] Proctor, A. and Sherwood, P. M. A.: Data Analysis Techniques in X-ray Photoelectron Spectroscopy, *Anal. Chem.* **1982**, *54*, p. 13-19.

[58] Tougaard, S.: Universality Classes of Inelastic Electron Scattering Cross-Sections, *Surf. Interface Anal.* **1997**, *25*, p. 137-154.

[59] Chastain, J.: *Handbook of X-ray Photoelectron Spectroscopy*, Perkin-Elmer Corp., Eden Prairie, MN, **1992**.

[60] Mayer, T.; Lebedev, M.; Hunger, R. and Jaegermann, W.: Elementary Processes at Semiconductor/Electrolyte Interfaces: Perspectives and Limits of Electron Spectroscopy, *Appl. Surf. Sci.* **2005**, *252*, p. 31-42.

[61] Tanuma, S.; C, J. P. and Penn, D. R.: Calculations of Electron Inelastic Mean Free Paths, *Surf. Interface Anal.* **1991**, *17*, p. 911-926.

[62] Dittrich, T.; Bitzer, T.; Rada, T.; Timoshenko, V. Y. and Rappich, J.: Non-Radiative Recombination at Reconstructed Si Surfaces, *Solid State Electron.* **2002**, *46*, p. 1863-1872.

[63] Timoshenko, V. Y.; Petrenko, A. B.; Stolyarov, M. N.; Dittrich, T.; Fuessel, W. and Rappich, J.: Quantitative Analysis of Room Temperature Photoluminescence of c-Si Wafers Excited by Short Laser Pulses, *J. Appl. Phys.* **1999**, *85*, p. 4171-4175.

[64] Yablonovitch, E. and Gmitter, T.: Auger Recombination in Silicon at Low Carrier Densities, *Appl. Phys. Lett.* **1986**, *49*, p. 587-589.

[65] Yablonovitch, E.; Allara, D. L.; Chang, C. C.; Gmitter, T. and Bright, T. B.: Unusually Low Surface-Recombination Velocity on Silicon and Germanium Surfaces, *Phys. Rev. Lett.* **1986**, *57*, p. 249-252.

[66] Kronik, L. and Shapira, Y.: Surface Photovoltage Phenomena: Theory, Experiment, and Applications., *Surf. Sci. Rep.* **1999**, *37*, p. 1-205.

[67] Rappich, J. and Dittrich, T.: *Handbook of Thin Film Materials (vol. 4: Electrochemical passivation of Si and SiGe surfaces)*, H. S. Nalwa. ed., Semiconductor and Supersemiconductor Thin Films, Academic Press, New York, **2002**.

[68] Heilig, K.; Flietner, H. and Reineke, J.: Investigation of Energetic Surface State Distributions at Real Surfaces of Silicon After Treatment with HF and H_2O Using Large-Signal Photovoltage Pulses, *J. Phys. D: Appl. Phys.* **1979**, *12*, p. 927-940.

[69] Laades, A.: *Preparation and Characterization of Amorphous/Crystalline Silicon Heterojunctions (a-Si:H/c-Si)*, TU Berlin Studies in Solid States Physics, Mensch & Buch Verlag, Berlin, **2005**.

[70] Reimer, L.: *Scanning Electron Microscopy*, Springer, Berlin, **1998**.

[71] Wartewig, S.: *IR and Raman Spectroscopy*, Wiley-VCH, Weinheim, **2003**.

[72] Allongue, P.; Villeneuve, C. H. d.; Morin, S.; Boukherroub, R. and Wayner, D. D. M.: The Preparation of Flat H-Si(111) Surfaces in 40% NH_4F Revisited, *Electrochim. Acta* **2000**, *45*, p. 4591-4598.

[73] Munford, M. L.; Cortés, R. and Allongue, P.: The Preparation of Ideally Ordered Flat H-Si(111) Surfaces, *Sensor. Mater.* **2001**, *13*, p. 259-269.

[74] Trucks, G. W.; Raghavachari, K.; Higashi, G. S. and Chabal, Y. J.: Mechanism of HF Etching of Silico Surfaces: A Theoretical Understanding of Hydrogen Passivation, *Phys. Rev. Lett.* **1990**, *65*, p. 504-507.

[75] Higashi, G. S.; Chabal, Y. J.; Trucks, G. W. and Raghavachari, K.: Ideal Hydrogen Termination of the Si(111) Surface, *Appl. Phys. Lett.* **1990**, *56*, p. 656-658.

[76] Chabal, Y. J.; Higashi, G. S.; Raghavachari, K. and Burrows, V. A.: Infrared Spectroscopy of Si(111) and Si(100) Surfaces After HF Treatment: Hydrogen Termination and Surface Morphology, *J. Vac. Sci. Technol. A* **1989**, *7*, p. 2104-2109.

[77] Mazzara, C.; Jupille, J.; Zheng, W.-Q.; Tanguy, M.; Tadjeddine, A. and Dumas, P.: Hydrogen-Terminated Si(111) and Si(100) by Wet Chemical Treatment: Linear and Non-Linear Infrared Spectroscopy, *Surf. Sci.* **1999**, *428*, p. 208-213.

[78] Stewart, M. P. and Buriak, J. M.: Chemical and Biological Applications of Porous Silicon Technology, *Adv. Mater.* **2000**, *12*, p. 859-869.

[79] Föll, H.; Christophersen, M.; Carstensen, J. and Hasse, G.: Formation and Application of Porous Silicon, *Mater. Sci. Eng. R* **2002**, *39*, p. 93-141.

[80] Yamaguchi, R.; Miyamoto, K.; Ishibashi, K.; Hirano, A.; Said, S. M.; Kimura, Y. and Niwano, M.: DNA Hybridization Detection by Porous Silicon-Based DNA Microarray in Conjugation with Infrared Microspectroscopy, *J. Appl. Phys.* **2007**, *102*, p. 014303 1-7.

[81] Ogata, Y. H.; Tsuboi, T.; Sakka, T. and Naito, S.: Oxidation of Porous Silicon in Dry and Wet Environments under Mild Temperature Conditions, *J. Porous Mat.* **2000**, *7*, p. 63-66.

[82] Borghesi, A.; Sassella, A.; Pivac, B. and Pavesi, L.: Characterization of Porous Silicon Inhomegeneities by High Spatial Resolution Infrared Spectroscopy, *Solid State Commun.* **1993**, *87*, p. 1-4.

[83] Maruyama, T. and Ohtani, S.: Photoluminescence of Porous Silicon Exposed to Ambient Air, *Appl. Phys. Lett.* **1994**, *65*, p. 1346-1348.

[84] Miura, T.; Niwano, M.; Shoji, D. and Miyamoto, N.: Kinetics of Oxidation on Hydrogen-Terminated Si(100) and (111) Surfaces Stored in Air, *J. Appl. Phys.* **1996**, *79*, p. 4973-4980.

[85] Lehmann, V. and Ronnebeck, S.: The Physics of Macropore Formation in Low-Doped p-Type Silicon, *J. Electrochem. Soc.* **1999**, *146*, p. 2968-2975.

[86] Smith, R. L. and Collins, S. D.: Porous Silicon Formation Mechanisms, *J. Appl. Phys.* **1992**, *71*, p. R1.

[87] Yahyaoui, F.; Dittrich, T.; Burke, T.; Aggour, M.; Lust, S.; Lévy-Clément, C. and Rappich, J.: Band Bending and Nonradiative Recombination at Si Surfaces During Electrochemical Treatment in Aqueous Fluoride Solution, *J. Electrochem. Soc.* **2002**, *148*, p. E472-E478.

[88] Hunger, R.; Fritsche, R.; Jaeckel, B.; Jaegermann, W.; Webb, L. J. and Lewis, N. S.: Chemical and Electronic Characterization of Methyl-Terminated Si(111) Surfaces by High-Resolution Synchrotron Photoelectron Spectroscopy, *Phys. Rev. B* **2005**, *72*, p. 045317 1-7.

[89] Webb, L. J.; Nemanick, E. J.; Biteen, J. S.; Knapp, D. W.; Michalak, D. J.; Traub, M. C.; Chan, A. S. Y.; Brunschwig, B. S. and Lewis, N. S.: High-Resolution X-ray Photoelectron Spectroscopic Studies of Alkylated Silicon(111) Surfaces, *J. Phys. Chem. B* **2005**, *109*, p. 3930-3937.

[90] Smith, B.: *Infrared Spectral Interpretation: a Systematic Approach*, CRC Press LLC, **1999**.

[91] Kaltchev, M. and Tysoe, W. T.: An Infrared Spectroscopic Investigation of Thin Alumina Films: Measurement of Acid Sites and Surface Reactivity, *Surf. Sci.* **1999**, *430*, p. 29-36.

[92] Canaria, C. A.; Lees, I. N.; Wun, A. W.; Miskelly, G. M. and Sailor, M. J.: Characterization of the Carbon-Silicon Stretch in Methylated Porous Silicon - Observation of an Anomalous Isotope Shift in the FTIR Spectrum, *Inorg. Chem. Commun.* **2002**, *5*, p. 560-564.

[93] Ignatyev, I. S.; Partal, F.; González, J. J. L. and Sundius, T.: Vibrational Spectra of Trimethylsilanol. The Problem of the Assignment of the SiOH Group Frequencies, *Spectrochim. Acta A* **2004**, *60*, p. 1169-1178.

[94] Rivillon, S. and Chabal, Y. J.: Alkylation of Silicon(111) Surfaces, *J. Phys. IV* **2006**, *132*, p. 195-198.

[95] Roodenko, K.; Rappich, J.; Yang, F.; Zhang, X.; Esser, N. and Hinrichs, K.: Anisotropy in Hydrogen-Passivated and Organically Modified Nanoporous Silicon Surfaces Studied by Polarization Dependent IR Spectroscopy, *Langmuir* **2009**, *25*, p. 1445-1452.

[96] Dubois, T.; Ozanam, F. and Chazalviel, J.-N.: Stabilization of the Porous Silicon Surface by Grafting of Organic Groups: Direct Electrochemical Methylation, *Proc. Electrochem. Soc.* **1997**, *97*, p. 296-310.

[97] Briggs, D.: *Handbook of X-ray and Ultraviolet Photoelectron Spectroscopy*, Heyden & Son, Cheshire, England, **1977**.

[98] Terry, J.; Linford, M. R.; Wigren, C.; Cao, R.; Pianetta, P. and Chidsey, C. E. D.: Alkyl-Terminated Si(111) Surfaces: A High-Resolution, Core Level Photoelectron Spectroscopy Study, *J. Appl. Phys.* **1999**, *85*, p. 213-221.

[99] Terry, J.; Mo, R.; Wigren, C.; Cao, R.; Mount, G.; Pianetta, P.; Linford, M. R. and Chidsey, C. E. D.: Reactivity of the H-Si (111) Surface, *Nucl. Instrum. Meth. B* **1997**, *133*, p. 94-101.

[100] Pauling, L.: *The Nature of the Chemical Bond*, 2nd. ed., Cornell University Press, Ithaca, NY, **1945**.

[101] Jaeckel, B.; Hunger, R.; Webb, L. J.; Jaegermann, W. and Lewis, N. S.: High-Resolution Synchrotron Photoemission Studies of the Electronic Structure and Thermal Stability of CH_3- and C_2H_5-Functionalized Si(111) Surfaces, *J. Phys. Chem. C* **2007**, *111*, p. 18204-18213.

[102] Barr, T. L.: *Modern ESCA: The Principles and Practice of X-ray Photoelectron Spectroscopy*, CRC Press, Inc., Boca Raton, Florida, **1994**.

[103] Beamson, G. and Briggs, D.: *High-Resolution XPS of Organic Polymers: the Scienta ESCA300 Database*, Wiley, New York, **1992**.

[104] Lud, S. Q.; Steenackers, M.; Jordan, R.; Bruno, P.; Gruen, D. M.; Feulner, P.; Garrido, J. A. and Stutzmann, M.: Chemical Grafting of Biphenyl Self-Assembled Monolayers on Ultrananocrystalline Diamond, *J. Am. Chem. Soc.* **2006**, *128*, p. 16884-16891.

[105] Voicu, R.; Boukherroub, R.; Bartzoka, V.; Ward, T.; Wojtyk, J. T. C. and Wayner, D. D. M.: Formation, Characterization, and Chemistry of Undecanoic Acid-Terminated Silicon Surfaces: Patterning and Immobilization of DNA, *Langmuir* **2004**, *20*, p. 11713-11720.

[106] Osaka, T.; Matsugana, M.; Kudo, S.; Niwa, D.; Shacham-Diamand, Y.; Jaegermann, W. and Hunger, R.: Electrical and Electrochemical Properties of Alkyl-Monolayer Modified Si(111) in the Presence of Water, *J. Electrochem. Soc.* **2007**, *154*, p. H919-H926.

[107] Wallart, X.; Villeneuve, C. H. d. and Allongue, P.: Truly Quantitative XPS Characterization of Organic Monolayers on Silicon: Study of Alkyl and Alkoxy Monolayers on H-Si(111), *J. Am. Chem. Soc.* **2005**, *127*, p. 7871-7878.

[108] Moras, P.; Mahne, N.; Ferrari, L.; Pesci, A.; Capozi, M.; Aversa, L.; Jha, S. N.; Verucchi, R.; Iannotta, S. and Pedio, M.: SiC(100) Ordered Film Growth by C60 Decomposition on Si(100) Surfaces, *Appl. Surf. Sci.* **2001**, *184*, p. 50-54.

[109] Smith, K. L. and Black, K. M.: Characterization of the Treated Surfaces of Silicon Alloyed Pyrolytic Carbon and SiC, *J. Vac. Sci. Technol. A* **1984**, *2*, p. 744-747.

[110] Faucheux, A.; Yang, F.; Allongue, P.; Villeneuve, C. H. d.; Ozanam, F. and Chazalviel, J.-N.: Thermal Decomposition of Alkyl Monolayers Covalently Grafted on (111) Silicon, *Appl. Phys. Lett.* **2006**, *88*, p. 193123 1-3.

[111] Basu, R.; Kinser, C. R.; Tovar, J. D. and Hersam, M. C.: Bromine Functionalized Molecular Adlayers on Hydrogen Passivated Silicon Surfaces, *Chem. Phys.* **2006**, *326*, p. 144-150.

[112] Hollinger, G. and Himpsel, F. J.: Probing the Transition Layer at the SiO_2-Si Interface Using Core Level Photoemission, *Appl. Phys. Lett.* **1984**, *44*, p. 93-95.

[113] Lu, Z. H.; Graham, M. J.; Jiang, D. T. and Tan, K. H.: SiO_2/Si(100) Interface Studied by Al*K*α X-ray and Synchrotron Radiation Photoelectron Spectroscopy, *Appl. Phys. Lett.* **1993**, *63*, p. 2941-2943.

[114] Karlsson, C. J.; Owman, F.; Landemark, E.; Chao, Y.-C.; Martensson, P. and Uhrberg, R. I. G.: Si2p Core-Level Spectroscopy of the Si(111)-(1x1)-H and Si(111)-(1x1)-D Surfaces - Vibrational Effects and Phonon Broadening, *Phys. Rev. Lett.* **1994**, *72*, p. 4145-4148.

[115] Grupp, C. and Taleb-Ibrahimi, A.: Core-Level Broadening Mechanisms at Silicon Surfaces, *J. Electron Spectrosc.* **1999**, *103*, p. 309-313.

[116] Köppe, M.; Itchkawitz, B. S.; Kilcoyne, A. L. D.; Feldhaus, J.; Kemgens, B.; Kivimäki, A.; Neeb, M. and Bradshaw, A. M., *Phys. Rev. A* **1996**, *53*, p. 4120.

[117] Hunger, R.; Pettenkofer, C. and Scheer, R.: Dipole Formation and Band Alignment at the Si(111)/$CuInS_2$ Heterojunction, *J. Appl. Phys.* **2002**, *91*, p. 6560-6570.

[118] Renzi, V. D.; Rousseau, R.; Marchetto, D.; Biagi, R.; Scandolo, S. and Pennino, U. d.: Metal Work-Function Changes Induced by Organic Adsorbates: A Combined Experimental and Theoretical Study, *Phys. Rev. Lett.* **2005**, *95*, p. 046804 1-4.

[119] Fukidome, H.; Pluchery, O.; Queeney, K. T.; Caudano, Y.; Raghavachari, K.; Weldon, M. K.; Chaban, E. E.; Christman, S. B.; Kobayashi, H. and Chabal, Y. J.: In situ vibrational study of SiO_2/liquid interfaces, *Surf. Sci.* **2002**, *502-503*, p. 498-502.

[120] Aristov, V. Y.; Lay, G. L.; Hricovini, K.; Taleb-Ibrahimi, A.; Dumas, P.; Gunther, R.; Osvald, J. and Indlekofer, G.: Nearly Complete Tuning of the Fermi-Level Position at a Prototypical Metal-Silicon Interface Lead on Unpinned Si(111)1x1-H, *J. Electron Spectrosc.* **1994**, *68*, p. 419-426.

[121] Angermann, H. and Rappich, J.: Surface States and Recombination Loss on Wet-Chemically Passivated Si Studied by Surface Photovoltage (SPV) and Photoluminescence (PL), *Solid State Phenom.* **2008**, *134*, p. 41-44.

[122] Roodenko, K.; Yang, F.; Hunger, R.; Esser, N.; Hinrichs, K. and Rappich, J.: Passivation of Si(111) Surfaces with Electrochemically Grafted Thin Organic Films, *Surf. Sci.* **2009**, *submitted*.

[123] Angermann, H.; Henrion, W.; Rebien, M. and Röseler, A.: Wet-Chemical Preparation and Spectroscopic Characterization of Si Interfaces, *Appl. Surf. Sci.* **2004**, *235*, p. 322-339.

[124] Osipov, A. V.; Patzner, P. and Hess, P.: Kinetics of Laser-Induced Oxidation of Silicon Near Room Temperature, *Appl. Phys. A- Mater.* **2006**, *82*, p. 275-280.

[125] Yoshinobu, J.; Tsuda, H.; Onchi, M. and Nishijima, M.: Rehybridization of Acetylene on the Si(111) (7x7) Surface - A Vibrational Study, *Chem. Phys. Lett.* **1986**, *130*, p. 170-174.

[126] Ferguson, G. A. and Raghavachari, K.: Collective Vibrations in Cluster Models for Semiconductor Surfaces: Vibrational Spectra of Acetylenyl and Methylacetylenyl Functionalized Si(111), *J. Chem. Phys.* **2007**, *127*, p. 194706 1-7.

[127] Sieval, A. B.; Demirel, A. L.; Nissink, J. W. M.; Linford, M. R.; Maas, J. H. v. d.; Jeu, W. H. d.; Zuilhof, H. and Sudhölter, E. J. R.: Highly Stable Si-C Linked Functionalized Monolayers on the Silicon (100) Surface, *Langmuir* **1998**, *14*, p. 1759-1768.

[128] Lin-Vien, D.; Colthup, N. B.; Fateley, W. G. and Grasselli, J. G.: *The Handbook of Infrared and Raman Characteristic Frequencies of Organic Molecules*, Academic Press, San Diego, **1991**.

[129] Allongue, P.; Villeneuve, C. H. d.; Pinson, J.; Ozanam, F.; Chazalviel, J.-N. and Wallart, X.: Organic Monolayers on Si(111) by Electrochemical Method, *Electrochim. Acta* **1998**, *43*, p. 2791-2798.

[130] Terry, J.; Linford, M. R.; Wingren, C.; Cao, R. Y.; Pianetta, P. and Chidsey, C. E. D.: Determination of the Bonding of Alkyl Monolayers to the Si(111) Surface Using Chemical-Shift, Scanned-Energy Photoelectron Diffraction, *Appl. Phys. Lett.* **1997**, *71*, p. 1056-1058.

[131] Cicero, R. L.; Linford, M. R. and Chidsey, C. E. D.: Photoreactivity of Unsaturated Compounds with Hydrogen-Terminated Silicon(111), *Langmuir* **2000**, *16*, p. 5688-5695.

[132] Hurley, P. T.; Nemanick, E. J.; Brunschwig, B. S. and Lewis, N. S.: Covalent Attachment of Acetylene and Methylacetylene Functionality to Si(111) Surfaces: Scaffolds for Organic Surface Functionalization while Retaining Si-C Passivation of Si(111) Surfaces Sites, *J. Am. Chem. Soc.* **2006**, *128*, p. 9990-9991.

[133] He, T.; Ding, H.; Peor, N.; Lu, M.; Corley, D. A.; Chen, B.; Ofir, Y.; Gao, Y.; Yizchaik, S. and Tour, J. M.: Silicon/Molecule Interfacial Electronic Modifications, *J. Am. Chem. Soc.* **2008**, *130*, p. 1699-1710.

[134] Musa, I. and Eccleston, W.: Electrical Properties of Polymer Si Heterojunctions, *Thin Solid Films* **1999**, *343-344*, p. 469-475.

[135] Onganer, Y.; Saglam, M.; Türüt, A.; Efeoglu, H. and Tüzemen, S.: High Barrier Metallic Polymer p-Type Silicon Schottky Diodes, *Solid State Electron.* **1996**, *39*, p. 677-680.

[136] Poddar, R. and Luo, C.: A Novel Approach to Fabricate a PPy/p-Type Si Heterojunction, *Solid State Electron.* **2006**, *50*, p. 1687-1691.

[137] Guo, Z. P.; Wang, J. Z.; Liu, H. K. and Dou, S. X.: Study of Silicon/Polypyrrole Composite as Anode Materials for Li-ion Batteries, *J. Power Sources* **2005**, *146*, p. 448-451.

[138] Skotheim, T. A.: *Handbook of Conducting Polymers (vol. 1)*, Marcel Dekker, New York, **1986**.

[139] Skotheim, T. A.: *Handbook of Conducting Polymers (vol. 2)*, Marcel Dekker, New York, **1986**.

[140] Intelmann, C. M.; Rammelt, U.; Plieth, W.; Cai, X.; Jähne, E. and Adler, H.-P.: Preparation of Ultrathin Polypyrrole Films Using an Adhesion Promoter, *J. Solid State Electr.* **2006**, *11*, p. 1-9.

[141] Intelmann, C. M.; Syritski, V.; Tsankov, D.; Hinrichs, K. and Rappich, J.: Ultrathin Polypyrrole Films on Silicon Substrates, *Electrochim. Acta* **2008**, *53*, p. 4046-4050.

[142] Ping, Z. and Nauer, G. E.: In Situ FTIR-ATR Spectroscopic Investigations on the Polymerization Process and the Redox Behavior of Poly(thienylpyrrole) Thin Film Electrodes in Aqueous and Non-Aqueous Solutions. Part 1. Characterization of the Polymerization Process in Acetonitrile Containing Different Supporting Salts, *J. Electroanal. Chem.* **1996**, *416*, p. 157-166.

[143] Zhang, X.; Zhang, J.; Song, W. and Liu, Z.: Controllable Synthesis of Conducting Polypyrrole Nanostuctures, *J. Phys. Chem. B* **2006**, *110*, p. 1158-1165.

[144] Li, X.; Wan, M.; Wei, Y.; Shen, J. and Chen, Z.: Electromagnetic Functionalized and Core−Shell Micro/Nanostructured Polypyrrole Composites, *J. Phys. Chem. B* **2006**, *110*, p. 14623-14626.

[145] Tian, B. and Zerbi, G.: Lattice Dynamics and Vibrational Spectra of Polypyrrole, *J. Chem. Phys.* **1990**, *92*, p. 3886-3891.

[146] Wang, J. G.; Neoh, K. G. and Kang, E. T.: Comparative Study of Chemically Synthesized and Plasma Polymerized Pyrrole and Thiophene Thin Films, *Thin Solid Films* **2004**, *446*, p. 205-217.

[147] Fabre, B.; Lopinski, G. P. and Wayner, D. D. M.: Functionalization of Si(111) Surfaces with Alkyl Chains Terminated by Electrochemically Polymerizable Thienyl Units, *Chem. Commun.* **2002**, p. 2904-2905.

List of abbreviations

BE	Binding energy
BrBu	Bromobutane
CV	Cyclovoltammetry
Cv	Current-voltage
Ct	Current-time
DEE	Diethyl ether
FTIR	Fourier-Transform infrared spectroscopy
FZ	Float zone
HF	Hydrogen fluoride
IMFP	Inelastic mean free path
IR	Infrared
IRSE	Infrared spectroscopic ellipsometry
MCT	Mercury-Cadmium-Telluride
MePSi	Methylated porous silicon
NH_4F	Ammonium fluoride
PPy	Polypyrrole
PSi	Porous silicon
PL	Photoluminescence
PT	Polythiophene
PV	Photovoltage
Pyl-MgBr	Pyrrylmagnesium bromide
R•	Radical
RMgX	Grignard solution
SEM	Scanning electron microscopy
Solv	Solvent
SPV	Surface photovoltage
SXPS	Synchrotron X-ray photoemission spectroscopy
THF	Tetrahydrofuran
Tyl-MgBr	Thiophen-2-yl magnesium bromide
UHV	Ultrahigh vacuum
XPS	X-ray photoemission spectroscopy

Acknowledgements

I have been exceptionally fortunate to have spent my time as a graduate student working with a number of colleagues at the department Si-Photovoltaik (SE1) at the Helmholtz-Zentrum Berlin für Materialien und Energie GmbH (HZB) who are not only great scientists, but also wonderful and interesting people. Now the time has come to express my thanks to them.

First and foremost I would like to thank Prof. Dr. Klaus Rademann at the HU-Berlin for supervising this work, for his critical analysis, for the interesting and helpful discussions, and encouragement.

I want to express my sincere gratitude to Dr. Jörg Rappich from HZB-SE1 for his guidance, for the interesting and enlightening discussions, for being a constant source of ideas and also for his ongoing support. I wholeheartedly appreciated his availability and all the freedom he gave me to lead this research on my own. Thank you again for everything.

My thanks also go to Prof. Dr. Norbert Esser at the ISAS Institute Berlin for the interesting discussions, his encouragement, and for accepting to be the second referee of this thesis.

Dr. Karsten Hinrichs and Dr. Katy Roodenko from ISAS-Berlin have also been invaluable in measuring the IRSE spectra of my samples and for the fruitful discussions on IR spectroscopy techniques.

I am very grateful to Dr. Ralf Hunger from TU-Darmstadt and Dr. Iver Lauermann of HZB-SE2 for their unfailing service at the SXPS and XPS machines, and their constant interesting and illuminating discussions about the obtained results, which gave me a better understanding of the XPS techniques used.

I thank Dr. Silvia Janietz from IAP-Golm for providing me the synthesized pyrrylmagnesium bromide compound.

I would also like to thank Mrs. Klimm (HZB-SE1) for carefully recording the SEM micrographs and the members of the organic/Si hybrid group at HZB-SE1, Dr. Matthias Intelmann and Xin Zhang, for their constant and invaluable sources of help and the nice atmosphere besides all science.

I am grateful to the support by Dr. Manfred Schmidt at HZB-SE1 and his permanent interest in this work of Si surface modification.

Thanks to all people of the department SE1, especially Mrs. Krusche, for their help on all the “little things” along the way.

I am also thankful to all my friends and my family for their encouragement.

Finally, I would like to thank the people without whom none of this work would have been possible, especially my parents, and my sisters Roseline, Irèna, and Lina for their constant support throughout my thesis.

List of publications

Faucheux, A.; Yang, F.; Allongue, P.; Henry de Villeneuve, C.; Ozanam, F. and Chazalviel, J.-N.: Thermal Decomposition of Alkyl Monolayers Covalently Grafted on (111) Silicon, *Appl. Phys. Lett.* **2006**, *88*, p.193123 1-3.

Güell, A. G.; Roodenko, K.; Yang, F.; Hinrichs, K.; Gensch, M.; Sanz, F. and Rappich, J.: Interface Properties and Passivation of p-Si(111) Surfaces by Electrochemical Organic Layer Deposition, *Mater. Sci. Eng. B-Solid* **2006**, *134*, p. 273-276.

Yang, F.; Roodenko, K.; Hinrichs, K. and Rappich, J.: Electronic and Surface Properties During the Etch-Back of Anodic Oxides on Si(111) Surfaces in 40% NH_4F Solution, *J. Micromech. Microeng.* **2007**, *17*, p. S56-S60.

Intelmann, C. M.; Hinrichs, K.; Syritski, V.; Yang, F. and Rappich, J.: Recombination Behavior at the Ultrathin Polypyrrole Films/Silicon Interface Investigated by In-Situ Pulsed Photoluminescence, *Jpn. J. Appl. Phys.* **2008**, *47*, p. 554-557.

Roodenko, K.; Rappich, J.; Yang, F.; Zhang, X.; Esser, N. and Hinrichs, K.: Optical Effects and Anisotropy in Hydrogen Passivated and Organically Modified Porous Silicon Surfaces Studied by IR Polarized Spectroscopies, *Langmuir* **2009**, *25*, p. 1445-1452.

Yang, F.; Hunger, R.; Roodenko, K.; Hinrichs, K.; Rademann, K. and Rappich, J.: Vibrational and Electronic Characterization of Ethynyl Derivatives Grafted onto Hydrogenated Si(111) Surfaces, *Langmuir* **2009**, *25*, p. 9313-9318.

Yang, F.; Hunger, R.; Rademann, K. and Rappich, J.: Photoluminescence and Surface Photovoltage of Ethynyl Derivatives-Terminated Si(111) Surfaces, *Phys. Status Solidi C*, **accepted**.

Part of the works submitted:

Yang, F.; Roodenko, K.; Hunger, R.; Hinrichs, K.; Rademann, K. and Rappich, J.: One-Step Electrochemical Grafting of CD_3 onto Si(111) Surfaces: An IR Ellipsometry, Synchrotron XPS, and Photoluminescence Study, *J. Am. Chem. Soc.*, **submitted**.

Yang, F.; Hunger, R.; Rademann, K. and Rappich, J.: Electronic Properties of Methyl and Ethynyl Derivatives Electrochemically Anchored onto Si(111) Surfaces, *Angew. Chem. Int. Edit.*, **submitted**.

Roodenko, K.; Yang, F.; Hunger, R.; Esser, N.; Hinrichs, K. and Rappich, J.: Passivation of Si(111) Surfaces with Electrochemically Grafted Thin Organic Films, *Surf. Sci.* **submitted**.

Part of the work in progress:

Yang, F.; Hunger, R.; Hinrichs, K.; Roodenko, K.; Rademann, K. and Rappich, J.: Passivation and Stability of Methylated Si(111) Surfaces in Ambient Air: A SXPS, IRSE, and PL Study, *Adv. Mater.*, **to be submitted**.

Selbständigkeitserklärung

Hiermit versichere ich, Florent Yang, dass ich die vorliegende Dissertation selbständig und nur unter Verwendung der angegebenen Quellen und Hilfsmittel angefertigt habe.

Berlin, den 16.10.2008